DOKUZ EYLÜL UNIVERSITY
GRADUATE SCHOOL OF NATURAL AND APPLIED SCIENCES

ELECTRIC, MAGNETIC AND ELASTIC WAVES IN ANISOTROPIC MATERIALS

by
Handan ÇERDİK YASLAN

May, 2011
İZMİR

ELECTRIC, MAGNETIC AND ELASTIC WAVES IN ANISOTROPIC MATERIALS

A Thesis Submitted to the

Graduate School of Natural and Applied Sciences of Dokuz Eylül University

In Partial Fulfilment of the Requirements for the Degree of Doctor of Philosophy in Mathematics

by
Handan ÇERDİK YASLAN

May, 2011
İZMİR

Ph.D. THESIS EXAMINATION RESULT FORM

We have read the thesis entitled **"ELECTRIC, MAGNETIC AND ELASTIC WAVES IN ANISOTROPIC MATERIALS "** completed by **HANDAN ÇERDİK YASLAN** under supervision of **PROF. DR. VALERY YAKHNO** and we certify that in our opinion it is fully adequate, in scope and in quality, as a thesis for the degree of Doctor of Philosophy.

Prof. Dr. Valery YAKHNO

Supervisor

Prof. Dr. Gonca ONARGAN

Thesis Committee Member

Prof. Dr. Taner OĞUZER

Thesis Committee Member

Doç. Dr. Fatma AYAZ

Examining Committee Member

Yrd. Doç. Dr. Melda DUMAN

Examining Committee Member

Prof. Dr. Mustafa SABUNCU
Director
Graduate School of Natural and Applied Sciences

ACKNOWLEDGEMENTS

I would like to express my deepest gratitude to my supervisor Prof. Dr. Valery YAKHNO for his advice, encouragement, patience and belief in me. I would like to thank his invaluable contribution to this thesis. He also helped me improve my mathematical background. He is not only a very good scientist, but also a very good teacher. I am proud to be his PhD student.

Also, I would like to express my gratitude to TUBİTAK (The Scientific and Technical Research Council of Turkey) for its support during my PhD research.

Finally, I am grateful to my family for their never ending love, trust, encouragement throughout my life.

Handan ÇERDİK YASLAN

ELECTRIC, MAGNETIC AND ELASTIC WAVES IN ANISOTROPIC MATERIALS

ABSTRACT

In this thesis new methods for the fundamental solutions of elastodynamics of anisotropic crystals, quasicrystals and fundamental solutions of electromagnetodynamics of anisotropic materials are suggested. These methods are based on the Fourier transformation with respect to space variables and some matrix computations. Robustness of the methods are confirmed by computational examples. Simulation of elastic, electric and magnetic waves arising from pulse point sources in crystals and quasicrystals, electrically and magnetically anisotropic materials are obtained. Moreover, a new method for solving the initial value problem for the system of electromagnetoelasticity is proposed and theorems about existence and uniqueness of the solution of the initial value problem are proved.

Keywords: Time-dependent equations of anisotropic elasticity in crystals, quasicrystals, Maxwell's equations of anisotropic electrodynamics, equations of the electromagnetoelasticity, fundamental solution, analytical method, computational experiments, simulation.

İSOTROPİK OLMAYAN MATERYALLERDE ELEKTRİK, MANYETİK VE ELASTİK DALGALAR

ÖZ

Bu tezde isotropik olmayan kristaller ile yarı kristallerde ve isotropik olmayan materyallerde elastodinamiğin ve elektromagnetodinamiklerin temel çözümlerini bulmak için yeni metodlar sunulmuştur. Bu metodlar uzay değişkenlerine göre Fourier dönüşümlerine ve bazı matris hesaplamalarına dayanır. Metodların doğruluğu hesaplamalı örneklere dayanarak gösterilmiştir. Kristallerde, yarı kristallerde, elektriksel ve manyetiksel isotropik olmayan materyallerde nokta kaynaktan doğan elastik, manyetik ve elektrik dalgaların simülasyonları elde edilmiştir. Ayrıca elektromagnetoelastik sisteminin başlangıç değer problemini çözmek için yeni bir metod önerilmiştir. Bu başlangıç değer probleminin çözümüyle ilgili varlık ve teklik teoremlerinin ispatları verilmiştir.

Anahtar sözcükler: Kristallerde ve yarı kristallerde isotropik olmayan elastiğin zamana bağlı denklemleri, isotropik olmayan elektrodinamiğin Maxwell denklemleri, elektromagnetoelastiğin denklemleri, temel çözüm, analitik metod, hesaplamalı örnekler, simülasyon.

CONTENTS

Page

CHAPTER ONE
INTRODUCTION

Search and development of new materials with specific properties are needed for different industries such as chemistry, microelectronics, etc. When new materials are created we must be able to have the possibility to model and study their properties. Mathematical models of physical processes can provide cutaway views that let you see aspects of something that would be invisible in the real artifact but computer models can also provide visualization tools.

The physical properties of a homogeneous isotropic medium do not depend on the direction and the position inside the medium. Physical properties of anisotropic media essentially depend on orientation and position. An anisotropic medium is called homogeneous when its physical properties depend on orientation and do not depend on position. The medium can be isotropic relative to some physical properties and anisotropic with respect to others. For example, anisotropic crystals and dielectrics are magnetically isotropic but electrically anisotropic. Some of materials are magnetically anisotropic but electrically isotropic and some of materials are electrically and magnetically anisotropic. Anisotropy of materials is related to their atomic lattice. A smallest block (three dimensional array of atoms) of anisotropic materials is determined by repeated replication in three dimensions. Its symmetry tells how the constituent atoms are arranged in a regular repeating configuration. The structure of these three- dimensional unit cell of atoms in anisotropic materials may have one of seven basic shapes: cubic, hexagonal, tetragonal, trigonal, orthorhombic, monoclinic and triclinic (see, for example, Nye (1967)). Thesis includes mathematical modeling and simulating the wave propagation in anisotropic solids and crystals.

Crystal is a solid in which the constituent atoms, molecules, or ions are packed in a regularly ordered. The physical and chemical properties of a crystal to depend not

only on the nature of the atoms in each cell, but also on the geometrical arrangement of the cells, that is the lattice symmetry. Thus, independently of the cell contents, crystals with the same point symmetry give related behaviour for physical quantities, in corresponding orientations. Tensor analysis expresses this behaviour well. Physical properties of crystals are represented by tensors.

The crystalline medium is characterized by an infinity of geometrical points, each equivalent to any point O in the crystal. All of these equivalent points have the same atomic environment, and they can be deduced from one another by means of a succession of elementary translations along three vectors a, b, c. The set of all these points forms a three-dimensional lattice. In classifying crystals according to the point symmetry of the lattice, we define the seven crystal systems. A crystal system is characterized by the geometrical form of the cell. These forms vary from the most general parallelepiped as follows (Dieulesaint & Royer (1980))

- Triclinic $\alpha \neq \beta \neq \gamma$; $a \neq b \neq c$
- Monoclinic $\alpha = \beta, \gamma > 90$; $a \neq b \neq c$
- Orthorhombic $\alpha = \beta = \gamma = 90$; $a \neq b \neq c$
- Trigonal $\alpha = \beta = \gamma \neq 90$; $a = b = c$
- Tetragonal $\alpha = \beta = \gamma = 90$; $a = b \neq c$
- Hexagonal $\alpha = \beta = 90, \gamma = 120$; $a = b \neq c$
- Cubic $\alpha = \beta = \gamma = 90$; $a = b = c$.

Here α is an angle between c and b, β is an angle between a and c, γ is an angle between a and b.

Numerous significant problems of structural mechanics, geophysics and material sciences are closely related to studies of wave propagations in continuous anisotropic elastic media. The main core of these problems consists in the determination of displacement and stresses fields induced by impulsive loading as well as calculations of the behavior of structures subjected to sudden shocks. The behavior of the wave processes essentially depends on properties of materials and media (density and elastic moduli). We note that the forms of wave fronts from the pulse point sources in elastic materials with general structure of anisotropy (monoclinic, triclinic) are not spherical and have very peculiar forms. If elastic waves arise from an impulsive force concentrated at the fixed point then the computation of the displacement and stresses at the points near by the source is complicated because the displacements and stresses are generalized functions (distributions) (see Vladimirov (1971), Vladimirov (1979), Reed & Simon (1975), Hormander (1963)). The mathematical model of the motion of homogeneous anisotropic elastic media is presented by the dynamic system of equations of linear theory of elasticity (Ting (1996), Ting & Barnett & Wu (1990), Dieulesaint & Royer (1980), Federov (1968), Poruchikov (1993)). This system consists of three partial differential equations of the second order with constant coefficients (Ting (1996), Ting & Barnett & Wu (1990), Dieulesaint & Royer (1980), Donida & Bernetti (1991), Yakhno & Akmaz (2007), Yakhno & Akmaz (2005)). The differential equations of anisotropic elastodynamics describe the dynamic processes of the wave phenomena in anisotropic materials and media. The problems of elastodynamics are often stated in the form of computing displacement components at internal points of anisotropic solids. Analytical and numerical methods play the important role in the study of these problems (see, for example, Poruchikov (1993), Chang & Wu (2003), Carrer & Mansur (1999), Sladek & Sladek & Zhang (2005), Moosavi & Khelil (2009), Dauksher & Emery (2000)). Besides that fundamental solutions (FSs) or Green's functions (GFs) of equations of elastodynamics are important tools for solving these problems (see for example, Mansur & Loureiro

(2009), Mansur & Loureiro & Soares & Dors (2007), Soares & Mansur (2005), Vea-Tudela & Telles (2005), Rangelov & Manolis & Dineva (2008), Rangelov (2003), Berger & Tewary (1996), Tewary (1995), Wang & Achenbach (1994), Wang & Achenbach (1995)). Fundamental solutions of partial differential equations play an important role in both applied and theoretical studies on physics of solids (Stokes (1883),Volterra (1894), Mindlin (1936), Huang & Wang (1991)).

The existence proofs for fundamental solutions (FSs) in the spaces of generalized functions for any linear differential equations with constant coefficients were given by Malgrange (1955-1956), Ehrenpreis (1960), Hormander (1963). Ignoring here many approaches of finding FSs for scalar differential equations with constant coefficients we point out only some of methods to determine FSs for equations of elastodynamics. The analytical computation of the explicit formulae for FSs in homogeneous isotropic linearly elastic solids offers no difficulty (see, for example, Aki & Richard (1980), Payton (1983)). But this is not the case for general homogeneous anisotropic media.

The fundamental solutions for anisotropic elastic media have been studied by Buchwald (1959), Lighthill (1960), Burridge (1967a),Burridge (1967b), Burridge (1971), Kraut (1963), Musgrave (1970), Willis (1973), Payton (1983), Tsvankin & Chesnokov (1989), Wu & Ting & Barnett (1990), Payton (1992), Wang & Achenbach (1992), Tewary & Fortunko (1992), Zhu (1992), Budreck (1993) and other authors. The fundamental solutions of anisotropic elasticity in the papers mentioned above are either approximations or they have complicated mathematical forms which are difficult to evaluate numerically. Most of approaches for finding the time-dependent fundamental solutions are related with the Fourier-Laplace presentation in a wave-vector-frequency space. The oscillatory nature of the Fourier-Laplace representation and the principal value calculation at the singularities create computational difficulties.

An interesting approach of finding fundamental solutions by the Radon transform for 3D and 2D time-domain elastodynamic has been suggested by Wang & Achenbach (1994). They found fundamental solutions in the form of a surface integral over a unit sphere for 3D case. Physically, the integral can be interpreted as superpositions of plane waves propagating in all directions. The resulting expression has a complicated form containing the integration over the slowness surface. We note that for some anisotropic materials (cubic, transversely isotropic) fundamental solutions can be evaluated numerically using this approach (see, Wang & Achenbach (1994)). In the paper of Tewary (1995) the formula for the time-dependent fundamental solution in three dimensional anisotropic elastic infinite solids has been derived by Radon transform and solving the Christoffel equation in terms of the delta function. The computational advantages of this method and method of Wang & Achenbach (1994) are following: it does not require integration over frequency, the integration is made over two out of three variables. However the method of Tewary (1995) calculates numerically the transient displacement field due to a point source in infinite anisotropic cubic solids. The numerical realization of this method for general anisotropic elastic solids (triclinic, monoclinic and etc) is questionable because the computation of the weight function in the obtained Radon representation is not clear for the general case.

The computation of fundamental solutions for general linear equations of elastodynamics with three space and one time variables has been obtained only for particular cases of anisotropy (cubic, isotropic, transversely isotropic, orthotropic structures)(Wang & Achenbach (1994), Tewary (1995),Wang & Achenbach (1995), Yang & Pan & Tewary (2004), Rangelov (2003), Kocak (2009), Khojasteh & Rahimian & Pak (2008), Wang & Pan & Feng (2007), Rangelov & Manolis & Dineva (2008)). The computation of the fundamental solutions in such anisotropic elastic media as trigonal, monoclinic, triclinic has not been achieved so far.

Since the icosahedral quasicrystal structure was discovered in Al-Mn alloys in 1984

(Shechtman & Blech & Gratias & Cahn (1980)), great progress has been made in experimental and theoretical studies in physics of quasicrystals (Wang & Chen & Kuo (1987), Wollgarten & Beyss & Urban & Liebertz & Koster (1987), Ovidko (1998)). These experiments and theoretical analyses have shown that quasicrystals(QCs) are new materials with a complex structure and unusual properties (Ronchetti (1987), Socolar & Lubensky & Steinhardt (1986), Wang & Yang & Hu (1997), Fan (1999), Fan & Mai (2004) etc.). This has created an important opportunity for new basic research. For large single-grain quasicrystals, over one hundred different alloys with thermodynamic stability have been produced. This suggests that quasicrystals may become a new class of functional and structural materials, which have many prospective engineering applications. The significance of quasi-crystals, in theory and practice, has created a great deal of attention by researchers in a range of fields, such as solid state physics, crystallography, materials science, applied mathematics, and solid mechanics. Thesis includes mathematical modeling and simulating the elastic wave propagation in quasicrystals.

Quasicrystalline materials (QCs) are clearly fascinating materials: crystal structures and properties are surprising and could be remarkably useful. Most of these properties combine effectively to give technologically interesting applications which have been protected recently by several patents (Blaaderen (2009), Dubois (2005)). For instance, the combination of such kind of properties as high hardness, low friction and corrosive resistance of QCs gives almost ideal material for motor-car engines. The application of QCs in motor-car engines would be undoubtedly result in reduced air pollution and increase engine lifetimes. The same set of associated properties (hardness, low friction, corrosive resistance) combined with bio-compatibility is also very promising for introducing QCs in surgical applications as parts used for bone repair and prostheses (Blaaderen (2009), Dubois (2005), Dubois (2000)).

1D, 2D and 3D QCs are defined as three dimensional body with the special atom

arrangements. The atom arrangement of 1D QC is quasi-periodic in direction and periodic in the plane which is orthogonal to this direction. The atom arrangement of 2D QC is quasi-periodic in a plane and periodic in the orthogonal direction. The atom arrangement of 3D QC is quasi-periodic in three dimensions without periodic direction. Three-dimensional QCs such as icosahedral QCs (e.g. Al-Cu-Fe and Al-Li-Cu) are quasiperiodic in three dimensions, without periodic direction. They play a central role in the study of QCs.

Elasticity is one of important properties of QCs. The expressions of the generalized Hooke's law, equations of the equilibrium and motion have been analyzed in works Yang & Wang & Ding & Hu (1993), Ding & Wang & Yang & Hu (1995), Ding & Yang & Hu & Wang (1993), Fan (1999), Fan & Mai (2004), Fan & Guo (2005), Gao & Zhao (2006), Gao & Zhao & Xu (2008), Gao (2009), Liu & Fan & Guo (2003), Peng & Fan & Zhang & Sun (2001), Peng & Fan (2002).

Among various QCs, one-dimensional QCs are of particular interest for the researchers after the success of Merlin & Bajema & Clarke & Juang & Bhattacharya (1985) in growing model systems, where quasi-periodicity is built up. Wang & Yang & Hu (1997) derived all the possible point groups and space groups of 1D QCs; Liu & Fu & Dong (1997) studied the physical properties of 1D QCs. Gao (2009) and Chen & Ma & Ding (2004) have presented general solutions of three-dimensional elastostatic problems for 1D hexagonal quasicrystals. Gao & Zhao & Xu (2008) have developed theory of general solutions of three-dimensional elastostatic(3D) problems for 1D hexagonal quasicrystals. Peng & Fan & Zhang & Sun (2001) have solved the three-dimensional elasticity equations of 1D hexagonal quasicrystals for static case using a new perturbation technique. Gao & Zhao (2006) have obtained the general solutions of three-dimensional elasticity equations of 2D dodecagonal and 1D hexagonal quasicrystals for static case using a new perturbation technique. Peng & Fan (2000) have obtained the general solutions of three-dimensional elasticity equations of

1D hexagonal quasicrystals for static case in terms of four harmonic functions. Peng & Fan & Zhang & Sun (2001) have obtained the general solutions of three-dimensional elasticity equations of 1D hexagonal quasicrystals for static case using Fourier series and Hankel transform. Wang (2006) has given a general solution of 1D hexagonal quasicrystals for dynamic and static elasticity. Fan & Mai (2004) have discussed three dimensional elasticity of 1D, 2D and 3D QCs for dynamic case.

The fundamental theory based on the motion of continuum model to describe the elastic behavior of QCs is well known (see, for example, Ding & Yang & Hu & Wang (1993), Hu & Wang & Ding (2000), Gao & Zhao (2006), Rochal & Lorman (2002)). The elastic equations in 3D elasticity of QCs are more complicated than those of classical elasticity. In QCs a phason displacement field exits in addition to a phonon displacement. All existing models of QC elastodynamics are given by partial differential equations. The exam of the consistency of models, given by partial differential equations, is related to the comparison values of solutions for these equations with experimental data. Solutions of elastodynamic equations for QCs are difficult to obtain than for crystals. Computation values of solutions of elastodynamic equations for 3D QCs are more complicated than those of 1D and 2D QCs. Because of the complexities of the solution of elastodynamic equations most authors consider only elastic plane problems for QCs (Ding & Yang & Hu & Wang (1993), Akmaz & Akinci (2009), Fan & Mai (2004)), i.e. they suppose that the elastic fields induced in QCs are independent of the variable z. The plane elasticity problems of 3D and 2D quasicrystals has been studied for static case in Ding & Wang & Yang & Hu (1995). Based on the stress potential function general solution of the plane elasticity problems of icosahedral quasicrystals has been studied for static case in Li & Fan (2006). Gao (2009) has established general solutions for plane elastostatic of cubic quasicrystals using an operator method. Fan & Guo (2005) has developed the potential function theory for plane elastostatic of three-dimensional

icosahedral quasicrystals. The dynamic plane elastic problems in 2D QCs with dodecagonal, pentagonal and decagonal structures have been studied in Akmaz & Akinci (2009). The time-dependent elastic problems in QCs have been studied in Fan & Mai (2004), Wang (2006), Akmaz & Akinci (2009), Akmaz (2009) Yakhno & Yaslan (2011). Using decomposition and superposition procedures 2D dynamic problems for 1D and 2D hexagonal QCs have been solved Fan & Mai (2004). Wang (2006) has found a general solution for 3D dynamic problem in 1D hexagonal QCs. Using PS method related with polynomial presentation of data 3D elastic problems in 3D QCs have been solved in Akmaz (2009). A method for the derivation of the time-dependent fundamental solution with three space variables in 2D QCs with arbitrary system of anisotropy have been proposed in Yakhno & Yaslan (2011).

Three-dimensional quasicrystals, such as icosahedral quasicrystals (e.g., Al-Cu-Fe and Al-Li-Cu) play a central role in the study of quasicrystalline solids. It is more difficult to obtain rigorous analytic solutions for the elasticity problems of 3D QCs. Yang & Wang & Ding & Hu (1993) have discussed the expressions of the generalized Hooke's law and equilibrium for cubic QCs in static case. Zhou & Fan (2000) have studied axisymmetric elasticity problem of cubic quasicrystal. The plane elasticity problems of 3D and 2D quasicrystals has been studied for static case in Ding & Wang & Yang & Hu (1995). Based on the stress potential function general solution of the plane elasticity problems of icosahedral quasicrystals has been studied for static case in Li & Fan (2006). Gao (2009) has established general solutions for plane elastostatic of cubic quasicrystals using an operator method. Fan & Guo (2005) has developed the potential function theory for plane elastostatic of three-dimensional icosahedral quasicrystals.

It is well known that fundamental solutions (Green's functions in free space) play a crucial role in the elasticity theory. An analytical presentation of elastostatic fundamental solution (FS) has been derived for icosahedral quasicrystals in the paper

Bachteler & Trebin (1998). In De & Pelcovits (1987) have computed fundamental solution (FS) for the elastic equations and used them for finding general solutions of the inhomogenous linear elastostatic equations of pentagonal QCs. In Akmaz & Akinci (2009) have obtained Fourier images of a fundamental solution (FS) for dynamic plane elasticity problems of 2D dodecagonal, pentagonal and decagonal QCs. In Ding & Wang & Yang & Hu (1995) have studied the elastic fundamental solution (FS) for QCs in the static case. We note that computation of FSs for equations of elastodynamics and elastostatics in 2D QCs has been obtained only for particular cases of anisotropy (Ding & Wang & Yang & Hu (1995), Gao & Zhao & Xu (2008), Gao (2009), Liu & Fan & Guo (2003), Peng & Fan (2002), Akmaz & Akinci (2009)). The computation of FSs for general equations of elastodynamics in 1D, 2D and 3D QCs with arbitrary system of anisotropy has not been achieved so far.

Many technically important materials (media) which become popular in new technologies are anisotropic. For example, the widely used substrate material sapphire and the lithium niobate (LiNbO3), which is used in the design of integrated optics devices, are anisotropic. The medium can be isotropic relative to some physical properties and anisotropic with respect to others. For example, for the study of the light propagation in crystals (the problems of the crystal optics), we can assume that a medium is magnetically isotropic but electrically anisotropic. Materials react to applied electromagnetic fields in a variety of ways. For example, if a point pulse source is located in an optical homogeneous isotropic crystal, then fronts of electric and magnetic waves have spherical shapes. The shapes of the fronts in anisotropic materials are not spherical and have very peculiar forms. The simulation of invisible electromagnetic wave phenomena is a very important issue of modern inter-discipline engineering areas.

Analytic methods of fundamental solutions (Green's function of the free space) constructions have been studied for isotropic and anisotropic materials in Haba (2004),

Li & Liu & Leong & Yeo (2001), Ortner & Wagner (2004), Yakhno (2005). An analytical method for solving IVP for the time-dependent electromagnetic fields in homogenous electrically and magnetically anisotropic media is studied in Yakhno & Yakhno (2007), Yakhno (2008). Most of the electromagnetic wave problems have been solved by numerical methods, in particular finite element method, boundary elements method, finite difference method, nodal method (see, for example, Cohen (2002), Cohen & Heikkola & Joly & Neittaanmaki (2003), Monk (2003)).

To deal with electromagnetic wave propagation different problems and methods of their solving have been applied. For the isotropic materials decomposition method is applied (see, Lindell (1990)). Analytic method of Green's functions constructions have been studied for isotropic and anisotropic materials in Haba (2004), Wijnands & Pendry & Garcia-Vidal & Bell & Roberts & Moreno (1997), Li & Liu & Leong & Yeo (2001), Gottis & Kondylis (1995), Ortner & Wagner (2004), Yakhno (2005), Dmitriev & Silkin & Farzan (2002). To modeling lossy anisotropic dielectric wave-guides in inhomogeneous biaxial anisotropic media the method of lines has been made (see, Berrini & Wu (1996)). An analytical method for solving IVP for the system of crystal optics with polynomial data and a polynomial inhomogeneous term is suggested in Yakhno & Altunkaynak (2008), and also time-dependent electromagnetic fields in homogenous anisotropic media is studied in Yakhno (2008).

When an electrical-conducting elastic body oscillates in an electromagnetic field, variations of the electrical and magnetic fields are observed as a result of this motion. Similar processes are observed when seismic waves propagate in the Earth's crust. Variations of elastic and electromagnetic fields arising in this case are called electromagnetoelastic waves. Such waves contain a certain information about electromagnetic and elastic parameters of the medium. In this case, as a rule, the following types of electromagnetoelastic interactions are distinguished: the interaction based on the electrokinetic properties of a medium, the interaction based on the

piezoelectric properties of a medium, the interaction based on the velocity effect.

The theory of electromagnetoelasticity is concerned with the interacting effects of an externally applied electromagnetic field on the elastic deformations of a solid body. The theory has developed quickly in recent decades because of the possibilities of its extensive practical applications in diverse fields such as geophysics, mechanics of continua, electrodynamics and other relevant areas. In recent years mathematical problems on the propagation of electromagnetoelastic waves have been studied in Priimenko & Vishnevskii (2010), Priimenko & Vishnevskii (2008), Priimenko & Vishnevskii (2005).

Mathematical models of wave propagations in anisotropic elasticity and electromagneticity are described by systems of partial differential equations. Due to their special characteristics, research on the behavior of magneto-electro-elastic structures has been widely carried out. There is a great interest to develop new methods for solving initial value problems and initial boundary value problems for these systems and simulate invisible elastic and electromagnetic waves. Magneto-electro-elastic materials also have important applications in the fields of electric, microwave, supersonics, acoustic, hydrophones, medical ultrasonic imaging, laser, infrared and so on. Unfortunately the exact solutions can not be found for all complex equations and systems. And so using the computer programming the approximate solutions can be found for these problems. Literature dealing with research on the behaviour of magneto-electro-elastic structures has gained more importance recently. Two-dimensional and three-dimensional time-harmonic Green's functions for linear magnetoelectroelastic solids have been derived by means of Radon-transform by Diaz & Saez & Sanchez & Zhang (2008). The dynamic potentials of a quasi-plane magneto-electro-elastic medium of transversely isotropic symmetry with an inclusion of arbitrary shape have been derived and the explicit expressions of the dynamic Greens functions of this medium have been also obtained both in the space-time domain

and in the space-frequency domain by Chen & Shen & Tian (2006). An analytical treatment on the propagation of harmonic waves in an infinitely extended, magneto-electro-elastic (6mm crystal), and multilayered plate have been presented using the method of propagator (or transfer) matrix by Chen & Pan & Chen (2007). Free vibrations of infinite magneto-electro-elastic cylinders for hexagonal crystal have been studied using a finite element formulation by Buchanan (2003).

The functionally graded (FG) material structure has attracted wide and increasing attentions to scientists and engineers. FG materials plays an essential role in most advanced integrated systems for vibration control and health monitoring. Recently, a new class of smart (or intelligent) materials, called functionally graded materials, has been rapidly developed and used in engineering applications for sensing, actuating and controlling purposes due to their direct and converse multi-field effects. The performance of intelligent devices whose responses depend upon the coupled properties of magneto- electroelastic composites is of increasing current interest. Thus, there is considerable motivation in studying defects in these media. Unlike the conventional multilayered devices of which material properties suddenly change at the interfaces between adjacent layers, the material properties of these FG plates and shells are gradually varied through the thickness coordinate. That largely improves the working performance and lifetime of the devices composed of the FG material. Tsai & Wu (2008) have presented the 3D dynamics responses of FG magneto-electro-elastic shells (orthotropic solid) with open-circuit surface conditions using the method of multiple scales. Wu & Lu (2009) have studied the 3D dynamic responses of FG magneto-electro-elastic plates (orthotropic solid) using a modified Pagano method. The dynamic versions for the 3D solutions of the smart structures (orthotropic solid) have been presented by Chen & Chen & Pan & Heyliger (2007) and Pan & Heyliger (2002). Chen & Lee (2003) and Chen & Lee & Ding (2005) have proposed the alternative state space formulation to determine 3D solutions for the static and dynamic

responses of functionally graded transversely isotropic magneto-electro-elastic plates using the method of propagator (or transfer) matrix. A three-dimensional (3D) free vibration analysis of simply supported, doubly curved functionally graded (FG) time dependent magneto-electro-elastic shells (orthotropic solid) with closed-circuit surface conditions has been presented using the method of perturbation by Wu & Tsai (2010). A dynamic solution have been presented for the propagation of harmonic waves in inhomogeneous (FG) magneto-electroelastic hollow cylinders and plates composed of piezoelectric $BaTiO_3$ and magnetostrictive $CoFe_2O_4$ by Yu & Ma & Su (2008), Wu & Yu & He (2008). Based on Legendre orthogonal polynomial series expansion approach, a dynamic solution has been presented for the propagation of circumferential harmonic waves in piezoelectric-piezomagnetic FG cylindrical curved plates by Yu & Wu (2009). Zhong & Yu (2006) have proposed a state space formulation to study 3D free and forced vibration of FG piezoelectric plates (orthotropic solid).

The goal of the thesis is to

- develop methods for the computation of fundamental solutions of differential equations of elastodynamics and electrodynamics for general anisotropic solids, crystals, quasicrystals, dielectrics, electrically and magnetically anisotropic materials;
- obtain the visualization of the pure elastic, phonon elastic, phason elastic, electric and magnetic waves in different crystals, quasicrystals and anisotropic materials;
- create an analytical method of finding a solution of equations of electromagnetoelasticity for a general anisotropic vertically inhomogenous electromagnetoelastic material with given initial data.

The plan of the thesis as follows. In Chapter 2 to find the fundamental solution for the dynamic system of anisotropic elasticity three different methods are presented.

In the first and second method the second order partial differential equations of elastodynamics are written in the form of the first order symmetric hyperbolic system with respect to the displacement velocity and stresses. The first method consists in the following. The Fourier transform image of the fundamental solution with respect to space variables is presented as a power series expansion relative to the Fourier parameters. This presentation is based on the properties of generalized solutions of the initial value problems for symmetric hyperbolic system and Paley-Wiener theorem. Then explicit formulae for the coefficients of this power series are derived successively. The inverse Fourier transform of the obtained Fourier image of the fundamental solution as 3D integration over a bounded domain has been implemented numerically. As a result of this integration we find the fundamental solution in a regularized form. This regularized form of the fundamental solution belongs to the class of classical functions and has finite values for any space and time variables. Let us note that the fundamental solution of the motion equations for indefinite isotropic solids can be given by explicit formulae. We use these formulae for evaluation of our method. Using our method the computer calculation of fundamental solution components (displacement velocity and stresses components arising from pulse point forces) has been made and the simulation of elastic waves has been obtained in general anisotropic media (orthorhombic, monoclinic).

We note here that the approach to reduce the second order system of elastodynamics in frequency domain for isotropic heterogeneous media into a system containing the partial derivatives of the first order has been applied by Manolis & Shaw & Pavlou (1998). The first order system obtained in Manolis & Shaw & Pavlou (1998) is written in a matrix form with non symmetric matrix coefficients.

In the second method we derive a new method for deriving the time-dependent FSs for indefinite linear homogeneous media (solids) with arbitrary anisotropy which is based on its natural mathematical and physical properties. Namely, the FSs of motion

equations for elastic media are generalized functions (distributions) with a compact supports for a fixed time variable. Physically it means that the perturbation from the pulse point force is propagated in a bounded domain of isotropic or anisotropic indefinite solids for a fixed time and therefore there is a quiet in all points outside of this bounded domain. Using the Paley-Wiener theorem (see, for example, Reed & Simon (1975)) we obtain that the Fourier transform of the FS with respect to space variables is an analytic function depending on wave-vector variables (Fourier parameters). Hence the expression of the FSs presented in terms of wave-vector variables does not contain singularities and this expression is integrable over an arbitrary 3D bounded domain of wave-vector variables. The inverse Fourier transform of this expression as 3D integration over a bounded domain can be implemented numerically. As a result of this integration we find the FS in a regularized form. This regularized FS belongs to the class of classical functions and has finite values for any space and time variables. Let us note that the FS of the motion equations for indefinite isotropic (transversely isotropic) solids can be given by explicit formula in terms of wave-vector variables as well as space variables. We use these formulae for testing our method. The first part of the numerical experiments of the present paper has shown that values of the FS in terms of wave-vector variables found by the suggested method and values of the FS obtained by the explicit formula for the isotropic (transversely isotropic) indefinite solids are almost the same (the accuracy in these experiments is less or equal to 10^{-10}). Moreover, we have shown that values of the FSs found by the suggested method can be efficiently used for the computation of the integrals when the integrand contains the FSs as terms. By computational experiments we have obtained very close values of integrals when we use either values of the FS found by the suggested method or values of the explicit formula in the case of isotropic or transversely isotropic infinite solids. The suggested method consists of the several steps: equations for each column of the fundamental matrix (FS) are reduced to a symmetric hyperbolic system; the Fourier transform with respect to the space variables is applied to this symmetric hyperbolic

system; as a result of it we obtain a system of the ordinary differential equations with respect to the time variable whose coefficients depend on the Fourier parameters; using the matrix transformation an explicit formula for a solution of the obtained system is computed; as a result of these computations we obtain explicit formulae for Fourier images of the fundamental matrix columns; finally, the FS is computed by the inverse Fourier transform to the obtained Fourier image of fundamental matrix. Using the suggested method the following new computational aspects of FSs for anisotropic solids have been obtained: the values of FSs have been computed in homogeneous solids with trigonal (aluminum oxide), monoclinic (diopside) and triclinic (albite) structures of anisotropy; the simulation of the wave propagation in these solids has been made. Computational examples confirm the robustness of the suggested approach for the computation of FS of elastodynamics in general homogeneous anisotropic media. As an application of the FSs an explicit formula for the displacement components of general homogeneous anisotropic media arising from an arbitrary force is obtained.

In the third method a new approach for finding the displacement in unbounded general anisotropic media is suggested. This approach consists of the following. The equations of elastodynamics are written in terms of displacement. These equations form a system of the partial differential equations of the second order. Applying the Fourier transform with respect to space variables to these equations we obtain a system of second order ordinary differential equations whose coefficients depend on Fourier parameters. Using the matrix transformations and properties of coefficients the Fourier image of the fundamental solution is computed. Finally, the fundamental solution is computed by the inverse Fourier transform to obtained Fourier image. The implementation and justification of the suggested method have been made by computational experiments in MATLAB. Computational experiments confirm the robustness of the suggested method. The visualization of the displacement components in general homogeneous anisotropic solids by modern computer tools allows us to see

and evaluate the dependence between the structure of solids and the behavior of the displacement field. Our method allows users to observe the elastic wave propagation arising from pulse point forces of the form $\mathbf{e}^m\delta(x)\delta(t)$ in monoclinic, triclinic and other anisotropic solids. The visualization of displacement components gives knowledge about the form of fronts of elastic wave propagation in Sodium Thiosulfate with monoclinic and Copper Sulphate Pentahydrate with triclinic structures of anisotropy.

Chapter 3 consist of three sections. In these sections the dynamic three dimensional motion equations of 1D, 2D and 3D QCs are considered, respectively. We studied a method for the derivation of the time-dependent fundamental solution (Green's function) with three space variables in QCs with arbitrary system of anisotropy. This method consists of the following. The dynamic equations of the motion for QCs are written in terms of the Fourier transform with respect to space variables as a vector ordinary differential equation with matrix coefficients depending on the Fourier parameters. Applying the matrix transformations and properties of matrix coefficients a solution of the vector ordinary differential equation is computed. Finally, the fundamental solution is computed by the inverse Fourier transform. Computational examples confirm the robustness of the suggested method for computation of FS in 1D, 2D and 3D QCs with arbitrary type of anisotropy. Computational images of phonon and phason displacements for anisotropic 1D QCs with triclinic, monoclinic, orthorhombic, tetragonal, trigonal structures are given at the end of the first section. Computational images of phonon and phason displacements for anisotropic 2D QCs with dodecagonal, octagonal, decagonal, pentagonal, hexagonal, triclinic structures are given at the end of the second section. And in the third section simulations of the fundamental solution of the icosahedral QCs are given. It is shown that the constructed fundamental solution of elasticity for QCs can be efficiently used for computation of the initial value problem for the considered dynamic differential equations of elasticity for QCs with arbitrary given external force and initial data.

In chapter 4 a homogeneous non-dispersive electrically and magnetically anisotropic media, characterized by a symmetric positive definite permittivity and permeability tensors are considered. An analytic method for deriving the time-dependent fundamental solution (Green's function of the free space) in these anisotropic media is studied. This method consists of the following: equations for each column of the fundamental solution are reduced to a symmetric hyperbolic system; using the Fourier transform with respect to the space variables and matrix transformations we obtain formulae for Fourier images of the fundamental solution columns, finally, the fundamental solution is computed by the inverse Fourier transform. Computational examples confirm the robustness of the suggested method.

In chapter 5 IVP for the system of linear, inhomogenous, anisotropic dynamics of electromagnetoelasticity (EME) is considered. An analytic method of solving IVP for EME is given. First of all IVP is rewritten in terms of the Fourier images with respect to the space lateral variables. We denote this problem as FIVP. After that the obtained FIVP is transformed into an equivalent second kind vector integral equation of the Volterra type. Applying the successive approximations method to this integral equation we have constructed its solution. At last using the equivalence of this vector integral equation to FIVP and the real Paley-Wiener theorem we found a solution of IVP for the system of linear, inhomogenous, anisotropic dynamics of electromagnetoelasticity.

CHAPTER TWO
MODELLING AND SIMULATION OF ELASTIC WAVES IN CRYSTALS

In this chapter of the thesis fundamental solution of anisotropic elastodynamics is calculated using three different methods.

2.1 Equations of anisotropic elastodynamics as a symmetric hyperbolic system: deriving the time-dependent fundamental solution

2.1.1 Equations of anisotropic elastodynamics

A body which is acted on by external forces is said to be in a state of stress. If we consider a volume element situated within a stressed body there are forces exerted on the surface of the element by the material surrounding it. These forces are proportional to the area of the surface of the element, and the force per unit area is called the stress (Nye (1957)).

Strain is the geometrical expression of deformation caused by the action of stress on a physical body. Strain is calculated by first assuming a change between two body states: the beginning state and the final state. Then the difference in placement of two points in this body in those two states expresses the numerical value of strain. Strain therefore expresses itself as a change in size or shape. If strain is equal over all parts of a body, it is referred to as homogeneous strain; otherwise, it is inhomogeneous strain. In its most general form, the strain is a symmetric tensor. Hooke's law of elasticity is an approximation that states that the amount by which a material body is deformed (the strain) is linearly related to the force causing the deformation (the stress).

Here, the stress is denoted by the components τ_{jk} of τ. The resistance of the material is called strain tensor is denoted by ε. The stress-strain law can be written as

$$\tau_{ij} = c_{ijkl}\varepsilon_{kl} \tag{2.1}$$

Here, c_{ijkl} are the components of fourth rank tensor $\mathbf{C}$ which denotes the elastic moduli and determines the properties of the material. And it must satisfy the following symmetry property

$$c_{ijkl} = c_{jikl}, \quad c_{ijkl} = c_{jilk}, \quad c_{ijkl} = c_{klij} \tag{2.2}$$

To show the second condition of symmetry property in (2.2), we use the first and the third conditions, i.e

$$c_{ijkl} = c_{klij} = c_{lkij} = c_{ijlk}$$

The first condition of the symmetry property in (2.2), follows from the symmetry property of the stress

$$\tau_{ij} = \tau_{ji}, \quad \text{for } i,j = 1,2,3. \tag{2.3}$$

To show the third condition of the symmetry property in (2.2), it is not enough to use the symmetry property of strain tensor

$$\varepsilon_{ij} = \varepsilon_{ji}, \quad \text{for } i,j = 1,2,3. \tag{2.4}$$

By using the symmetry property of the strain in (2.4), we can write

$$\tau_{ij} = \frac{1}{2}c_{ijkl}\varepsilon_{kl} + \frac{1}{2}c_{ijkl}\varepsilon_{kl} = \frac{1}{2}c_{ijkl}\varepsilon_{kl} + \frac{1}{2}c_{ijlk}\varepsilon_{lk} = \frac{1}{2}(c_{ijkl} + c_{ijlk})\varepsilon_{kl}$$

The strain energy W of per unit volume of the material is

$$W = \int_0^{\varepsilon_{pq}} \tau_{ij}\, d\varepsilon_{ij} = \int_0^{\varepsilon_{pq}} c_{ijkl}\varepsilon_{kl}\, d\varepsilon_{ij} \tag{2.5}$$

This integral is independent of the path taken by ε_{ij}. Otherwise, we extract amount of the energy which is impossible for a real material. The integral depends only the final strain ε_{pq}. Then this implies that it is the total differential of dW,i.e

$$c_{ijkl}\varepsilon_{kl}d\varepsilon_{ij} = dW = \frac{\partial W}{\partial \varepsilon_{ij}}d\varepsilon_{ij}$$

Then for arbitrary $d\varepsilon_{ij,}$

$$\tau_{ij} = c_{ijkl}\varepsilon_{kl} = \frac{\partial W}{\partial \varepsilon_{ij}} \tag{2.6}$$

The differentiation of the above equality follows that

$$c_{ijkl} = \frac{\partial W^2}{\partial \varepsilon_{kl}\partial \varepsilon_{ij}}$$

The double differentiation is interchangeable so

$$c_{ijkl} = c_{klij} \quad \text{for } i,j,k,l = 1,2,3.$$

So we have the full symmetry property,

$$c_{ijkl} = c_{klij} = c_{lkij} = c_{ijlk} \tag{2.7}$$

Additionally, the equation (2.6) follows that

$$W = \frac{1}{2}c_{ijkl}\varepsilon_{ij}\varepsilon_{kl}$$

Since the strain energy must be positive then

$$c_{ijkl}\varepsilon_{ij}\varepsilon_{kl} > 0, \qquad \text{for } i,j,k,l = 1,2,3.$$

so, the quadratic form,

$$\sum_{i,j,k,l=1}^{3} c_{ijkl}\varepsilon_{ij}\varepsilon_{kl} > 0, \quad \varepsilon_{ij} \neq 0,\ \varepsilon_{kl} \neq 0. \tag{2.8}$$

These notations and definitions can be found in Ting (1996).

The transformation between the subscripts $ijkl$ and $\alpha\beta$ is accomplished by replacing the subscripts ij(or kl) with the subscript α(or β) using the following rules:

$$\alpha = \begin{cases} i, & \text{if } i = j; \\ 9 - i - j, & \text{if } i \neq j. \end{cases} \qquad \beta = \begin{cases} k, & \text{if } k = l; \\ 9 - k - l, & \text{if } k \neq l. \end{cases} \tag{2.9}$$

So, the subscripts are taken as

$$\begin{aligned} ij \text{ or } kl \quad &\rightarrow \quad \alpha(\text{ or } \beta) \\ 11 \quad &\rightarrow \quad 1 \\ 22 \quad &\rightarrow \quad 2 \\ 33 \quad &\rightarrow \quad 3 \\ 23 \text{ or } 32 \quad &\rightarrow \quad 4 \\ 31 \text{ or } 13 \quad &\rightarrow \quad 5 \\ 21 \text{ or } 12 \quad &\rightarrow \quad 6. \end{aligned} \tag{2.10}$$

So the matrix

$$\mathbf{C} = (c_{\alpha\beta})_{6\times 6}, \tag{2.11}$$

of all moduli is symmetric. The stress-strain law in (2.1) can be written as

$$\tau_\alpha = c_{\alpha\beta}\varepsilon_\beta, \quad c_{\alpha\beta} = c_{\beta\alpha}. \tag{2.12}$$

The quadratic form in (2.8) can be written

$$\sum_{\alpha,\beta=1}^{6} c_{\alpha\beta}\varepsilon_\alpha\varepsilon_\beta > 0, \quad \varepsilon_\alpha \neq 0,\ \varepsilon_\beta \neq 0 \tag{2.13}$$

and implies the positive-definiteness of the 6×6 matrix $\mathbf{C}$.

Let $x=(x_1,x_2,x_3)\in R^3$. We assume that R^3 is an elastic medium, whose small vibrations

$$\mathbf{u}(x,t)=(u_1(x,t),u_2(x,t),u_3(x,t))$$

are governed by the system of partial differential equations

$$\rho\frac{\partial^2 u_i}{\partial t^2}=\sum_{j=1}^{3}\frac{\partial \tau_{ij}}{\partial x_j}+f_i,\ x=(x_1,x_2,x_3)\in R^3,\ t\in R,\ i=1,2,3, \tag{2.14}$$

where $\rho>0$ is the density of the medium; $\mathbf{f}=(f_1,f_2,f_3)$ is an external force, $f_i=f_i(x,t), i=1,2,3$; $f_i(x,t)$ is a given function.

Stresses $\tau_{ij}=\tau_{ij}(x,t)$ are defined as

$$\tau_{ij}=\sum_{k,l=1}^{3} c_{ijkl}\frac{\partial u_k}{\partial x_l},\ i,j=1,2,3, \tag{2.15}$$

where $\{c_{ijkl}\}_{i,j,k,l=1}^{3}$ are the elastic moduli of the medium.

2.1.2 Reduction of (2.14) to a symmetric hyperbolic system

Using the symmetry properties of the elastic moduli and the rule (2.10) the relation (2.15) can be written as

$$\begin{aligned}\tau_\alpha &= c_{\alpha 1}\frac{\partial u_1}{\partial x_1}+c_{\alpha 6}\frac{\partial u_1}{\partial x_2}+c_{\alpha 5}\frac{\partial u_1}{\partial x_3}+c_{\alpha 6}\frac{\partial u_2}{\partial x_1}+c_{\alpha 2}\frac{\partial u_2}{\partial x_2}\\ &+ c_{\alpha 4}\frac{\partial u_2}{\partial x_3}+c_{\alpha 5}\frac{\partial u_3}{\partial x_1}+c_{\alpha 4}\frac{\partial u_3}{\partial x_2}+c_{\alpha 3}\frac{\partial u_3}{\partial x_3},\ \alpha = 1,2,...,6. \end{aligned} \tag{2.16}$$

Here $\tau = (\tau_1,\tau_2,\tau_3,\tau_4,\tau_5,\tau_6)$. Let

$$U_i = \frac{\partial u_i}{\partial t},\ i = 1,2,3, \tag{2.17}$$

$$\mathbf{Y} = (\frac{\partial U_1}{\partial x_1},\frac{\partial U_2}{\partial x_2},\frac{\partial U_3}{\partial x_3},(\frac{\partial U_3}{\partial x_2}+\frac{\partial U_2}{\partial x_3}),(\frac{\partial U_3}{\partial x_1}+\frac{\partial U_1}{\partial x_3}),(\frac{\partial U_2}{\partial x_1}+\frac{\partial U_1}{\partial x_2})),$$

$$\mathbf{U} = (U_1,U_2,U_3). \tag{2.18}$$

Differentiating (2.16) with respect to t and using vectors τ and $\mathbf{Y}$ we have

$$\frac{\partial \tau}{\partial t} = \mathbf{C}\mathbf{Y}, \tag{2.19}$$

where $\mathbf{C}$ is defined by (2.11). Multiplying (2.19) by the inverse of $\mathbf{C}$, denoted $\mathbf{C}^{-1}$, we find

$$\mathbf{C}^{-1}\frac{\partial \tau}{\partial t} - \mathbf{Y} = 0. \tag{2.20}$$

Equation (2.20) can be written in the form

$$\mathbf{C}^{-1}\frac{\partial \tau}{\partial t}+\sum_{j=1}^{3}(\mathbf{A}_j^1)^*\frac{\partial \mathbf{U}}{\partial x_j}=0, \tag{2.21}$$

where $*$ is the transposition of sign,

$$\mathbf{A}_1^1=\begin{bmatrix} -1 & 0 & 0 & 0 & 0 & 0 \\ 0 & 0 & 0 & 0 & 0 & -1 \\ 0 & 0 & 0 & 0 & -1 & 0 \end{bmatrix},\ \mathbf{A}_2^1=\begin{bmatrix} 0 & 0 & 0 & 0 & 0 & -1 \\ 0 & -1 & 0 & 0 & 0 & 0 \\ 0 & 0 & 0 & -1 & 0 & 0 \end{bmatrix},$$

$$\mathbf{A}_3^1=\begin{bmatrix} 0 & 0 & 0 & 0 & -1 & 0 \\ 0 & 0 & 0 & -1 & 0 & 0 \\ 0 & 0 & -1 & 0 & 0 & 0 \end{bmatrix}. \tag{2.22}$$

Using the notation mentioned above the left-hand side of (2.14) can be written as

$$\rho\frac{\partial^2 u}{\partial t^2}=\rho\frac{\partial \mathbf{U}}{\partial t}. \tag{2.23}$$

Now let us consider the term $\sum\limits_{j=1}^{3}\frac{\partial \tau_{ij}}{\partial x_j}$ in the right-hand side of (2.14). Taking into account the symmetry properties of the elastic moduli and the rule (2.10) we have

$$\sum_{j=1}^{3}\frac{\partial \tau_{1j}}{\partial x_j}=\frac{\partial \tau_1}{\partial x_1}+\frac{\partial \tau_6}{\partial x_2}+\frac{\partial \tau_5}{\partial x_3},$$

$$\sum_{j=1}^{3}\frac{\partial \tau_{2j}}{\partial x_j}=\frac{\partial \tau_6}{\partial x_1}+\frac{\partial \tau_2}{\partial x_2}+\frac{\partial \tau_4}{\partial x_3},$$

$$\sum_{j=1}^{3}\frac{\partial \tau_{3j}}{\partial x_j}=\frac{\partial \tau_5}{\partial x_1}+\frac{\partial \tau_4}{\partial x_2}+\frac{\partial \tau_3}{\partial x_3}.$$

Using these equations and (2.23) equations (2.14) can be written as

$$\rho\frac{\partial \mathbf{U}}{\partial t}+\sum_{j=1}^{3}(\mathbf{A}_j^1)\frac{\partial \tau}{\partial x_j}=\mathbf{f}. \tag{2.24}$$

The relations (2.21) and (2.24) can be presented by a single system as (Yakhno & Akmaz (2005))

$$\mathbf{A}_0\frac{\partial \mathbf{V}}{\partial t}+\sum_{j=1}^{3}\mathbf{A}_j\frac{\partial \mathbf{V}}{\partial x_j}=\mathbf{F},\ x\in R^3,\ t\in R, \tag{2.25}$$

where $\mathbf{F}=(\mathbf{f},0_{6,1})$,

$$\mathbf{V}=(U_1,U_2,U_3,\tau_1,\tau_2,\tau_3,\tau_4,\tau_5,\tau_6),$$

$$\mathbf{A}_0=\begin{bmatrix}\rho\mathbf{I}_{3,3} & 0_{3,6}\\ 0_{6,3} & \mathbf{C}^{-1}\end{bmatrix},\mathbf{A}_j=\begin{bmatrix}0_{3,3} & \mathbf{A}_j^1\\ (\mathbf{A}_j^1)^* & 0_{6,6}\end{bmatrix}. \tag{2.26}$$

Here $\mathbf{I}_{m,m}$ is the unit matrix of the order $m\times m$ and $0_{l,m}$ is the zero matrix of the order $l\times m$, matrices $\mathbf{A}_j^1,\ j=1,2,3$, are defined by (2.22).

We note that the matrix $\mathbf{A}_0$ is symmetric positive definite and matrices $\mathbf{A}_j^1,\ j=1,2,3$ are symmetric. Therefore the system (2.25) is a symmetric hyperbolic system (see, for example, Lax (2006), Courant & Hilbert (1962)). In this section we call (2.25) as the symmetric hyperbolic system of elasticity (SHSE) and the second order system (2.14) as the anisotropic elastic system (AES).

2.1.3 Some properties of fundamental solution for the system of anisotropic elasticity

Let us consider (2.14) and (2.15) with initial conditions

$$\mathbf{u}(x,0)=\psi(x),\ \frac{\partial \mathbf{u}}{\partial t}(x,0)=\varphi(x),\ x\in R^3, t\in R. \tag{2.27}$$

Here $\psi(x)=(\psi_1(x),\psi_2(x),\psi_3(x))$ and $\varphi(x)=(\varphi_1(x),\varphi_2(x),\varphi_3(x))$. Using equalities

$$U_i(x,0)=\varphi_i(x),\ \tau_{ij}\mid_{t=0}=\sum_{k,l=1}^{3} c_{ijkl}\frac{\partial \psi_k}{\partial x_l},\ i,j=1,2,3.$$

Initial conditions (2.27) can be written in the vector form

$$\mathbf{V}(x,0)=\mathbf{V}_0(x),\ x\in R^3. \tag{2.28}$$

Lemma 2.1. *System (2.25) can be transformed into the following form (see, similar reasoning in Yakhno & Akmaz (2005))*

$$I_9\frac{\partial \widetilde{V}}{\partial t}\ +\ \sum_{j=1}^{3}\widetilde{A}_j\frac{\partial \widetilde{V}}{\partial x_j}=\widetilde{F}(x,t),\ x\in R^3, t\in R, \tag{2.29}$$

which is a symmetric hyperbolic system.

Proof. For the symmetric positive definite matrix $\mathbf{C}$ there exists a symmetric positive definite matrix $\mathbf{M}$ such that $\mathbf{C}^{-1}=\mathbf{M}^2$ (Goldberg (1992)) and the matrix $\mathbf{M}^{-1}$, which is inverse of $\mathbf{M}$, is symmetric (see Appendix). Let

$$\mathbf{S}=\begin{bmatrix} \rho^{-\frac{1}{2}}\mathbf{I}_{3,3} & 0_{3,6} \\ 0_{6,3} & \mathbf{M}^{-1} \end{bmatrix}.$$

Applying the transformation $\mathbf{V}(x,t)=\mathbf{S}\widetilde{\mathbf{V}}(x,t)$ into (2.25) and multiplying it by the

matrix $\mathbf{S}$ from the left hand side we find (2.29). Here

$$\widetilde{\mathbf{A}}_j = \mathbf{S}\mathbf{A}_j\mathbf{S},\ \widetilde{\mathbf{F}} = \mathbf{S}\mathbf{F}. \tag{2.30}$$

We note that $\widetilde{\mathbf{A}}_j,\ j = 1,2,3$, are still symmetric, which implies that (2.29) is symmetric hyperbolic system. □

Initial conditions (2.28) can be written as

$$\widetilde{\mathbf{V}}(x,0) = \mathbf{S}^{-1}\mathbf{V}_0(x) = \widetilde{\mathbf{V}}_0(x) \tag{2.31}$$

Theorem 2.2. *Let T be a fixed positive number, $\psi(x)$; $\varphi(x)$ and $\mathbf{f}(x,t)$ be given functions such that $\psi(x) \in H^2(R^3)$; $\varphi(x) \in H^1(R^3)$ and $\mathbf{f}(x,t) \in C([0,T];H^1(R^3))$. Then there exists a unique solution of Cauchy problem (2.29),(2.31) (see, similar reasoning in Yakhno & Akmaz (2005))*

$$\widetilde{\boldsymbol{V}}(x,t) \in C^1([0,T];L^2(R^3)) \cap C([0,T];H^1(R^3)).$$

Proof. Using existence theorem for symmetric hyperbolic system of the first order (Mizohata (1973), see Appendix) it can be shown that there exists a unique solution of (2.29),(2.31) in the class $C^1([0,T];L^2(R^3)) \cap C([0,T];H^1(R^3))$. □

Theorem 2.3. *Let T be a fixed positive number, $\psi(x)$; $\varphi(x)$ and $\mathbf{f}(x,t)$ be given functions such that $\psi(x) \in C_0^\infty(R^3)$; $\varphi(x) \in C_0^\infty(R^3)$ and $\mathbf{f}(x,t) \in C([0,T];C_0^\infty(R^3))$. Then the solution $\widetilde{\boldsymbol{V}}(x,t)$ of Cauchy problem (2.29), (2.31) belongs to*

$$C^1([0,T];C_0^\infty(R^3)).$$

Proof. Using Theorem 2.2 it can be found that if $D^\alpha\psi(x) \in H^4(R^3)$; $D^\alpha\varphi(x) \in H^3(R^3)$ and $D^\alpha\mathbf{f}(x,t) \in C([0,T];H^3(R^3))$ where T is a fixed positive number, $\alpha = (\alpha_1,\alpha_2,\alpha_3)$

is an arbitrary multi-index, $|\alpha| = \alpha_1 + \alpha_2 + \alpha_3$, α_i; $i = 1,2,3$ are nonnegative integers, $D^\alpha = \frac{\partial^{|\alpha|}}{\partial x_1^{\alpha_1} \partial x_2^{\alpha_2} \partial x_3^{\alpha_3}}$. Then $D^\alpha \widetilde{\mathbf{V}}(x,t)$ belongs to the class (see, similar reasoning in Yakhno & Akmaz (2005))

$$D^\alpha \widetilde{\mathbf{V}}(x,t) \in C^1([0,T];H^2(R^3)) \cap C([0,T];H^3(R^3)).$$

Using this fact and applying Sobolev's lemma (see Appendix) it can be proved that

$$\widetilde{\mathbf{V}}(x,t) \in C^1([0,T];C^\infty(R^3)).$$

Now we need to prove that the function $\widetilde{\mathbf{V}}(x,t)$ has a compact support. Let us consider symmetric hyperbolic system of the first order (2.29) where all matrices $\widetilde{\mathbf{A}}_k$ are real symmetric matrices with constant elements. Let T be a fixed positive number, $\xi = (\xi_1, \xi_2, \xi_3) \in R^3$ be a parameter; $A(\xi)$ be a matrix defined by $A(\xi) = \sum_{k=1}^3 \widetilde{\mathbf{A}}_k \xi_k$; $\lambda_i(\xi)$, $i = 1,2,...,9$ be eigenvalues of $A(\xi)$. The positive number M is defined by

$$M = \max_{n=1,2,...,9} \max_{|\xi|=1} |\lambda_i(\xi)|. \tag{2.32}$$

We claim that M is the upper bound on the speed of waves in any direction.

Using T and M we define the following domains

$$S(x_0,h) = \{x \in R^3 : |x - x_0| \le M(T-h),\ 0 \le h \le T\}$$
$$\Gamma(x_0,T) = \{(x,t) : 0 \le t \le T,\ |x - x_0| \le M(T-t)\}$$
$$R(x_0,h) = \{(x,t) : 0 \le t \le h,\ |x - x_0| = M(T-t)\}$$

Here $\Gamma(x_0,T)$ is the conoid with vertex (x_0,T); $S(x_0,h)$ is the surface constructed by the intersection of the plane $t = h$ and the conoid $\Gamma(x_0,T)$; $R(x_0,h)$ is the lateral surface of the conoid $\Gamma(x_0,T)$ bounded by $S(x_0,0)$ and $S(x_0,h)$. Let Ω be the region in $R^3 \times (0,\infty)$

bounded by $S(x_0,0)$, $S(x_0,h)$ and $R(x_0,h)$ with boundary $\partial\Omega = S(x_0,0) \cup S(x_0,h) \cup R(x_0,h)$.

Applying the energy inequality (Courant & Hilbert (1962), see Appendix) we find the following estimate for the solution of (2.29), (2.31)

$$\int_{S(h)} |\widetilde{\mathbf{V}}(x,h)|^2 dx \le e^h \Big[\int_{S(0)} |\widetilde{\mathbf{V}}_0(x)|^2 dx + \int_0^h \Big(\int_{S(t)} |\widetilde{\mathbf{F}}(x,t)|^2 dx \Big) dt \Big]. \qquad (2.33)$$

Let us define $P(K) = \{x \in R^3 : |x| \le K\}$. Since $\psi(x) \in C_0^\infty(R^3)$; $\varphi(x) \in C_0^\infty(R^3)$ and $\mathbf{f}(x,t) \in C([0,T]; C_0^\infty(R^3))$ then there exits $K > 0$ such that $supp\ \psi \subseteq P(K)$, $supp\ \varphi \subseteq P(K)$ and $\mathbf{f}(x,t)$ as a function of the variable x, has a finite support which is located in $P(K)$ for any fixed t from $[0,T]$.

Also let us denote

$$D(T,K) = \{(x,t) : 0 \le t \le T,\ \Gamma(x,t) \cap P(K) = \emptyset\}.$$

If $(x,t) \in D(T,K)$ then $\widetilde{\mathbf{V}}(x,t) = 0$. This means $\widetilde{\mathbf{V}}(x,t) = 0$ for any $t \in [0,T]$ and $|x| > MT + K$.

Hence, $supp\ \widetilde{\mathbf{V}} \subseteq P(MT+K)$. As a result $\widetilde{\mathbf{V}}(x,t)$ belongs to the class

$$\widetilde{\mathbf{V}}(x,t) \in C^1([0,T]; C_0^\infty(R^3)).$$

□

Theorem 2.4. *Let $\widetilde{W^m}$ be a fundamental solution of*

$$\begin{aligned} \mathbf{I}_{9,9} \frac{\partial \widetilde{W^m}}{\partial t} &+ \sum_{j=1}^{3} \widetilde{A}_j \frac{\partial \widetilde{W^m}}{\partial x_j} = E^m \delta(x)\delta(t),\ x \in R^3, t \in R, \qquad (2.34) \\ \widetilde{W^m}(x,t)|_{t<0} &= 0. \end{aligned}$$

And $\mathbf{W}^m(x,t)$ *be a solution of the following IVP*

$$\begin{aligned} \mathbf{I}_{9,9}\frac{\partial \boldsymbol{W}^m}{\partial t} &+ \sum_{j=1}^{3} \widetilde{\boldsymbol{A}}_j \frac{\partial \boldsymbol{W}^m}{\partial x_j} = 0,\ x \in R^3, t \in R, \\ \boldsymbol{W}^m(x,0) &= \mathsf{E}^m \delta(x). \end{aligned} \tag{2.35}$$

Then $\widetilde{\boldsymbol{W}^m}(x,t) = \theta(t)\boldsymbol{W}^m$. *Here* $m = 1,2,3$; $\mathsf{E}^1 = (1,0,0,0,0,0,0,0,0)^*$, $\mathsf{E}^2 = (0,1,0,0,0,0,0,0,0)^*$, $\mathsf{E}^3 = (0,0,1,0,0,0,0,0,0)^*$; $\delta(t)$ *is the Dirac delta function with support at* $t = 0$; $\delta(x)$ *is the Dirac delta function with respect to space variables, i.e.* $\delta(x) = \delta(x_1)\delta(x_2)\delta(x_3)$; *matrices* $\widetilde{\boldsymbol{A}}_j$, $j = 1,2,3$, *are defined by (2.30).*

Proof. Since $\widetilde{\mathbf{W}^m}(x,t) = \theta(t)\mathbf{W}^m(x,t)$, derivative of $\widetilde{\mathbf{W}^m}$ with respect to t is

$$\frac{\partial \widetilde{\mathbf{W}^m}}{\partial t} = \delta(t)\mathbf{W}^m(x,0) + \theta(t)\frac{\partial \mathbf{W}^m}{\partial t}$$

and

$$\begin{aligned} \mathbf{I}_{9,9}\frac{\partial \widetilde{\mathbf{W}^m}}{\partial t} + \sum_{j=1}^{3} \widetilde{\mathbf{A}}_j \frac{\partial \widetilde{\mathbf{W}^m}}{\partial x_j} &= \mathsf{E}^m \delta(x)\delta(t) + \theta(t)(\mathbf{I}_{9,9}\frac{\partial \mathbf{W}^m}{\partial t} + \sum_{j=1}^{3} \widetilde{\mathbf{A}}_j \frac{\partial \mathbf{W}^m}{\partial x_j}) \\ &= \mathsf{E}^m \delta(x)\delta(t). \end{aligned}$$

□

It is well known that Hormander-Lojasiewicz theorem (Vladimirov (1979), see Appendix) the arbitrary differential equation and system with constant coefficients has a fundamental solution of slow growth. Thus, system with constant coefficients given with equations (2.35) has a fundamental solution

$$\mathbf{W}^m(x,t) \in C^1([0,T];\mathbb{S}'(R^3)).$$

Our aim is to study some of the properties of this fundamental solution and suggest a method to find fundamental solutions.

Let us denote convolution of functions $\mathbf{W}^m(x,t)$ with cap-shaped function $w_\varepsilon(x)$ by $\mathbf{W}^m_\varepsilon(x,t)$. Taking convolution with cap-shaped function, the problem (2.35) can be written as

$$\begin{aligned} \mathbf{I}_{9,9}\frac{\partial \mathbf{W}^m_\varepsilon}{\partial t} &+ \sum_{j=1}^{3} \widetilde{\mathbf{A}}_j \frac{\partial \mathbf{W}^m_\varepsilon}{\partial x_j} = 0,\ x \in R^3, t \in R, \\ \mathbf{W}^m_\varepsilon(x,0) &= \mathsf{E}^m w_\varepsilon(x). \end{aligned} \tag{2.36}$$

Using Theorem 2.3, it can be proved that problem (2.36) has a unique solution $\mathbf{W}^m_\varepsilon(x,t) \in C^1([0,T];C_0^\infty(R^3))$ where $supp\ \mathbf{W}^m_\varepsilon(x,t) \subseteq P(MT+\varepsilon_0)\ \forall \varepsilon \in (0,\varepsilon_0)$.

Property 1. As $\varepsilon \to +0$, $\mathbf{W}^m_\varepsilon(x,t)$ approaches to $\mathbf{W}^m(x,t)$ in $\mathbb{S}'(R^3)$; $\forall t \in [0,T]$.

Proof of property 1. It can be proved that as $\varepsilon \to +0$, $w_\varepsilon(x)$ approaches to $\delta(x)$ in $\mathbb{S}'(R^3)$. Using this fact and using the continuity of the convolution, property is proved.

Property 2. Let T be a fixed positive number. There exists a solution of Cauchy problem (2.35)

$$\mathbf{W}^m(x,t) \in C^1([0,T];\mathcal{E}'(R^3)).$$

Proof of property 2. We need to show that

$$(\mathbf{W}^m,\varphi) = 0;\ \forall \varphi \in \mathbb{S} \ \text{ and } supp\ \varphi \subseteq R^3 \setminus P(MT+\varepsilon_0).$$

From property 1, we know that

$$\begin{aligned} (\mathbf{W}^m,\varphi) &= \lim_{\varepsilon \to +0} (\mathbf{W}^m_\varepsilon,\varphi);\ \forall \varphi \in \mathbb{S} \\ &= 0. \end{aligned}$$

This means $supp\ \mathbf{W}^m \subseteq P(MT+\varepsilon_0)\ \forall \varepsilon \in (0,\varepsilon_0)$. So we prove that $\mathbf{W}^m(x,t)$ is a

tempered distribution with compact support, solution of the Cauchy problem (2.35) belongs to the following space

$$\mathbf{W}^m(x,t) \in C^1([0,T];\mathcal{E}'(R^3)).$$

Property 3. Since $\mathbf{W}^m(x,t) \in C^1([0,T];\mathcal{E}'(R^3))$, according to Paley-Wiener theorem (Reed & Simon (1975), see Appendix), Fourier transform of the function $\mathbf{W}^m(x,t)$ is an entire analytic function with respect to $\nu = (\nu_1,\nu_2,\nu_3) \in R^3$, and can be written as a power series

$$\hat{\mathbf{W}}^m(\nu,t) = \sum_{n=0}^{\infty}\sum_{p=0}^{\infty}\sum_{k=0}^{\infty}(\mathbf{W}^m)^{n+1,p+1,k+1}(t)\nu_1^n\nu_2^p\nu_3^k. \tag{2.37}$$

2.1.4 Fundamental solutions of SHSE and AES

The fundamental solution of SHSE (2.25) is defined as a matrix $\mathbf{G}(x,t)$ of the order 9×3 whose columns $\mathbf{V}^m(x,t) = (V_1^m(x,t),...,V_9^m(x,t))$ satisfy

$$\mathbf{A}_0\frac{\partial \mathbf{V}^m}{\partial t} + \sum_{j=1}^{3}\mathbf{A}_j\frac{\partial \mathbf{V}^m}{\partial x_j} = \mathsf{E}^m\delta(x)\delta(t),\ x\in R^3,\ t\in R, \tag{2.38}$$

$$\mathbf{V}^m(x,t)\mid_{t<0} = 0, \tag{2.39}$$

where $m = 1,2,3$; $\mathsf{E}^1 = (1,0,0,0,0,0,0,0,0)^*$, $\mathsf{E}^2 = (0,1,0,0,0,0,0,0,0)^*$, $\mathsf{E}^3 = (0,0,1,0,0,0,0,0,0)^*$; $\delta(t)$ is the Dirac delta function with support at $t=0$; $\delta(x)$ is the Dirac delta function with respect to space variables, i.e. $\delta(x) = \delta(x_1)\delta(x_2)\delta(x_3)$; matrices $\mathbf{A}_0,\ \mathbf{A}_j,\ j=1,2,3$, are defined by (2.22), (2.26).

Remark 1. The fundamental solution of the system of the form (2.25) with a vector function $\mathbf{F}(x,t)$, whose nine components are arbitrary functions for $t \geq 0$ and equal

to zero for $t < 0$, can be defined as a matrix $\mathcal{G}(x,t)$ of the order 9×9 for which the formula

$$\mathbf{V}(x,t) = \int_{-\infty}^{\infty}\int_{-\infty}^{\infty}\int_{-\infty}^{\infty}\int_{-\infty}^{\infty} \mathcal{G}(x-\xi, t-\eta)\mathbf{F}(\xi,\eta)d\xi_1 d\xi_2 d\xi_3 d\eta \tag{2.40}$$

gives a solution of (2.25). Here $\xi = (\xi_1, \xi_2, \xi_3) \in R^3$, $x = (x_1, x_2, x_3) \in R^3$, $t \in R$. Using the fact that the first three components of

$$\mathbf{F} = (f_1(\xi,\eta), f_2(\xi,\eta), f_3(\xi,\eta), 0, ..., 0)$$

are nonzero and other components are identically equal to zero we find that columns of $\mathcal{G}(x,t)$ started from fourth do not have any influence on the solution $\mathbf{V}(x,t)$ defined by (2.40). Therefore the fundamental solution of SHSE (2.25) is naturally defined as a matrix $\mathbf{G}(x,t)$ of the order 9×3 for which the formula

$$\mathbf{V}(x,t) = \int_{-\infty}^{\infty}\int_{-\infty}^{\infty}\int_{-\infty}^{\infty}\int_{-\infty}^{\infty} \mathbf{G}(x-\xi, t-\eta)\mathbf{f}(\xi,\eta)d\xi_1 d\xi_2 d\xi_3 d\eta$$

gives a solution of SHSE (2.25), where $\mathbf{f}(\xi,\eta) = (f_1(\xi,\eta), f_2(\xi,\eta), f_3(\xi,\eta))$ is 3D vector column. We note also that each column of the fundamental solution $\mathbf{G}(x,t)$ of SHSE (2.25) satisfies (2.38), (2.39).

A fundamental solution of AES (2.14) is defined as a matrix $G(x,t)$ of the order 3×3 whose columns $\mathbf{u}^m(x,t) = (u_1^m(x,t), u_2^m(x,t), u_3^m(x,t))^*$ satisfy equations (2.14) for $f_i = \delta_i^m \delta(x)\delta(t)$. Here δ_i^m is the Kroneker symbol, i.e. $\delta_i^m = 1$ if $i = m$ and $\delta_i^m = 0$ if $i \neq m$; $i = 1,2,3$; $m = 1,2,3$; $\delta(x) = \delta(x_1) \cdot \delta(x_2) \cdot \delta(x_3)$ is the Dirac delta function concentrated at $x_1 = 0$, $x_2 = 0$, $x_3 = 0$; $\delta(t)$ is the Dirac delta function concentrated at $t = 0$.

Remark 2. If the fundamental solution $\mathbf{G}(x,t)$ of SHSE (2.25) is given (found)

then elements of the fundamental solution $G(x,t)$ of AES (2.14) can be computed by the following formulae

$$u_j^m(x,t) = \int_0^t V_j^m(x,\eta)d\eta,\ m = 1,2,3;\ j = 1,2,3. \tag{2.41}$$

2.1.5 Deriving the fundamental solution of SHSE

In this section we derive the explicit formulae for all components of the fundamental solution $\mathbf{G}(x,t)$. The derivation of fundamental solution columns have the following steps. In the first step equations (2.38)-(2.39) are written in terms of Fourier transform with respect to space variables x_1,x_2,x_3 and then the images $\tilde{\mathbf{V}}^m(\nu,t)$ of the Fourier transform of $\mathbf{V}^m(x,t)$ are found in the form of the power series with respect to 3-D Fourier parameter $\nu \in R^3$ with unknown coefficients depending on the time variable t. We obtain recurrence relations for unknown coefficients in the next step. Using these relations all power series coefficients are derived explicitly. Applying the inverse Fourier transform to the found formulae for $\tilde{\mathbf{V}}^m(\nu,t)$ we obtain explicit formulae for each column $\mathbf{V}^m(x,t)$ of the fundamental solution $\mathbf{G}(x,t)$ in the last step.

2.1.5.1 Symmetric hyperbolic system in terms of Fourier transform

Let $\tilde{\mathbf{V}}^m(\nu,t)$ be the Fourier transform image of $\mathbf{V}^m(x,t)$ with respect to $x = (x_1,x_2,x_3) \in R^3$, i.e.

$$\tilde{V_j}^m(\nu,t) = F_x[V_i^m](\nu,t),\ j = 1,2,...,9,$$

where

$$F_x[V_j^m](\nu,t) = \int_{-\infty}^{\infty}\int_{-\infty}^{\infty}\int_{-\infty}^{\infty} V_j^m(x,t)e^{ix\cdot\nu}dx_1dx_2dx_3,$$
$$\nu = (\nu_1,\nu_2,\nu_3) \in R^3,\ x\cdot\nu = x_1\nu_1 + x_2\nu_2 + x_3\nu_3,\ i^2 = -1.$$

Equations (2.38)-(2.39) can be written in terms of the Fourier image $\tilde{\mathbf{V}}^m(\nu,t)$ as follows:

$$\mathbf{A}_0\frac{\partial\tilde{\mathbf{V}}^m}{\partial t} - i(\nu_1\mathbf{A}_1 + \nu_2\mathbf{A}_2 + \nu_3\mathbf{A}_3)\tilde{\mathbf{V}}^m = \mathsf{E}^m\delta(t),\ t \in R, \tag{2.42}$$

$$\tilde{\mathbf{V}}^m(\nu,t)|_{t\le 0} = 0,\ \nu \in R^3. \tag{2.43}$$

Using the matrix formalism in MATLAB we construct a non-singular matrix $\mathbf{T}$ and a diagonal matrix $\mathbf{D}$ with real-valued elements such that

$$\mathbf{T}^*\mathbf{A}_0\mathbf{T} = \mathbf{I},\ \mathbf{T}^*\mathbf{A}_3\mathbf{T} = \mathbf{D}, \tag{2.44}$$

where $\mathbf{I}$ is the identity matrix, $\mathbf{T}^*$ is the transposed matrix to $\mathbf{T}$. The technique of this diagonalization can be found in Yakhno & Yakhno & Kasap (2006).

We find a solution of (2.42) and (2.43) in the form

$$\tilde{\mathbf{V}}^m(\nu,t) = \mathbf{T}(\mathbf{X}^m(\nu,t) + i\mathbf{Y}^m(\nu,t)), \tag{2.45}$$

where the matrix $\mathbf{T}$ satisfies the relations (2.44). Vector functions $\mathbf{X}^m(\nu,t)$ and $\mathbf{Y}^m(\nu,t)$ are unknown. Substituting (2.45) into (2.42)-(2.43) and multiplying by $\mathbf{T}^*$ from left

hand side and using the relations (2.44) we find

$$\frac{\partial \mathbf{X}^m}{\partial t} + \nu_1 \mathcal{B}\mathbf{Y}^m + \nu_2 \mathcal{C}\mathbf{Y}^m + \nu_3 \mathbf{D}\mathbf{Y}^m = \mathbf{T}^* \mathsf{E}^m \delta(t),\ \mathbf{X}^m(\nu,t) \mid_{t\le 0} = 0, \tag{2.46}$$

$$\frac{\partial \mathbf{Y}^m}{\partial t} - \nu_1 \mathcal{B}\mathbf{X}^m - \nu_2 \mathcal{C}\mathbf{X}^m - \nu_3 \mathbf{D}\mathbf{X}^m = 0,\ \mathbf{Y}^m(\nu,0) \mid_{t\le 0} = 0 \tag{2.47}$$

where $\mathcal{B} = \mathbf{D}^* \mathbf{A}_1 \mathbf{D}$ and $\mathcal{C} = \mathbf{T}^* \mathbf{A}_2 \mathbf{T}$.

2.1.5.2 Explicit formula for a solution of IVP (2.42), (2.43)

Using properties of the fundamental solution in section 2.1.3 the vector functions $\mathbf{X}^m(\nu,t)$, $\mathbf{Y}^m(\nu,t)$ can be written as

$$\mathbf{X}^m(\nu,t) = \sum_{n=0}^{\infty}\sum_{p=0}^{\infty}\sum_{k=0}^{\infty} (\mathbf{X}^m)^{n+1,p+1,k+1}(t)\nu_1^n \nu_2^p \nu_3^k, \tag{2.48}$$

$$\mathbf{Y}^m(\nu,t) = \sum_{n=0}^{\infty}\sum_{p=0}^{\infty}\sum_{k=0}^{\infty} (\mathbf{Y}^m)^{n+1,p+1,k+1}(t)\nu_1^n \nu_2^p \nu_3^k, \tag{2.49}$$

Substituting these series into (2.46)-(2.47) we have

$$\frac{\partial (\mathbf{X}^m)^{1,1,1}}{\partial t} = 0,\ (\mathbf{X}^m)^{1,1,1}(t) \mid_{t=0} \ = \ \mathbf{T}^* \mathsf{E}^m.$$

$$\begin{aligned} \frac{\partial (\mathbf{X}^m)^{n+1,p+1,k+1}}{\partial t} \ &+ \ \mathcal{B}(\mathbf{Y}^m)^{n,p+1,k+1} + \mathcal{C}(\mathbf{Y}^m)^{n+1,p,k+1} \\ &+ \ \mathbf{D}(\mathbf{Y}^m)^{n+1,p+1,k} = 0,\ n,p,k = 0,1,..., \end{aligned}$$

$$(\mathbf{X}^m)^{n+1,p+1,k+1}(t) \mid_{t=0} = 0,\ n,p,k = 0,1,...;\ n+p+k \neq 0 \tag{2.50}$$

and

$$\begin{aligned}\frac{\partial(\mathbf{Y}^m)^{n+1,p+1,k+1}}{\partial t} &- \mathcal{B}(\mathbf{X}^m)^{n,p+1,k+1} - \mathcal{C}(\mathbf{X}^m)^{n+1,p,k+1} \\ &- \mathbf{D}(\mathbf{X}^m)^{n+1,p+1,k} = 0,\ \ n,p,k = 0,1,...,\end{aligned}$$

$$(\mathbf{Y}^m)^{n+1,p+1,k+1}(t)\mid_{t=0} = 0,\ \ n,p,k = 0,1,.... \tag{2.51}$$

where

$$\begin{aligned}(\mathbf{X}^m)^{0,r,s}(t) &= 0,\ (\mathbf{X}^m)^{l,0,s}(t) = 0,\ (\mathbf{X}^m)^{l,r,0}(t) = 0, \\ (\mathbf{Y}^m)^{0,r,s}(t) &= 0,\ (\mathbf{Y}^m)^{l,0,s}(t) = 0,\ (\mathbf{Y}^m)^{l,r,0}(t) = 0,\ \ l,r,s = 0,1,2,...\end{aligned}$$

Solving IVP (2.50)-(2.51) we have the following recurrence relations

$$\begin{aligned}&(\mathbf{X}^m)^{1,1,1}(t) = \mathbf{T}^*\ \mathsf{E}^m,\ \ (\mathbf{Y}^m)^{1,1,1}(t) = 0, \\ &(\mathbf{X}^m)^{n+1,p+1,k+1}(t) = \int_0^t \{-\mathcal{B}(\mathbf{Y}^m)^{n,p+1,k+1} - \mathcal{C}(\mathbf{Y}^m)^{n+1,p,k+1} \\ - &\ \mathbf{D}(\mathbf{Y}^m)^{n+1,p+1,k}\}(\tau)d\tau\ \ (n,p,k = 0,1,2,...;\ \ n+k+p \neq 0),\end{aligned} \tag{2.52}$$

$$\begin{aligned}&(\mathbf{Y}^m)^{n+1,p+1,k+1}(t) = \int_0^t \{\mathcal{B}(\mathbf{X}^m)^{n,p+1,k+1} + \mathcal{C}(\mathbf{X}^m)^{n+1,p,k+1} \\ + &\ \mathbf{D}(\mathbf{X}^m)^{n+1,p+1,k}\}(\tau)d\tau\ \ (n,p,k = 0,1,2,...)\end{aligned} \tag{2.53}$$

Using the recurrence relations (2.52)-(2.53) unknown vector coefficients

$$(\mathbf{X}^m)^{n+1,p+1,k+1},\quad (\mathbf{Y}^m)^{n+1,p+1,k+1},\quad n,p,k = 0,1,...$$

are determined.

Substituting the obtained vector coefficients into the series (2.48)-(2.49) we find the solution of the systems (2.46)-(2.47) and then, using (2.45), the solution $\tilde{\mathbf{V}}^m(\nu,t)$ of (2.42), (2.43).

2.1.5.3 Explicit formula for a solution of IVP (2.38)-(2.39)

Let $\tilde{\mathbf{V}}^m(\nu,t)$ be the found solution of (2.42), (2.43). The solution $\mathbf{V}^m(x,t) = (V_1^m(x,t),...,V_9^m(x,t))$ of IVP (2.38)-(2.39) is determined by the inverse Fourier transform of $\tilde{\mathbf{V}}^m(\nu,t)$, i.e. by the formula:

$$\mathbf{V}^m(x,t) = \frac{\theta(t)}{(2\pi)^3}\int_{-\infty}^{\infty}\int_{-\infty}^{\infty}\int_{-\infty}^{\infty}\tilde{\mathbf{V}}^m(\nu,t)e^{-ix\cdot\nu}d\nu_1 d\nu_2 d\nu_3, \tag{2.54}$$

where $\theta(t)$ is the Heaviside step function, i.e. $\theta(t)=1$ for $t\geq 0$ and $\theta(t)=0$ for $t<0$.

We get from (2.45) the following relation

$$\begin{aligned}\tilde{\mathbf{V}}^m(\nu,t)e^{-ix\cdot\nu} = &[\mathbf{TX}^m(\nu,t)\cos(x\cdot\nu)+\mathbf{TY}^m(\nu,t)\sin(x\cdot\nu)]\\ &+i[\mathbf{TY}^m(\nu,t)\cos(x\cdot\nu)-\mathbf{TY}^m(\nu,t)\sin(x\cdot\nu)].\end{aligned} \tag{2.55}$$

Taking into account that components of the vector function $\mathbf{V}^m(x,t)$ as well as components of vector functions $\mathbf{TX}^m(\nu,t)$ and $\mathbf{TY}^m(\nu,t)$ have real values, the imaginary part of the right hand side of (2.54) is equal to zero. As a result of it we find from (2.54) and (2.55) the following formula for mth column of the fundamental solution of SHSE:

$$\begin{aligned}\mathbf{V}^m(x,t) = &\frac{\theta(t)}{(2\pi)^3}\int_{-\infty}^{\infty}\int_{-\infty}^{\infty}\int_{-\infty}^{\infty}[\mathbf{TX}^m(\nu,t)\cos(x_1\nu_1+x_2\nu_2+x_3\nu_3)\\ &+\mathbf{TY}^m(\nu,t)\sin(x_1\nu_1+x_2\nu_2+x_3\nu_3)]\,d\nu_1 d\nu_2 d\nu_3.\end{aligned} \tag{2.56}$$

2.1.6 Computational experiments: implementation and justification

2.1.6.1 The regularization of some singular generalized functions

An explicit formula of the FS of equations of isotropic elastodynamics is well known (see, for example, Aki & Richard (1980)). For example, components of the first column of FS can be written in the form

$$G_1^1(x_1,x_2,x_3,t) = \frac{1}{4\pi\rho}(\frac{3x_1^2}{|x|^5} - \frac{1}{|x|^3})\theta(t-\frac{|x|}{C_L})\ \theta(\frac{|x|}{C_T}-t)t$$
$$+\frac{1}{4\pi\rho C_P^2}\frac{x_1^2}{|x|^3}\delta(t-\frac{|x|}{C_L}) + \frac{1}{4\pi\rho C_T^2|x|}(1-\frac{x_1^2}{|x|^2})\delta(t-\frac{|x|}{C_T}), \tag{2.57}$$

$$G_2^1(x_1,x_2,x_3,t) = \frac{1}{4\pi\rho}\frac{3x_1x_2}{|x|^5}\theta(t-\frac{|x|}{C_L})\ \theta(\frac{|x|}{C_T}-t)t$$
$$+\frac{1}{4\pi\rho C_L^2}\frac{x_1x_2}{|x|^3}\delta(t-\frac{|x|}{C_L}) - \frac{1}{4\pi\rho C_T^2}\frac{x_1x_2}{|x|^3})\delta(t-\frac{|x|}{C_T}), \tag{2.58}$$

$$G_3^1(x_1,x_2,x_3,t) = \frac{1}{4\pi\rho}\frac{3x_1x_3}{|x|^5}\theta(t-\frac{|x|}{C_L})\ \theta(\frac{|x|}{C_T}-t)t$$
$$+\frac{1}{4\pi\rho C_L^2}\frac{x_1x_3}{|x|^3}\delta(t-\frac{|x|}{C_L}) - \frac{1}{4\pi\rho C_T^2}\frac{x_1x_3}{|x|^3})\delta(t-\frac{|x|}{C_T}), \tag{2.59}$$

where $C_T^2 = \frac{\mu}{\rho}$, $C_L^2 = \frac{\lambda+2\mu}{\rho}$. These formulae contain singular terms $\delta(C_Tt - |x|)/(4\pi C_T^2\rho|x|)$ and $\delta(C_Lt-|x|)/(4\pi C_L^2\rho|x|)$. The supports of these singular terms are the characteristic cones $tC_T = |x|$ and $tC_L = |x|$ in the space of variables x_1,x_2,x_3,t. Usually the classical functions are defined by the point-wise manner and we can draw their graphs. Unfortunately this point-wise definition and its graphic presentation is not adequate to singular generalized functions (Vladimirov (1979), Vladimirov (1971), Reed & Simon (1975)). For this reason they are very often replaced by regularized functions which are classical and have graphic presentations. This regularization has

a parameter of the regularization and the singular generalized function is a limit in the sense of the generalized functions space when the parameter of this regularization tends to $+\infty$ (or $+0$). For example, the singular generalized function $\delta(t)$ can be regularized by $\frac{1}{2\sqrt{\pi\varepsilon}}\exp\left(-t^2/(4\varepsilon)\right)$ and the singular generalized function $\delta(C_T t-|x|)$ by $\frac{1}{2\sqrt{\pi\varepsilon}}\exp\left[-(C_T t-|x|)^2/(4\varepsilon)\right]$ (see Vladimirov (1979)).

On the other hand $\delta(C_T t-|x|)/(4\pi C_T^2\rho|x|)$ can be regularized by

$$h_A(x,t)=\frac{1}{(2\pi)^3}\int_{-A}^{A}\int_{-A}^{A}\int_{-A}^{A}\frac{\sin(C_T|\nu|t)}{\rho C_T|\nu|}\,e^{-ix\cdot\nu}d\nu_1 d\nu_2 d\nu_3,\ t>0, \tag{2.60}$$

$i^2=-1,\ \nu=(\nu_1,\nu_2,\nu_3)\in R^3,\ x=(x_1,x_2,x_3)\in R^3,\ x\cdot\nu=x_1\nu_1+x_2\nu_2+x_3\nu_3.$

when $A\to+\infty$, because we know that (see Vladimirov (1979))

$$\lim_{A\to+\infty}\frac{1}{(2\pi)^3}\int_{-A}^{A}\int_{-A}^{A}\int_{-A}^{A}\frac{\sin(C_T|\nu|t)}{\rho C_T|\nu|}\,e^{-ix\nu}d\nu_1 d\nu_2 d\nu_3=F_\nu^{-1}[\frac{\sin(C_T|\nu|t)}{\rho C_T|\nu|}](x)$$

and

$$F_\nu^{-1}[\frac{\sin(C_T|\nu|t)}{\rho C_T|\nu|}](x)=\frac{1}{4\pi C_T^2|x|\rho}\delta(C_T t-|x|).$$

Here F_ν^{-1} is the 3D inverse Fourier transform defined by (2.54). Since the function $\sin(C_T|\nu|t)/(\rho C_T|\nu|)$ is even we can replace the $3D$ integral of (2.60) by

$$\int_{-A}^{A}\int_{-A}^{A}\int_{-A}^{A}\frac{\sin(C_T|\nu|t)}{\rho C_T|\nu|}\cos(x\cdot\nu)d\nu_1 d\nu_2 d\nu_3$$

and then approximately the obtained integral can be written by the following triple

sums

$$\sum_{n=-N}^{N}\sum_{m=-N}^{N}\sum_{l=-N}^{N}\frac{\sin(C_T|\nu|t)}{\rho C_T|\nu|}\Big|_{\nu=(n\Delta\nu,m\Delta\nu,l\Delta\nu)}\cos(\Delta\nu(nx_1+mx_2+lx_3))(\Delta\nu)^3,$$

where N is a natural number for which $A = N\Delta\nu$ and real numbers A and $\Delta\nu$ have been chosen from empirical observations and natural logic. Namely, using the obtained integral sums we compute the values of $h_A(x,t)$ for $\Delta\nu = 1$, $\Delta\nu = 0.5$, $\Delta\nu = 0.025$, $A = 20$, $A = 30$, $A = 40$, $A = 50$ and so on numerically in MATLAB . We compare the results of computation with values of the function $\frac{1}{2\sqrt{\pi\varepsilon}}\exp\left[-(C_Tt-|x|)^2/(4\varepsilon)\right]/(4\pi C_T^2\rho|x|)$ $(\varepsilon = 0.0001)$ which is a regularization of $\delta(C_Tt-|x|)/(4\pi C_T^2\rho|x|)$. We have observed that the difference between values of $h_A(x,t)$ and $\frac{1}{2\sqrt{\pi\varepsilon}}\exp\left[-(C_Tt-|x|)^2/(4\varepsilon)\right]/(4\pi C_T^2\rho|x|)$, $(\varepsilon = 0.0001)$ corresponding to $\Delta\nu = 0.5$ and $A = 40$, $A = 50$, $A = 60$, $A = 70$ becomes small and the increment of the regularization for the parameter A is not essential according to the case $\Delta\nu = 0.5$, $A = 40$. For this reason we choose $\Delta\nu = 0.5$, $A = 40$ as suitable parameters for $h_A(x,t)$ as regularization of $\delta(C_Tt-|x|)/(4\pi C_T^2\rho|x|)$ by the $3D$ integral sum.

2.1.6.2 Correctness of the method

For the computation of the fundamental solution of SHSE we use the formula (2.56) and then we derive the fundamental solution of AES by (2.41). The formula (2.56) contains 3D integral over the whole space R^3. We replace this integral by the integral over the bounded domain $(-A,A)\times(-A,A)\times(-A,A)$, where the number A is chosen by the empirical observation on the singular terms of the fundamental solution corresponding to isotropic elastic media which is described in section 2.1.6.1

We note also that terms $\mathbf{X}^m(\nu,t)$ and $\mathbf{Y}^m(\nu,t)$, appearing in (2.56), are presented in the form of triple series (2.48), (2.49) with infinite number of terms. We replace these

triple series by sums with finite number of terms of the form

$$\sum_{n=0}^{M}\sum_{p=0}^{M}\sum_{k=0}^{M}(\mathbf{X}^m)^{n+1,p+1,k+1}(t)\nu_1^n\nu_2^p\nu_3^k,$$
$$\sum_{n=0}^{M}\sum_{p=0}^{M}\sum_{k=0}^{M}(\mathbf{Y}^m)^{n+1,p+1,k+1}(t)\nu_1^n\nu_2^p\nu_3^k, \tag{2.61}$$

where the number M is chosen by the following natural logic. An explicit formula for the fundamental solution of isotropic elastodynamics as well as an explicit formula for its Fourier transform image with respect to space variables are well known (Aki & Richard (1980)). Thus the formula for the Fourier transform image of the first column of this fundamental solution has the form

$$\hat{\mathbf{u}}^1(\nu,t)=(\hat{u}_1^1(\nu,t),\hat{u}_2^1(\nu,t),\hat{u}_3^1(\nu,t)),$$

where

$$\begin{aligned}
\hat{u}_1^1(\nu,t) &= \frac{\theta}{\rho\mid\nu\mid^3}\{\frac{\sin(C_T\mid\nu\mid t)}{C_T}(\nu_2^2+\nu_3^2)+\frac{\sin(C_L\mid\nu\mid t)}{C_L}\nu_1^2\},\\
\hat{u}_2^1(\nu,t) &= \frac{\theta(t)}{\rho\mid\nu\mid^3}\nu_2\nu_1\{\frac{\sin(C_L\mid\nu\mid t)}{C_L}-\frac{\sin(C_T\mid\nu\mid t)}{C_T}\},\\
\hat{u}_3^1(\nu,t) &= \frac{\theta(t)}{\rho\mid\nu\mid^3}\nu_3\nu_1\{\frac{\sin(C_L\mid\nu\mid t)}{C_L}-\frac{\sin(C_T\mid\nu\mid t)}{C_T}\}.
\end{aligned}$$

Here elastic moduli for the isotropic medium are defined as $c_{ijkl}=\lambda\delta_i^j\delta_k^l+\mu(\delta_i^k\delta_j^l+\delta_i^l\delta_j^k)$, where μ and λ are Lame parameters; δ_i^j is the Kronecker symbol.

On the other hand we can find the first column of the Fourier transform image of the fundamental solution by our method using formulae (2.48) - (2.49), where triple series with infinite number of terms are replaced by sums (2.61) with finite number of terms. We have chosen M such that difference between components of $\hat{\mathbf{u}}^1(\nu,t)$ and components of $\tilde{\mathbf{u}}^1(\nu,t)$ computed by our method was negligible (of the order 10^{-4}) when $|\nu_j|<A$, $j=1,2,3$. The similar has been done for the second and third columns

of this fundamental solution. As a result we have got that suitable values are: $A \geq 40$ and $M \geq 60$.

For the justification of these values and evaluation of our method we have used the following properties of the fundamental solution of isotropic elastodynamics:

$$\int_{-\infty}^{\infty}\int_{-\infty}^{\infty} u_1^1(x_1,x_2,x_3,t)dx_1dx_2 = \frac{1}{2\rho C_T}\theta(C_T t - |x_3|),$$
$$\int_{-\infty}^{\infty} u_1^1(x_1,x_2,x_3,t)dx_1 = \frac{1}{2\pi\rho C_T}\frac{\theta(C_T t - \sqrt{x_2^2+x_3^2})}{\sqrt{C_T^2 t^2 - x_2^2 - x_3^2}},$$

where $u_1^1(x_1,x_2,x_3,t)$ is the first element of the first column of the fundamental solution of isotropic elastodynamics.

For the illustration we have considered the isotropic elastic material sillica (SiO_2) characterized by $\mu = 3.12$, $\lambda = 1.61$ ($10^{10}Pa$), $\rho = 2.203$ $(10^3 kg/m^3)$ (see, for example, Dieulesaint & Royer (2000), p.163). Using reasoning described above we have chosen numbers $A = 45$ and $M = 90$ and then applied our method based on formulae (2.41), (2.56). As a result of it we have computed $V_1^1(x_1,x_2,x_3,t)$ and $u_1^1(x_1,x_2,x_3,t)$. After that we have derived integrals

$$\int_{-\infty}^{\infty}\int_{-\infty}^{\infty} u_1^1(x_1,x_2,x_3,t)dx_1dx_2, \quad \int_{-\infty}^{\infty} u_1^1(x_1,x_2,x_3,t)dx_1. \tag{2.62}$$

For the computation of the integrals we have used the natural property

$$u_1^1(x_1,x_2,x_3,t) = 0, \text{ if } \sqrt{x_2^2+x_3^2} \geq tC_L, \text{ or } |x_3| \geq tC_L$$

and the integration has been taken over the bounded interval and bounded domain. The results of the computation and comparison are presented in the Fig.2.1-Fig.2.2. In Fig.2.1 we have computed the first integral in (2.62) for $M = 60$, $A = 45$, $t = 2$.

Fig.2.1 gives 2D plot of this integral. Here the horizontal axis is x_3. In Fig.2.2 we have computed the second integral in (2.62) for $x_2 = x_3 = a, M = 60, A = 40, t = 0.5$. Figure 2.2 gives 2D plot of this integral. Here the horizontal axis is a.

2.1.7 Images of elements of the fundamental solution of SHSE

The computational experiments of this section confirm the robustness of our method to produce images of elements of fundamental solution of SHSE (2.25). These images are the simulation of wave propagations arising from directional pulse point forces in general anisotropic media. We consider the following homogeneous elastic materials with orthorhombic and monoclinic structures of anisotropy.

Orthorhombic crystal α-iodic acid (HIO_3) (see Dieulesaint & Royer (2000)) has the following properties: $\rho = 4.640\ (10^3 kg/m^3)$; and

$$\begin{aligned} c_{11} &= 3.01,\ c_{12} = c_{21} = 1.61,\ c_{13} = c_{31} = 1.11, \\ c_{22} &= 5.8,\ c_{23} = c_{23} = 0.80,\ c_{33} = 4.29, \\ c_{44} &= 1.69,\ c_{55} = 2.06,\ c_{66} = 1.58,\ (10^{10}\ Pa) \end{aligned}$$

other elements of the matrix **C** are equal to zero.

Monoclinic crystal AT-cut quartz (see Batra & Qian & Chen (2004)) has the density $\rho = 2.649\ (10^3 kg/m^3)$; elements of the matrix C defined by

$$\begin{aligned} c_{11} &= 8.67,\ c_{12} = c_{21} = -0.83,\ c_{13} = c_{31} = 2.71,\ c_{14} = c_{41} = -0.37, \\ c_{22} &= 12.98,\ c_{23} = c_{23} = -0.74, c_{24} = c_{24} = 0.57\ c_{33} = 10.28, \\ c_{34} &= c_{43} = 0.99,\ c_{44} = 3.86,\ c_{55} = 6.88,\ c_{66} = 2.9, c_{56} = c_{65} = 0.25 \end{aligned}$$

(10^{10}Pa) and other elements of the matrix **C** are equal to zero.

In computational experiments we compute the third column of the fundamental solution of SHSE (2.25), i.e. we take $m = 3$ in (2.38), (2.39). Using the matrix formalism from Yakhno & Yakhno & Kasap (2006) the matrices $\mathbf{T}$, $\mathbf{T}^*$, $\mathbf{D}$ have been computed in MATLAB. Further, using formula (2.56) and procedures, described in section 2.1.5, we have derived values of $V_k^3(x,t),\ k = 1,2,...,9$; i.e. all components of the displacement speed and stresses for each anisotropic material. We have used the following parameters for the computations : $A = 40$ and $M = 60$.

Figs.2.3a-c are the screen shots of 3-D level plots of $V_3^3(x_1,0,x_3,0.25)$, $V_3^3(x_1,0,x_3,2)$ and $V_3^3(x_1,0,x_3,3.5)$. The horizontal axes are x_1 and x_3. The vertical axis is the magnitude of $V_3(x_1,0,x_3,t)$ for $t = 0.25,2,3.5$. Figs.2.4a-c are the screen shots of 2-D level plots of the same surfaces $V_3^3(x_1,0,x_3,0.25)$, $V_3^3(x_1,0,x_3,2)$ and $V_3^3(x_1,0,x_3,3.5)$. This is a view from the top of z-axis (the plan). The Figs.2.3 and 2.4 demonstrate dynamics of the wave propagation in the orthorhombic crystal.

The Figs.2.5a-c contain 2-D plots (a view from the top of z-axis) of $z = V_k^3(x_1,0,x_3,t),\ k = 1,5,9$ for $t = 0.8$ corresponding to the monoclinic crystal.

The obtained results of simulations give the information about fronts of elastic wave propagations and behavior of the displacement speeds and stresses in elastic media with general structure of anisotropy (orthorhombic, monoclinic). We note here that for isotropic media we can get such kind of information by explicit formulae for columns of the fundamental solutions. These explicit formulae contain terms with singularities on the surface of characteristic cones in (x,t) space, where $x = (x_1,x_2,x_3)$ is a 3D space variable and t is a 1D time variable. If the time variable is fixed then singularities are located on the surfaces of spheres. These surfaces of spheres are fronts of elastic waves (longitudinal and transverse waves) in isotropic

media. There are three waves in the general anisotropic elastic media. One wave is quasi-longitudinal and two waves are quasi-transverse (Aki & Richard (1980)). The speed of the quasi-longitudinal is the biggest one. The results of the computational experiments presented in Figs.2.4-2.5 demonstrate configurations of the front traces of quasi-longitudinal waves for $x_2 = 0$ and $t = const$. These front traces have very peculiar forms as compared with the isotropic case. We note that the front traces of quasi-transverse waves are unrecognizable through other fluctuations arising in the disturbed domains.

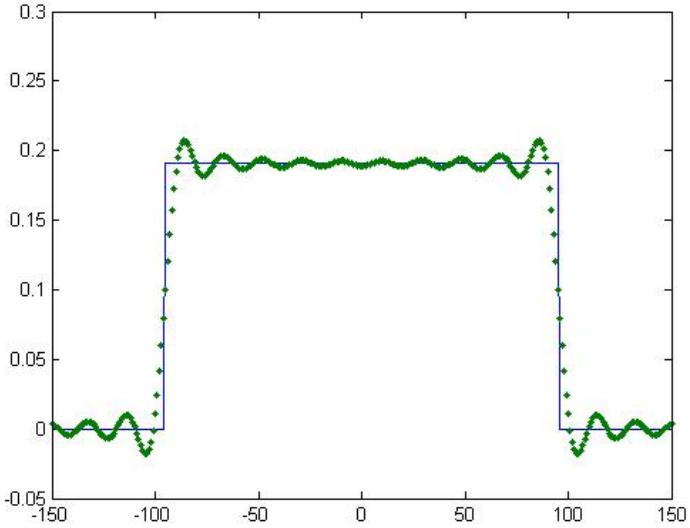

Figure 2.1: The graph of $I_2(x_3,t) = \int_{-\infty}^{\infty}\int_{-\infty}^{\infty} u_1^1(x_1,x_2,x_3,t)dx_1dx_2$ at $t = 2$ computed by **...** our method; — exact values of $I(x_3,t)$ at $t = 2$.

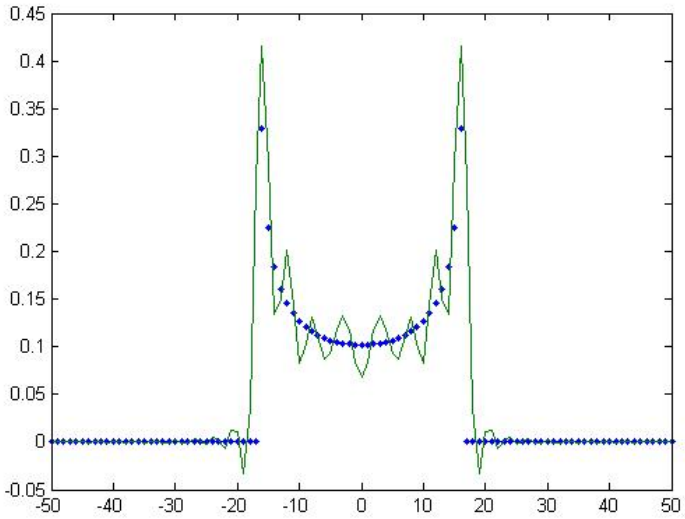

Figure 2.2: The graph of $I_1(x_2,x_3,t) = \int_{-\infty}^{\infty} u_1^1(x_1,x_2,x_3,t)dx_1$ at $t = 0.5$, $x_2 = x_3$ computed by — our method; **...** exact values of $I_1(x_2,x_3,t)$ solution at $t = 0.5$, $x_2 = x_3$.

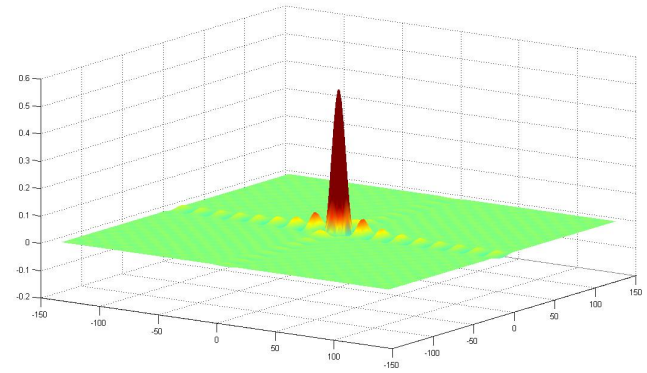

(a) t=0.25

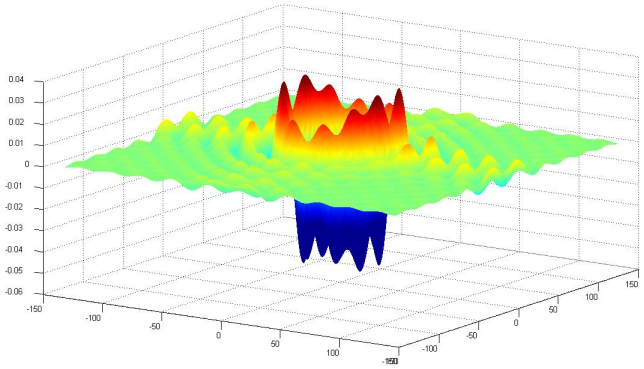

(b) t=2

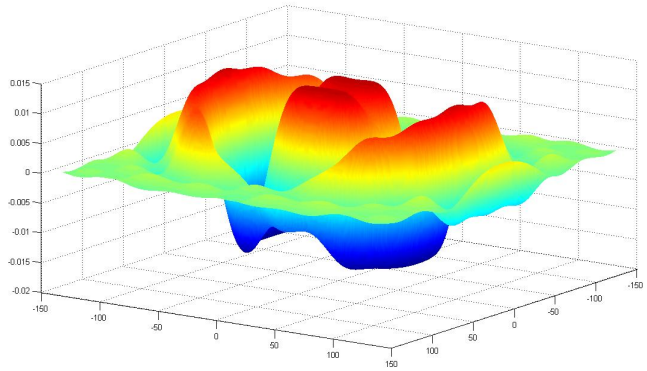

(c) t=3.5

Figure 2.3: Images of $z = V_3^3(x_1, 0, x_3, t)$ at $t = 0.25$, $t = 2$, $t = 3.5$ in orthorhombic crystal; the horizontal axes are x_1 and x_3, the vertical axis is the magnitude of $V_3^3(x_1, 0, x_3, t)$.

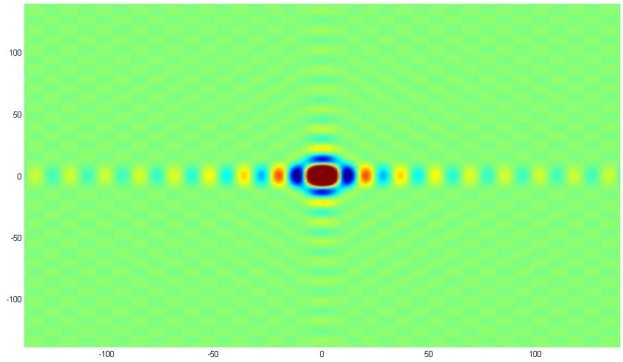

(a) t=0.25

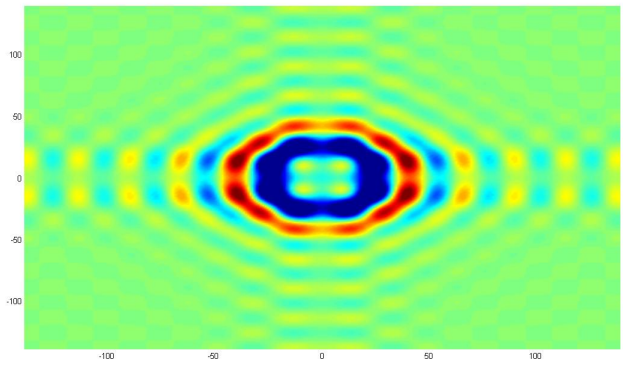

(b) t=2

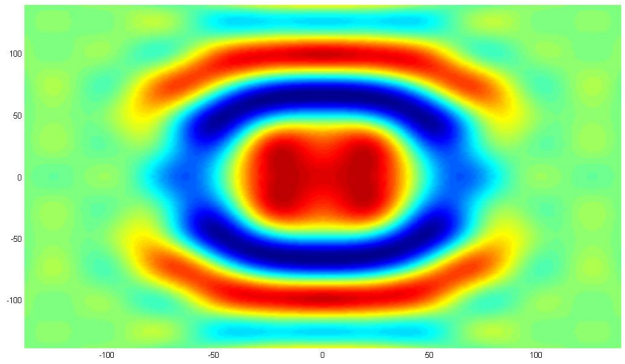

(c) t=3.5

Figure 2.4: Images of $V_3^3(x_1,0,x_3,t)$ at $t=0.25$, $t=2$, $t=3.5$ in orthorhombic crystal; the view from the top of z-axis on the surfaces $z=V_3^3(x_1,0,x_3,t)$ (plan).

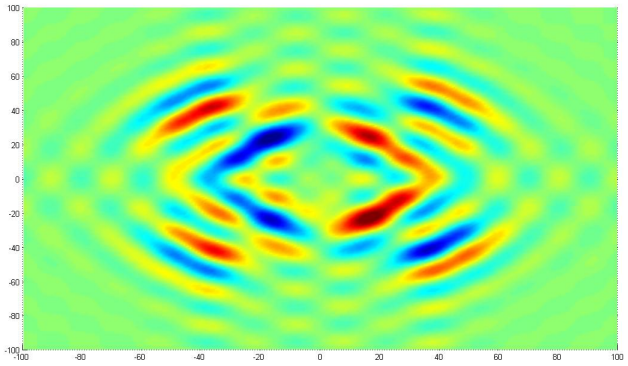

(a) 2-D plot of $V_1^3(x_1,0,x_3,0.8)$

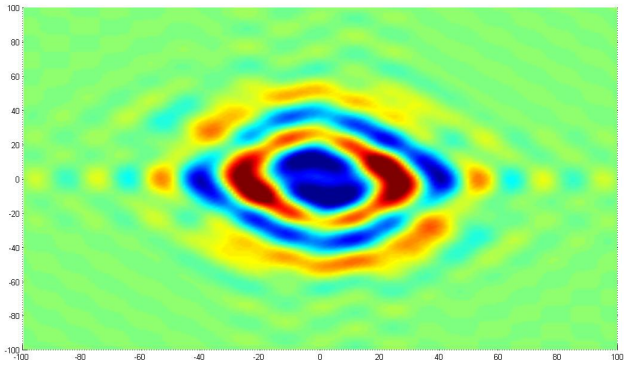

(b) 2-D plot of $V_5^3(x_1,0,x_3,0.8)$

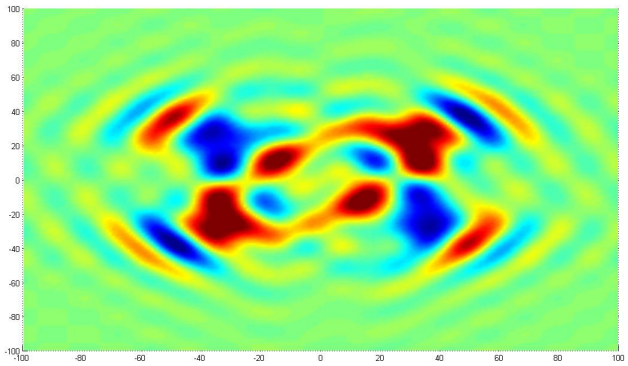

(c) 2-D plot of $V_9^3(x_1,0,x_3,0.8)$

Figure 2.5: Images of the third column components of the fundamental solution of SHSE at $t = 0.8$, $x_2 = 0$ in the monoclinic crystal; the view from the top of z axis on surfaces $z = V_j^3(x_1,0,x_3,3.5)$, $j = 1,5,9$.

2.2 Computation of the time-dependent fundamental solution for equations of elastodynamics in general anisotropic media

2.2.1 Statement of the problem

The time-dependent FS of anisotropic elastodynamics (2.14) (AES) is defined as a matrix $G(x,t)$ of the order 3×3 whose columns

$$\mathbf{u}^m(x,t) = (u_1^m(x,t), u_2^m(x,t), u_3^m(x,t))$$

satisfy equalities

$$\rho\frac{\partial^2 u_i^m}{\partial t^2} = \sum_{j=1}^{3}\frac{\partial \tau_{ij}^m}{\partial x_j} + \delta_i^m\delta(x)\delta(t),\ x=(x_1,x_2,x_3)\in R^3,\ t\in R,\ i=1,2,3, \quad (2.63)$$

$$u_i^m|_{t<0} = 0,\ \ i=1,2,3, \quad (2.64)$$

where δ_i^m is the Kronecker symbol, i.e. $\delta_i^m = 1$ if $i=m$ and $\delta_i^m = 0$ if $i\neq m$; $i=1,2,3$; $m=1,2,3$.

From the physical point of view the m-th column of FS is the displacement of the considered anisotropic medium arising from the pulse point force $\mathbf{e}^m\delta(x)\delta(t)$, where $\mathbf{e}^1=(1,0,0)$, $\mathbf{e}^2=(0,1,0)$, $\mathbf{e}^3=(0,0,1)$ are basis vectors of the Cartesian coordinates.

(2.14) can be reduce to the first order symmetric hyperbolic system (2.25) (see section 2.1.2). The main problem of this section is to find fundamental solution of SHSE (2.25), i.e. to solve the initial value problem (2.38)-(2.39) and to find fundamental solution of AES (2.14), i.e. to solve the initial value problem

(2.63)-(2.64).

2.2.2 Method of the solution

Applying the Fourier transform with respect to x in the initial value problem (2.38)-(2.39) we have

$$\mathbf{A}_0\frac{\partial\tilde{\mathbf{V}}^m}{\partial t} - i\mathbf{B}(\nu)\tilde{\mathbf{V}}^m = \mathsf{E}^m\delta(t), \tag{2.65}$$

$$\tilde{\mathbf{V}}^m(\nu,t)|_{t<0} = 0,, \tag{2.66}$$

where $\mathbf{B}(\nu) = (\nu_1\mathbf{A}_1 + \nu_2\mathbf{A}_2 + \nu_3\mathbf{A}_3)$.

Step 1: Diagonalization $\mathbf{A}_0$ *and* $\mathbf{B}(\nu)$ *simultaneously.* The matrix $\mathbf{A}_0$ is symmetric positive definite and $\mathbf{B}(\nu)$ is symmetric. In this step we construct a non-singular matrix $\mathbf{T}(\nu)$ and a diagonal matrix $\mathbf{D}(\nu) = diag(d_k(\nu),\ k = 1,2,...,9)$ with real valued elements such that

$$\mathbf{T}^*(\nu)\mathbf{A}_0\mathbf{T}(\nu) = \mathbf{I},\ \mathbf{T}^*(\nu)\mathbf{B}(\nu)\mathbf{T}(\nu) = \mathbf{D}(\nu), \tag{2.67}$$

where $\mathbf{I}$ is the identity matrix, $\mathbf{T}^*(\nu)$ is the transposed matrix to $\mathbf{T}(\nu)$.

Computing $\mathbf{T}(\nu)$ and $\mathbf{D}(\nu)$ can be made by the following way: we find $\mathbf{A}_0^{-1/2}$ and then using the matrix $\mathbf{A}_0^{-1/2}\mathbf{B}(\nu)\mathbf{A}_0^{-1/2}$ we construct $\mathbf{T}(\nu)$ and $\mathbf{D}(\nu)$.

Finding $\mathbf{A}_0^{-1/2}$. For the given positive definite matrix $\mathbf{A}_0$ we compute an orthogonal matrix $\mathcal{R}$ by the eigenfunctions of $\mathbf{A}_0$ such that $\mathcal{R}^*\mathbf{A}_0\mathcal{R} = \mathcal{L}$, where $\mathcal{R}^*$ is the transpose matrix to $\mathcal{R}$ and $\mathcal{L} = diag(\lambda_k,\ k = 1,2,...,9)$ is the diagonal matrix with positive elements λ_k which are eigenvalues of $\mathbf{A}_0$. The matrix $\mathcal{L}^{1/2}$ is defined by the formula $\mathcal{L}^{1/2} = diag(\sqrt{\lambda_k},\ k = 1,2,...,9)$ and $\mathbf{A}_0^{1/2}$ is defined by $\mathbf{A}_0^{1/2} = \mathcal{R}\mathcal{L}^{1/2}\mathcal{R}^*$.

The matrix $\mathbf{A}_0^{-1/2}$ is the inverse to $\mathbf{A}_0^{1/2}$.

Finding $\mathbf{T}(\nu)$ *and* $\boldsymbol{D}(\nu)$. Let matrix $\mathbf{B}(\nu)$ be given and matrix $\mathbf{A}_0^{-1/2}$ be found.

Let us consider the matrix $\mathbf{A}_0^{-1/2}\mathbf{B}(\nu)\mathbf{A}_0^{-1/2}$ which is symmetric with real valued elements. The diagonal matrix $\mathbf{D}(\nu)$ is constructed by eigenvalues of $\mathbf{A}_0^{-1/2}\mathbf{B}(\nu)\mathbf{A}_0^{-1/2}$. The columns of the orthogonal matrix $Q(\nu)$ are formed by normalized orthogonal eigenfunctions of $\mathbf{A}_0^{-1/2}\mathbf{B}(\nu)\mathbf{A}_0^{-1/2}$ corresponding to eigenvalues $d_k(\nu),\ k=1,2,...,9$. The matrix $\mathbf{T}(\nu)$ is defined by the formula $\mathbf{T}(\nu)=\mathbf{A}_0^{-1/2}Q(\nu)$.

Step 2: Deriving a solution of (2.65)-(2.66). Let $\mathbf{D}(\nu)$ and $\mathbf{T}(\nu)$, satisfying (2.67), be constructed. We find the solution of (2.65)-(2.66) in the form

$$\tilde{\mathbf{V}}^m(\nu,t)=\mathbf{T}(\nu)\mathbf{Y}^m(\nu,t), \tag{2.68}$$

where $\mathbf{Y}^m(\nu,t)$ is unknown vector function. Substituting (2.68) into (2.65)-(2.66) and then multiplying the obtained vector differential equation by $\mathbf{T}^*(\nu)$ and using (2.67) we find

$$\frac{\partial \mathbf{Y}^m}{\partial t}-i\mathbf{D}(\nu)\mathbf{Y}^m = \mathbf{T}^*(\nu)\mathsf{E}^m\delta(t),\ t\in R \tag{2.69}$$

$$\mathbf{Y}^m(\nu,t)|_{t\le 0} = 0. \tag{2.70}$$

Using the ordinary differential equations technique (see, for example, Boyce & DiPrima (1992)), a solution of this initial value problem (2.69)-(2.70) is given by

$$\mathbf{Y}^m(\nu,t)=\theta(t)\left[\cos(\mathbf{D}(\nu)t)+i\sin(\mathbf{D}(\nu)t)\right]\mathbf{T}^*(\nu)\mathsf{E}^m,$$

where $\theta(t)$ is the Heaviside function, i.e. $\theta(t)=1$ for $t\ge 0$ and $\theta(t)=0$ for $t<0$; $\cos(\mathbf{D}(\nu)t)$ and $\sin(\mathbf{D}(\nu)t)$ are diagonal matrices whose diagonal elements are $\cos(d_k(\nu)t)$ and $\sin(d_k(\nu)t),\ k=1,2,...,9$, respectively.

Finally, a solution of (2.65)-(2.66) is determined by

$$\tilde{\mathbf{V}}^m(\nu,t) = \theta(t)\mathbf{T}(\nu)\left[\cos(\mathbf{D}(\nu)t) + i\sin(\mathbf{D}(\nu)t)\right]\mathbf{T}^*(\nu)\mathsf{E}^m. \tag{2.71}$$

Step 3: Deriving a solution of Problem (2.38). Noting that every solution of (2.38) is a real valued vector function and using formulae (2.54), (2.71) we find that a solution of (2.38) is given by

$$\mathbf{V}^m(x,t) = \frac{\theta(t)}{(2\pi)^3}\int\limits_{-\infty}^{\infty}\int\limits_{-\infty}^{\infty}\int\limits_{-\infty}^{\infty}\mathbf{T}(\nu)\cos\Big(\mathbf{D}(\nu)t - \mathbf{I}(\nu\cdot x)\Big)\mathbf{T}^*(\nu)\mathsf{E}^m d\nu_1 d\nu_2 d\nu_3, \tag{2.72}$$

where $\cos\Big(\mathbf{D}(\nu)t - \mathbf{I}(\nu\cdot x)\Big)$ is the diagonal matrix with diagonal elements $\cos\Big(d_k(\nu)t - \nu\cdot x\Big),\ k = 1,2,...,9.$

2.2.3 Explicit formulae for FS of displacement, displacement speed and stress

Let $\mathsf{E}^m,\ m = 1,2,3,$ be defined in the statement of (2.38). Let us consider the formula (2.72). The first three components of the vector function $\mathbf{V}^m(x,t)$ in (2.72) are elements of m-th column of the matrix $\frac{\partial G(x,t)}{\partial t}$, where $G(x,t)$ is FS of anisotropic elasticity (fundamental solution of AES). To find m-th column of $G(x,t)$ we need to integrate the right hand side of (2.72) with respect to t from zero to t. Since $\mathbf{T}(\nu),\mathbf{T}^*(\nu),\mathsf{E}^m$ do not depend on t the integration of the right hand side of (2.72) is related with the calculation of the integral of the matrix $\cos(\mathbf{D}(\nu)\tau - \mathbf{I}(\nu\cdot x))$ with respect to τ from 0 to t. We find this integral explicitly. The result of this integration is

the matrix $\mathbf{S}(\nu,t,x)$ whose elements are found by formulae

$$\begin{aligned} S_{kj}(\nu,t,x) &= 0,\ j \neq k; \\ S_{kk}(\nu,t,x) &= t\cos(\nu\cdot x)\ if\ d_k(\nu)=0; \\ S_{kk}(\nu,t,x) &= \frac{\sin(d_k(\nu)t-\nu\cdot x)}{d_k(\nu)}+\frac{\sin(\nu x)}{d_k(\nu)}\ if\ d_k(\nu)\neq 0;\ k,j=1,...,9. \end{aligned} \quad (2.73)$$

As a result of it we find explicit formulae for components of the vector function $\mathbf{u}^m$ (m-th column of $G(x,t)$) in the form

$$u_n^m(x,t)=\frac{\theta(t)}{(2\pi)^3}\int_{-\infty}^{\infty}\int_{-\infty}^{\infty}\int_{-\infty}^{\infty}[\mathbf{T}(\nu)\mathbf{S}(\nu,t,x)\mathbf{T}^*(\nu)\mathsf{E}^m]_n d\nu_1 d\nu_2 d\nu_3, \quad (2.74)$$

where $n=1,2,3$; elements of the matrix $\mathbf{S}(\nu,t,x)$ are defined by (2.73); $[\mathbf{T}(\nu)\mathbf{S}(\nu,t,x)\mathbf{T}^*(\nu)\mathsf{E}^m]_n$ is the n-th component of the vector $\mathbf{T}(\nu)\mathbf{S}(\nu,t,x)\mathbf{T}^*(\nu)\mathsf{E}^m$.

The last six components of the vector function $\mathbf{V}^m(x,t)$ in (2.72) are fundamental solution of stress. The first three components of the vector function $\mathbf{V}^m(x,t)$ in (2.72) are fundamental solution of displacement speed.

2.2.4 Formulae of the displacement, displacement speed and stress from an arbitrary force

As one of important applications of FS we describe the derivation of the displacement, displacement speed and stress arising from an arbitrary force in the considered anisotropic media. Here we base on the suggested method for the FS construction. Let $\mathbf{G}(x,t)$ be FS of SHSE and $\widetilde{\mathbf{G}}(\nu,t)$ be the Fourier transform of $\mathbf{G}(x,t)$ with respect to the space variable $x=(x_1,x_2,x_3)\in R^3$. We note that the first three components of the vector function $\widetilde{\mathbf{V}}^m(\nu,t)$ defined by (2.71) for E^m are components of m-th column of $\frac{\partial}{\partial t}\widetilde{G}(\nu,t)$. Integrating (2.71) with respect to t from 0 to t we find

components of m-th column of $\widetilde{G}(\nu,t)$ (FS of AES) by the following formulae

$$\widetilde{u}_n^m(\nu,t) = \theta(t)[\mathbf{T}(\nu)P(\nu,t)\mathbf{T}^*(\nu)\mathsf{E}^m]_n, \tag{2.75}$$

where $n = 1,2,3$, $P(\nu,t)$ is the diagonal matrix whose diagonal elements are defined by

$$\begin{aligned} P_{kk}(\nu,t) &= t \ for \ d_k(\nu) = 0, \\ P_{kk}(\nu,t) &= \frac{\sin(d_k(\nu)t)}{d_k(\nu)} + i\frac{(1-\cos(d_k(\nu)t))}{d_k(\nu)} \ for\, d_k(\nu) \neq 0;\ k = 1,...,9 \end{aligned} \tag{2.76}$$

This means that the Fourier image $\widetilde{G}(\nu,t)$ of $G(x,t)$ can be derived immediately after steps 1 and 2 by formulae (2.75), (2.76). The Fourier image $\widetilde{G}(\nu,t)$ of FS can be applied for the computation of the displacement $\mathbf{u}(x,t) = (u_1(x,t),u_2(x,t),u_3(x,t))$ arising from an arbitrary given force $\mathbf{f}(x,t) = (f_1(x,t),f_2(x,t),f_3(x,t))$ satisfying $\mathbf{f}(x,t)$ for $t < 0$. Really, let $\widetilde{\mathbf{f}}(\nu,t)$ be the Fourier transform of $\mathbf{f}(x,t)$ with respect to $x = (x_1,x_2,x_3) \in R^3$. Then

$$\mathbf{u}(x,t) = \frac{\theta(t)}{(2\pi)^3}\int_0^t\int_{-\infty}^{\infty}\int_{-\infty}^{\infty}\int_{-\infty}^{\infty}\widetilde{G}(\nu,t-\tau)\widetilde{\mathbf{f}}(\nu,\tau)e^{-i\nu\cdot x}d\nu_1 d\nu_2 d\nu_3 d\tau. \tag{2.77}$$

Similarly, the computation of the displacement speed and stress arising from an arbitrary given force $\mathbf{F}(x,t) = (f_1(x,t),f_2(x,t),f_3(x,t),0,0,0,0,0,0)$ satisfying $\mathbf{F}(x,t)$ for $t < 0$ are given by

$$\mathbf{V}(x,t) = \frac{\theta(t)}{(2\pi)^3}\int_0^t\int_{-\infty}^{\infty}\int_{-\infty}^{\infty}\int_{-\infty}^{\infty}\widetilde{\mathbf{G}}(\nu,t-\tau)\widetilde{\mathbf{F}}(\nu,\tau)e^{-i\nu\cdot x}d\nu_1 d\nu_2 d\nu_3 d\tau. \tag{2.78}$$

2.2.5 Computational examples

2.2.5.1 General characteristics of computations and visualizations

We have implemented two types of computational experiments. The first one shows a high accuracy in computing values of FSs in terms of wave-vector variables for isotropic (transversely isotropic) elastic indefinite media. In these experiments we consider the isotropic material Sillica (SiO_2) and transversely isotropic material graphite-epoxy composite. The values of FSs have been derived for these materials in two ways: by explicit formulae as well as by the method of Section 2.2.2. The results of the comparison are presented in Tables 2.1-2.2. Moreover, we have obtained that values of the FSs found by the method of Sections 2.2.2, 2.2.3 can be efficiently used for the computation of integrals when the integral contains the FS as terms.

In the second type of computational experiments we have considered three homogenous anisotropic materials with trigonal, monoclinic and triclinic structures of anisotropy, respectively. They are aluminium oxide (Al_2O_3), diopside ($CaMgSi_2O_6$) and albite ($NaAlSi_3O_8$). For these experiments we have taken the pulse force situated in each material and modeled by $\mathbf{e}^3\delta(x_1)\delta(x_2)\delta(x_3)\delta(t)$, where $\mathbf{e}^3 = (0,0,1)$, $\delta(\cdot)$ is the Dirac delta function. The responses of the considered anisotropic materials on this source are the displacement, displacement speed and stress vectors depending on the position and the time. Using the method of Sections 2.2.2, 2.2.3 (see steps 1-3) we compute $\mathbf{T}(\nu), \mathbf{T}^*(\nu), \mathbf{D}(\nu)$ and then using the formula (2.72), (2.74) we have derived numerically components of $\mathbf{u}^3$ and $\mathbf{V}^3$.

The pulse point force $\mathbf{e}^3\delta(x_1)\delta(x_2)\delta(x_3)\delta(t)$ produces diverging elastic waves. The behavior of elastic fields (dynamics of wave propagations, the traces of fronts and distribution of magnitudes of the displacement for three different anisotropic media

(aluminum oxide, diopside and albite) are presented in the form of components $\mathbf{u}^3$ in the Figures 2.8-2.10. The traces of fronts and distribution of magnitudes of the displacement, displacement speed and stress for triclinic anisotropic media (albite) are presented in the form of the second and fifth components $\mathbf{V}^3$ in the Figures 2.11-2.12.

2.2.5.2 Description of input data and corresponding images

Example 1. **Isotropic material - sillica(SiO_2)**

The density and Lame parameters of this material are equal to (Dieulesaint & Royer (2000))

$$\rho = 2.203(10^3 kg/m^3),\ \lambda = 1.61,\ \mu = 3.12(10^{10} Pa).$$

For this example we take the pulse force of the form $\mathbf{e}^1\delta(x_1)\delta(x_2)\delta(x_3)\delta(t)$, where $\mathbf{e}^1 = (1,0,0)$. Using the method of Section 2.2.2 we compute $\mathbf{T}(\nu)$, $\mathbf{T}^*(\nu)$, $\mathbf{D}(\nu)$ and then using the formulae (2.75), (2.76) we find elements of the FS (matrix) $\widetilde{G}(\nu,t)$ in terms of wave-vector values $\nu = (\nu_1,\nu_2,\nu_3)$ for any fixed time t. The first column of this FS is the displacement vector $\widetilde{\mathbf{u}}^1(\nu,t) = (\widetilde{u}_1^1(\nu,t),\widetilde{u}_2^1(\nu,t),\widetilde{u}_3^1(\nu,t))$ depending on wave-vector parameter $\nu = (\nu_1,\nu_2,\nu_3)$ and time t. On the other hand for the pulse force $\mathbf{e}^1\delta(x_1)\delta(x_2)\delta(x_3)\delta(t)$ we can use the explicit formula for the first column of FS for isotropic elastic infinite materials (Aki & Richard (1980), Kausel (2006)). We denote the FS for isotropic elastic materials in terms of wave-vector and time variables as $\widetilde{\mathcal{E}}(\nu,t)$ and in terms of space and time variables as $\mathcal{E}(x,t)$. Here $\nu = (\nu_1,\nu_2,\nu_3)$ is the wave-vector variable and $x = (x_1,x_2,x_3)$ is the space variable. The components of

the first column of $\widetilde{\mathcal{E}}(\nu,t)$ can be written explicitly as follows

$$\begin{aligned}
\widetilde{\mathcal{E}}_1^1(\nu,t) &= \frac{\theta(t)}{\rho \mid \nu \mid^3}\{\frac{\sin(C_T \mid \nu \mid t)}{C_T}(\nu_2^2+\nu_3^2)+\frac{\sin(C_L \mid \nu \mid t)}{C_L}\nu_1^2\}, \qquad (2.79)\\
\widetilde{\mathcal{E}}_2^1(\nu,t) &= \frac{\theta(t)}{\rho \mid \nu \mid^3}\nu_2\nu_1\{\frac{\sin(C_L \mid \nu \mid t)}{C_L}-\frac{\sin(C_T \mid \nu \mid t)}{C_T}\},\\
\widetilde{\mathcal{E}}_3^1(\nu,t) &= \frac{\theta(t)}{\rho \mid \nu \mid^3}\nu_3\nu_1\{\frac{\sin(C_L \mid \nu \mid t)}{C_L}-\frac{\sin(C_T \mid \nu \mid t)}{C_T}\},
\end{aligned}$$

where $C_T^2=\frac{\mu}{\rho},\ C_L^2=\frac{\lambda+2\mu}{\rho}$.

Some values of $\widetilde{u}_1^1(\nu,t)$ and $\widetilde{\mathcal{E}}_1^1(\nu,t)$ and their comparison are given in Table 2.1. In this table the following notations are used: $\Delta = 25.10^{-4}$; $\widetilde{\mathcal{E}}_1^1(\nu_1,\nu_2,\nu_3,t)$ are values computed by the formula (2.79); $\widetilde{u}_1^1(\nu_1,\nu_2,\nu_3,t)$ are values of the first component of the first column of FS $\tilde{G}(\nu_1,\nu_2,\nu_3,t)$ computed by our method; $\widetilde{u}_1^1-\widetilde{\mathcal{E}}_1^1$ are values of $\widetilde{u}_1^1(\nu_1,\nu_2,\nu_3,t)-\widetilde{\mathcal{E}}_1^1(\nu_1,\nu_2,\nu_3,t)$ which mean the error between values $\widetilde{u}_1^1(\nu_1,\nu_2,\nu_3,t)$ found by our method and exact values $\widetilde{\mathcal{E}}_1^1(\nu_1,\nu_2,\nu_3,t)$.

Using computed values $\mathbf{T}(\nu)$ and $\mathbf{D}(\nu)$ (2.73)-(2.74), we can derive $u_1^1(x_1,x_2,x_3,t)$ and then compute numerically the integral

$$g_1^1(z,t)=\int_0^t\int_{-\infty}^{\infty}u_1^1(x_1,x_2,x_3,\tau)dx_1d\tau\mid_{x_2=x_3=z}.$$

At the same time the integral

$$e_1^1(z,t)=\int_0^t\int_{-\infty}^{\infty}\mathcal{E}_1^1(x_1,x_2,x_3,\tau)dx_1d\tau\mid_{x_2=x_3=z}$$

can be derived explicitly as follows

$$e_1^1(z,t) = \frac{1}{2\pi\rho C_T^2}[\ln\left(t+\sqrt{t^2-(\frac{\mid x \mid}{C_T})^2}\right)-\ln\left(\frac{\mid x \mid}{C_T}\right)].$$

The graphs of functions $g_1^1(z,t)$ and $e_1^1(z,t)$ for $t=1$ and their comparison are presented

in the Fig.2.6.

Example 2. **Transversely isotropic solid - graphite-epoxy composite**

The elastic constants in units of $10^{10}Pa$ are given by (Wang & Achenbach (1994))

$$\begin{aligned} c_{11} &= c_{22} = 13.92,\ c_{12} = c_{21} = 6.92, \\ c_{13} &= c_{23} = c_{31} = c_{32} = 6.44,\ c_{33} = 160.7, \\ c_{44} &= c_{55} = 7.07\ c_{66} = \frac{13.92 - 160.7}{2}. \end{aligned}$$

Other elastic constants are equal to zero. The density $\rho = 1(10^3 kg/m^3)$.

In this example we take the pulse force of the form $\mathbf{e}^2\delta(x_1)\delta(x_2)\delta(x_3)\delta(t)$, where $\mathbf{e}^2 = (0,1,0)$. Using the method of Section 2.2.2 we compute $\mathbf{T}(\nu)$, $\mathbf{T}^*(\nu)$, $\mathbf{D}(\nu)$ and then using the formulae (2.75), (2.76) we find elements of the fundamental matrix $\widetilde{G}(\nu,t)$ in terms of wave-vector values $\nu = (\nu_1,\nu_2,\nu_3)$ for the fixed time t. The second column of the fundamental matrix is the displacement $\widetilde{\mathbf{u}}^2(\nu,t) = (\widetilde{u}_1^2(\nu,t),\widetilde{u}_2^2(\nu,t),\widetilde{u}_3^2(\nu,t))$ depending on wave-vector parameter $\nu = (\nu_1,\nu_2,\nu_3)$ and time t. On the other hand for the pulse force $\mathbf{e}^2\delta(x_1)\delta(x_2)\delta(x_3)\delta(t)$ we can use the explicit formula for the second column of $\widetilde{\mathcal{E}}(\nu,t)$ for $\nu_2 = 0$. Here $\widetilde{\mathcal{E}}(\nu,t)$ is the FS of transversely isotropic material (graphite-epoxy composite) in terms of wave-vector variable $\nu = (\nu_1,\nu_2,\nu_3)$ and time variable t. The components of the second column of $\widetilde{\mathcal{E}}(\nu,t)$ for $\nu_2 = 0$ can be written explicitly as follows

$$\begin{aligned} \widetilde{\mathcal{E}}_1^2(\nu,t) &= \widetilde{\mathcal{E}}_3^2(\nu,t) = 0,\ (\nu_2 = 0) \\ \widetilde{\mathcal{E}}_2^2(\nu,t)\mid_{\nu_2=0} &= \frac{\theta(t)}{\sqrt{\rho(c_{66}\nu_1^2 + c_{44}\nu_3^2)}} \sin\left(t\sqrt{\frac{(c_{66}\nu_1^2 + c_{44}\nu_3^2)}{\rho}}\right). \end{aligned} \quad (2.80)$$

Values of $\widetilde{u}_2^2(\nu,t)$, $\widetilde{\mathcal{E}}_2^2(\nu,t)$ for $\nu_2 = 0$ and their comparison are given in Table 2.2. In this table the following notations are used: $\Delta = 25.10^{-4}$; $\widetilde{\mathcal{E}}_2^2(\nu_1,0,\nu_3,t)$ are values

computed by the formula (2.80); $\widetilde{u}_2^2(\nu_1,0,\nu_3,t)$ are values of the second component of the second column of FS $\tilde{G}(\nu_1,0,\nu_3,t)$ computed by our method. $\widetilde{u}_2^2-\widetilde{\mathcal{E}}_2^2$ are values of $\widetilde{u}_2^2(\nu_1,0,\nu_3,t)-\widetilde{\mathcal{E}}_2^2(\nu_1,0,\nu_3,t)$ which mean the error between values $\widetilde{u}_2^2(\nu_1,0,\nu_3,t)$ found by our method and exact values $\widetilde{\mathcal{E}}_2^2(\nu_1,0,\nu_3,t)$.

Using computed values $\mathbf{T}(\nu)$, $\mathbf{D}(\nu)$ and formulae (2.73), (2.74) we derive the second column $\mathbf{u}^2(x,t)$ of the fundamental matrix $G(x,t)$ for graphite-epoxy composite in terms of space and time variables and then compute numerically the integral

$$g_2^2(z,t)=\int_0^t\int_{-\infty}^{\infty}u_2^2(x_1,x_2,x_3,t-\tau)f(\tau)dx_2d\tau\,|_{x_1=x_3=z},$$

where $u_2^2(x_1,x_2,x_3,t)$ is the second component of the vector column $\mathbf{u}^2(x,t)$, $x=(x_1,x_2,x_3)$; $f(\tau)=\tau^2\exp(-3\tau^2)$ (see similar example in Wang & Achenbach (1994)).

Let $\mathcal{E}(x,t)$ be the FS of the graphite-epoxy composite in terms of the space and time variables; $\mathcal{E}_2^2(x,t)$ be the second element of the second column of $\mathcal{E}(x,t)$. We can derive explicitly

$$\int_{-\infty}^{\infty}\mathcal{E}_2^2(x_1,x_2,x_3,t)dx_2=\frac{\theta(t-\sqrt{\frac{x_1^2\rho}{c_{66}}+\frac{x_3^2\rho}{c_{44}}})}{2\pi\sqrt{c_{66}c_{44}}\sqrt{t^2-(\frac{x_1^2\rho}{c_{66}}+\frac{x_3^2\rho}{c_{44}})}}$$

and then, compute the integral

$$\begin{aligned}e_2^2(z,t) &= \int_0^t\int_{-\infty}^{\infty}\mathcal{E}_2^2(x_1,x_2,x_3,\tau)f(\tau)dx_2d\tau|_{x_1=x_3=z}\\ &= \frac{1}{2\pi}\int_0^t\frac{\theta(t-\tau-\sqrt{\frac{x_1^2\rho}{c_{66}}+\frac{x_3^2\rho}{c_{44}}})}{\sqrt{c_{66}c_{44}}\sqrt{(t-\tau)^2-(\frac{x_1^2\rho}{c_{66}}+\frac{x_3^2\rho}{c_{44}})}}f(\tau)d\tau.\end{aligned}$$

The graphs of functions $g_2^2(z,t)$ and $e_2^2(z,t)$ for $t=1$ and their comparison are

presented on the Fig.2.7.

Example 3. **A crystal of trigonal anisotropic structure - aluminum oxide(Al_2O_3)**

The density ρ is equal to $3.986(10^3 kg/m^3)$ and the matrix of elastic moduli $C = (c_{\alpha\beta})_{6\times 6}$ is given by (see, for example, Dieulesaint & Royer (2000))

$$\begin{aligned} c_{11} &= 49.7,\ c_{12} = c_{21} = 16.4,\ c_{13} = c_{31} = 11.2, \\ c_{14} &= c_{41} = -2.35,\ c_{33} = 49.9,\ c_{44} = 14.7 \\ c_{56} &= c_{65} = -2.35,\ c_{66} = \frac{49.7 - 16.4}{2}(10^{10} Pa). \end{aligned}$$

Other elements of the symmetric matrix **C** are equal to zero. Fig.2.8 show dynamic of the distribution the first component of the displacement $\mathbf{u}^3(x_1, 0, x_3, t)$ in the aluminum oxide at $t = 0.8$. Fig.2.8 contain screen shot of 2-D level plot of the same surface $u_1^3(x_1, 0, x_3, 0.8)$, i.e. a view of the surface from the top of z-axis. The figure illustrate the behavior of the first component of the displacement vector $\mathbf{u}^3(x_1, 0, x_3, t)$ in aluminum oxide at $t = 0.8$.

Example 4. **A crystal of the monoclinic structure - diopside($CaMgSi_2O_6$)**

The density $\rho = 3.31(10^3 kg/m^3)$ and elements of the matrix $\mathbf{C} = (c_{\alpha\beta})_{6\times 6}$ are defined by (see, for example, Alexandrov (1964))

$$\begin{aligned} c_{11} &= 2.040,\ c_{12} = c_{21} = 0.884,\ c_{13} = c_{31} = 0.0883,\ c_{15} = c_{51} = -0.193, \\ c_{22} &= 1.750,\ c_{23} = c_{32} = 0.482,\ c_{25} = c_{52} = -0.196,\ c_{33} = 2.38, \\ c_{35} &= c_{53} = -0.336,\ c_{44} = 0.675,\ c_{46} = c_{64} = -0.113,\ c_{55} = 0.588, \\ c_{66} &= 0.705(10^{11} Pa). \end{aligned}$$

Other elements are equal to zero. Fig.2.9 presents of the first component of the

displacement speed $\mathbf{u}^3(x_1,0,x_3,t)$ at the time $t=3$ in diopside. The different colors correspond to different values $u_1^3(x_1,0,x_3,3)$. Fig.2.9 present the view from the top of z-axis.

Example 5. **A crystal of the triclinic structure - albite($NaAlSi_3O_8$)**

The density $\rho = 2(10^3 kg/m^3)$ and elastic moduli $\mathbf{C} = (c_{\alpha\beta})_{6\times 6}$ are defined by (see, for example, Brown & Abramson & Angel (2006))

$$\begin{aligned}
c_{11} &= 69.1,\ c_{12}=c_{21}=34.0,\ c_{13}=c_{13}=30.8,\ c_{14}=c_{41}=5.1,\\
c_{15} &= c_{15}=-2.4,\ c_{16}=c_{61}=-0.9\ c_{22}=183.5,\ c_{23}=c_{32}=5.5,\\
c_{24} &= c_{42}=-3.9\ c_{25}=c_{52}=-7.7,\ c_{26}=c_{62}=-5.8,\ c_{33}=179.5\\
c_{34} &= c_{43}=-8.7,\ c_{35}=c_{53}=7.1,\ c_{36}=c_{63}=-9.8,\ c_{44}=24.9,\\
c_{45} &= c_{54}=-2.4,\ c_{46}=c_{64}=-7.2\ c_{55}=26.8,\ c_{56}=c_{65}=0.5, c_{66}=33.5(GPa).
\end{aligned}$$

Fig.2.10 show the first component of the displacement $\mathbf{u}^3(x_1,0,x_3,t)$, at the time $t=0.3$ in albite. Fig.2.11, Fig.2.12 show the second component of the displacement speed and stress of $\mathbf{V}^3(x_1,0,x_3,t)$, at the time $t=0.3$ in albite. Fig.2.10-Fig.2.12 present the view from the top of z-axis.

2.2.5.3 Analysis of the visualization

The simulation of the displacement, displacement speed, stress components in general anisotropic media by modern computer tools allow us to see and evaluate dependence between media structures and behavior of displacement, displacement speed, stress components. The method allows users to observe the elastic wave propagation arising from pulse point sources of the form $\mathbf{e}^m\delta(x_1)\delta(x_2)\delta(x_3)\delta(t)$ in trigonal, monoclinic, triclinic and other anisotropic materials. We can see in the

Figures 2.8 - 2.12 that the different anisotropic structures of media produce different responses of displacement, displacement speed, stress inside these media. The visualization of the displacement components, presented on the Figures 2.8 - 2.12 gives knowledge about the form of fronts of elastic wave propagations in aluminum oxide, diopside and albite. We see that fronts are not spherical and have very peculiar forms.

Table 2.1. The accuracy of computing $\widetilde{u}_1^1(\nu_1,\nu_2,\nu_3,t)$ in isotropic material sillica (SiO_2)

t	ν_1	ν_2	ν_3	$\widetilde{u}_1^1(\nu_1,\nu_2,\nu_3,t)$	$\widetilde{u}_1^1-\widetilde{\mathcal{E}}_1^1$
1	Δ	Δ	Δ	0.4539234397	-0.4×10^{-15}
	Δ	$\Delta\times10$	$\Delta\times10^2$	0.4471914039	0.3×10^{-12}
	$\Delta\times10$	$\Delta\times10^2$	$\Delta\times10^5$	$0.1227898668\times10^{-2}$	0.5×10^{-11}
	$\Delta\times10^5$	$\Delta\times10^5$	$\Delta\times10^5$	$0.1540383945\times10^{-3}$	0.3×10^{-10}
2	Δ	Δ	Δ	0.9078287344	-0.3×10^{-14}
	Δ	$\Delta\times10$	$\Delta\times10^2$	0.8546908803	0.2×10^{-11}
	$\Delta\times10$	$\Delta\times10^2$	$\Delta\times10^5$	$-0.1457632983\times10^{-2}$	0.5×10^{-11}
	$\Delta\times10^5$	$\Delta\times10^5$	$\Delta\times10^5$	$0.2754393629\times10^{-3}$	0.6×10^{-10}
3	Δ	Δ	Δ	1.361697740	-0.1×10^{-13}
	Δ	$\Delta\times10$	$\Delta\times10^2$	1.186330242	0.7×10^{-11}
	$\Delta\times10$	$\Delta\times10^2$	$\Delta\times10^5$	$0.5024509308\times10^{-3}$	-0.3×10^{-10}
	$\Delta\times10^5$	$\Delta\times10^5$	$\Delta\times10^5$	$0.3418815169\times10^{-3}$	0.7×10^{-10}

Table 2.2. The accuracy of computing $\widetilde{u}_2^2(\nu_1, 0, \nu_3, t)$ in transversely isotropic material graphite epoxy composite.

t	ν_1	ν_3	$\widetilde{u}_2^2(\nu_1, 0, \nu_3, t)$	$\widetilde{u}_2^2 - \widetilde{\mathcal{E}}_2^2$
1	Δ	Δ	0.9999889896	0
	Δ	$\Delta \times 10^4$	$-0.7215342900 \times 10^{-2}$	-0.9×10^{-18}
	$\Delta \times 10$	$\Delta \times 10$	0.9988993220	0
	$\Delta \times 10^5$	$\Delta \times 10^5$	$0.9514609420 \times 10^{-3}$	-0.4×10^{-16}
2	Δ	Δ	1.999911918	-0.2×10^{-15}
	Δ	$\Delta \times 10^4$	$0.1266250282 \times 10^{-1}$	0.2×10^{-17}
	$\Delta \times 10$	$\Delta \times 10$	1.991203297	0
	$\Delta \times 10^5$	$\Delta \times 10^5$	$-0.1206444628 \times 10^{-2}$	-0.3×10^{-16}
3	Δ	Δ	2.999702728	0
	Δ	$\Delta \times 10^4$	$-0.1500660552 \times 10^{-1}$	0.2×10^{-16}
	$\Delta \times 10$	$\Delta \times 10$	2.970360126	0
	$\Delta \times 10^5$	$\Delta \times 10^5$	$0.5783008964 \times 10^{-3}$	0.2×10^{-15}
4	Δ	Δ	3.999295371	-0.4×10^{-15}
	Δ	$\Delta \times 10^4$	$0.1367320809 \times 10^{-1}$	0
	$\Delta \times 10$	$\Delta \times 10$	3.929904814	0
	$\Delta \times 10^5$	$\Delta \times 10^5$	$0.4731638603 \times 10^{-3}$	-0.3×10^{-15}

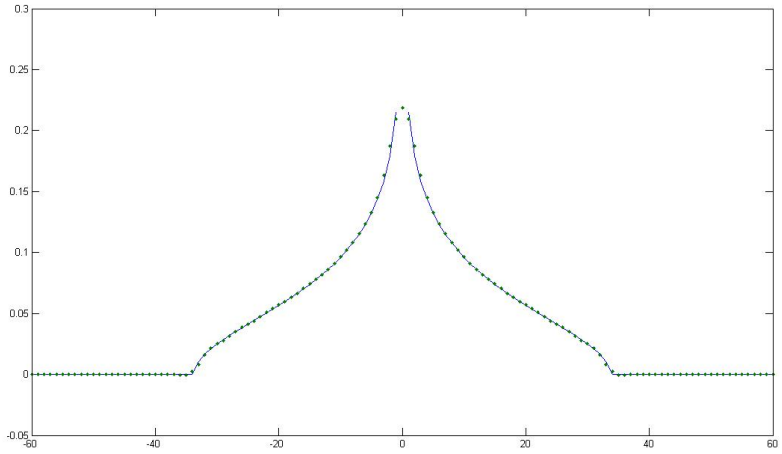

Figure 2.6: Graphs of $g_1^1(z,t)$ and $e_1^1(z,t)$. The dotted line represents $g_1^1(z,t)$ at $t = 1$ (our method). The continuous line represents $e_1^1(z,t)$ at $t = 1$ (the explicit formula (2.80)).

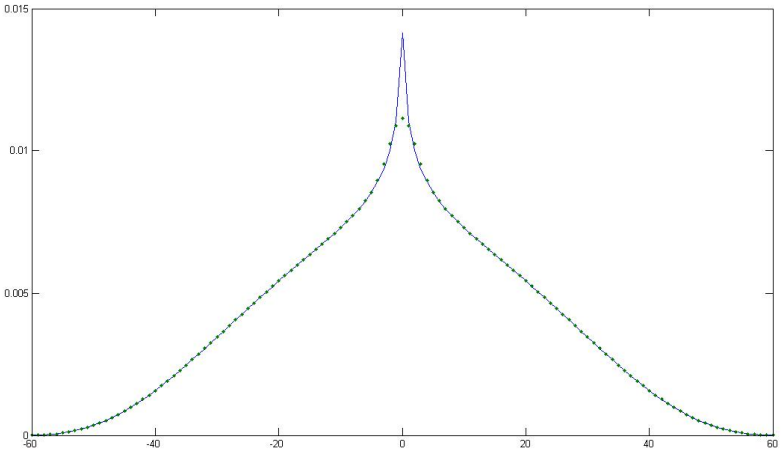

Figure 2.7: Graphs of $g_2^2(z,t)$ and $e_2^2(z,t)$. The dotted line represents $g_2^2(z,t)$ at $t = 1$ (our method). The continuous line represents $e_2^2(z,t)$ at $t = 1$ (the explicit formula (2.81)).

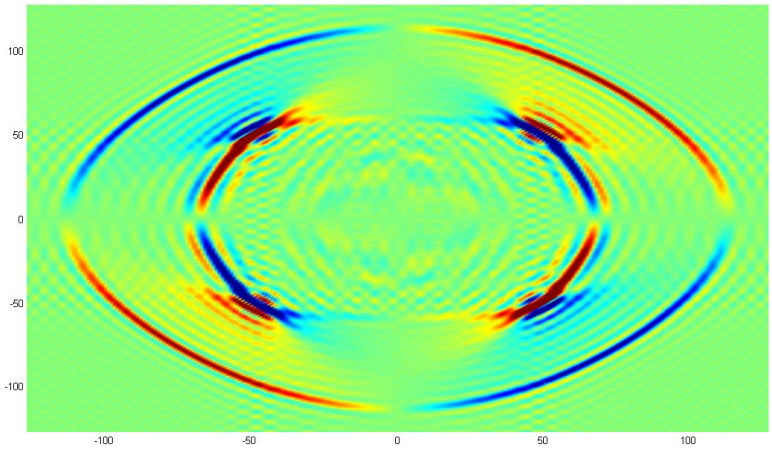

Figure 2.8: 2-*D* plot of the first component of the displacement $\mathbf{u}^3(x_1,0,x_3,t)$ for $t = 0.8$ in aluminum oxide (trigonal structure of anisotropy)

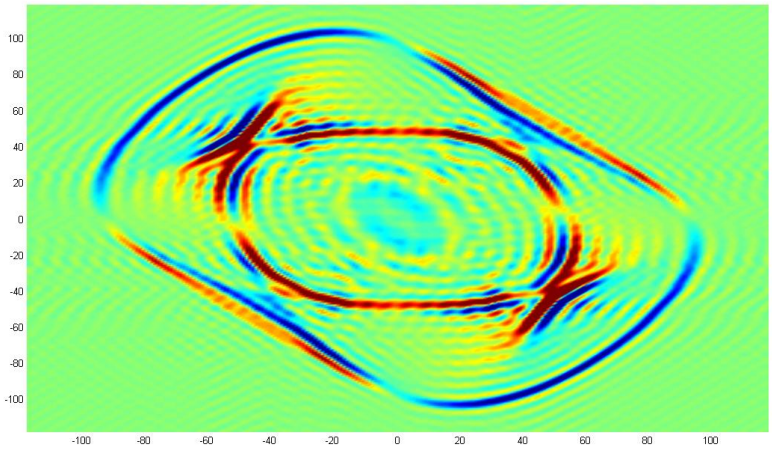

Figure 2.9: 2-*D* plot of the first component for the displacement $\mathbf{u}^3(x_1,0,x_3,t)$ for $t = 3$ in diopside (monoclinic structure of anisotropy)

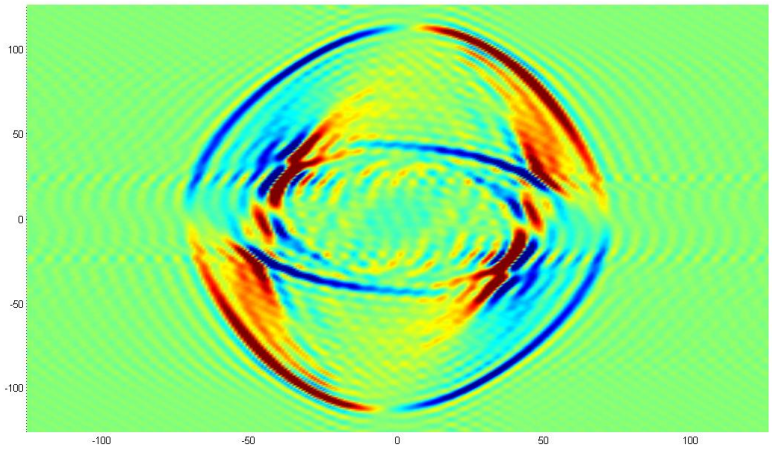

Figure 2.10: 2-*D* plot of the first component of the displacement $\mathbf{u}^3(x_1,0,x_3,t)$ for $t = 0.3$ in albite (triclinic structure of anisotropy)

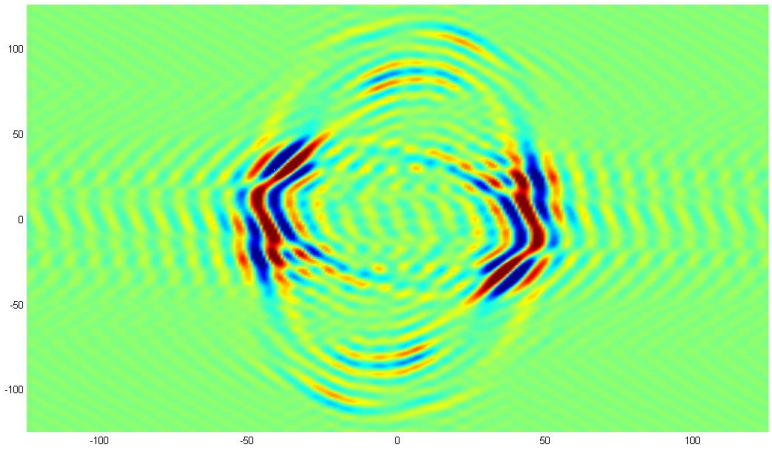

Figure 2.11: 2-*D* plot of the second component of the displacement speed $\mathbf{V}_2^3(x_1,0,x_3,t)$ for $t = 0.3$ in albite (triclinic structure of anisotropy)

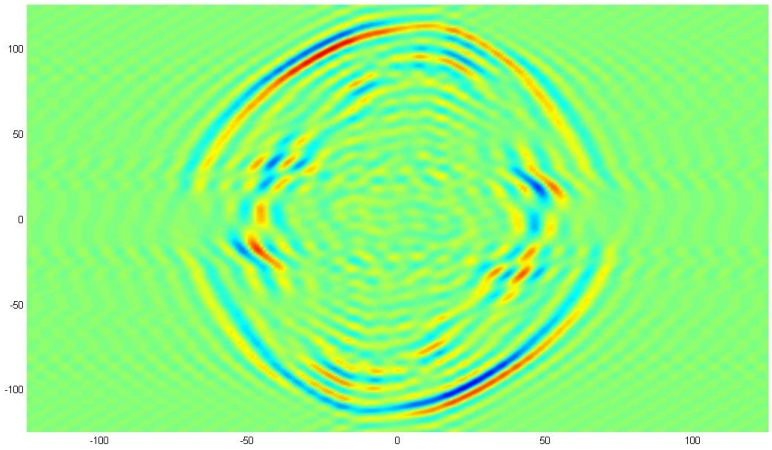

Figure 2.12: 2-*D* plot of the second component of the stress $\mathbf{V}_5^3(x_1,0,x_3,t)$ for $t = 0.3$ in albite (triclinic structure of anisotropy)

2.3 Solids with general structure of anisotropy: computation of the time-dependent fundamental solution and wave fronts

2.3.1 Statement of the problem

Let us consider (2.14) and (2.15). Substituting (2.15) into (2.14) we have

$$\rho\frac{\partial^2 u_i(x,t)}{\partial t^2} = \sum_{j,k,l=1}^{3} c_{ijkl}\frac{\partial^2 u_k(x,t)}{\partial x_j \partial x_l} + f_i(x,t),\ x \in R^3, t \in R. \tag{2.81}$$

System (2.81) can be written as follows

$$\rho\frac{\partial^2 \mathbf{u}(x,t)}{\partial t^2} = \sum_{j,l=1}^{3} \mathbf{A}_{jl}\frac{\partial^2 \mathbf{u}(x,t)}{\partial x_j \partial x_l} + \mathbf{f}(x,t),\ x \in R^3, t \in R, \tag{2.82}$$

where $\mathbf{f}(x,t) = (f_1(x,t), f_2(x,t), f_3(x,t))$,

$$\mathbf{A}_{jl} = \begin{bmatrix} c_{1j1l} & c_{1j2l} & c_{1j3l} \\ c_{2j1l} & c_{2j2l} & c_{2j3l} \\ c_{3j1l} & c_{3j2l} & c_{3j3l} \end{bmatrix}. \tag{2.83}$$

Let us consider the point forces of the form $\mathbf{e}^m\delta(x)h(t)$, where $m = 1,2,3$; $\mathbf{e}^1 = (1,0,0)$, $\mathbf{e}^2 = (0,1,0)$, $\mathbf{e}^3 = (0,0,1)$ are basis vectors of the space R^3; $\delta(x) = \delta(x_1)\delta(x_2)\delta(x_3)$ is the $3D$ Dirac delta function concentrated at the point $(0,0,0)$ from R^3; $h(t)$ is a function such that $h(t) = 0$ for $t < 0$.

Let $\mathbf{u}^m(x,t) = (u_1^m(x,t), u_2^m(x,t), u_3^m(x,t))$ be a solution of (2.82) for $\mathbf{f}(x,t) = \mathbf{e}^m\delta(x)h(t)$ satisfying $\mathbf{u}^m(x,t)|_{t<0} = 0$, i.e.

$$\rho\frac{\partial^2\mathbf{u}^m(x,t)}{\partial t^2} = \sum_{j,l=1}^{3}\mathbf{A}_{jl}\frac{\partial^2\mathbf{u}^m(x,t)}{\partial x_j\partial x_l} + \mathbf{e}^m\delta(x)h(t), \tag{2.84}$$

$$\mathbf{u}^m(x,t)|_{t<0} = 0, \tag{2.85}$$

The time-dependent FS of equations of linear anisotropic elastodynamics is defined as a matrix $G(x,t)$ of the order 3×3 whose columns $G^m(x,t) = (G_1^m(x,t), G_2^m(x,t), G_3^m(x,t))$, $m = 1,2,3$ satisfy (2.84), (2.85) for $h(t) = \delta(t)$, where $\delta(t)$ is the $1D$ Dirac delta function concentrated at $t = 0$. From the physical point of view the mth column of the FS of equations of linear anisotropic elastodynamics is the displacement of the considered anisotropic elastic solid arising from the pulse point force $\mathbf{e}^m\delta(x)\delta(t)$. The computation of the vector function $\mathbf{u}^m(x,t)$ satisfying (2.84), (2.85) is the main problem of this section.

2.3.2 Computation of a solution of (2.84), (2.85)

The method of deriving $\mathbf{u}^m(x,t)$ satisfying (2.84) and (2.85) consists of the following. In the first step equations (2.84) and (2.85) are written in terms of the Fourier transform with respect to $x \in R^3$. In the second step, a solution of the obtained initial value problem is derived by matrix transformations and the ordinary differential equations technique. In the last step, the solution of (2.84), (2.85) is found by the inverse Fourier transform.

2.3.2.1 Equations (2.84), (2.85) in terms of Fourier images

Let $\tilde{\mathbf{u}}^m(\nu,t) = (\tilde{u_1}^m(\nu,t), \tilde{u_2}^m(\nu,t), \tilde{u_3}^m(\nu,t))$ be the Fourier image of $\mathbf{u}^m(x,t)$ with respect to $x = (x_1,x_2,x_3) \in R^3$. Equations (2.84) and (2.85) can be written in terms of $\tilde{\mathbf{u}}^m(\nu,t)$ as follows

$$\rho \frac{d^2\tilde{\mathbf{u}}^m}{dt^2} + \mathbf{A}(\nu)\tilde{\mathbf{u}}^m = \mathbf{e}^m h(t),\ \nu \in R^3, t \in R, \tag{2.86}$$

$$\tilde{\mathbf{u}}^m(\nu,t)|_{t<0} = 0. \tag{2.87}$$

Here

$$\mathbf{A}(\nu) = \sum_{j,l=1}^{3} \mathbf{A}_{jl}\nu_j\nu_l, \tag{2.88}$$

where matrices $\mathbf{A}_{jl}$ are defined by (2.83).

2.3.2.2 *Formula for a solution of (2.86), (2.87) for* $\nu = 0$

A solution of (2.86), (2.87) for $\nu_1 = 0$, $\nu_2 = 0$, $\nu_3 = 0$ is given by

$$\tilde{\mathbf{u}}^m(0,t) = \frac{\theta(t)}{\rho}\left(\int_0^t (t-\tau)h(\tau)d\tau\right)\mathbf{e}^m, \tag{2.89}$$

where $\theta(t)$ is the Heaviside function, i.e. $\theta(t) = 1$ for $t \geq 0$ and $\theta(t) = 0$ for $t < 0$.

2.3.2.3 *Diagonalization of the matrix* $\boldsymbol{A}(\nu)$ *for* $\nu \neq 0$

Using the symmetry and positivity of elastic constants c_{ijkl} (see conditions (2.12), (2.13)) we obtain that the matrix $\mathbf{A}(\nu)$, defined by (2.88), is symmetric positive definite for $\nu \neq 0$ (see Appendix). Using the linear algebra technique for the given matrix $\mathbf{A}(\nu)$ we construct an orthogonal matrix $\mathbf{T}(\nu)$ and a diagonal matrix $\mathbf{D}(\nu) = diag(d_k(\nu),\ k = 1,2,3)$ with positive elements such that

$$\mathbf{T}^*(\nu)\mathbf{A}(\nu)\mathbf{T}(\nu) = \mathbf{D}(\nu), \tag{2.90}$$

where $\mathbf{T}^*(\nu)$ is the transposed matrix to $\mathbf{T}(\nu)$.

2.3.2.4 *The derivation of a solution of (2.86), (2.87) for* $\nu \neq 0$

Let $\mathbf{T}(\nu)$ and $\mathbf{D}(\nu) = diag(d_k(\nu),\ k = 1,2,3)$ be constructed. A solution of (2.86), (2.87) can be found as

$$\tilde{\mathbf{u}}^m(\nu,t) = \mathbf{T}(\nu)\mathbf{Y}^m(\nu,t), \tag{2.91}$$

where $\mathbf{Y}^m(\nu,t)$ is unknown vector function. Substituting (2.91) into (2.86), (2.87) and then multiplying the obtained equations by $\mathbf{T}^*(\nu)$ and using (2.90) we find

$$\rho\frac{d^2\mathbf{Y}^m}{dt^2}+\mathbf{D}(\nu)\mathbf{Y}^m = \mathbf{T}^*(\nu)\mathbf{e}^m h(t), \tag{2.92}$$

$$\mathbf{Y}^m(\nu,t)|_{t<0} = 0,\ t\in R,\ \nu\in R^3. \tag{2.93}$$

We note that the explicit formula of the fundamental solution for the ordinary differential operator $(\rho d^2/dt^2+d_k(\nu))$, when $d_k(\nu)>0$, is given by (see, for example, Vladimirov (1971))

$$\mathcal{E}_k(\nu,t)=\frac{\theta(t)}{\sqrt{\rho d_k(\nu)}}\sin(t\sqrt{d_k(\nu)/\rho}). \tag{2.94}$$

Each component of the vector solution of the problem (2.92), (2.93) can be found by (see, for example, Vladimirov (1971)) the convolution of the FS $\mathcal{E}_k(\nu,t)$ and $[\mathbf{T}^*(\nu)\mathbf{e}^m]_k h(t)$ i.e.

$$\mathbf{Y}^m_k(\nu,t)=\mathcal{E}_k * [\mathbf{T}^*(\nu)\mathbf{e}^m]_k h(t),$$

where the notation $[\mathbf{T}^*(\nu)\mathbf{e}^m]_k$ means kth component of the vector $\mathbf{T}^*(\nu)\mathbf{e}^m$.

Using formula (2.94) the convolution can be computed explicitly and as a result of it we find for $d_k(\nu)>0$:

$$\mathbf{Y}^m_k(\nu,t)=\theta(t)\int_0^t \frac{[\mathbf{T}^*(\nu)\mathbf{e}^m]_k h(\tau)}{\sqrt{\rho d_k(\nu)}}\sin\left((t-\tau)\sqrt{\frac{d_k(\nu)}{\rho}}\right)d\tau. \tag{2.95}$$

Finally, a solution of (2.86), (2.87) is determined by (2.89), (2.91), (2.95).

2.3.2.5 A formula for the Fourier image of the FS of equations of anisotropic elastodynamics

The Fourier image of the FS of equations of linear anisotropic elastodynamics is a matrix of the order 3×3 whose columns $\tilde{G}^m(\nu,t) = (\tilde{G}^m_1(\nu,t), \tilde{G}^m_2(\nu,t), \tilde{G}^m_3(\nu,t))$, $m = 1,2,3$ satisfy

$$\rho \frac{d^2\tilde{G}^m}{dt^2} + \mathbf{A}(\nu)\tilde{G}^m = \mathbf{e}^m\delta(t), \tag{2.96}$$

$$\tilde{G}^m(\nu,t)|_{t<0} = 0,\ \nu \in R^3,\ t \in R. \tag{2.97}$$

Similar to Sections 2.3.2.2 and 2.3.2.3 we find $\tilde{G}^m(0,t)$ by

$$\tilde{G}^m(0,t) = \frac{\theta(t)}{\rho} t\mathbf{e}^m \tag{2.98}$$

and we compute $\tilde{G}^m(\nu,t)$ for $\nu \neq 0$ as follows

$$\tilde{G}^m(\nu,t) = \mathbf{T}(\nu)\mathbf{Y}^m(\nu,t), \tag{2.99}$$

where components of

$$\mathbf{Y}^m(\nu,t) = (Y^m_1(\nu,t), Y^m_2(\nu,t), Y^m_3(\nu,t))$$

are given by

$$\mathbf{Y}^m_k(\nu,t) = \theta(t)\frac{[\mathbf{T}^*(\nu)\mathbf{e}^m]_k}{\sqrt{\rho d_k(\nu)}} \sin\left(\sqrt{\frac{d_k(\nu)}{\rho}}t\right). \tag{2.100}$$

2.3.2.6 *Formulae for a solution of (2.86), (2.87) and for the FS of equations of anisotropic elastodynamics*

Let $\tilde{\mathbf{u}}^m(\nu,t)$ be the solution of (2.86), (2.87) defined by (2.89), (2.91), (2.95). A solution $\mathbf{u}^m(x,t)$ of (2.84), (2.85) is defined by the inverse Fourier transform of $\tilde{\mathbf{u}}^m(\nu,t)$, i.e. by the formula

$$\mathbf{u}^m(x,t) = F_\nu^{-1}[\tilde{\mathbf{u}}^m(\nu,t)](x) = \frac{1}{(2\pi)^3}\int\limits_{-\infty}^{+\infty}\int\limits_{-\infty}^{+\infty}\int\limits_{-\infty}^{+\infty}\tilde{\mathbf{u}}^m(\nu,t)\, e^{-ix\cdot\nu}d\nu_1 d\nu_2 d\nu_3,$$
$$\nu = (\nu_1,\nu_2,\nu_3)\in R^3,\ x=(x_1,x_2,x_3)\in R^3. \tag{2.101}$$

Taking into account that the components of the vector function $\mathbf{u}^m(x,t)$ as well as the components of vector functions $\tilde{\mathbf{u}}^m(\nu,t)$ have real values, the imaginary part of the right hand side of (2.101) is equal to zero. As a result of it we find the following formula for a solution of (2.86), (2.87) from (2.101):

$$\mathbf{u}^m(x,t) = \frac{\theta(t)}{(2\pi)^3}\int\limits_{-\infty}^{\infty}\int\limits_{-\infty}^{\infty}\int\limits_{-\infty}^{\infty}\tilde{\mathbf{u}}^m(\nu,t)\,\cos(x_1\nu_1+x_2\nu_2+x_3\nu_3)d\nu_1 d\nu_2 d\nu_3. \tag{2.102}$$

Using the similar reasonings and formulae (2.98), (2.99) and (2.100) we obtain a formula for mth column of the FS of equations of anisotropic elastodynamics

$$G^m(x,t) = \frac{\theta(t)}{(2\pi)^3}\int\limits_{-\infty}^{\infty}\int\limits_{-\infty}^{\infty}\int\limits_{-\infty}^{\infty}\tilde{G}^m(\nu,t)\,\cos(x_1\nu_1+x_2\nu_2+x_3\nu_3)d\nu_1 d\nu_2 d\nu_3, \tag{2.103}$$

where $\tilde{G}^m(\nu,t)$ is defined by (2.98), (2.99) and (2.100).

2.3.3 Computational experiments: implementation and justification

2.3.3.1 The accuracy of the suggested method in finding the Fourier image of the FS

We consider the isotropic material Silica (SiO_2) characterized by the density $\rho = 2.203\ (10^3 kg/m^3)$ and Lame parameters $\lambda = 1.61$, $\mu = 3.12\,(10^{10} Pa)$ (see, for example, Dieulesaint & Royer (2000), p.163). For this computational experiment we take the pulse point force $\mathbf{e}^3\delta(x_1)\delta(x_2)\delta(x_3)\delta(t)$, where $\mathbf{e}^3 = (0,0,1)$. Using our method we compute $\mathbf{T}(\nu)$, $\mathbf{T}^*(\nu)$, $\mathbf{D}(\nu)$ and then using the formula (2.98), (2.99) and (2.100) we find the third column of the Fourier image of the FS $\tilde{G}^3(\nu,t)$ for arbitrary $\nu = (\nu_1,\nu_2,\nu_3) \in R^3$ and any fixed time t. On the other hand the FS of motion equations of the indefinite isotropic solid as well as its Fourier image can be given by explicit formulae (see, for example, Aki & Richard (1980)). If we denote the FS of equations of isotropic elastodynamics by 3×3 matrix $\mathcal{E}(x,t)$ with columns $\mathbf{E}^m(x,t) = (E_1^m(x,t), E_2^m(x,t), E_3^m(x,t))$ and the Fourier image of $\mathcal{E}(x,t)$ by 3×3 matrix $\tilde{\mathcal{E}}(\nu,t)$ with columns $\tilde{\mathbf{E}}^m(\nu,t) = (\tilde{E}_1^m(\nu,t), \tilde{E}_2^m(\nu,t), \tilde{E}_3^m(\nu,t))$ then, for example, for components of the third column $\tilde{\mathbf{E}}^3(\nu,t)$ the following explicit formulae take place

$$\tilde{E}_1^3(\nu,t) = \frac{\theta(t)}{\rho\mid\nu\mid^3}\nu_1\nu_3\left(\frac{\sin(C_L\mid\nu\mid t)}{C_L} - \frac{\sin(C_T\mid\nu\mid t)}{C_T}\right), \tag{2.104}$$

$$\tilde{E}_2^3(\nu,t) = \frac{\theta(t)}{\rho\mid\nu\mid^3}\nu_2\nu_3\left(\frac{\sin(C_L\mid\nu\mid t)}{C_L} - \frac{\sin(C_T\mid\nu\mid t)}{C_T}\right), \tag{2.105}$$

$$\tilde{E}_3^3(\nu,t) = \frac{\theta(t)}{\rho\mid\nu\mid^3}\left(\frac{\sin(C_L\mid\nu\mid t)}{C_L}\nu_3^2 + \frac{\sin(C_T\mid\nu\mid t)}{C_T}(\nu_1^2+\nu_2^2)\right), \tag{2.106}$$

where $C_T^2 = \mu/\rho,\ C_L^2 = (\lambda+2\mu)/\rho$.

Using our method and explicit formulae (2.104)–(2.106) we have computed values

$\tilde{G}^3(\nu,t)$ and $\tilde{\mathbf{E}}^3(\nu,t)$. Some values of $\tilde{G}_3^3(\nu,t)$ and $\tilde{G}_3^3(\nu,t)-\tilde{E}_3^3(\nu,t)$ are given in Table 2.3. The results of this computational experiment have shown that values of the Fourier image of the FS found by our method and by the explicit formulae are almost the same (the accuracy in this experiment is less or equal to 10^{-15}).

2.3.3.2 Correctness of computation of integrals (2.102) and (2.103)

In this section we consider several computational experiments confirming the correctness of our method. For the numerical computation of (2.102) and (2.103) in MATLAB we have replaced the $3D$ integration over the whole space R^3 by the integration over the bounded domain $(-A,A)\times(-A,A)\times(-A,A)$ and then approximated $3D$ integrals over this bounded domain by the triple sums, similar to Section 2.1.6.1, with $A=40$ and $\Delta\nu=0.5$.

Example 1. In this example we consider an isotropic solid with wave speed quotient $C_L/C_T=2$, ($\mu=1$, $\lambda=2\,(10^{10}Pa)$, $\rho=0.75\,(10^3 kg/m^3)$) similar to Wang & Achenbach (1994), Payton (1983). Using formula (2.102) and our method we have computed $\mathbf{u}^3(x,t)$ for

$$h(t)=\theta(t)t^2\exp(-3t^2). \tag{2.107}$$

On the other hand there exists explicit formulae for components of the solution $\mathbf{u}^3(x,t)$ of (2.84), (2.85) for the case of homogeneous isotropic solids (see Aki & Richard (1980)). Using these formulae we have found for $u_3^3(0,0,z,t)$ and $u_3^3(\sqrt{6}z/4,\sqrt{6}z/4,z/2,t)$:

$$u_3^3(0,0,z,t)=\frac{1}{2\pi\rho\mid z\mid^3}\int\limits_{|z|/C_L}^{|z|/C_T}\tau\theta(t-\tau)(t-\tau)^2\exp\left(-3(t-\tau)^2\right)d\tau$$

$$+\frac{1}{4\pi\rho C_L^2 \mid z \mid}\theta(t-\frac{|z|}{C_L})(t-\frac{|z|}{C_L})^2\exp\left(-3(t-\frac{|z|}{C_L})^2\right), \tag{2.108}$$

$$u_3^3(\frac{\sqrt{6}}{4}z,\frac{\sqrt{6}}{4}z,\frac{z}{2},t) = -\frac{1}{16\pi\rho \mid z \mid^3}\int\limits_{|z|/C_L}^{|z|/C_T}\tau\theta(t-\tau)(t-\tau)^2\exp\left(-3(t-\tau)^2\right)d\tau$$

$$+\frac{1}{16\pi\rho C_L^2 \mid z \mid}\theta(t-\frac{|z|}{C_L})(t-\frac{|z|}{C_L})^2\exp\left(-3(t-\frac{|z|}{C_L})^2\right)$$

$$+\frac{3}{16\pi\rho C_T^2 \mid z \mid}\theta(t-\frac{|z|}{C_T})(t-\frac{|z|}{C_T})^2\exp\left(-3(t-\frac{|z|}{C_T})^2\right). \tag{2.109}$$

We note that the function $h(t)$ of the form (2.107) has been taken from the paper Wang & Achenbach (1994) to compare results of computation by our method with results of computation by methods of Payton (1983) and Wang & Achenbach (1994) presented in the paper Wang & Achenbach (1994) by graphs. The graphs of functions $u_3^3(0,0,z,t)$ and $u_3^3(\sqrt{6}z/4,\sqrt{6}z/4,z/2,t)$ for $t = 5\sqrt{\rho/\mu}$ obtained by our method and by explicit presentations (2.108), (2.109) are presented in Figs 2.13 and 2.14. As we can see these graphs have excellent agreement.

Example 2. In this example we consider the isotropic material Silica (SiO_2) and in equation (2.84) we take $m = 1$, $h(t) = \theta(t)$, where $\theta(t)$ is the Heaviside step function. Using our method we have found values of matrices $\mathbf{T}(\nu)$, $\mathbf{T}^*(\nu)$, $\mathbf{D}(\nu)$ and then using the formula (2.102) we have computed $\mathbf{u}^1(x,t)$. On the other hand we have used the explicit formulae for the components of the solution $\mathbf{u}^1(x,t)$ of (2.84), (2.85) for the case of homogeneous isotropic solids (Aki & Richard (1980)). Using these formulae we have found the following presentations for $u_1^1(z,z,z,t)$ and $u_2^1(z,z,z,t)$:

$$u_1^1(z,z,z,t) = \frac{1}{12\sqrt{3}\pi\rho|z|}\left[\frac{1}{C_L^2}\theta\left(t-\frac{\sqrt{3}|z|}{C_L}\right)+\frac{2}{C_T^2}\theta\left(t-\frac{\sqrt{3}|z|}{C_T}\right)\right], \tag{2.110}$$

$$u_2^1(z,z,z,t) = \frac{1}{24\sqrt{3}\pi\rho|z|}\left(\frac{1}{C_T^2}-\frac{1}{C_L^2}\right) \quad \text{for} \quad t > \frac{\sqrt{3}|z|}{C_T};$$
$$u_2^1(z,z,z,t) = \frac{1}{24\sqrt{3}\pi\rho}\left(\frac{t^2}{|z|^3}-\frac{1}{|z|C_L^2}\right) \quad \text{for} \quad \frac{\sqrt{3}|z|}{C_L} < t < \frac{\sqrt{3}|z|}{C_T};$$
$$u_2^1(z,z,z,t) = 0 \quad \text{for} \quad t < \frac{\sqrt{3}|z|}{C_L}. \tag{2.111}$$

The graphs of the functions $u_1^1(z,z,z,t)$ and $u_2^1(z,z,z,t)$ for $t = 1$ obtained by our method and by explicit formulae (2.110) and (2.111) are presented in Figs 2.15 and 2.16. As we can see these graphs have excellent agreement.

Example 3. In this example we consider the isotropic material silica (SiO_2). We take $m = 1$ and $h(t) = \delta(t)$ in equation (2.84), where $\delta(t)$ is the Dirac delta function. Using formula (2.102) and our method we have computed $G^1(x,t)$, i.e. the first column of the FS of elastodynamics. On the other hand we have used the explicit formulae (2.57)-(2.59) for the components of the first column of the FS of elastodynamics (Aki & Richard (1980)). For drawing graphs of components of $G^1(x,t)$ we replace singular terms $\delta(t-|x|/C_T)$ and $\delta(t-|x|/C_L)$ by $\frac{1}{2\sqrt{\pi\varepsilon}}\exp\left[-(t-|x|/C_T)^2/(4\varepsilon)\right]$ and $\frac{1}{2\sqrt{\pi\varepsilon}}\exp\left[-(t-|x|/C_L)^2/(4\varepsilon)\right]$ with $\varepsilon = 0.0001$, respectively.

The graphs of functions $G_1^1(z,z,z,t)$ and $G_2^1(z,z,z,t)$ for $t = 1$ obtained by our method and by formulae (2.57)- (2.59) are presented in Figs. 2.17 and 2.18. The curves of graphs $G_1^1(z,z,z,1)$ and $G_2^1(z,z,z,1)$ obtained by our method fluctuate around curves of graphs of the functions $G_1^1(z,z,z,1)$ and $G_2^1(z,z,z,1)$ obtained by formulae (2.57)- (2.59). We can see in Figs. 2.17 and 2.18 that all peaks of graphs obtained by our method and by formulae (2.57)- (2.59) have the same positions and similar magnitudes.

Taking into account that $G^m(x,t)$ is the elastic field arising from the pulse source $\mathbf{e}^m\delta(x)\delta(t)$ we have a chance to compute and visualize behavior of the elastic field at fixed time on a fixed plane, for example, on the plane $x_2 = 0$ at $t = 1.5$. The graphs of

$G_1^1(x_1, 0, x_3, 1.5)$ obtained by formula (2.57) and by our method are presented in Figs. 2.19 and 2.20, respectively. In these Figures the horizontal axis is x_1 and vertical axis is x_2. The graphs of these Figures mean the view from the top of the magnitude axis of G_1^1 and different colors correspond to different magnitudes. In these Figures we see clearly two fronts related to longitudinal and transverse waves. We can see also that these waves propagate perpendicular to each other.

2.3.3.3 Computational examples of the FS of equations of anisotropic elastodynamics

In this section the following two examples of homogeneous elastic solids with general structure of anisotropy are considered.

Example 4. **The solid of monoclinic structure: Sodium Thiosulfate** ($Na_2S_2O_3$). The density $\rho = 1.7499\ kg/cm^3$ and elastic constants are defined (see, for example, Hearmon (1956)) by

$$\begin{aligned}
c_{1111} &= 0.3323,\ c_{1122} = c_{2211} = 0.1814,\ c_{1133} = c_{3311} = 0.1875,\\
c_{1113} &= c_{1311} = 0.0225,\ c_{2222} = 0.2953,\ c_{2233} = c_{3322} = 0.1713,\\
c_{2213} &= c_{1322} = 0.0983,\ c_{3333} = 0.459,\ c_{3313} = c_{1333} = -0.0678,\\
c_{2323} &= 0.0569,\ c_{2312} = c_{1223} = -0.0268,\ c_{1313} = 0.107,\ c_{1212} = 0.0598(GPa).
\end{aligned}$$

Other elastic constants are equal to zero.

Example 5. **The solid of triclinic structure: Copper Sulphate Pentahydrate** . The density $\rho = 2.649\ kg/cm^3$ and elastic moduli are defined (see, for example, Brown

& Abramson & Angel (2006)) by

$$
\begin{aligned}
c_{1111} &= 5.65,\ c_{1122}=c_{2211}=2.65,\ c_{1133}=c_{3311}=3.21,\ c_{1123}=c_{2311}=-0.33,\\
c_{1113} &= c_{1311}=-0.08,\ c_{1112}=c_{1211}=-0.39,\ c_{2222}=4.33,\ c_{2233}=c_{3322}=3.47,\\
c_{2223} &= c_{2322}=-0.07,\ c_{2213}=c_{1322}=-0.21,\ c_{2212}=c_{1222}=0.02,\ c_{3333}=5.69,\\
c_{3323} &= c_{2333}=-0.44,\ c_{3313}=c_{1333}=-0.21,\ c_{3312}=c_{1233}=-0.16,\\
c_{2323} &= 1.73,\ c_{2313}=c_{1323}=0.09,\ c_{2312}=c_{1223}=0.03,\\
c_{1313} &= 1.22,\ c_{1312}=c_{1213}=-0.26,\ c_{1212}=1(GPa).
\end{aligned}
$$

For the computational experiments we take equation (2.84) with $h(t)=\delta(t)$. The goal of these computational experiments is to derive the FS of elastodynamics and to obtain the graphic presentations of the elements of the FS using formula (2.102), our method and MATLAB tools. The physical meaning of *mth* column of the FS is the vector of displacement depending on the position (i.e. space variables x_1, x_2, x_3) and the time variable t arising from the pulse point force of the form $\mathbf{e}^m\delta(x)\delta(t)$ in the considered elastic anisotropic solid. The graphic presentation of the components of this displacement in points of the space gives a possibility to observe the wave propagation phenomenon, in particular, wave fronts arising from pulse point sources at different times in general anisotropic solids.

Using our method we have computed numerically the components of $G^m(x,t)$.

Fig.2.21 presents the first component of the displacement $G^1(x_1,0,x_3,t)$ at $t=4$. Here the horizontal and vertical axes are x_1 and x_3, respectively. Fig.2.21 presents a view from the top of the magnitude axis G_1^1 (i.e. the view of the surface $z=G_1^1(x_1,0,x_3,4)$ from the top of z axis).

Similar, Fig. 2.22 presents the second component of the displacement $G^1(x_1,x_2,0,t)$ at $t=5$. Here the horizontal and vertical axes are x_1 and x_2, respectively. Fig.2.23

presents the third component of the displacement $G^1(x_1,0,x_3,t)$ at the time $t=4$. Here the horizontal and vertical axes are x_1 and x_3, respectively.

In Figs 2.21- 2.23 we can see the behavior of the components of the elastic field in the monoclinic solid Sodium Thiosulfate arising from the pulse point force $\mathbf{e}^1\delta(x)\delta(t)$. We can see peculiar forms of the traces of wave fronts which we observe on the planes $x_2=0$, $x_3=0$.

Fig.2.24 presents the first component of the displacement $G^3(x_1,0,x_3,t)$ at $t=1.75$. Fig.2.25 presents the second component of the displacement $G^3(0,x_2,x_3,t)$ at $t=1.75$. Fig.2.26 presents the third component of the displacement $G^3(0,x_2,x_3,t)$ at the time $t=1.75$. Figs.2.24-2.26 are the screen shots of $2-D$ level plots of the surfaces $G^3_1(x_1,0,x_3,1.75)$, $G^3_2(0,x_2,x_3,1.75)$, $G^3_3(0,x_2,x_3,1.75)$, respectively. This is a view from the top of z-axis (the plan). In Figs. 2.24-2.26 we can see the behavior of components of the elastic field in the triclinic solid Copper Sulphate Pentahydrate arising from the pulse point force $\mathbf{e}^3\delta(x)\delta(t)$. We can see peculiar forms of the traces of wave fronts which we observe on the planes $x_1=0$, $x_2=0$.

Table 2.3. The accuracy of computing $\tilde{G}_3^3(\nu,t)$ in isotropic material silica (SiO_2)

t	ν_1	ν_2	ν_3	$\tilde{G}_3^3(\nu,t)$	$\tilde{G}_3^3(\nu,t)-\tilde{E}_3^3(\nu,t)$
1	10^{-5}	10^{-5}	10^{-5}	0.4539264639	-0.1×10^{-15}
	10^{-5}	10^{-4}	10^{-3}	0.4539261932	-0.1×10^{-15}
	10^{-4}	10^{-4}	10^{-4}	0.4539264591	0.6×10^{-16}
	10^{-3}	10^{-3}	10^{-3}	0.4539259800	0.1×10^{-15}
	10^{-2}	10^{-2}	10^{-2}	0.4538780786	0
	10^{-1}	10^{-2}	10^{-3}	0.4528447980	0
	10^{-1}	10^{-1}	10^{-1}	0.4491066612	0
	1	1	1	0.1236007290	0.6×10^{-16}
	10^{1}	10^{1}	10^{1}	$0.1884405489\times10^{-1}$	-0.3×10^{-17}
	10^{2}	10^{2}	10^{2}	$-0.1273480138\times10^{-2}$	-0.4×10^{-16}
	10^{1}	10^{2}	10^{3}	$-0.7528755459\times10^{-4}$	-0.5×10^{-16}
	10^{3}	10^{3}	10^{3}	$0.8709300174\times10^{-4}$	-0.4×10^{-16}
	10^{5}	10^{4}	10^{3}	$-0.3012966019\times10^{-5}$	-0.3×10^{-16}
2	10^{-5}	10^{-5}	10^{-5}	0.9078529274	-0.1×10^{-15}
	10^{-5}	10^{-4}	10^{-3}	0.9078507625	-0.2×10^{-15}
	10^{-4}	10^{-4}	10^{-4}	0.9078528891	0
	10^{-3}	10^{-3}	10^{-3}	0.9078490569	0.1×10^{-15}
	10^{-2}	10^{-2}	10^{-2}	0.9074658907	-0.1×10^{-15}
	10^{-1}	10^{-2}	10^{-3}	0.8992181580	-0.2×10^{-15}
	10^{-1}	10^{-1}	10^{-1}	0.8697446556	0
	1	1	1	-0.1102871416	0.1×10^{-16}
	10^{1}	10^{1}	10^{1}	$-0.2958623228\times10^{-2}$	0.5×10^{-16}
	10^{2}	10^{2}	10^{2}	$-0.7422665165\times10^{-3}$	0.2×10^{-16}
	10^{1}	10^{2}	10^{3}	$-0.1514006209\times10^{-3}$	-0.8×10^{-16}
	10^{3}	10^{3}	10^{3}	$0.5202463403\times10^{-4}$	-0.8×10^{-16}
	10^{5}	10^{4}	10^{3}	$-0.3663436948\times10^{-5}$	0.3×10^{-16}
3	10^{-5}	10^{-5}	10^{-5}	0.9078529274	-0.1×10^{-15}
	10^{-5}	10^{-4}	10^{-3}	1.361779390	-0.2×10^{-15}
	10^{-4}	10^{-4}	10^{-4}	1.361779261	0.2×10^{-15}
	10^{-3}	10^{-3}	10^{-3}	1.361766327	0.4×10^{-15}
	10^{-2}	10^{-2}	10^{-2}	1.360473397	0.4×10^{-15}
	10^{-1}	10^{-2}	10^{-3}	1.332741143	0
	10^{-1}	10^{-1}	10^{-1}	1.235652336	0.2×10^{-15}
	1	1	1	$-0.3190631567\times10^{-1}$	-0.2×10^{-15}
	10^{1}	10^{1}	10^{1}	$-0.1528018422\times10^{-1}$	0.5×10^{-16}
	10^{2}	10^{2}	10^{2}	$-0.1021957343\times10^{-2}$	0.6×10^{-16}
	10^{1}	10^{2}	10^{3}	$-0.1988284129\times10^{-3}$	-0.2×10^{-17}
	10^{3}	10^{3}	10^{3}	$0.1567941374\times10^{-3}$	-0.5×10^{-16}
	10^{5}	10^{4}	10^{3}	$-0.1442495824\times10^{-5}$	0.2×10^{-15}

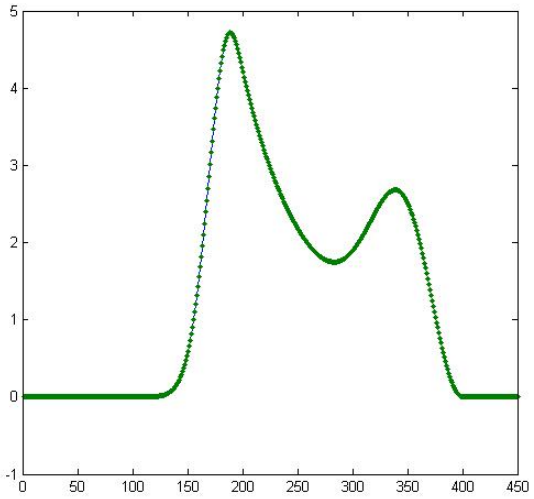

Figure 2.13: Graphs of the third component $u_3^3(0,0,z,t)$ of solutions (2.84), (2.85) for $h(t) = \theta(t)t^2\exp(-3t^2)$ at $t = 5\sqrt{\frac{\rho}{\mu}}$ for an isotropic solid with wave speed quotient $C_L/C_T = 2$. The dotted line represents analytical solution found by (2.108). The continuous line represents our method.

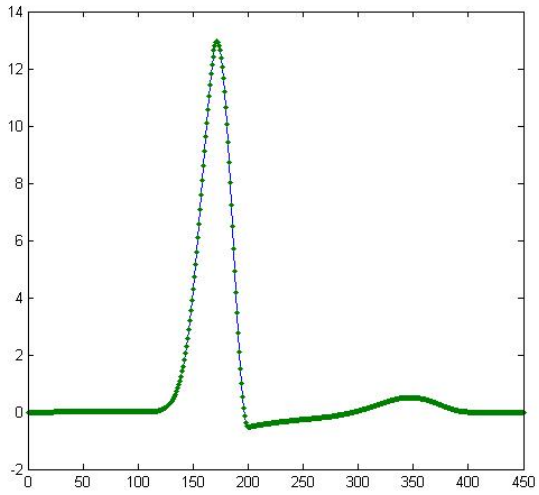

Figure 2.14: Graphs of the third component $u_3^3(\sqrt{6}z/4, \sqrt{6}z/4, z/2, t)$ of solutions (2.84), (2.85) for $h(t) = \theta(t)t^2\exp(-3t^2)$ at $t = 5\sqrt{\frac{\rho}{\mu}}$ for an isotropic solid with wave speed quotient $C_L/C_T = 2$. The dotted line represents analytical solution found by (2.109). The continuous line represents our method.

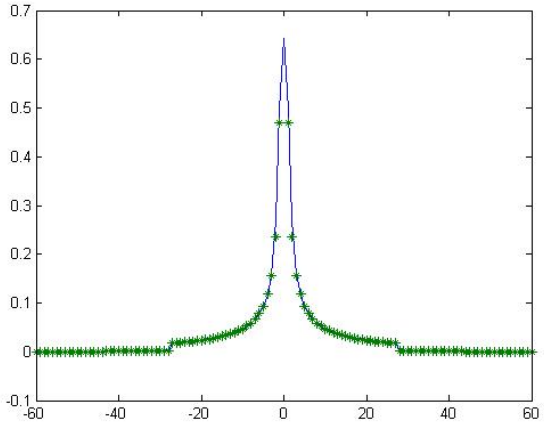

Figure 2.15: Graphs of the first component $u_1^1(z,z,z,t)$ of solutions (2.84), (2.85) for $h(t) = \theta(t)$ at $t = 1$ for the isotropic solid Silica (SiO_2). The line denoted by *** represents analytical solution found by formula (2.110). The line denoted by —— represents our method.

2.4 Concluding Remarks

In this chapter of the thesis fundamental solution of anisotropic elastodynamics is derived using three different methods. The first method is based on Fourier transformation, Paley-Wiener theorem and some properties of fundamental solutions. In the second method and third method system of anisotropic elastodynamics is reduced to a first order symmetric hyperbolic system and a second order matrix equation, respectively. And using Fourier transformation and some matrix computations fundamental solution of anisotropic elastodynamics is derived. Computational examples confirm robustness of the given methods.

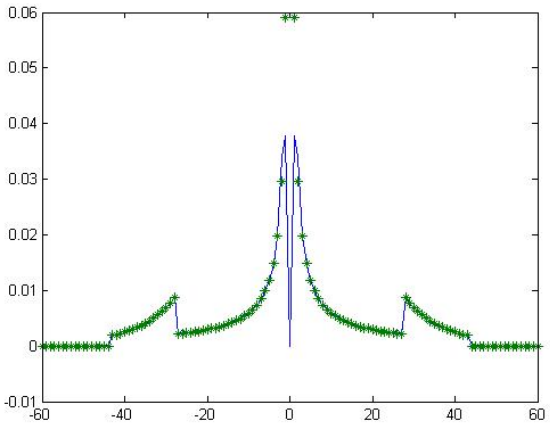

Figure 2.16: Graphs of the second component $u_2^1(z,z,z,t)$ of solutions (2.84), (2.85) for $h(t) = \theta(t)$ at $t = 1$ for the isotropic solid Silica (SiO_2). The line denoted by *** represents analytical solution found by formulae (**??**) and (2.111). The line denoted by —— represents our method.

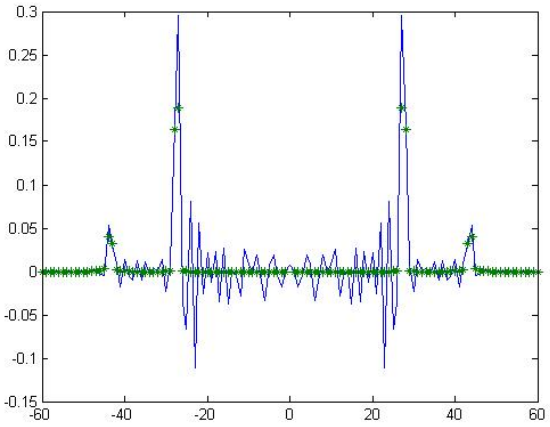

Figure 2.17: Graphs of the first component $G_1^1(z,z,z,t)$ of solutions (2.84), (2.85) for $h(t) = \delta(t)$ at $t = 1$ for the isotropic solid Silica (SiO_2). The line denoted by *** represents analytical solution found by formula (2.57), where $\delta(t)$ is approximated by $\exp\left[-t^2/(4\varepsilon)\right]/(2\sqrt{\pi\varepsilon})$, $\varepsilon = 0.0001$. The line denoted by —— represents our method.

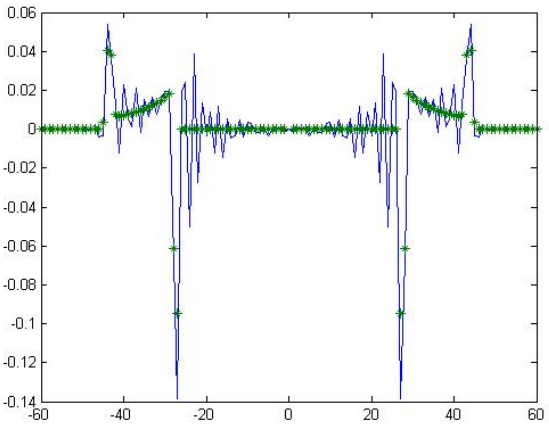

Figure 2.18: Graphs of the second component $G_2^1(z,z,z,t)$ of solutions (2.84), (2.85) for $h(t) = \delta(t)$ at $t = 1$ for the isotropic solid Silica (SiO_2). The line denoted by *** represents analytical solution found by formula (2.58), where $\delta(t)$ is approximated by $\exp\left[-t^2/(4\varepsilon)\right]/(2\sqrt{\pi\varepsilon})$, $\varepsilon = 0.0001$. The line denoted by —— represents our method.

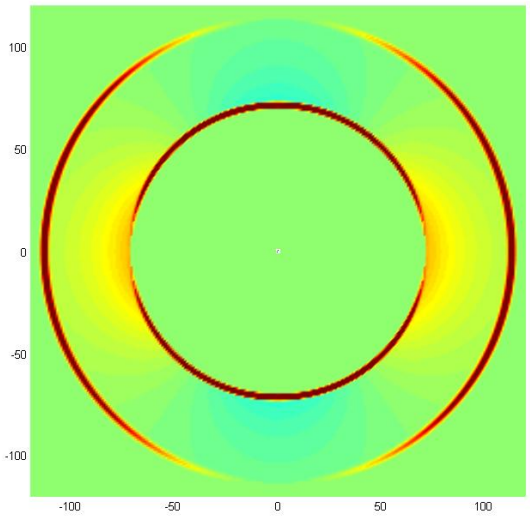

Figure 2.19: The map surface plot of 3D surface $z = G_1^1(x_1,0,x_3,1.5)$, where $G_1^1(x_1,x_2,x_3,t)$ is computed by formula (2.57) for the isotropic elastic solid Silica (SiO_2); the Dirac delta function $\delta(t)$ is approximated in (2.57) by $\exp\left[-t^2/(4\varepsilon)\right]/(2\sqrt{\pi\varepsilon})$, $\varepsilon = 0.0001$.

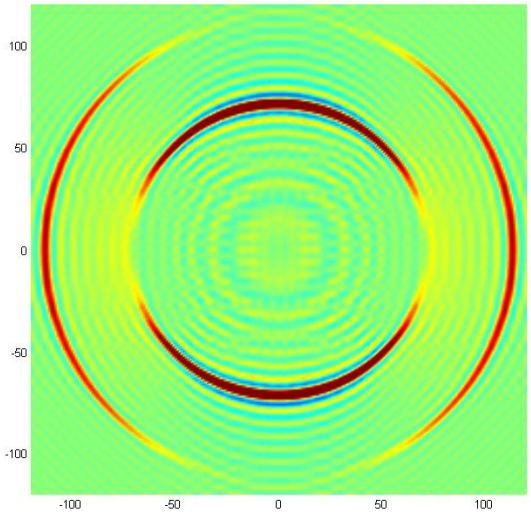

Figure 2.20: The map surface plot of 3D surface $z = G_1^1(x_1, 0, x_3, 1.5)$, where $G_1^1(x_1, x_2, x_3, t)$ is computed by our method for the isotropic elastic solid Silica (SiO_2).

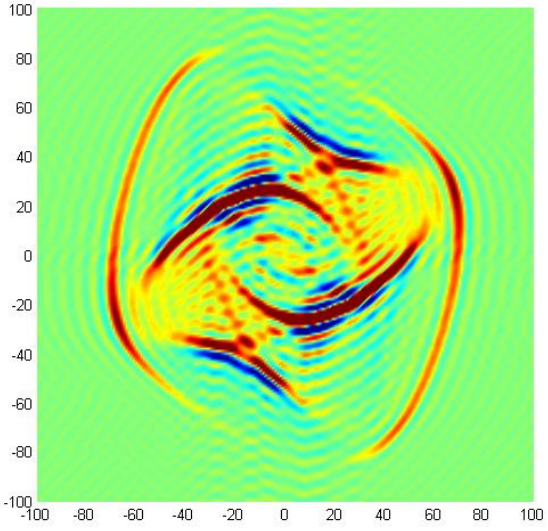

Figure 2.21: The map surface plot of 3D surface $z = G_1^1(x_1, 0, x_3, 4)$, where $G_1^1(x_1, x_2, x_3, t)$ is computed by our method for Sodium Thiosulfate (monoclinic structure of anisotropy).

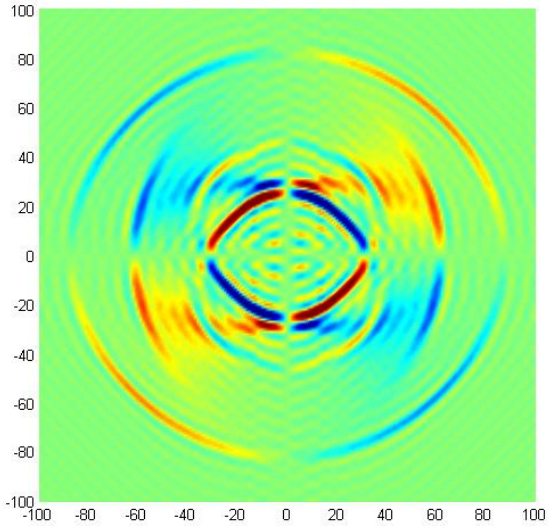

Figure 2.22: The map surface plot of 3D surface $z = G_2^1(x_1, x_2, 0, 5)$, where $G_2^1(x_1, x_2, x_3, t)$ is computed by our method for Sodium Thiosulfate (monoclinic structure of anisotropy).

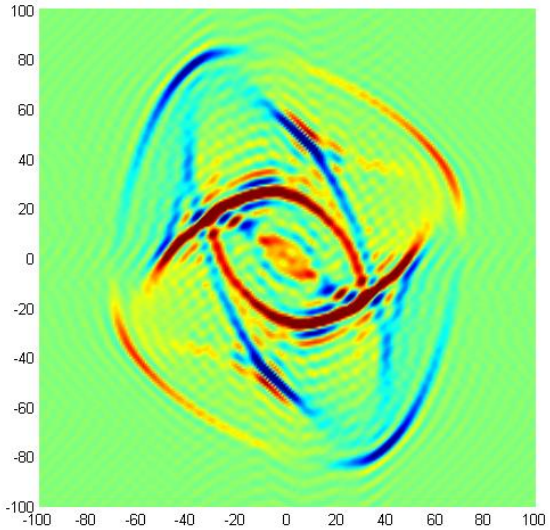

Figure 2.23: The map surface plot of 3D surface $z = G_3^1(x_1, 0, x_3, 4)$, where $G_3^1(x_1, x_2, x_3, t)$ is computed by our method for Sodium Thiosulfate (monoclinic structure of anisotropy).

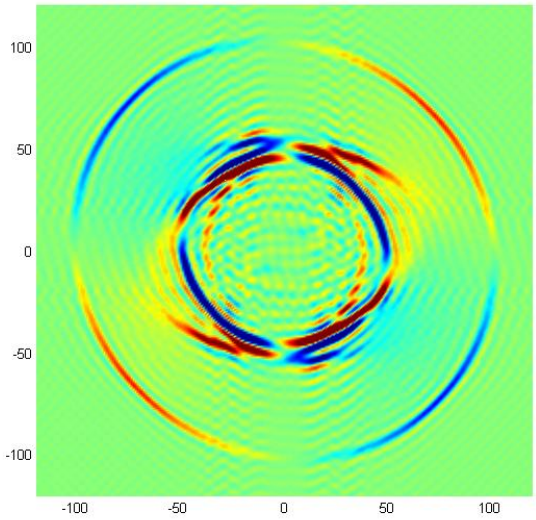

Figure 2.24: The map surface plot of 3D surface $z = G_1^3(x_1, 0, x_3, 1.75)$, where $G_1^3(x_1, x_2, x_3, t)$ is computed by our method for Copper Sulphate Pentahydrate (triclinic structure of anisotropy).

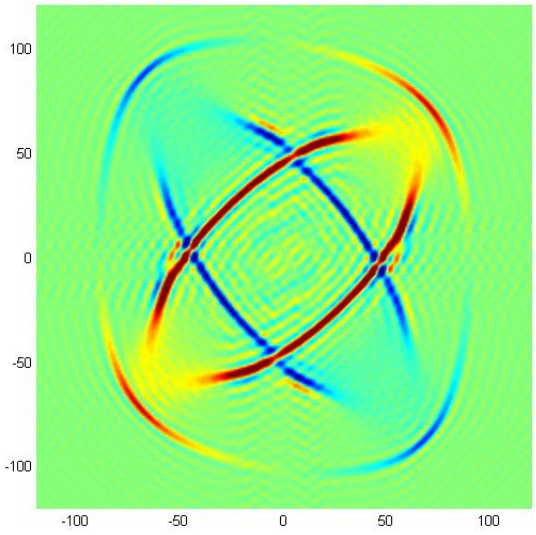

Figure 2.25: The map surface plot of 3D surface $z = G_2^3(x_1, 0, x_3, 1.75)$, where $G_2^3(x_1, x_2, x_3, t)$ is computed by our method for Copper Sulphate Pentahydrate (triclinic structure of anisotropy).

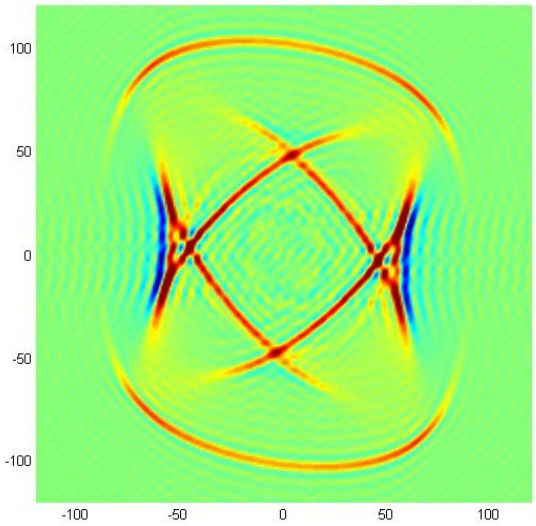

Figure 2.26: The map surface plot of 3D surface $z = G_3^3(x_1, 0, x_3, 1.75)$, where $G_3^3(x_1, x_2, x_3, t)$ is computed by our method for Copper Sulphate Pentahydrate (triclinic structure of anisotropy).

CHAPTER THREE
MODELLING AND SIMULATION OF ELASTIC WAVES IN QUASICRYSTALS

In this chapter the dynamic three dimensional elasticity problems of 1D, 2D and 3D quasicrystals are considered. This chapter consist of three sections. In these sections the fundamental solutions of the dynamic three dimensional elasticity problems of 1D, 2D and 3D quasicrystals are computed.

3.1 Three dimensional elastodynamics of 1D quasicrystals: the derivation of the time-dependent fundamental solution

3.1.1 The basic equations for 1D QCs

Let $x = (x_1, x_2, x_3) \in R^3$ be a space variable, $t \in R$ be a time variable. According to the generalized elasticity theory (Ding & Yang & Hu & Wang (1993), Wang & Yang & Hu (1997), Gao & Zhao (2006)), Hooke's law for 1-D QCs can be written in the form

$$\sigma_{ij} = c_{ijkl}\varepsilon_{kl} + R_{ij3l}w_{3l}, \tag{3.112}$$

$$H_{3j} = R_{kl3j}\varepsilon_{kl} + K_{3j3l}w_{3l}, \ i,j,k,l = 1,2,3. \tag{3.113}$$

where ε_{kl} and w_{3l} are defined as follows

$$\varepsilon_{kl} = \frac{1}{2}(\frac{\partial u_k}{\partial x_l} + \frac{\partial u_l}{\partial x_k}), \ w_{3l} = \frac{\partial w_3}{\partial x_l}, \ k,l = 1,2,3. \tag{3.114}$$

Here $u_k, k = 1,2,3$ the phonon displacements and w_3 is phason displacement.

c_{ijkl} represents the elastic constants of the phonon field which satisfy symmetry properties

$$c_{ijkl} = c_{jikl} = c_{ijlk} = c_{klij}. \tag{3.115}$$

K_{3j3l} represents the elastic constants of the phason field which satisfy symmetry properties

$$K_{3j3l} = K_{3l3j}, \tag{3.116}$$

and R_{ij3l} are phonon-phason coupling elastic constants which satisfy symmetry properties

$$R_{ij3l} = R_{ji3l}. \tag{3.117}$$

The positivity of elastic strain energy density requires that the elastic constant tensors $c_{ijkl},\ K_{3j3l},\ R_{ij3l}$ must be positive definite. Namely, when the strain tensors ε_{kl}, w_{3l} are not zero entirely, the elastic constant tensors satisfy the following inequality (Gao & Zhao (2006))

$$\sum_{i,j,l=1}^{3} c_{ijkl}\varepsilon_{ij}\varepsilon_{kl} > 0,\ \sum_{j,l=1}^{3} K_{3j3l}w_{3j}w_{3l} > 0,\ \sum_{i,j,l=1}^{3} R_{ij3l}\varepsilon_{ij}w_{3l} > 0. \tag{3.118}$$

The dynamic equilibrium equations can be written in the following form (Ding & Yang & Hu & Wang (1993))

$$\rho\frac{\partial^2 u_i(x,t)}{\partial t^2} = \sum_{j=1}^{3}\frac{\partial \sigma_{ij}(x,t)}{\partial x_j} + f_i(x,t),\ i = 1,2,3, \tag{3.119}$$

$$\rho\frac{\partial^2 w_3(x,t)}{\partial t^2} = \sum_{j=1}^{3}\frac{\partial H_{3j}(x,t)}{\partial x_j} + g_3(x,t),\ x \in R^3,\ t \in R, \tag{3.120}$$

where $\rho > 0$ is the density; $\mathbf{f}(x,t) = (f_1(x,t), f_2(x,t), f_3(x,t)),\ g_3(x,t)$ are body forces

densities for the phonon and phason displacements, respectively; σ_{ij} and H_{3j}, $i,j=1,2,3$ are phonon and phason stresses (see, for example, Ding & Yang & Hu & Wang (1993),Hu & Wang & Ding (2000),Gao & Zhao (2006),Yang & Wang & Ding & Hu (1993)).

There exits the following classification of 1-D QCs (Wang & Yang & Hu (1997)): Triclinic, Monoclinic, Orthorhombic, Tetragonal, Trigonal and Hexagonal crystal systems (see Appendix.).

3.1.2 Time-dependent fundamental solution of elasticity for 1D QCs

Substituting (3.112) and (3.113) into (3.119) and (3.120) we have for $i=1,2,3$

$$\rho\frac{\partial^2 u_i(x,t)}{\partial t^2}=\sum_{j,k,l=1}^{3}c_{ijkl}\frac{\partial^2 u_k(x,t)}{\partial x_j\partial x_l}+\sum_{j,l=1}^{3}R_{ij3l}\frac{\partial^2 w_3(x,t)}{\partial x_j\partial x_l}+f_i, \tag{3.121}$$

$$\rho\frac{\partial^2 w_3(x,t)}{\partial t^2}=\sum_{j,k,l=1}^{3}R_{kl3j}\frac{\partial^2 u_k(x,t)}{\partial x_j\partial x_l}+\sum_{j,l=1}^{3}K_{3j3l}\frac{\partial^2 w_3(x,t)}{\partial x_j\partial x_l}+g_3. \tag{3.122}$$

The system (3.121)-(3.122) can be written in the form of one vector partial differential equation as follows (Akmaz (2009))

$$\rho\frac{\partial^2 \mathbf{V}}{\partial t^2}=\sum_{j,l=1}^{3}\mathbf{P}_{jl}\frac{\partial^2 \mathbf{V}}{\partial x_j\partial x_l}+\mathbf{F}(x,t), x\in R^3, t\in R, \tag{3.123}$$

where $\mathbf{V}=(u_1,u_2,u_3,w_3)$, $\mathbf{F}=(f_1,f_2,f_3,g_3)$ and matrices $\mathbf{P}_{jl}$ are defined by

$$\mathbf{P}_{jl}=\begin{bmatrix} \frac{c_{1j1l}+c_{1l1j}}{2} & \frac{c_{1j2l}+c_{1l2j}}{2} & \frac{c_{1j3l}+c_{1l3j}}{2} & \frac{R_{1j3l}+R_{1l3j}}{2} \\ \frac{c_{2j1l}+c_{2l1j}}{2} & \frac{c_{2j2l}+c_{2l2j}}{2} & \frac{c_{2j3l}+c_{2l3j}}{2} & \frac{R_{2j3l}+R_{2l3j}}{2} \\ \frac{c_{3j1l}+c_{3l1j}}{2} & \frac{c_{3j2l}+c_{3l2j}}{2} & \frac{c_{3j3l}+c_{3l3j}}{2} & \frac{R_{3j3l}+R_{3l3j}}{2} \\ \frac{R_{1j3l}+R_{1l3j}}{2} & \frac{R_{2j3l}+R_{2l3j}}{2} & \frac{R_{3j3l}+R_{3l3j}}{2} & \frac{K_{3j3l}+K_{3l3j}}{2} \end{bmatrix}. \tag{3.124}$$

The time-dependent fundamental solution (FS) of elastodynamics in 3D QCs is a 4×4 matrix whose mth column is a vector function

$$\mathbf{V}^m(x,t) = (u_1^m(x,t), u_2^m(x,t), u_3^m(x,t), w_3^m(x,t))$$

satisfying

$$\rho\frac{\partial^2\mathbf{V}^m}{\partial t^2} = \sum_{j,l=1}^{3}\mathbf{P}_{jl}\frac{\partial^2\mathbf{V}^m}{\partial x_j\partial x_l} + \mathsf{E}^m\delta(x)\delta(t),\ x\in R^3, t\in R, \tag{3.125}$$

$$\mathbf{V}^m(x,t)|_{t<0} = 0, \tag{3.126}$$

Here $\delta(x) = \delta(x_1)\delta(x_2)\delta(x_3)$ is the Dirac delta function of the space variable concentrated at $x_1 = 0,\ x_2 = 0,\ x_3 = 0$; $\delta(t)$ is the Dirac delta function of the time variable concentrated at $t = 0$; $m = 1,...,4$; $\mathsf{E}^m = (\delta_1^m, \delta_2^m, \delta_3^m, \delta_4^m)$, δ_n^m is the Kronecker symbol i.e. $\delta_n^m = 1$ if $n = m$ and $\delta_n^m = 0$ if $n \neq m$, $n = 1,...,4$. $\mathbf{P}_{jl}$ are matrices defined by (3.124).

3.1.3 Computation of mth column for time-dependent FS of 1D QCs

In this section we will solve IVP (3.125)-(3.126). Let

$$\tilde{\mathbf{V}}^m(\nu,t) = (\tilde{u_1}^m, \tilde{u_2}^m, \tilde{u_3}^m, \tilde{w_3}^m)$$

be the Fourier image of $\mathbf{V}^m(x,t)$ with respect to $x = (x_1,x_2,x_3)\in R^3$, i.e.

$$\tilde{V_j}^m(\nu,t) = \int_{-\infty}^{\infty}\int_{-\infty}^{\infty}\int_{-\infty}^{\infty} V_j^m(x,t)e^{ix\cdot\nu}dx_1dx_2dx_3,$$

where

$$\nu \;=\; (\nu_1,\nu_2,\nu_3)\in R^3,\ x\cdot\nu = x_1\nu_1+x_2\nu_2+x_3\nu_3,\ i^2=-1,\ j=1,2,3,4.$$

The IVP (3.125)-(3.126) can be written in terms of $\tilde{\mathbf{V}}^m(\nu,t)$ as follows

$$\rho\frac{\partial^2\tilde{\mathbf{V}}^m}{\partial t^2}+\mathbf{A}(\nu)\tilde{\mathbf{V}}^m \;=\; \mathsf{E}^m\delta(t),\ \nu\in R^3, t\in R, \tag{3.127}$$

$$\tilde{\mathbf{V}}^m(\nu,t)|_{t<0} \;=\; 0. \tag{3.128}$$

Here

$$\mathbf{A}(\nu)=\sum_{j,l=1}^{3}\mathbf{P}_{jl}\nu_j\nu_l, \tag{3.129}$$

$\mathbf{P}_{jl}$ are matrices defined by (3.124).

3.1.3.1 Explicit formula for a solution of (3.127), (3.128)

From (3.118) $\mathbf{A}(\nu)$ is a positive semi definite matrix (see Appendix) and from (3.115), (3.116), (3.117) $\mathbf{A}(\nu)$ is a symmetric matrix. Then we can construct an orthogonal matrix $\mathbf{T}(\nu)$ and a diagonal matrix $\mathbf{D}(\nu)=diag(d_k(\nu),\ k=1,2,3,4)$ with nonnegative elements such that

$$\mathbf{T}^*(\nu)\mathbf{A}(\nu)\mathbf{T}(\nu)=\mathbf{D}(\nu), \tag{3.130}$$

where $\mathbf{T}^*(\nu)$ is the transposed matrix to $\mathbf{T}(\nu)$.

Using the transformation

$$\tilde{\mathbf{V}}^m(\nu,t)=\mathbf{T}(\nu)\mathbf{Y}^m(\nu,t), \tag{3.131}$$

where $\mathbf{Y}^m(\nu,t)$ is unknown vector function, for (3.127)-(3.128) and then multiplying the obtained vector differential equation by $\mathbf{T}^*(\nu)$ and using (3.130) we find

$$\rho\frac{\partial^2\mathbf{Y}^m}{\partial t^2}+\mathbf{D}(\nu)\mathbf{Y}^m = \mathbf{T}^*(\nu)\mathsf{E}^m\delta(t),\ t\in R,\ \nu\in R^3 \tag{3.132}$$

$$\mathbf{Y}^m(\nu,t)|_{t\le 0} = 0. \tag{3.133}$$

Using the ordinary differential equations technique (see, for example, Boyce & DiPrima (1992)), a solution of the initial value problem (3.132)-(3.133) is given by

$$\mathbf{Y}^m_k(\nu,t)=\theta(t)\frac{(\mathbf{T}^*(\nu)\mathsf{E}^m)_k}{\sqrt{\rho d_k(\nu)}}\sin(t\frac{\sqrt{d_k(\nu)}}{\sqrt{\rho}}),\ for\ d_k(\nu)>0,$$

$$\mathbf{Y}^m_k(\nu,t)=\theta(t)\frac{(\mathbf{T}^*(\nu)\mathsf{E}^m)_k}{\rho}t,\ for\ d_k(\nu)=0,$$

where $k=1,2,3,4$, $\theta(t)$ is the Heaviside function, i.e. $\theta(t)=1$ for $t\ge 0$ and $\theta(t)=0$ for $t<0$. Finally, a solution of (3.127), (3.128) is determined by

$$\tilde{\mathbf{V}}^m(\nu,t)=\theta(t)\mathbf{T}(\nu)\mathbf{Y}^m(\nu,t). \tag{3.134}$$

3.1.3.2 Explicit formula for mth column for time-dependent FS of 1D QCs

The values of $\mathbf{V}^m(x,t)$, $\tilde{\mathbf{V}}^m(\nu,t)$, $\mathbf{T}(\nu)$ and $\mathbf{D}(\nu)=diag(d_k(\nu),\ k=1,2,3,4)$ are real. So applying the inverse Fourier transform to (3.134) (see, for example Vladimirov (1971)) we find that a solution of (3.125), (3.126) is given by

$$\begin{aligned}\mathbf{V}^m(x,t) &= \frac{\theta(t)}{(2\pi)^3}Re\left[\int_{-\infty}^{\infty}\int_{-\infty}^{\infty}\int_{-\infty}^{\infty}\mathbf{T}(\nu)\mathbf{Y}^m(\nu,t)\cos(\nu\cdot x)d\nu_1 d\nu_2 d\nu_3\right]\\ &= \frac{\theta(t)}{(2\pi)^3}\int_{-\infty}^{\infty}\int_{-\infty}^{\infty}\int_{-\infty}^{\infty}\mathbf{T}(\nu)\mathbf{Y}^m(\nu,t)\cos(\nu\cdot x)d\nu_1 d\nu_2 d\nu_3.\end{aligned} \tag{3.135}$$

3.1.4 Computational examples

3.1.4.1 General characteristics of computations and visualizations

In this section, we consider six 1D quasicrystals for anisotropic dynamic elasticity: hexagonal, trigonal, tetragonal, orthorhombic, monoclinic and triclinic structures, respectively. For our examples we take the pulse force situated in each crystal and modeled by $\mathsf{E}^3\delta(x_1)\delta(x_2)\delta(x_3)\delta(t)$ and $\mathsf{E}^4\delta(x_1)\delta(x_2)\delta(x_3)\delta(t)$, where $\mathsf{E}^3=(0,0,1,0)$, $\mathsf{E}^4=(0,0,0,1)$ and $\delta(.)$ is the Dirac delta function. The responses of the considered anisotropic quasicrystals on this source are the phonon and phason displacement vectors depending on the position (i.e. space variables x_1,x_2,x_3) and the time variable t. Using the method of Section 3.1.3 we compute $\mathbf{T}(\nu),\mathbf{T}^*(\nu),\mathbf{D}(\nu)$ and then using the formula (3.135) we have derived numerically components of $\mathbf{V}^3(x,t)$ and $\mathbf{V}^4(x,t)$. The first three components of the vector function $\mathbf{V}^i(x,t), i=3,4$, are components of the phonon displacement $u_1^i(x,t),u_2^i(x,t),u_3^i(x,t)$ and the fourth component is the phason displacement $w_3^i(x,t), i=3,4$.

We note here that the vectors $\mathbf{V}^3(x,t)$ and $\mathbf{V}^4(x,t)$ are the third and fourth columns of $\mathbf{G}(x,t)$, where $\mathbf{G}(x,t)$ is the FS of anisotropic elasticity for quasicrystals.

3.1.4.2 Description of input data and corresponding images

Example 1. (**Hexagonal Crystal.**) The density ρ is equal to 1.848 and the independent elastic constants are

$$\begin{aligned}
c_{1111} &= 29.23,\ c_{1122}=c_{2211}=2.67,\ c_{1133}=c_{3311}=1.4,\ c_{3333}=33.64,\\
c_{2323} &= c_{2332}=c_{3223}=c_{3232}=16.25,\ c_{1212}=c_{1221}=c_{2112}=c_{2121}=13.28;\\
R_{1133} &= 1.35,\ R_{3333}=1,\ R_{3131}=R_{1331}=0.4,\ R_{2331}=R_{3231}=-2.1;\\
K_{3333} &= 1,\ K_{3131}=2.
\end{aligned}$$

Figures 3.27, 3.28 show dynamics of the distribution of the first phonon displacement $u_1^3(x_1,0,x_3,0.75)$ and phason displacement $w_3^3(x_1,0,x_3,0.75)$, respectively. These figures contain screen shots of 2-D level plots of the $u_1^3(x_1,0,x_3,0.75)$ and $w_3^3(x_1,0,x_3,0.75)$, i.e. a view of these surfaces from the top of z-axis.

Example 2. (**Trigonal Crystal.**) The density ρ is equal to 3.986 and the independent elastic constants are

$$\begin{aligned}
c_{1111} &= 49.7,\ c_{1122}=c_{2211}=16.4,\ c_{1133}=c_{3311}=11.2,\\
c_{1123} &= c_{2311}=c_{1132}=c_{3211}=-2.35,\ c_{3333}=49.9,\\
c_{2323} &= c_{3223}=c_{3232}=c_{2332}=14.7,\ c_{1212}=c_{1221}=c_{2112}=c_{2121}=16.65;\\
R_{1133} &= 1,\ R_{3333}=0.4,\ R_{2332}=R_{3232}=0.1,\ R_{1132}=2.1;\ K_{3333}=1,\ K_{3131}=2.
\end{aligned}$$

Figures 3.29, 3.30 present 2-D plot of the first phonon displacement $u_1^3(x_1,0,x_3,0.8)$ and pahon displacement $w_3^4(x_1,0,x_3,3.75)$. All pictures are the view from the top of z-axis.

Example 3. (**Tetragonal Crystal.**) The density ρ is equal to 4.255 and the

independent elastic constants are

$$\begin{aligned}
c_{1111} &= 14.5,\ c_{1122}=c_{2211}=6.6,\ c_{1133}=c_{3311}=4.46,\ c_{3333}=12.65\\
c_{1112} &= c_{1211}=c_{2111}=c_{1121}=1.3,\ c_{2323}=c_{2332}=c_{3223}=c_{3232}=3.69,\\
c_{1212} &= c_{1221}=c_{2112}=c_{2121}=4.5;\ R_{1133}=1.35,\ R_{3333}=0.4,\\
R_{2332} &= R_{3232}=1,\ R_{2331}=R_{3231}=2;\ K_{3333}=1,\ K_{3131}=2.
\end{aligned}$$

Figures 3.31, 3.32 present of the first phonon displacement $u_1^3(x_1,0,x_3,1.75)$ and the phason displacement $w_3^3(x_1,0,x_3,1.75)$. All pictures are the view from the top of z-axis.

Example 4. (**Orthorhombic Crystal.**) The density ρ is equal to 4.64 and the independent elastic constants are

$$\begin{aligned}
c_{1111} &= 3.01,\ c_{1122}=c_{2211}=1.61,\ c_{1133}=c_{3311}=1.11,\ c_{2222}=5.8,\\
c_{3131} &= c_{1331}=c_{3113}=c_{1313}=2.06,\ c_{2233}=c_{3322}=0.8,\ c_{3333}=4.29,\\
c_{2323} &= c_{2332}=c_{3223}=c_{3232}=1.69,\ c_{1212}=c_{1221}=c_{2112}=c_{2121}=1.58;\\
R_{1133} &= 1.5,\ R_{3333}=6.6,\ R_{2332}=R_{3232}=-2.5,\ R_{3131}=R_{1331}=1.11,\\
R_{2233} &= 2.1;\ K_{3333}=11.1,\ K_{3131}=1.3\ K_{3232}=4.
\end{aligned}$$

Figures 3.33, 3.34 present of the first phonon displacement $u_1^4(x_1,0,x_3,1.5)$ and the second phason displacement $w_3^3(x_1,0,x_3,1.5)$. All pictures are the view from the top of z-axis.

Example 5. (**Monoclinic Crystal.**) The density ρ is equal to 3.31 and the nonzero

elastic constants are

$$
\begin{aligned}
c_{1111} &= 2.040,\ c_{1122}=c_{2211}=0.884,\ c_{1133}=c_{3311}=0.0883,\\
c_{1131} &= c_{3111}=c_{1311}=c_{1113}=-0.193,\ c_{2222}=1.750,\ c_{3333}=2.38\\
c_{2233} &= c_{3322}=0.482,\ c_{2231}=c_{3122}=c_{1322}=c_{2213}=-0.196,\\
c_{3331} &= c_{3133}=c_{1333}=c_{3313}=-0.336,\ c_{2323}=c_{2332}=c_{3223}=c_{3232}=0.675,\\
c_{2312} &= c_{3212}=c_{1232}=c_{1223}=c_{3221}=c_{2132}=c_{2321}=c_{2123}=-0.113,\\
c_{3131} &= c_{1331}=c_{3113}=c_{1313}=0.588,\ c_{1212}=c_{1221}=c_{2112}=c_{2121}=0.705;\\
R_{1133} &= 0.035,\ R_{2233}=-1.04,\ R_{3333}=0.1,\ R_{3133}=R_{1333}=-0.2,\\
R_{1131} &= 0.1,\ R_{2231}=-2.5,\ R_{3331}=-0.1,\ R_{3131}=R_{1331}=1.5,\\
R_{2332} &= R_{3232}=0.01,\ R_{1232}=R_{2132}=-0.3;\ K_{3333}=4,\\
K_{3331} &= K_{3133}=3.1,\ K_{3131}=5,\ K_{3232}=3.
\end{aligned}
$$

Figures 3.35, 3.36 show dynamics of the distribution of the first phonon displacement $u_1^4(x_1,0,x_3,2)$ the phason displacement $w_3^4(x_1,0,x_3,2)$. Figures 3.35, 3.36 contain screen shots of 2-D level plots of the first phonon and phason displacements, respectively, i.e. a view of these surfaces from the top of z-axis.

Example 6. (**Triclinic Crystal**).

The density $\rho = 2$ and the nonzero elastic constants are

$$
\begin{aligned}
c_{1111} &= 69.1,\ c_{1122}=c_{2211}=34.0,\ c_{1133}=c_{3311}=30.8,\ c_{3333}=179.5,\\
c_{1123} &= c_{2311}=c_{3211}=c_{1132}=5.1, c_{1131}=c_{3111}=c_{1311}=c_{1113}-2.4,\\
c_{1112} &= c_{1121}=c_{2111}=c_{1211}=-0.9, c_{2222}=183.5,\ c_{2233}=c_{3322}=5.5,\\
c_{2223} &= c_{2322}=c_{3222}=c_{2232}=-3.9,\ c_{3131}=c_{3113}=c_{1331}=c_{1313}=26.8,\\
c_{2231} &= c_{3122}=c_{1322}=c_{2213}=-7.7,\ c_{2212}=c_{2221}=c_{2122}=c_{1222}=-5.8,
\end{aligned}
$$

$$
\begin{aligned}
c_{3323} &= c_{3332} = c_{3233} = c_{2333} = -8.7,\ c_{3331} = c_{3313} = c_{1333} = c_{3133} = 7.1,\\
c_{3312} &= c_{3321} = c_{2133} = c_{1233} = -9.8,\ c_{2323} = c_{2332} = c_{3223} = c_{3232} = 24.9,\\
c_{3112} &= c_{3121} = c_{2131} = c_{1231} = c_{1312} = c_{1213} = c_{1321} = c_{2113} = 0.5,\\
c_{2331} &= c_{2313} = c_{1323} = c_{3123} = c_{3231} = c_{3132} = c_{3213} = c_{1332} = -2.4,\\
c_{2312} &= c_{2321} = c_{2123} = c_{1223} = c_{3212} = c_{1232} = c_{3221} = c_{2132} = -7.2,\\
c_{1212} &= c_{1221} = c_{2112} = c_{2121} = 33.5;\ R_{1131} = -1.35,\ R_{1132} = -5.4,\\
R_{1231} &= R_{2131} = -2, R_{1133} = 1,\ R_{1232} = R_{2132} = 3,\ R_{1233} = R_{2133} = 4,\\
R_{1331} &= R_{3131} = -1.1,\ R_{1332} = R_{3132} = 0.5,\ R_{1333} = R_{3133} = 1.3,\\
R_{2231} &= 7.3,\ R_{2232} = 1.3,\ R_{2233} = 4.1,\ R_{2331} = R_{3231} = -0.7,\\
R_{2333} &= R_{3233} = 3.3,\ R_{2332} = R_{3232} = 1.5\ R_{3331} = 2.6,\ R_{3332} = 0.01,\\
R_{3333} &= 4.2;\ K_{3131} = 6,\ K_{3132} = K_{3231} = 1,\ K_{3133} = K_{3331} = 0.5,\\
K_{3232} &= 2.2,\ K_{3233} = K_{3332} = 2.1,\ K_{3333} = 3.
\end{aligned}
$$

Figures 3.37, 3.38 present of the first phonon displacement $u_1^3(x_1,0,x_3,0.3)$ and the phason displacement $w_3^4(x_1,0,x_3,1.5)$ on the plane $x_2 = 0$. Here the horizontal axes are x_1 and x_3. All pictures are the view from the top of z-axis.

3.1.4.3 Analysis of the visualization

The simulation of the phonon and phason displacements in general anisotropic media by modern computer tools allow us to see and evaluate dependence between media structures and behavior of these displacement. The approach of the method allows users to observe the elastic wave propagation arising from pulse point sources of the form $\mathsf{E}^m\delta(x_1)\delta(x_2)\delta(x_3)\delta(t)$ in 1D QCs (hexagonal, trigonal, tetragonal, orthorhombic monoclinic, triclinic). Here $\mathsf{E}^m = (\delta_1^m, \delta_2^m, \delta_3^m, \delta_4^m)$. We can see on the Figures 3.27-3.38 that the different 1D QCs structures of media produce different

responses of phonon and phason displacement fields inside these media. The various shapes of elastic waves (different forms of fronts and magnitude fluctuations of phonon and phason displacement fields) are shown in presented figures.

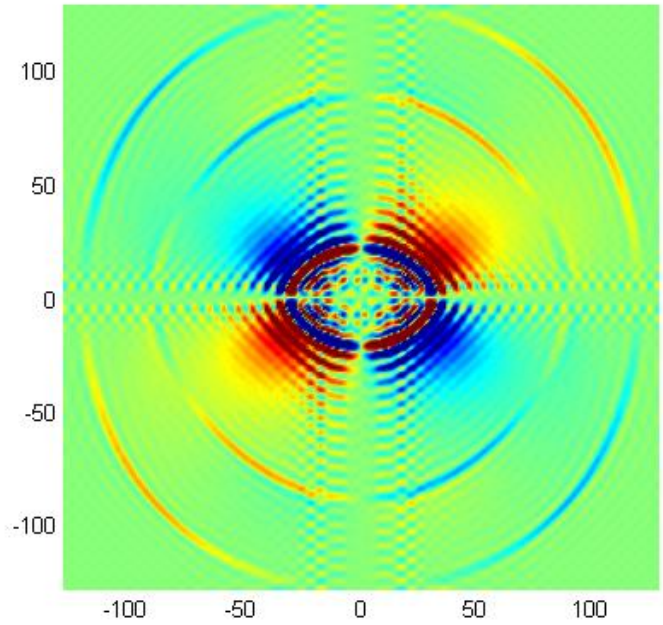

Figure 3.27: The map surface plot (plan) of 3D surface $z = u_1^4(x_1, 0, x_3, t)$ for $t = 0.75$ in hexagonal QC

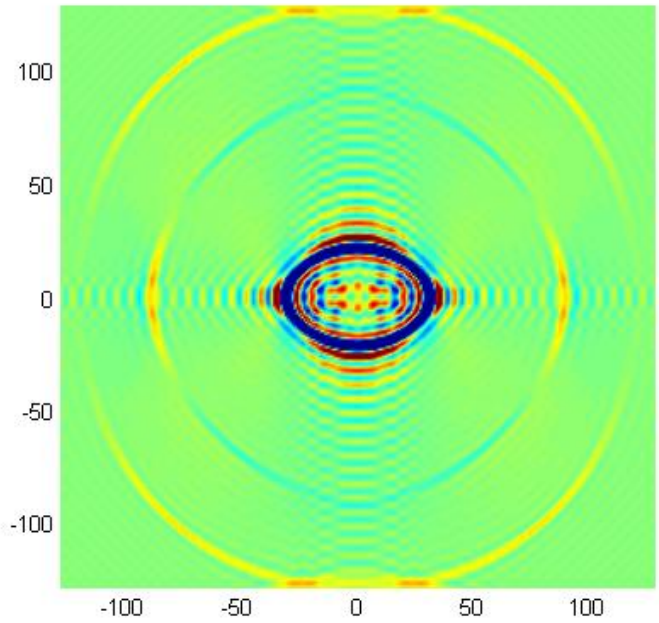

Figure 3.28: The map surface plot (plan) of 3D surface $z = w_3^3(x_1, 0, x_3, t)$ for $t = 0.75$ in hexagonal QC

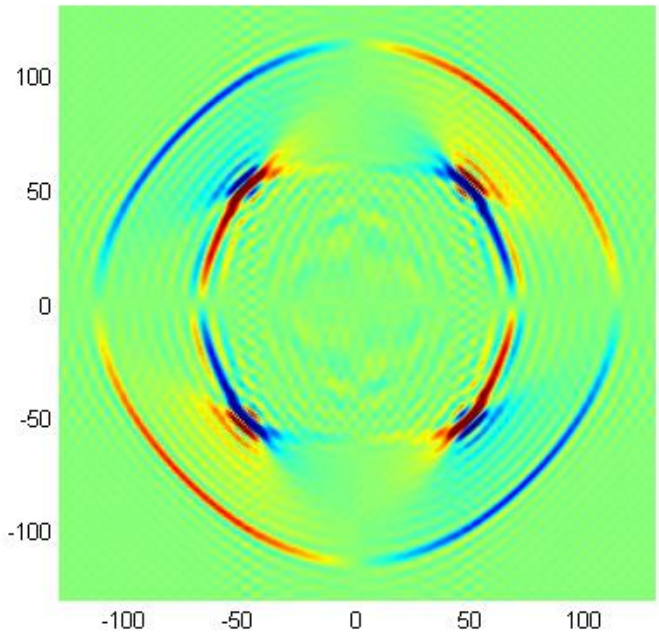

Figure 3.29: The map surface plot (plan) of 3D surface $z = u_1^3(x_1, 0, x_3, t)$ for $t = 0.8$ in trigonal QC

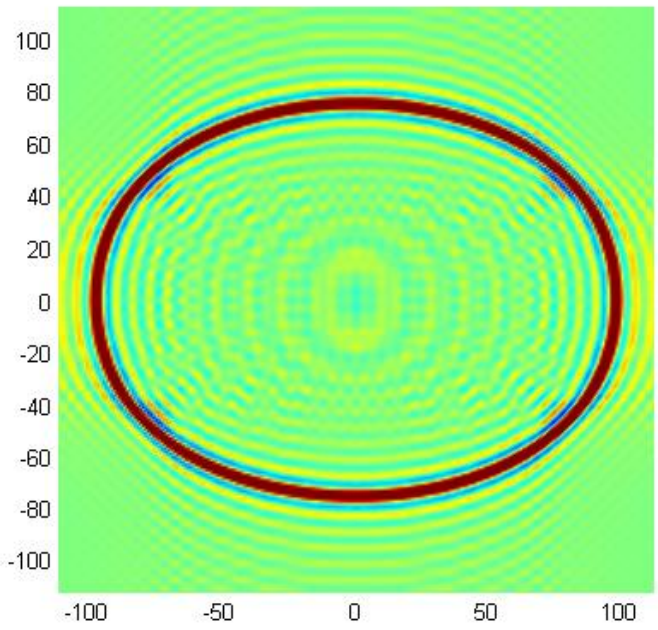

Figure 3.30: The map surface plot (plan) of 3D surface $z = w_3^4(x_1, 0, x_3, t)$ for $t = 3.75$ in trigonal QC

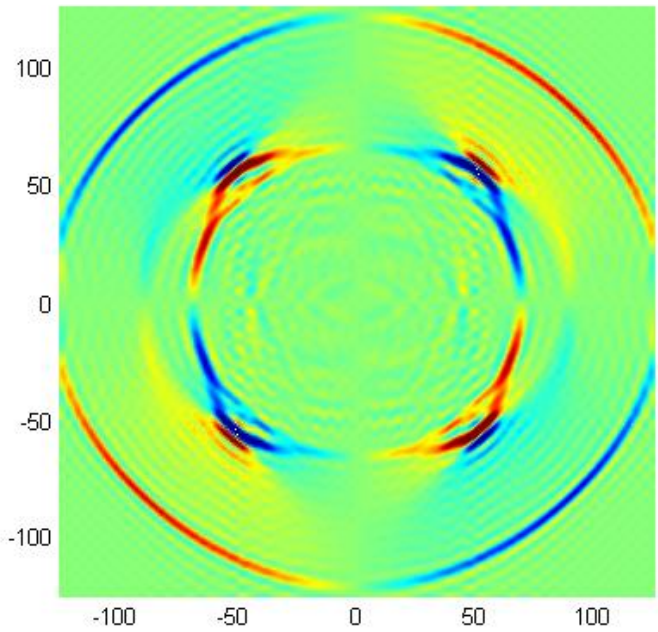

Figure 3.31: The map surface plot (plan) of 3D surface $z = u_1^3(x_1, 0, x_3, t)$ for $t = 1.75$ in tetragonal QC

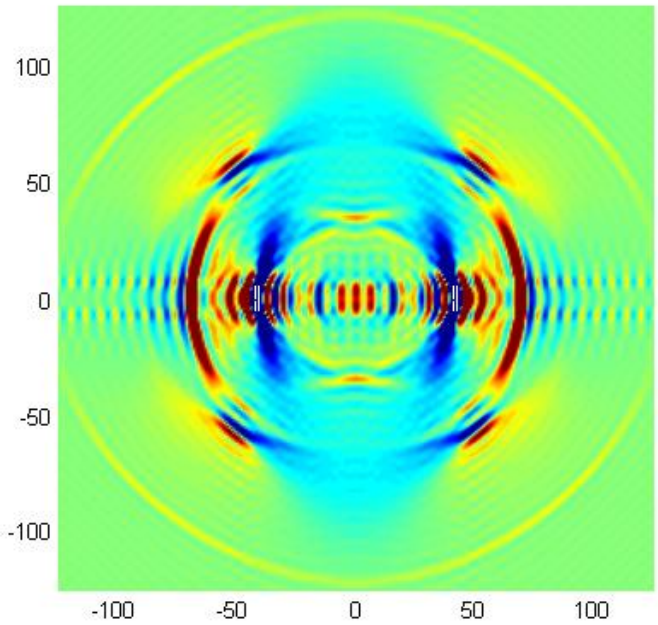

Figure 3.32: The map surface plot (plan) of 3D surface $z = w_3^3(x_1, 0, x_3, t)$ for $t = 1.75$ in tetragonal QC

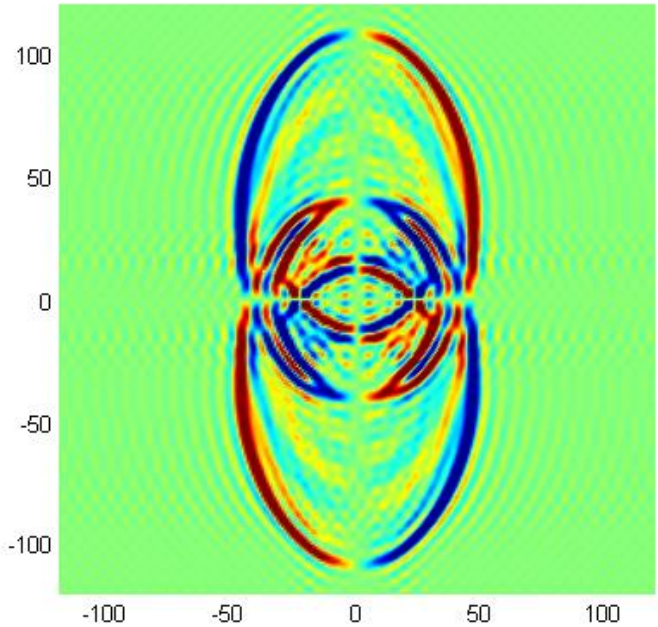

Figure 3.33: The map surface plot (plan) of 3D surface $z = u_1^4(x_1, 0, x_3, t)$ for $t = 1.5$ in orthorhombic QC

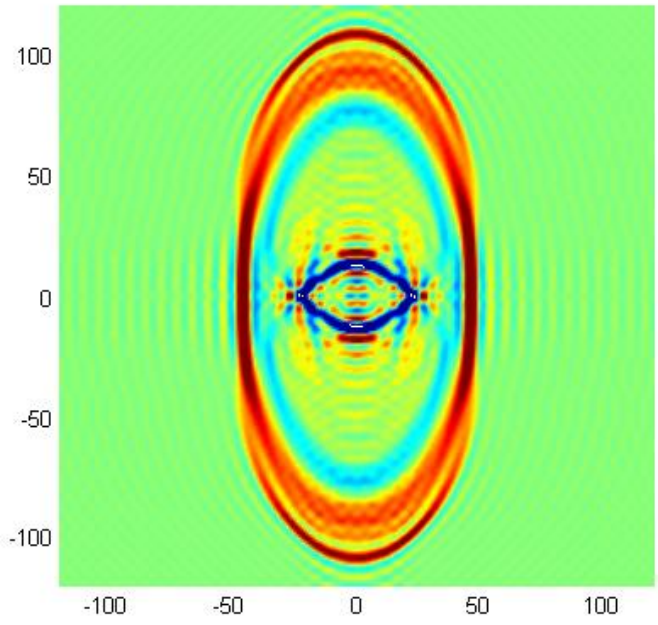

Figure 3.34: The map surface plot (plan) of 3D surface $z = w_3^3(x_1, 0, x_3, t)$ for $t = 1.5$ in orthorhombic QC

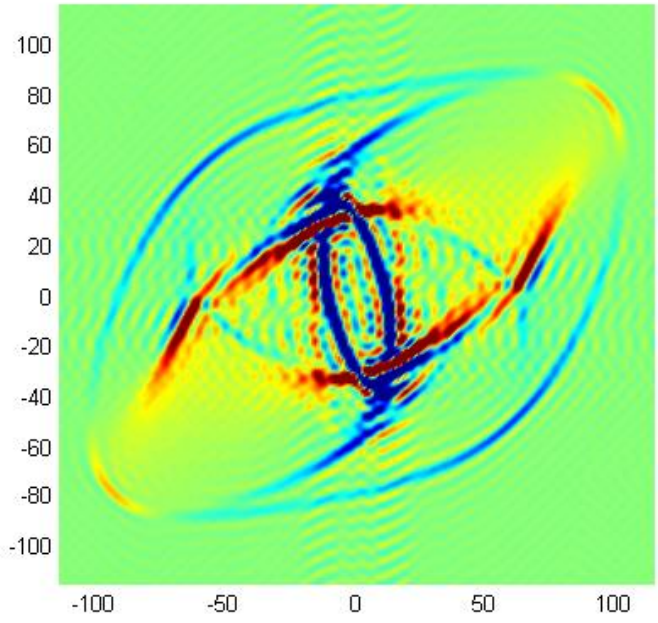

Figure 3.35: The map surface plot (plan) of 3D surface $z = u_1^4(x_1, 0, x_3, t)$ for $t = 2$ in monoclinic QC

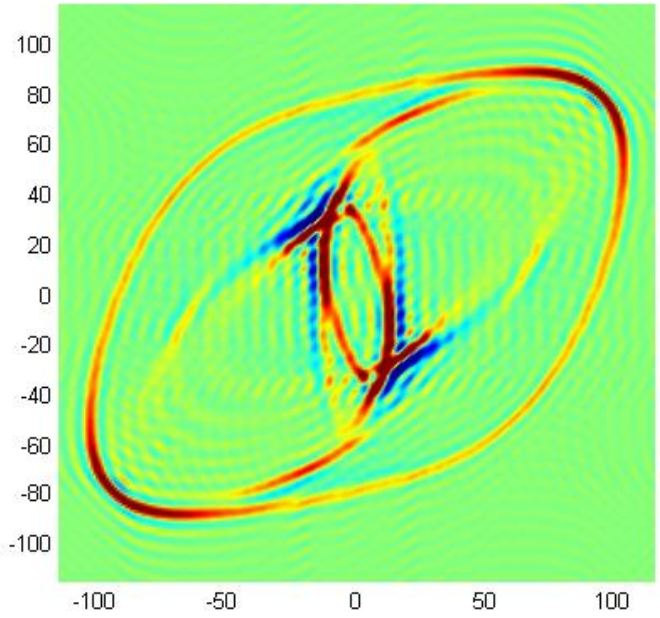

Figure 3.36: The map surface plot (plan) of 3D surface $z = w_3^4(x_1, 0, x_3, t)$ for $t = 2$ in monoclinic QC

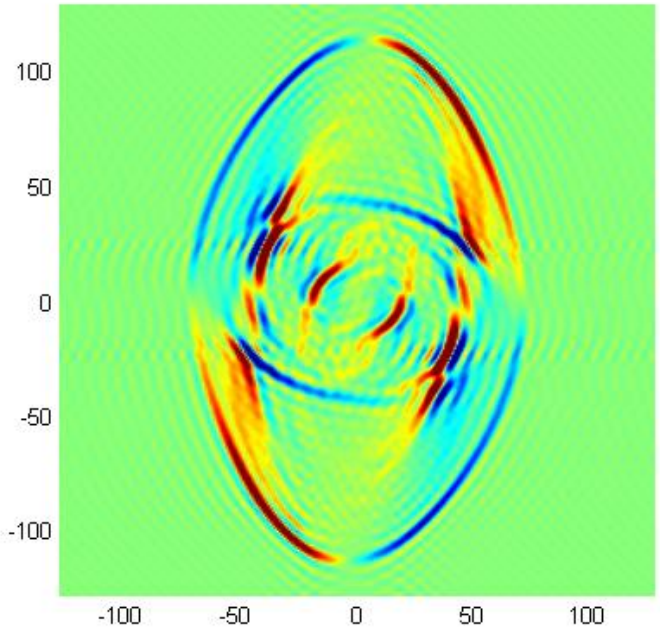

Figure 3.37: The map surface plot (plan) of 3D surface $z = u_1^4(x_1, 0, x_3, t)$ for $t = 2$ in triclinic QC

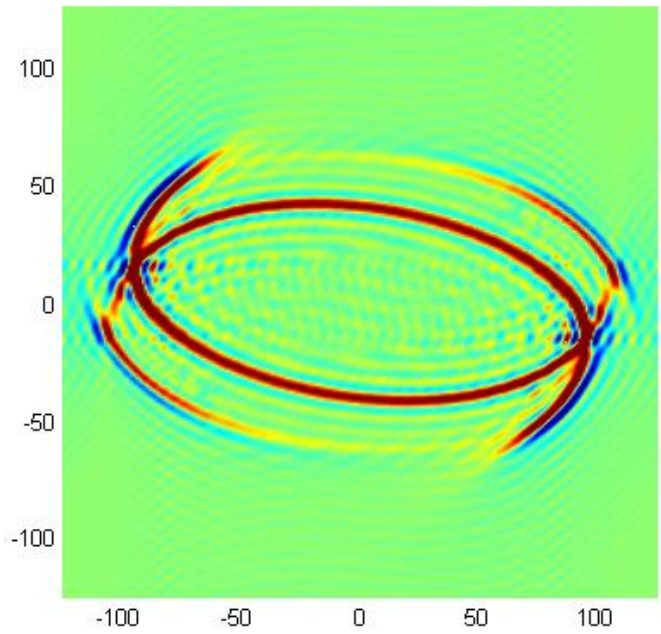

Figure 3.38: The map surface plot (plan) of 3D surface $z = w_3^4(x_1, 0, x_3, t)$ for $t = 1.5$ in triclinic QC

3.2 Three dimensional elastodynamics of 2D quasicrystals: the derivation of the time-dependent fundamental solution

3.2.1 The basic equations for 2D QCs

Let us consider a quasicrystal with two dimensional quasiperiodic and one dimensional periodic structure. Let $x = (x_1, x_2, x_3) \in R^3$ be a space variable, $t \in R$ be a time variable. The generalized Hooke's laws of the elasticity problem of 2D QCs is given by (Gao (2009), Grimmer (2008))

$$\sigma_{ij} = c_{ijkl}\varepsilon_{kl} + R_{ij\alpha l}w_{\alpha l}, \tag{3.136}$$

$$H_{\beta j} = R_{kl\beta j}\varepsilon_{kl} + K_{\beta j\alpha l}w_{\alpha l},\ i,j,k,l = 1,2,3,\ \alpha,\beta = 1,2, \tag{3.137}$$

where $\varepsilon_{kl}(x,t)$, $w_{\alpha l}(x,t)$, $l = 1,2,3$, $\alpha = 1,2$ are defined as follows

$$\varepsilon_{kl} = \frac{1}{2}(\frac{\partial u_k}{\partial x_l} + \frac{\partial u_l}{\partial x_k}),\ w_{\alpha l} = \frac{\partial w_\alpha}{\partial x_l},\ k,l = 1,2,3,\ \alpha = 1,2, \tag{3.138}$$

are phonon and phason strains, Here u_k, $k = 1,2,3$ and $w_\alpha, \alpha = 1,2$ are the phonon and phason displacements; $\varepsilon_{kl}(x,t)$, $w_{\alpha l}(x,t)$, $k,l = 1,2,3$, $\alpha = 1,2$ are phonon and phason strains.

c_{ijkl} represent the phonon elastic constants, $K_{\beta j\alpha l}$ are the phason elastic constants, $R_{ij\alpha l}$ are the phonon-phason coupling elastic constants. Similar to Ding & Yang & Hu & Wang (1993), we assume that the following symmetric properties are satisfied

$$c_{ijkl} = c_{jikl} = c_{ijlk} = c_{klij},\ K_{\beta j\alpha l} = K_{\alpha l\beta j},\ R_{ij\alpha l} = R_{ji\alpha l}. \tag{3.139}$$

The positivity of the elastic strain energy density requires that the elastic constant tensors c_{ijkl}, $R_{ij\alpha l}$, $K_{\beta j\alpha l}$ must be positive definite. Namely, when the strain tensors ε_{ij},

$w_{\alpha l}$ are not zero entirely, the elastic constant tensors satisfy the following inequality (see Gao & Zhao (2006))

$$\sum_{j,l,i,k=1}^{3} c_{ijkl}\varepsilon_{ij}\varepsilon_{kl} > 0, \ \sum_{j,l=1}^{3}\sum_{\alpha,\beta=1}^{2} K_{\beta j\alpha l}w_{\beta j}w_{\alpha l} > 0, \ \sum_{j,l,i=1}^{3}\sum_{\alpha=1}^{2} R_{ij\alpha l}\varepsilon_{ij}w_{\alpha l} > 0.$$

The dynamic equilibrium equations can be written in the following form (Ding & Yang & Hu & Wang (1993))

$$\rho\frac{\partial^2 u_i(x,t)}{\partial t^2} = \sum_{j=1}^{3}\frac{\partial\sigma_{ij}(x,t)}{\partial x_j} + f_i(x,t), \ i=1,2,3, \tag{3.140}$$

$$\rho\frac{\partial^2 w_\beta(x,t)}{\partial t^2} = \sum_{j=1}^{3}\frac{\partial H_{\beta j}(x,t)}{\partial x_j} + g_\beta(x,t), \ \beta=1,2, \ x\in R^3, \ t\in R, \tag{3.141}$$

where the constant $\rho > 0$ is the density; $f_i(x,t), i=1,2,3$ and $g_j(x,t), j=1,2$ are body forces densities for the phonon and phason displacements, respectively; σ_{ij} and $H_{\beta j}$, $i,j=1,2,3$, $\beta=1,2$ are phonon and phason stresses (see, for example, Ding & Yang & Hu & Wang (1993),Hu & Wang & Ding (2000),Gao & Zhao (2006),Yang & Wang & Ding & Hu (1993)).

3.2.2 Time-dependent fundamental solution of elasticity for 2D QCs

Let m run values $1,2,3,4,5$; δ_n^m be the Kronecker symbol i.e. $\delta_n^m = 1$ if $n=m$ and $\delta_n^m = 0$ if $n\neq m$; $n=1,2,3,4,5$; $m=1,2,3,4,5$. The time-dependent Green's function (GF) of elasticity for 2D QCs is a 5×5 matrix whose mth column is a vector function

$$\mathbf{V}^m(x,t) = (u_1^m(x,t), u_2^m(x,t), u_3^m(x,t), w_1^m(x,t), w_2^m(x,t))$$

satisfying the following equations

$$\rho\frac{\partial^2 u_i^m(x,t)}{\partial t^2} = \sum_{j,k,l=1}^{3} c_{ijkl}\frac{\partial^2 u_k^m(x,t)}{\partial x_j \partial x_l} + \sum_{j,l=1}^{3}\sum_{\alpha=1}^{2} R_{ij\alpha l}\frac{\partial^2 w_\alpha^m(x,t)}{\partial x_j \partial x_l} + \delta_i^m \delta(x)\delta(t), \tag{3.142}$$

$$\rho\frac{\partial^2 w_\beta^m(x,t)}{\partial t^2} = \sum_{j,k,l=1}^{3} R_{kl\beta j}\frac{\partial^2 u_k^m(x,t)}{\partial x_j \partial x_l} + \sum_{j,l=1}^{3}\sum_{\alpha=1}^{2} K_{\beta j\alpha l}\frac{\partial^2 w_\alpha^m(x,t)}{\partial x_j \partial x_l} + \delta_\beta^m \delta(x)\delta(t), \tag{3.143}$$

and conditions

$$u_i^m(x,t)\mid_{t<0} = 0,\ \ w_\beta^m(x,t)\mid_{t<0} = 0. \tag{3.144}$$

Here $i = 1,2,3;\ \beta = 1,2;\ \delta(x) = \delta(x_1)\delta(x_2)\delta(x_3)$ is the Dirac delta function of the space variable concentrated at $x_1 = 0,\ x_2 = 0,\ x_3 = 0$; $\delta(t)$ is the Dirac delta function of the time variable concentrated at $t = 0$. Equations (3.142)-(3.144) can be written in the following form

$$\rho\frac{\partial^2 \mathbf{V}^m}{\partial t^2} = \sum_{j,l=1}^{3} \mathbf{P}_{jl}\frac{\partial^2 \mathbf{V}^m}{\partial x_j \partial x_l} + \mathsf{E}^m \delta(x)\delta(t),\ x \in R^3, t \in R, \tag{3.145}$$

$$\mathbf{V}^m(x,t)\mid_{t<0} = 0, \tag{3.146}$$

where $\mathsf{E}^m = (\delta_1^m, \delta_2^m, \delta_3^m, \delta_4^m, \delta_5^m)$,

$$\mathbf{P}_{jl} = \frac{1}{2}\times\begin{bmatrix} c_{1j1l}+c_{1l1j} & c_{1j2l}+c_{1l2j} & c_{1j3l}+c_{1l3j} & R_{1j1l}+R_{1l1j} & R_{1j2l}+R_{1l2j} \\ c_{2j1l}+c_{2l1j} & c_{2j2l}+c_{2l2j} & c_{2j3l}+c_{2l3j} & R_{2j1l}+r_{2l1j} & R_{2j2l}+r_{2l2j} \\ c_{3j1l}+c_{3l1j} & c_{3j2l}+c_{3l2j} & c_{3j3l}+c_{3l3j} & R_{3j1l}+R_{3l1j} & R_{3j2l}+R_{3l2j} \\ R_{1j1l}+R_{1l1j} & R_{2j1l}+R_{2l1j} & R_{3j1l}+R_{3l1j} & K_{1j1l}+K_{1l1j} & K_{1j2l}+K_{1l2j} \\ R_{1j2l}+R_{1l2j} & R_{2j2l}+R_{2l2j} & R_{3j2l}+R_{3l2j} & K_{2j1l}+K_{2l1j} & K_{2j2l}+K_{2l2j} \end{bmatrix},$$

We note that matrices $\mathbf{P}_{jl}$ are symmetric here. The similar presentations of the motion equations of elastic crystals and QCs have been used before in papers of Yakhno & Akmaz (2005), Akmaz (2009).

The computation of mth column for the time-dependent fundamental solution (FS) This problem is related with finding a vector function $\mathbf{V}^m(x,t)$ satisfying (3.145) and (3.146).

3.2.3 Computation of mth column for time-dependent FS of 2D QCs

The method of deriving $\mathbf{V}^m(x,t)$ satisfying (3.145) and (3.146) consists of the following. In the first step equations (3.145) and (3.146) are written in terms of the Fourier transform with respect to $x \in R^3$. In the second step, a solution of the obtained initial value problem is derived by matrix transformations and the ordinary differential equations technique. In the last step, an explicit formula for mth column of FS is found by the inverse Fourier transform.

3.2.3.1 Equations for mth column of FS in terms of Fourier images

Let

$$\tilde{\mathbf{V}}^m(\nu,t) = (\tilde{u_1}^m(\nu,t), \tilde{u_2}^m(\nu,t), \tilde{u_3}^m(\nu,t), \tilde{w_1}^m(\nu,t), \tilde{w_2}^m(\nu,t))$$

be the Fourier image of $\mathbf{V}^m(x,t)$ with respect to $x = (x_1,x_2,x_3) \in R^3$, i.e.

$$\tilde{V_j}^m(\nu,t) = \int_{-\infty}^{\infty}\int_{-\infty}^{\infty}\int_{-\infty}^{\infty} V_j^m(x,t)e^{ix\cdot\nu}dx_1dx_2dx_3,$$

where

$$\nu = (\nu_1, \nu_2, \nu_3) \in R^3,\ x \cdot \nu = x_1\nu_1 + x_2\nu_2 + x_3\nu_3,\ i^2 = -1,\ j = 1,2,3,4,5.$$

Applying the Fourier transform with respect to $x = (x_1, x_2, x_3) \in R^3$ to equations (3.145) and (3.146) we find

$$\rho \frac{\partial^2 \tilde{\mathbf{V}}^m}{\partial t^2} + \mathbf{A}(\nu)\tilde{\mathbf{V}}^m = \mathsf{E}^m \delta(t),\ \nu \in R^3, t \in R, \tag{3.147}$$

$$\tilde{\mathbf{V}}^m(\nu, t)|_{t<0} = 0. \tag{3.148}$$

Here

$$\mathbf{A}(\nu) = \sum_{j,l=1}^{3} \mathbf{P}_{jl}\nu_j\nu_l, \tag{3.149}$$

where matrices $\mathbf{P}_{jl}$ are defined after condition (3.146).

We use the obtained equalities (3.147) and (3.148) for deriving unknown vector function $\tilde{\mathbf{V}}^m(\nu, t)$ depending on 3D parameter $\nu = (\nu_1, \nu_2, \nu_3) \in R^3$ and the time variable t.

3.2.3.2 Explicit formula for a solution of (3.147), (3.148)

Using the positivity of elastic constant tensors $c_{ijkl},\ R_{ij\alpha l},\ K_{\beta j\alpha l}$ we obtain that the matrix $\mathbf{A}(\nu)$, defined by (3.149), is symmetric positive semi-definite (see Appendix). For this matrix $\mathbf{A}(\nu)$ we construct an orthogonal matrix $\mathbf{T}(\nu)$ and a diagonal matrix $\mathbf{D}(\nu) = diag(d_k(\nu),\ k = 1,2,3,4,5)$ with nonnegative elements such that

$$\mathbf{T}^*(\nu)\mathbf{A}(\nu)\mathbf{T}(\nu) = \mathbf{D}(\nu), \tag{3.150}$$

where $\mathbf{T}^*(\nu)$ is the transposed matrix to $\mathbf{T}(\nu)$.

Let $\mathbf{T}(\nu)$ and $\mathbf{D}(\nu) = diag(d_k(\nu),\ k = 1,2,3,4,5)$ be constructed. A solution of (3.147), (3.148) can be found using the transformation

$$\tilde{\mathbf{V}}^m(\nu,t) = \mathbf{T}(\nu)\mathbf{Y}^m(\nu,t), \tag{3.151}$$

where $\mathbf{Y}^m(\nu,t)$ is unknown vector function. Substituting (3.151) into (3.147), (3.148) and then multiplying the obtained equations by $\mathbf{T}^*(\nu)$ and using (3.150) we find

$$\begin{aligned} \rho\frac{\partial^2\mathbf{Y}^m}{\partial t^2} + \mathbf{D}(\nu)\mathbf{Y}^m &= \mathbf{T}^*(\nu)\mathsf{E}^m\delta(t),\ t \in R,\ \nu \in R^3 \qquad (3.152)\\ \mathbf{Y}^m(\nu,t)|_{t\le 0} &= 0. \qquad (3.153) \end{aligned}$$

Using the ordinary differential equations technique (see, for example, Boyce & DiPrima (1992)) we find that a solution of (3.152)-(3.153) is defined by

$$\mathbf{Y}^m_k(\nu,t) = \theta(t)\frac{(\mathbf{T}^*(\nu)\mathsf{E}^m)_k}{\sqrt{\rho d_k(\nu)}}\sin(t\frac{\sqrt{d_k(\nu)}}{\sqrt{\rho}}),\ for\ d_k(\nu) > 0, \tag{3.154}$$

$$\mathbf{Y}^m_k(\nu,t) = \theta(t)\frac{(\mathbf{T}^*(\nu)\mathsf{E}^m)_k}{\rho}t,\ for\ d_k(\nu) > 0. \tag{3.155}$$

Here $\theta(t)$ is the Heaviside function, i.e. $\theta(t) = 1$ for $t \ge 0$ and $\theta(t) = 0$ for $t < 0$.

Finally, a solution of (3.147), (3.148) is determined by

$$\tilde{\mathbf{V}}^m(\nu,t) = \theta(t)\mathbf{T}(\nu)\mathbf{Y}^m(\nu,t). \tag{3.156}$$

3.2.3.3 Explicit formula for mth column for time-dependent FS of 2D QCs

We note that values of $\mathbf{V}^m(x,t)$, $\tilde{\mathbf{V}}^m(\nu,t)$, $\mathbf{T}(\nu)$ and $\mathbf{D}(\nu) = diag(d_k(\nu),\ k = 1,2,3,4,5)$ are real. Therefore, applying the inverse Fourier transform to (3.156), we find the following explicit formula for mth column for the time-dependent FS of 2D QCs

$$\mathbf{V}^m(x,t) = \frac{\theta(t)}{(2\pi)^3} \int_{-\infty}^{\infty} \int_{-\infty}^{\infty} \int_{-\infty}^{\infty} \mathbf{T}(\nu)\mathbf{Y}^m(\nu,t)\cos(\nu\cdot x)d\nu_1 d\nu_2 d\nu_3. \tag{3.157}$$

Here the components of the vector function $\tilde{\mathbf{V}}^m(\nu,t)$ are defined explicitly by (3.154) and (3.155).

3.2.4 Computational examples

3.2.4.1 General characteristics of computations and visualizations

The aim of computational examples is to derive values of elements for fundamental's matrices and then draw graphs of Green's matrix elements for different anisotropic 2D QCs. For the computational examples we consider six 2D QCs with different structures of anisotropy: dodecagonal, octagonal, decagonal, pentagonal, hexagonal, triclinic, respectively. We consider third, fourth and fifth columns of Green's matrix for the visualization. This means that we take $m = 3$, $m = 4$ and $m = 5$ in (3.145) and (3.146), i.e. the pulse point forces are situated in each QCs and modeled by

$$\mathsf{E}^3\delta(x_1)\delta(x_2)\delta(x_3)\delta(t), \quad \mathsf{E}^4\delta(x_1)\delta(x_2)\delta(x_3)\delta(t) \quad \text{and} \quad \mathsf{E}^5\delta(x_1)\delta(x_2)\delta(x_3)\delta(t),$$

where $\mathsf{E}^3 = (0,0,1,0,0)$, $\mathsf{E}^4 = (0,0,0,1,0)$, $\mathsf{E}^5 = (0,0,0,0,1)$ and $\delta(\cdot)$ is the Dirac delta function. The responses of the considered anisotropic QCs on these sources are the phonon and phason displacement vectors depending on the position (i.e. space variables x_1, x_2, x_3) and the time variable t. Using the method of Section 3.2.3 we compute $\mathbf{T}(\nu)$, $\mathbf{T}^*(\nu)$, $\mathbf{D}(\nu)$ and then using the formula (3.157) we have derived solutions $\mathbf{V}^3(x,t)$, $\mathbf{V}^4(x,t)$ and $\mathbf{V}^5(x,t)$ of (3.145), (3.146) numerically for $m=3$, $m=4$ and $m=5$, respectively. We note that the first three components of the vector function $\mathbf{V}^i(x,t)$ are components of the phonon displacement $u_1^i(x,t), u_2^i(x,t), u_3^i(x,t)$, the fourth and fifth components are the phason displacements $w_1^i(x,t)$, $w_2^i(x,t)$, $i = 3,4,5$. As a result of visualization in computational examples we have seen the fluctuations of phason and phonon displacement components at points located in the short distance from a pulse point force. Moreover we have got images of the wave fronts arising from pulse point sources in QCs with different structures of anisotropy.

3.2.4.2 Description of input data and corresponding images

Example 1. (**Dodecagonal Crystal.**) The density ρ is equal to 1. We assume that phonon, phason, phonon-phason coupling elastic constants satisfy conditions of the dodecagonal 2D QC system (see Appendix). We take the independent elastic constants as (Lei & Wang & Hu & Ding (2000))

$$
\begin{aligned}
c_{1111} &= 1,\ c_{1122} = c_{2211} = -0.6,\ c_{1133} = c_{3311} = -0.1,\ c_{3333} = 0.4,\\
c_{2323} &= c_{2332} = c_{3223} = c_{3232} = 0.2,\ c_{1212} = c_{1221} = c_{2112} = c_{2121} = 0.8;\\
K_{1111} &= K_{2222} = 0.6,\ K_{1221} = K_{2112} = 0.4,\ K_{1122} = K_{2211} = 0.5,\\
K_{2323} &= K_{1313} = 0.7,\ K_{1212} = K_{2121} = 1.5,\ K_{1112} = K_{1211} = K_{1121} = K_{2111} = 0.2.
\end{aligned}
$$

Figures 3.39-3.40 show the third phonon displacement $u_3^3(x_1,0,x_3,3.3)$ and the second phason displacement $w_2^5(x_1,0,x_3,2.5)$ corresponding to sources $\mathsf{E}^3\delta(x)\delta(t)$, $\mathsf{E}^5\delta(x)\delta(t)$. Figures 3.39-3.40 are the screen shots of $2-D$ level plots of $u_3^3(x_1,0,x_3,3.3)$, $w_2^5(x_1,0,x_3,2.5)$. This is a view from the top of z-axis (the plan).

Using the symbolic math toolbox in MATLAB we have calculated the matrix $\mathbf{T}(\nu)$ and $\mathbf{D}(\nu)$ as follows:

$$
\begin{aligned}
d_1(\nu) &= \frac{4\nu_1^2+4\nu_2^2+\nu_3^2}{5},\\
d_2(\nu) &= \frac{3}{5}\nu_1^2+\frac{3}{5}\nu_2^2+\frac{3}{10}\nu_3^2+\frac{1}{10}(\nu_3^4-7\nu_2^2\nu_3^2-7\nu_1^2\nu_3^2+16\nu_2^4+32\nu_1^2\nu_2^2+16\nu_1^4)^{\frac{1}{2}},\\
d_3(\nu) &= \frac{3}{5}\nu_1^2+\frac{3}{5}\nu_2^2+\frac{3}{10}\nu_3^2-\frac{1}{10}(\nu_3^4-7\nu_2^2\nu_3^2-7\nu_1^2\nu_3^2+16\nu_2^4+32\nu_1^2\nu_2^2+16\nu_1^4)^{\frac{1}{2}},\\
d_4(\nu) &= \frac{21}{20}\nu_1^2+\frac{21}{20}\nu_2^2+\frac{7}{10}\nu_3^2+\frac{\sqrt{97}}{20}\nu_1^2+\frac{\sqrt{97}}{20}\nu_2^2,\\
d_5(\nu) &= \frac{21}{20}\nu_1^2+\frac{21}{20}\nu_2^2+\frac{7}{10}\nu_3^2-\frac{\sqrt{97}}{20}\nu_1^2-\frac{\sqrt{97}}{20}\nu_2^2.
\end{aligned}
$$

And each row of the matrix $\mathbf{T}(\nu)$ is

$$
\begin{aligned}
\mathbf{T}_1(\nu) &= (1,\frac{\nu_1(-\nu_3^2+4\nu_2^2+4\nu_1^2+A)}{\nu_3(\nu_1^2+\nu_2^2)},-\frac{\nu_1(\nu_3^2-4\nu_2^2-4\nu_1^2+A)}{\nu_3(\nu_1^2+\nu_2^2)},0,0),\\
\mathbf{T}_2(\nu) &= (-\frac{\nu_1}{\nu_2},\frac{\nu_2(-\nu_3^2+4\nu_2^2+4\nu_1^2+A)}{\nu_3(\nu_1^2+\nu_2^2)},-\frac{\nu_2(\nu_3^2-4\nu_2^2-4\nu_1^2+A)}{\nu_3(\nu_1^2+\nu_2^2)},0,0),\\
\mathbf{T}_3(\nu) &= (0,1,1,0,0),\\
\mathbf{T}_4(\nu) &= (0,0,0,\frac{1}{2}\frac{9\nu_2^2-9\nu_1^2+\sqrt{97}\nu_1^2+\sqrt{97}\nu_2^2+8\nu_1\nu_2}{2\nu_1^2+9\nu_1\nu_2-2\nu_2^2}\\
&\quad , \quad \frac{-1}{2}\frac{-9\nu_2^2+9\nu_1^2+\sqrt{97}\nu_1^2+\sqrt{97}\nu_2^2-8\nu_1\nu_2}{2\nu_1^2+9\nu_1\nu_2-2\nu_2^2}),\\
\mathbf{T}_5(\nu) &= (0,0,0,1,1).
\end{aligned}
$$

Here $A=(\nu_3^4-7\nu_2^2\nu_3^2-7\nu_1^2\nu_3^2+16\nu_2^4+32\nu_1^2\nu_2^2+16\nu_1^4)^{\frac{1}{2}}$.

MATLAB commands to find the matrices $\mathbf{T}(\nu)$, $\mathbf{T}^*(\nu)$ and $\mathbf{D}(\nu)$ are listed below.

Input: ρ, c_{ijkl}, $R_{ij\alpha l}$, $K_{\beta j\alpha l}$

syms ν_1 ν_2 ν_3 real

$[EigVecA(\nu), EigValA(\nu)] = eig(A(\nu));$

$\mathcal{T}(\nu) = EigVecA(\nu);$

$\mathbf{D}(\nu) = EigValA(\nu);$

Output: $\mathbf{T}(\nu)$, $\mathbf{T}^*(\nu)$, $\mathbf{D}(\nu)$.

Example 2. (**Octagonal Crystal.**) The density ρ is equal to 1. We assume that phonon, phason, phonon-phason coupling elastic constants satisfy conditions of the octagonal 2D QC system (see Appendix). Similar to Lei & Hu & Wang & Ding (1999), we take

$$\begin{aligned}
c_{1111} &= 0.9,\ c_{1122} = c_{2211} = -0.3,\ c_{1133} = c_{3311} = 0.2,\ c_{3333} = 0.3,\\
c_{2323} &= c_{2332} = c_{3223} = c_{3232} = 0.5,\ c_{1212} = c_{1221} = c_{2112} = c_{2121} = 0.6;\\
R_{1111} &= R_{1122} = R_{1221} = R_{2121} = 0.04,\\
R_{1112} &= R_{2221} = R_{1211} = R_{2111} = R_{1222} = R_{2122} = 0.02;\ K_{1111} = K_{2222} = 0.9,\\
K_{1221} &= K_{2112} = -0.3,\ K_{1122} = K_{2211} = -0.2,\ K_{2323} = K_{1313} = 0.4,\\
K_{1212} &= K_{2121} = 0.4,\ K_{1112} = K_{1211} = K_{1121} = K_{2111} = 0.1.
\end{aligned}$$

Figures 3.41- 3.42 present the second phonon displacement $u_2^4(x_1,0,x_3,2.5)$ and the second phason displacement $w_2^4(x_1,0,x_3,3.3)$ on the plane $x_2 = 0$ corresponding to source $\mathsf{E}^4\delta(x)\delta(t)$. Figures 3.41- 3.42 contain $2-D$ plots of $u_2^4(x_1,0,x_3,2.5)$, $w_2^4(x_1,0,x_3,3.3)$ (i.e. a view of the surfaces $z = u_2^4(x_1,0,x_3,2.5)$, $z = w_2^4(x_1,0,x_3,3.3$ from the top of z axis, respectively).

Example 3. (**Decagonal Crystal.**) The density ρ is equal to 1. The phonon, phason, phonon-phason coupling elastic constants satisfy conditions of decagonal 2D QC system (see Appendix), and the nonzero phonon elastic constants of Al-Ni-Co (see, for example, Chernikov & Ott & Bianchi (1998)), phason, phonon-phason coupling elastic constants are

$$\begin{aligned}
c_{1111} &= 2.343,\ c_{1122}=c_{2211}=0.5736,\ c_{1133}=c_{3311}=0.6662,\ c_{3333}=2.3221,\\
c_{2323} &= c_{2332}=c_{3223}=c_{3232}=0.7019,\ c_{1212}=c_{1221}=c_{2112}=c_{2121}=0.8845;\\
R_{1111} &= R_{1122}=R_{1221}=R_{2121}=0.1;\ K_{2323}=K_{1313}=1.87\\
K_{1111} &= K_{2222}=K_{1212}=K_{2121}=10.1,\ K_{1122}=K_{2211}=-7.5.
\end{aligned}$$

Figures 3.43-3.44 show dynamics of the distribution for the second phonon displacement $u_2^5(x_1,0,x_3,1)$ and the first phason displacement $w_1^4(x_1,0,x_3,0.8)$ corresponding to source $\mathsf{E}^5\delta(x)\delta(t)$ and $\mathsf{E}^4\delta(x)\delta(t)$, respectively. Figures 3.45-3.48 show dynamics of the distribution for the third phonon displacement $u_3^3(x_1,0,x_3,t)$ at the time $t=0.5,\ 1.3$ arising from the force $\mathsf{E}^3\delta(x)\delta(t)$. Figures 3.46, 3.48 are 3D plots of $u_3^3(x_1,0,x_3,t)$ for $t=0.5,\ 1.3$. Here the horizontal axes are x_1 and x_3. The vertical axis is the magnitude of $u_3^3(x_1,0,x_3,t)$ for $t=0.5,\ 1.3$. The different colors correspond to different values of $u_3^3(x_1,0,x_3,t)$. Figures 3.45, 3.47 contain screen shots of 2D level plots of the same surfaces $u_3^3(x_1,0,x_3,0.5)$, $u_3^3(x_1,0,x_3,1.3)$, i.e. a view of these surfaces from the top of z-axis (the plan).

Example 4. (**Pentagonal Crystal.**) The density ρ is equal to 1 and the independent phonon, phason, phonon-phason coupling elastic constants are (similar to Lei & Wang

& Hu & Ding (1998))

$$
\begin{aligned}
c_{1111} &= 0.9,\ c_{1122}=c_{2211}=-0.3,\ c_{1133}=c_{3311}=-0.1,\ c_{3333}=0.6,\\
c_{2323} &= c_{2332}=c_{3223}=c_{3232}=0.5,\ c_{1212}=c_{1221}=c_{2112}=c_{2121}=0.6;\\
R_{1111} &= R_{1122}=R_{1221}=R_{2121}=0.05,\\
R_{1112} &= R_{2221}=R_{1211}=R_{2111}=R_{1222}=R_{2122}=0.06,\\
R_{2312} &= R_{3212}=R_{2321}=R_{3221}=R_{3122}=R_{1322}=-0.15,\\
R_{2311} &= R_{3211}=R_{3112}=R_{1312}=R_{3121}=R_{1321}=0.1,\ R_{1113}=0.08,\\
R_{1123} &= R_{1213}=R_{2113}=-0.04;\ K_{2323}=K_{1313}=0.8,\\
K_{1111} &= K_{2222}=K_{1212}=K_{2121}=0.9,\ K_{1122}=K_{2211}=1.3,\\
K_{1113} &= K_{1311}=K_{2213}=K_{1322}=K_{2312}=K_{1223}=0.3,\\
K_{1123} &= K_{2311}=K_{2223}=K_{2322}=K_{1321}=K_{2113}=0.2.
\end{aligned}
$$

These constants satisfy conditions of pentagonal 2D QC system (see Appendix). Figures 3.49- 3.50 show the third phonon displacement $u_3^3(x_1,0,x_3,t)$ and the first phason displacement $w_1^3(x_1,0,x_3,t)$ at the time $t=3$ on the plane $x_2=0$ corresponding to source $\mathsf{E}^3\delta(x)\delta(t)$. Figures 3.49- 3.50 contain $2-D$ plots (a view from the top of z-axis) of $z=u_3^3(x_1,0,x_3,t)$, $z=w_1^3(x_1,0,x_3,t)$ for $t=3$, respectively.

Example 5. (**Hexagonal Crystal.**) In this example the density ρ is equal to 1.848. The nonzero phonon elastic constant of hexagonal crystal $NbSi_2$ (see, for example, Chernikov & Ott & Bianchi (1998)), nonzero phason and phonon-phason coupling

elastic constants are

$$
\begin{aligned}
c_{1111} &= 3.8223,\ c_{1122}=c_{2211}=0.8124,\ c_{1133}=c_{3311}=0.8804,\ c_{3333}=4.6802,\\
c_{2323} &= c_{2332}=c_{3223}=c_{3232}=1.4474,\ c_{1212}=c_{1221}=c_{2112}=c_{2121}=1.5267;\\
R_{1111} &= R_{2222}=-0.02,\ R_{1122}=R_{2211}=-0.6,\ R_{3322}=R_{3311}=2.8,\\
R_{1313} &= R_{3113}=1.4,\ R_{1212}=R_{2112}=R_{1221}=R_{2121}=0.29;\\
K_{1111} &= K_{2222}=10.1,\ K_{1122}=K_{2211}=8.4,\ K_{1212}=K_{2121}=1.3,\\
K_{2323} &= K_{1313}=4.2,\ K_{1221}=K_{2112}=0.4.
\end{aligned}
$$

These constants satisfy conditions of hexagonal 2D QC system (see Appendix). Figures 3.51-3.52 present the third phonon displacement $u_3^3(x_1,0,x_3,1)$ and the first phason displacement $w_1^3(x_1,0,x_3,1)$ arising from the source $\mathsf{E}^3\delta(x)\delta(t)$. Figures 3.51-3.52 are the screen shots of $2-D$ level plots of the surfaces $u_3^3(x_1,0,x_3,1)$, $w_1^3(x_1,0,x_3,1)$, respectively. This is a view from the top of z-axis (the plan).

Example 6. (**Triclinic Crystal.**) In this example we take the density ρ is equal to 2. The phonon, phason and phonon-phason coupling elastic constants satisfy conditions of triclinic 2D QC system (see Appendix). We take

$$
\begin{aligned}
c_{1111} &= 69.1,\ c_{1122}=c_{2211}=34.0,\ c_{1133}=c_{3311}=30.8,\\
c_{1123} &= c_{2311}=c_{3211}=c_{1132}=5.1, c_{1131}=c_{3111}=c_{1311}=c_{1113}-2.4,\\
c_{1112} &= c_{1121}=c_{2111}=c_{1211}=-0.9, c_{2222}=183.5,\ c_{2233}=c_{3322}=5.5,\\
c_{2223} &= c_{2322}=c_{3222}=c_{2232}=-3.9,\ c_{3333}=179.5,\\
c_{2231} &= c_{3122}=c_{1322}=c_{2213}=-7.7,\ c_{2212}=c_{2221}=c_{2122}=c_{1222}=-5.8,\\
c_{3323} &= c_{3332}=c_{3233}=c_{2333}=-8.7,\ c_{3331}=c_{3313}=c_{1333}=c_{3133}=7.1,
\end{aligned}
$$

$$
\begin{aligned}
c_{3312} &= c_{3321} = c_{2133} = c_{1233} = -9.8,\ c_{2323} = c_{2332} = c_{3223} = c_{3232} = 24.9,\\
c_{3112} &= c_{3121} = c_{2131} = c_{1231} = c_{1312} = c_{1213} = c_{1321} = c_{2113} = 0.5,\\
c_{2331} &= c_{2313} = c_{1323} = c_{3123} = c_{3231} = c_{3132} = c_{3213} = c_{1332} = -2.3,\\
c_{2312} &= c_{2321} = c_{2123} = c_{1223} = c_{3212} = c_{1232} = c_{3221} = c_{2132} = -7.2\\
c_{3131} &= c_{3113} = c_{1331} = c_{1313} = 26.8,\ c_{1212} = c_{1221} = c_{2112} = c_{2121} = 33.5;\\
R_{1111} &= 8.35,\ R_{1112} = 1.4,\ R_{1113} = 15.5,\ R_{1211} = R_{2111} = 1.2,\\
R_{1212} &= R_{2112} = 4.3,\ R_{1213} = R_{2113} = -7.1,\ R_{1311} = R_{3111} = 2.1,\\
R_{1312} &= R_{3112} = -10.15,\ R_{1313} = R_{3113} = 6.3,\ R_{1121} = 7.3,\ R_{1122} = 1.3,\\
R_{1123} &= 8.01,\ R_{1221} = R_{2121} = 1.7,\ R_{1222} = R_{2122} = 16.5,\ R_{1223} = R_{2123} = 13.7,\\
R_{1321} &= R_{3121} = 1.06\ R_{1322} = R_{3122} = 18,\ R_{1323} = R_{3123} = -10.5,\\
R_{2211} &= 3.1,\ R_{2212} = 0.012,\ R_{2213} = 3.01,\ R_{2311} = R_{3211} = 0.02,\\
R_{2312} &= R_{3212} = 0.03,\ R_{2313} = R_{3213} = 1.04,\ R_{2221} = -10.11,\ R_{2222} = 7.2,\\
R_{2223} &= 0.4,\ R_{2321} = R_{3221} = -20.2,\ R_{2322} = R_{3222} = 3.3,\ R_{2323} = R_{3223} = 3.4,\\
R_{3311} &= 0.05,\ R_{3312} = 0.06,\ R_{3313} = -1.7,\ R_{3321} = 1.8,\ R_{3322} = -4.9,\\
R_{3323} &= 0.07;\ K_{1111} = 31.2,\ K_{1112} = K_{1211} = -10.2,\ K_{1113} = K_{1311} = 14.04,\\
K_{1212} &= 21.01,\ K_{1213} = K_{1312} = -9.1,\ K_{1313} = 13.3,\ K_{1121} = K_{2111} = -3.1,\\
K_{1122} &= K_{2211} = 10.6,\ K_{1123} = K_{2311} = -16.9,\ K_{1221} = K_{2112} = 8.5,\\
K_{1222} &= K_{2212} = 1.2,\ K_{1223} = K_{2312} = 1.11,\ K_{1321} = K_{2113} = 0.1,\\
K_{1322} &= K_{1322} = -0.1,\ K_{1323} = K_{2313} = -19.2,\ K_{2121} = 15.5,\ K_{2122} = K_{2221} = 1.6,\\
K_{2123} &= K_{2321} = 13.1,\ K_{2222} = 30,\ K_{2223} = K_{2322} = -0.15,\ K_{2323} = 60.5.
\end{aligned}
$$

Other components, which are not defined by given values and triclinic 2D QC conditions, are equal to zero. Figure 3.53 shows dynamic distribution of the first phonon displacement $u_1^3(x_1,0,x_3,0.2)$ arising from the force $\mathsf{E}^3\delta(x)\delta(t)$. Figure 3.54 shows dynamic distribution of the second phonon displacement $u_2^4(x_1,0,x_3,0.4)$ arising from the force $\mathsf{E}^4\delta(x)\delta(t)$. Figures 3.55-3.56 show dynamic distribution of the first

phason displacement $w_1^3(x_1,0,x_3,t)$ at $t = 0.1,\ 0.3$ arising from the force $\mathsf{E}^3\delta(x)\delta(t)$. Figures 3.53-3.56 contain $2-D$ plots (a view from the top of z-axis) of the surfaces $u_1^3(x_1,0,x_3,0.2)$, $u_2^4(x_1,0,x_3,0.4)$, $w_1^3(x_1,0,x_3,0.1)$, $w_1^3(x_1,0,x_3,0.3)$. In these figures the axes are x_1 and x_3; the different color correspond to different values of the displacement components.

3.2.4.3 Analysis of the visualization

The simulation of the phonon and phason displacements in anisotropic QCs by modern computer tools allows us to see and evaluate the dependence between media structures and behavior of these displacements. The approach of the method allows users to observe the elastic wave propagation arising from pulse point sources of the form $\mathsf{E}^m\delta(x_1)\delta(x_2)\delta(x_3)\delta(t)$ in 2D QCs (dodecagonal, octagonal, decagonal, pentagonal, hexagonal, triclinic). Here $\mathsf{E}^m = (\delta_1^m,\delta_2^m,\delta_3^m,\delta_4^m,\delta_5^m)$, where $\delta_i^m, i = 1,2,3,4,5$, is the Kronecker symbol. We can see on the Figures 3.39-3.56 that the different 2D QCs structures produce different responses of phonon and phason displacement fields inside these QCs. The various shapes of elastic waves (different forms of fronts and magnitude fluctuations of phonon and phason displacement fields) are shown in presented figures.

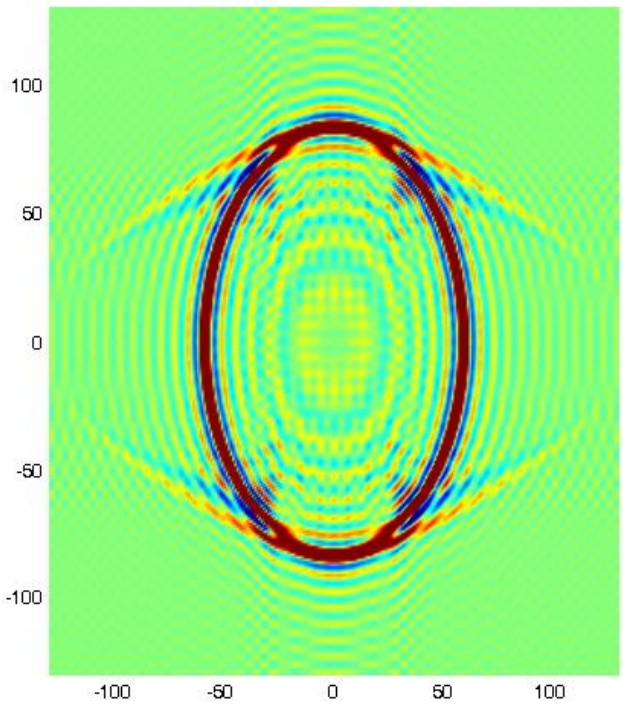

Figure 3.39: The map surface plot (plan) of 3D surface $z = u_3^3(x_1, 0, x_3, 3.3)$ (dodecagonal crystal).

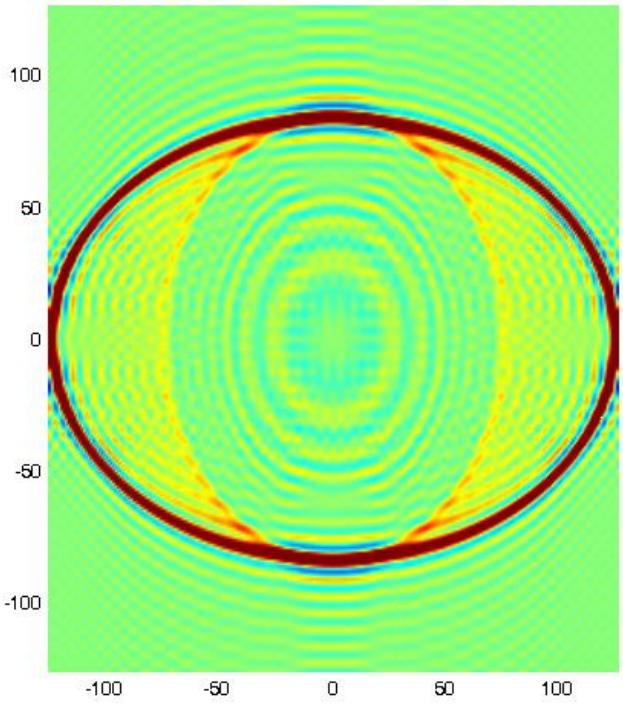

Figure 3.40: The map surface plot (plan) of 3D surface $z = w_2^5(x_1, 0, x_3, 2.5)$ (dodecagonal crystal).

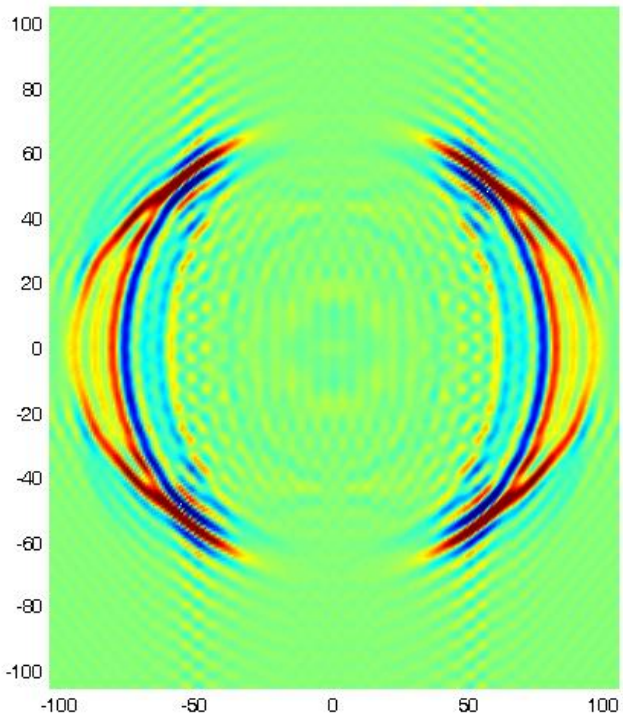

Figure 3.41: The map surface plot (plan) of 3D surface $z = u_2^4(x_1, 0, x_3, 2.5)$ (octagonal crystal1).

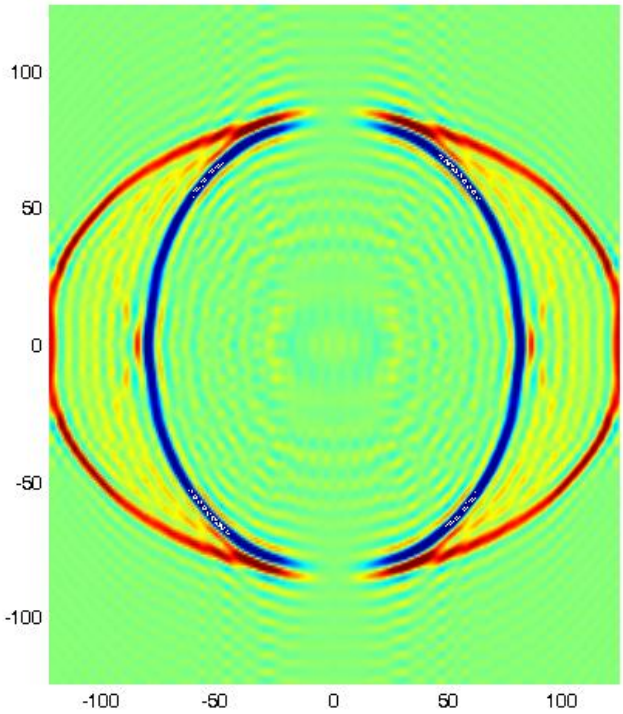

Figure 3.42: The map surface plot (plan) of 3D surface $z = w_2^4(x_1, 0, x_3, 3.3)$ (octagonal crystal).

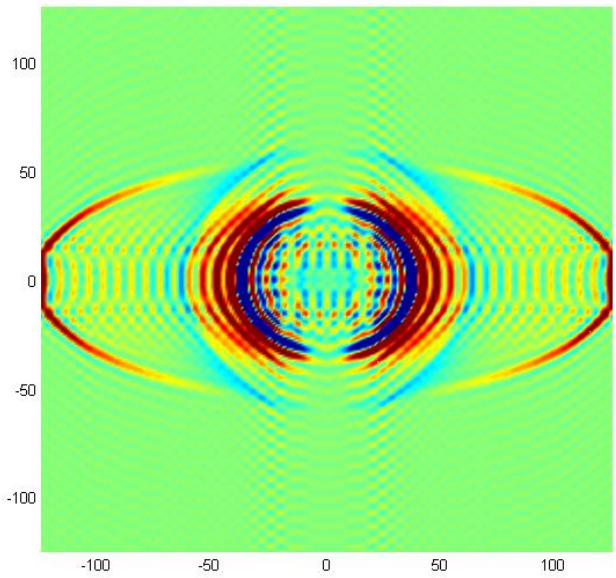

Figure 3.43: The map surface plot (plan) of 3D surface $z = u_2^5(x_1, 0, x_3, 1)$ (decagonal crystal).

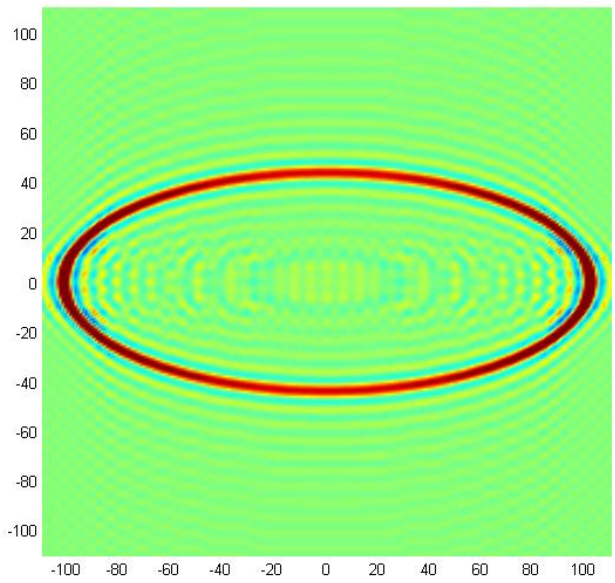

Figure 3.44: The map surface plot (plan) of 3D surface $z = w_1^4(x_1, 0, x_3, 0.8)$ (decagonal crystal).

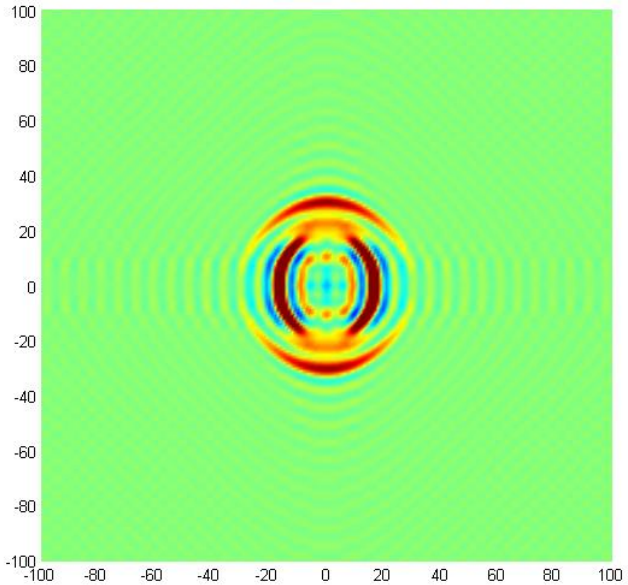

Figure 3.45: The map surface plot (plan) of 3D surface $z = u_3^3(x_1, 0, x_3, 0.5)$ (decagonal crystal).

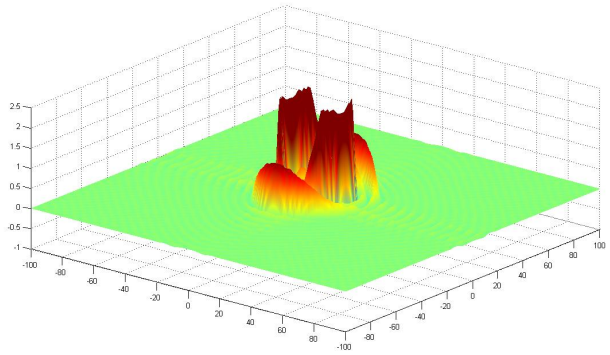

Figure 3.46: 3D surface $z = u_3^3(x_1, 0, x_3, 0.5)$ (decagonal crystal).

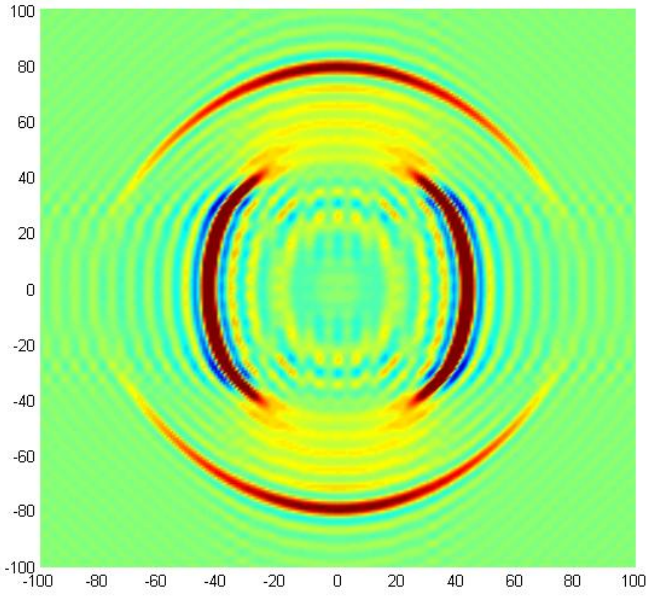

Figure 3.47: The map surface plot (plan) of 3D surface $z = u_3^3(x_1, 0, x_3, 1.3)$ (decagonal crystal).

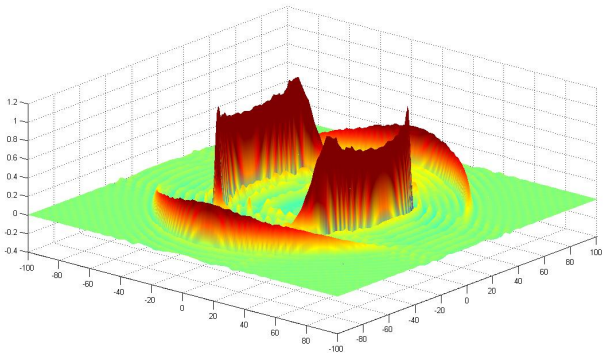

Figure 3.48: 3D surface $z = u_3^3(x_1, 0, x_3, 1.3)$ (decagonal crystal).

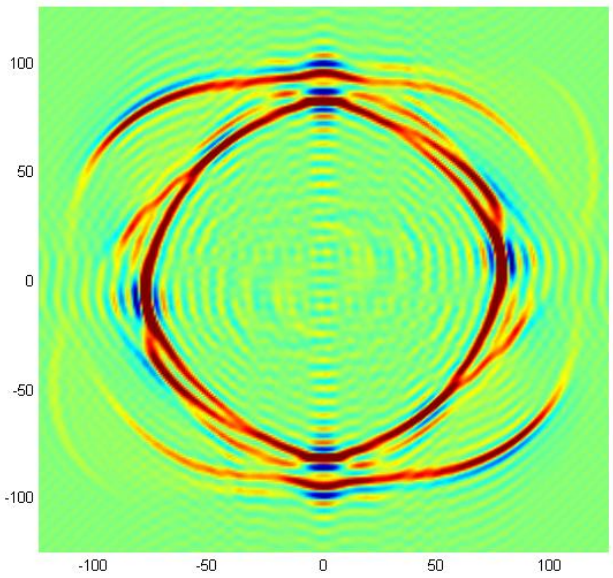

Figure 3.49: The map surface plot (plan) of 3D surface $z = u_3^3(x_1, 0, x_3, 3)$ (pentagonal crystal).

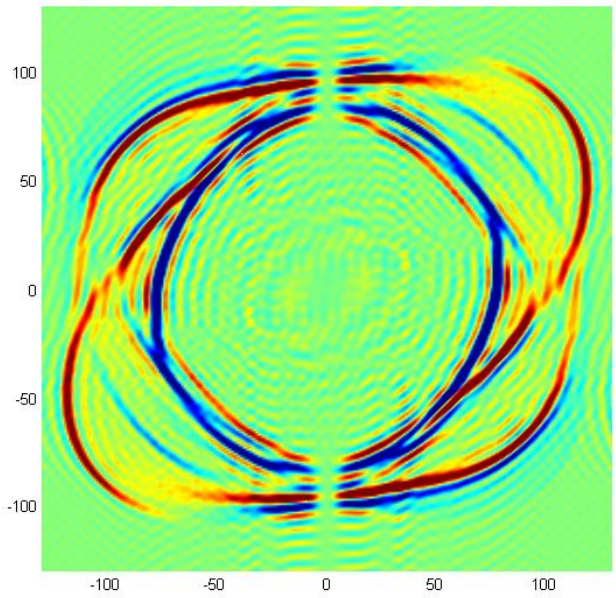

Figure 3.50: The map surface plot (plan) of 3D surface $z = w_1^3(x_1, 0, x_3, 3)$ (pentagonal crystal).

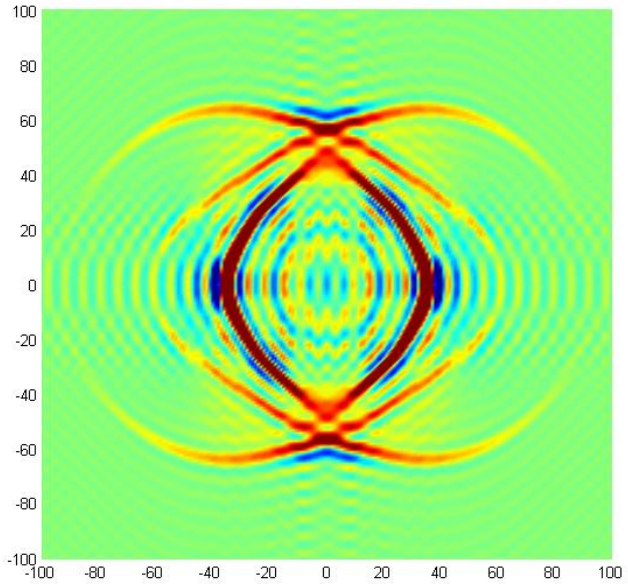

Figure 3.51: The map surface plot (plan) of 3D surface $z = u_3^3(x_1, 0, x_3, 1)$ (hexagonal crystal).

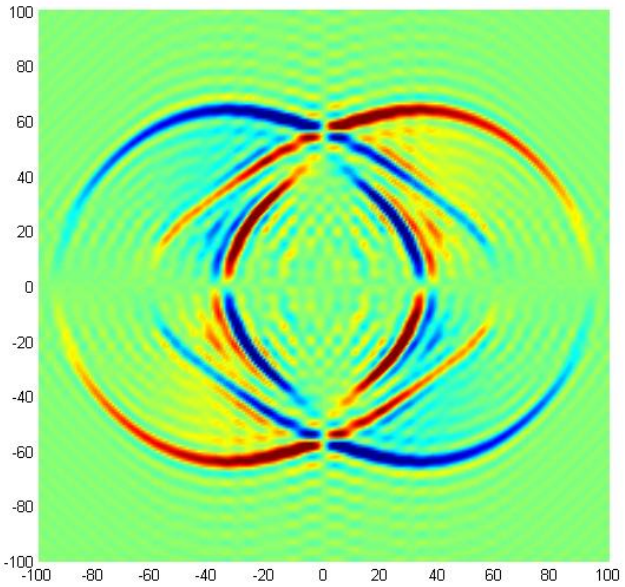

Figure 3.52: The map surface plot (plan) of 3D surface $z = w_1^3(x_1, 0, x_3, 1)$ (hexagonal crystal).

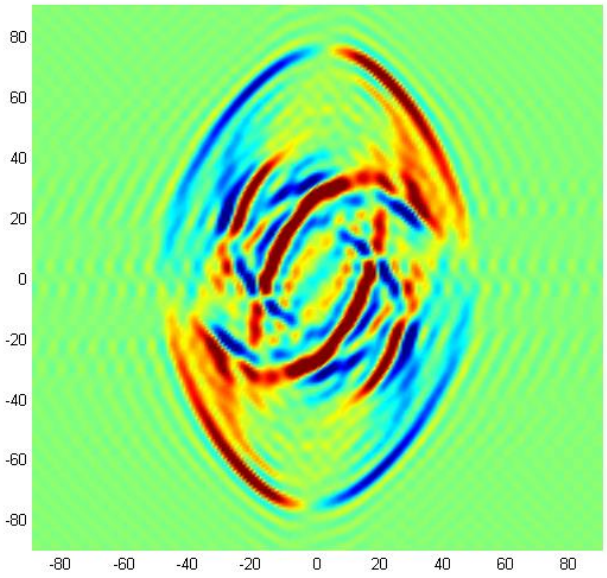

Figure 3.53: The map surface plot (plan) of 3D surface $z = u_1^3(x_1, 0, x_3, 0.2)$ (triclinic crystal).

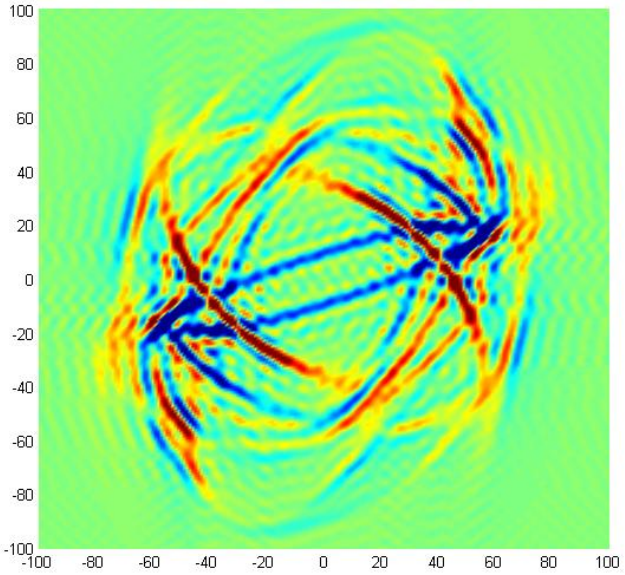

Figure 3.54: The map surface plot (plan) of 3D surface $z = u_2^4(x_1, 0, x_3, 0.4)$ (triclinic crystal).

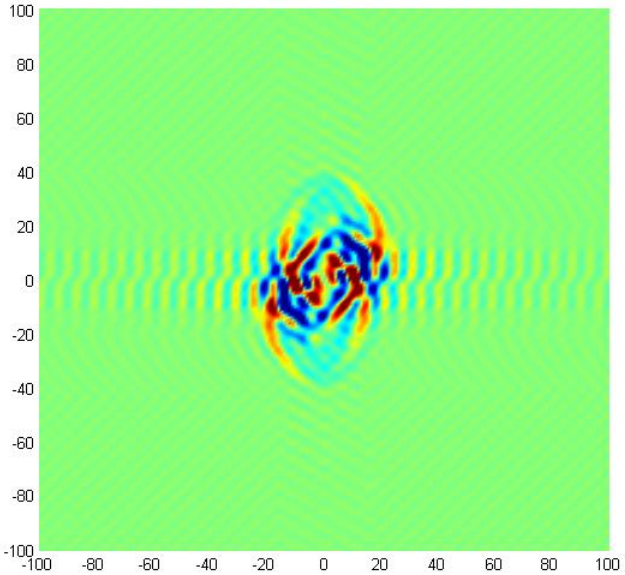

Figure 3.55: The map surface plot (plan) of 3D surface $z = w_1^3(x_1, 0, x_3, 0.1)$ (triclinic crystal).

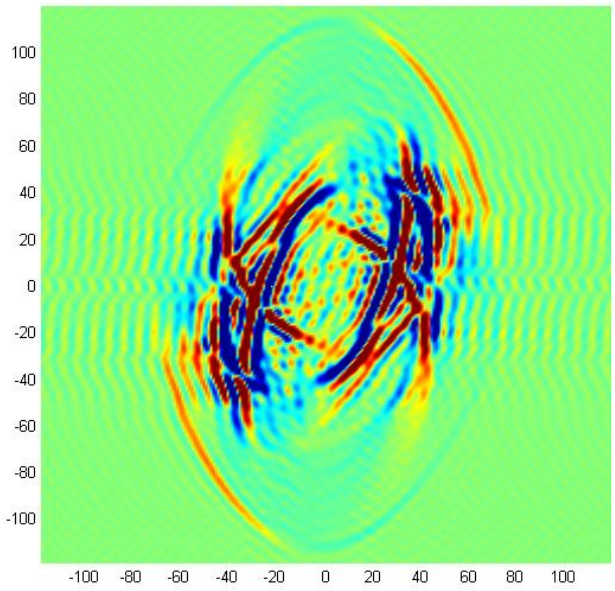

Figure 3.56: The map surface plot (plan) of 3D surface $z = w_1^3(x_1, 0, x_3, 0.3)$ (triclinic crystal).

3.3 Three dimensional elastodynamics of 3D quasicrystals: the derivation of the time-dependent fundamental solution

3.3.1 The basic equations for 3D QCs

Let $x = (x_1, x_2, x_3) \in R^3$ be a space variable, $t \in R$ be a time variable. The generalized Hooke's laws of the elasticity problem of 3D QCs are given by (see, for example, Ding & Yang & Hu & Wang (1993), Hu & Wang & Ding (2000), Gao & Zhao (2006))

$$\sigma_{ij} = c_{ijkl}\varepsilon_{kl} + R_{ijkl}w_{kl}, \tag{3.158}$$

$$H_{ij} = R_{klij}\varepsilon_{kl} + K_{ijkl}w_{kl}, \tag{3.159}$$

where ε_{kl} and w_{kl} are defined as follows

$$\varepsilon_{kl} = \frac{1}{2}(\frac{\partial u_k}{\partial x_l} + \frac{\partial u_l}{\partial x_k}),\ w_{kl} = \frac{\partial w_k}{\partial x_l},\ k,l = 1,2,3. \tag{3.160}$$

Here u_k and $w_k, k = 1,2,3$ are the phonon and phason displacements; $\varepsilon_{kl}(x,t)$, $w_{kl}(x,t),\ k,l = 1,2,3$ are phonon and phason strains.

c_{ijkl} are the phonon elastic constants, K_{ijkl} are the phason elastic constants, R_{ijkl} are the phonon-phason coupling elastic constants. Moreover, they satisfy the following symmetric properties

$$c_{ijkl} = c_{jikl} = c_{ijlk} = c_{klij},\ K_{ijkl} = K_{klij},\ R_{ijkl} = R_{jikl}. \tag{3.161}$$

The positivity of elastic strain energy density requires that the elastic constant tensors c_{ijkl}, K_{ijkl}, R_{ijkl} must be positive definite. Namely, when the strain tensors ε_{ij}, w_{ij} are not zero entirely, the elastic constant tensors satisfy the following inequality Gao &

Zhao (2006)

$$\sum_{i,j,k,l=1}^{3} c_{ijkl}\varepsilon_{ij}\varepsilon_{kl} > 0, \quad \sum_{i,j,k,l=1}^{3} K_{ijkl}w_{ij}w_{kl} > 0, \quad \sum_{i,j,k,l=1}^{3} R_{ijkl}\varepsilon_{ij}w_{kl} > 0. \tag{3.162}$$

The dynamic equilibrium equations can be written in the following form

$$\rho\frac{\partial^2 u_i(x,t)}{\partial t^2} = \sum_{j=1}^{3}\frac{\partial\sigma_{ij}(x,t)}{\partial x_j} + f_i(x,t), \tag{3.163}$$

$$\rho\frac{\partial^2 w_i(x,t)}{\partial t^2} = \sum_{j=1}^{3}\frac{\partial H_{ij}(x,t)}{\partial x_j} + g_i(x,t),\ i=1,2,3,\ x\in R^3,\ t\in R, \tag{3.164}$$

where the constant $\rho > 0$ is the density; $f_i(x,t)$ and $g_i(x,t), i = 1,2,3$ are body forces densities for the phonon and phason displacements, respectively; σ_{ij} and $H_{ij},\ i,j = 1,2,3$ are phonon and phason stresses (see, for example, Ding & Yang & Hu & Wang (1993),Hu & Wang & Ding (2000),Gao & Zhao (2006),Yang & Wang & Ding & Hu (1993)).

3.3.2 Time-dependent fundamental solution of elasticity for 3D QCs

Substituting (3.158) and (3.159) into (3.163) and (3.164) we have for $i = 1,2,3$

$$\rho\frac{\partial^2 u_i(x,t)}{\partial t^2} = \sum_{j,k,l=1}^{3} c_{ijkl}\frac{\partial^2 u_k(x,t)}{\partial x_j\partial x_l} + \sum_{j,l=1}^{3} R_{ijkl}\frac{\partial^2 w_k(x,t)}{\partial x_j\partial x_l} + f_i(x,t), \tag{3.165}$$

$$\rho\frac{\partial^2 w_i(x,t)}{\partial t^2} = \sum_{j,k,l=1}^{3} R_{klij}\frac{\partial^2 u_k(x,t)}{\partial x_j\partial x_l} + \sum_{j,l=1}^{3} K_{ijkl}\frac{\partial^2 w_i(x,t)}{\partial x_j\partial x_l} + g_i(x,t). \tag{3.166}$$

The system (3.165)-(3.166) can be written in the form of one vector partial differential equation as follows

$$\rho\frac{\partial^2 \mathbf{V}}{\partial t^2} = \sum_{j,l=1}^{3}\mathbf{P}_{jl}\frac{\partial^2 \mathbf{V}}{\partial x_j\partial x_l} + \mathbf{F}(x,t), x\in R^3, t\in R, \tag{3.167}$$

where $\mathbf{V} = (u_1, u_2, u_3, w_1, w_2, w_3)$, $\mathbf{F} = (f_1, f_2, f_3, g_1, g_2, g_3)$ and matrices $\mathbf{P}_{jl}$ are defined by

$$\mathbf{P}_{jl} = \frac{1}{2}\begin{bmatrix} C_{1j1l}+C_{1l1j} & C_{1j2l}+C_{1l2j} & C_{1j3l}+C_{1l3j} & R_{1j1l}+R_{1l1j} & R_{1j2l}+R_{1l2j} & R_{1j3l}+R_{1l3j} \\ C_{2j1l}+C_{2l1j} & C_{2j2l}+C_{2l2j} & C_{2j3l}+C_{2l3j} & R_{2j1l}+R_{2l1j} & R_{2j2l}+R_{2l2j} & R_{2j3l}+R_{2l3j} \\ C_{3j1l}+C_{3l1j} & C_{3j2l}+C_{3l2j} & C_{3j3l}+C_{3l3j} & R_{3j1l}+R_{3l1j} & R_{3j2l}+R_{3l2j} & R_{3j3l}+R_{3l3j} \\ R_{1j1l}+R_{1l1j} & R_{2j1l}+R_{2l1j} & R_{3j1l}+R_{3l1j} & K_{1j1l}+K_{1l1j} & K_{1j2l}+K_{1l2j} & K_{1j3l}+K_{3l1j} \\ R_{1j2l}+R_{1l2j} & R_{2j2l}+R_{2l2j} & R_{3j2l}+R_{3l2j} & K_{2j1l}+K_{2l1j} & K_{2j2l}+K_{2l2j} & K_{2j3l}+K_{3l2j} \\ R_{1j3l}+R_{1l3j} & R_{2j3l}+R_{2l3j} & R_{3j3l}+R_{3l3j} & K_{3j1l}+K_{3l1j} & K_{3j2l}+K_{3l2j} & K_{3j3l}+K_{3l3j} \end{bmatrix}.$$

The time-dependent fundamental solution (FS) of elastodynamics in 3D QCs is a 6×6 matrix whose mth column is a vector function

$$\mathbf{V}^m(x,t) = (u_1^m(x,t), u_2^m(x,t), u_3^m(x,t), w_1^m(x,t), w_2^m(x,t), w_3^m(x,t))$$

satisfying

$$\rho\frac{\partial^2 \mathbf{V}^m}{\partial t^2} = \sum_{j,l=1}^{3} \mathbf{P}_{jl}\frac{\partial^2 \mathbf{V}^m}{\partial x_j \partial x_l} + \mathsf{E}^m \delta(x)\delta(t), \tag{3.168}$$

$$\mathbf{V}^m(x,t)\mid_{t<0} = 0. \tag{3.169}$$

Here $\delta(x) = \delta(x_1)\delta(x_2)\delta(x_3)$ is the Dirac delta function of the space variable concentrated at $x_1 = 0,\ x_2 = 0,\ x_3 = 0$; $\delta(t)$ is the Dirac delta function of the time variable concentrated at $t = 0$; $m = 1,...,6$; $\mathsf{E}^m = (\delta_1^m, \delta_2^m, \delta_3^m, \delta_4^m, \delta_5^m, \delta_6^m)$, δ_n^m is the Kronecker symbol i.e. $\delta_n^m = 1$ if $n = m$ and $\delta_n^m = 0$ if $n \neq m$, $n = 1,...,6$. $\mathbf{P}_{jl}$ are matrices defined above.

The computation of mth column for the time-dependent FS of 3D QCs is the main problem of this section. This problem is related with finding a vector function $\mathbf{V}^m(x,t)$ satisfying (3.168) and (3.169).

3.3.3 Computation of mth column for time-dependent FS of 3D QCs

The method of deriving $\mathbf{V}^m(x,t)$ satisfying (3.168) and (3.169) consists of the following. In the first step equations (3.168) and (3.169) are written in terms of the Fourier transform with respect to $x \in R^3$. In the second step, a solution of the obtained initial value problem is derived by matrix transformations and the ordinary differential equations technique. In the last step, an explicit formula for mth column of FS is found by the inverse Fourier transform.

3.3.3.1 Equations for mth column of FS in terms of Fourier images

Let

$$\tilde{\mathbf{V}}^m(\nu,t) = (\tilde{u_1}^m, \tilde{u_2}^m, \tilde{u_3}^m, \tilde{w_1}^m, \tilde{w_2}^m, \tilde{w_3}^m)$$

be the Fourier image of $\mathbf{V}^m(x,t)$ with respect to $x = (x_1,x_2,x_3) \in R^3$, i.e.

$$\tilde{V_j}^m(\nu,t) = \int_{-\infty}^{\infty}\int_{-\infty}^{\infty}\int_{-\infty}^{\infty} V_j^m(x,t)e^{ix\cdot\nu}dx_1dx_2dx_3,$$
$$\nu = (\nu_1,\nu_2,\nu_3) \in R^3,\ x\cdot\nu = x_1\nu_1 + x_2\nu_2 + x_3\nu_3,\ i^2 = -1,\ j = 1,...,6.$$

The IVP (3.168) and (3.169) can be written in terms of $\tilde{\mathbf{V}}^m(\nu,t)$ as follows

$$\rho\frac{\partial^2\tilde{\mathbf{V}}^m}{\partial t^2} + \mathbf{A}(\nu)\tilde{\mathbf{V}}^m = \mathsf{E}^m\delta(t), \tag{3.170}$$

$$\tilde{\mathbf{V}}^m(\nu,t)|_{t<0} = 0,\ \nu \in R^3, t \in R,. \tag{3.171}$$

Here

$$\mathbf{A}(\nu) = \sum_{j,l=1}^{3} \mathbf{P}_{jl}\nu_j\nu_l, \tag{3.172}$$

where matrices $\mathbf{P}_{jl}$ are defined after (3.167).

We use the obtained equalities (3.170) and (3.171) for deriving unknown vector function $\tilde{\mathbf{V}}^m(\nu,t)$ depending on 3D parameter $\nu = (\nu_1,\nu_2,\nu_3) \in R^3$ and the time variable t.

3.3.3.2 Explicit formula for a solution of (3.170), (3.171)

Using the positivity of elastic constant tensors $c_{ijkl},\ R_{ijkl},\ K_{ijkl}$ we obtain that the matrix $\mathbf{A}(\nu)$, defined by (3.172), is symmetric positive semi-definite (see Appendix). For the matrix $\mathbf{A}(\nu)$ we construct an orthogonal matrix $\mathbf{T}(\nu)$ and a diagonal matrix $\mathbf{D}(\nu) = diag(d_k(\nu),\ k = 1,2,3,4,5,6)$ with nonnegative elements such that

$$\mathbf{T}^*(\nu)\mathbf{A}(\nu)\mathbf{T}(\nu) = \mathbf{D}(\nu), \tag{3.173}$$

where $\mathbf{T}^*(\nu)$ is the transposed matrix to $\mathbf{T}(\nu)$.

Let $\mathbf{T}(\nu)$ and $\mathbf{D}(\nu) = diag(d_k(\nu),\ k = 1,2,3,4,5,6)$ be constructed. A solution of (3.170), (3.171) can be found as

$$\tilde{\mathbf{V}}^m(\nu,t) = \mathbf{T}(\nu)\mathbf{Y}^m(\nu,t), \tag{3.174}$$

where $\mathbf{Y}^m(\nu,t)$ is unknown vector function. Substituting (3.174) into (3.170), (3.171) and then multiplying the obtained equations by $\mathbf{T}^*(\nu)$ and using (3.173) we find

$$\rho\frac{\partial^2\mathbf{Y}^m}{\partial t^2} + \mathbf{D}(\nu)\mathbf{Y}^m = \mathbf{T}^*(\nu)\mathsf{E}^m\delta(t), \tag{3.175}$$

$$\mathbf{Y}^m(\nu,t)|_{t\le 0} = 0,\ t \in R,\ \nu \in R^3. \tag{3.176}$$

Using the ordinary differential equations technique (Boyce & DiPrima (1992)), a

solution of the initial value problem (3.175)-(3.176) is given by for $d_k(\nu) > 0,\ k = 1,2,3,4,5,6,$

$$\mathbf{Y}_k^m(\nu,t) = \theta(t)\frac{(\mathbf{T}^*(\nu)\mathsf{E}^m)_k}{\sqrt{\rho d_k(\nu)}}\sin(t\frac{\sqrt{d_k(\nu)}}{\sqrt{\rho}}), \tag{3.177}$$

for $d_k(\nu) = 0$

$$\mathbf{Y}_k^m(\nu,t) = \theta(t)\frac{(\mathbf{T}^*(\nu)\mathsf{E}^m)_k}{\rho}t, \tag{3.178}$$

where $\theta(t)$ is the Heaviside function, i.e. $\theta(t) = 1$ for $t \geq 0$ and $\theta(t) = 0$ for $t < 0$. Finally, a solution of (3.170), (3.171) is determined by

$$\tilde{\mathbf{V}}^m(\nu,t) = \mathbf{T}(\nu)\mathbf{Y}^m(\nu,t). \tag{3.179}$$

3.3.3.3 Explicit formula for mth column for time-dependent FS of 3D QCs

We note that values of $\mathbf{V}^m(x,t)$, $\tilde{\mathbf{V}}^m(\nu,t)$, $\mathbf{T}(\nu)$ and $\mathbf{D}(\nu) = diag(d_k(\nu),\ k = 1,2,3,4,5,6)$ are real. Therefore, applying the inverse Fourier transform to (3.179) we find that a solution of (3.168), (3.169) is given by

$$\mathbf{V}^m(x,t) = \frac{\theta(t)}{(2\pi)^3}\int_{-\infty}^{\infty}\int_{-\infty}^{\infty}\int_{-\infty}^{\infty}\mathbf{T}(\nu)\mathbf{Y}^m(\nu,t)\cos(\nu\cdot x)d\nu_1 d\nu_2 d\nu_3. \tag{3.180}$$

3.3.4 Computational examples

3.3.4.1 General characteristics of computations and visualizations

The aim of computational examples is to derive values of elements for Green matrices and then draw graphs of Green's matrix elements for anisotropic 3D QC. In this section, we consider 3D icosahedral quasicrystal for anisotropic dynamic elasticity. For our example we take the pulse force situated in $\mathsf{E}^3\delta(x_1)\delta(x_2)\delta(x_3)\delta(t)$ and $\mathsf{E}^6\delta(x_1)\delta(x_2)\delta(x_3)\delta(t)$, where $\mathsf{E}^3 = (0,0,1,0,0,0)$, $\mathsf{E}^6 = (0,0,0,0,0,1)$ and $\delta(.)$ is the Dirac delta function. The responses of the considered anisotropic quasicrystal on this source are the phonon and phason displacement vectors depending on the position (i.e. space variables x_1, x_2, x_3) and the time variable t. Using the method of Section 3.3.3 we compute $\mathbf{T}(\nu), \mathbf{T}^*(\nu), \mathbf{D}(\nu)$ and then using the formula (3.180) we have derived numerically components of $\mathbf{V}^3(x,t)$ and $\mathbf{V}^6(x,t)$. The first three components of the vector function $\mathbf{V}^i(x,t), i = 3,6$, are the phonon displacements $u_1^i(x,t), u_2^i(x,t), u_3^i(x,t)$ and the other components are the phason displacements $w_1^i(x,t), w_2^i(x,t), w_3^i(x,t), i = 3,6$.

As a result of visualization in computational examples we have seen the fluctuations of phason and phonon displacement components at points located in the short distance from a pulse point force. Moreover we have got images of the wave fronts arising from pulse point sources in QCs with icosahedral structure of anisotropy.

Example. For three-dimensional icosahedral quasicrystals c_{ijkl} has the form (Akmaz (2009), Ding & Yang & Hu & Wang (1993), Hu & Wang & Ding (2000))

$$c_{ijkl} = \lambda\delta_{ij}\delta_{kl} + \mu(\delta_{jl}\delta_{ik} + \delta_{il}\delta_{jk}),$$

where λ and μ are Lame constants. The nonzero phason elastic constants are

$$\begin{aligned}
K_{1111} &= K_{2222} = K_{1212} = K_{2121} = K_1, \\
K_{1131} &= K_{1113} = K_{2213} = K_{2312} = -K_{2231} = -K_{2321} = -K_{1232} = -K_{3221} = K_2, \\
K_{3333} &= K_1 + K_2,\ K_{2323} = K_{3131} = K_{3232} = K_{1313} = K_1 - K_2.
\end{aligned}$$

The nonzero phonon-phason coupling elastic constants are

$$\begin{aligned}
R_{1111} &= R_{1122} = R_{1133} = R_{1113} = R_{2233} = R_{2332} = R_{3111} = R_{3131} = R_{1221} = R, \\
R_{2211} &= R_{2222} = R_{2213} = R_{2312} = R_{2321} = R_{3122} = R_{1223} = R_{1212} = -R, \\
R_{3333} &= -2R.
\end{aligned}$$

For icosahedral quasicrystal Al-Cu-Li $\lambda = 30.4GPa$, $\mu = 40.9GPa$, $K_1 = 300MPa$, $K_2 = 150MPa$ and $R = 0.8GPa$ (Li & Fan & Wu (2009)). We chosen density $\rho = 1(10^3 kg/m^3)$.

Figures 3.57 is the screen shot of 2-D level plot of the first phonon displacement $u_1^3(x_1,0,x_3,0.3)$. Figure 3.58 contains 2-D plot of the first phason displacement $w_1^3(0,x_2,x_3,0.19)$. Figure 3.59 shows dynamic of the distribution for the second phason displacement $w_2^3(x_1,x_2,0,0.15)$. Figure 3.60 presents 2-D plot of the first phonon displacement $u_1^6(x_1,0,x_3,0.15)$. Figure 3.61 is the screen shot of 2-D level plot of the second phonon displacement $u_2^6(0,x_2,x_3,0.15)$. Figure 3.62 contains 2-D plot of the third phonon displacement $u_3^6(x_1,x_2,0,0.15)$. Figure 3.63 contains screen shorts of 2D level plot of the second phason displacement $w_2^6(0,x_2,x_3,0.15)$. These figures are view from the top of z-axis (the plan). Figures 3.64, 3.66 show 2-D plot of the third phason displacement $w_3^6(x_1,x_2,0,t)$ for $t = 0.02,\ 0.15$, respectively. These figures are view from the top of z-axis (the plan). Figures 3.65, 3.67 are 3-D plots of $w_3^6(x_1,x_2,0,t)$ for $t = 0.02,\ 0.15$, respectively. Here the horizontal axes are x_1 and x_2. The vertical axis is the magnitude of $w_3^6(x_1,x_2,0,t)$ for $t = 0.02,\ 0.15$. The different colors correspond

to different values of $w_3^6(x_1, x_2, 0, t)$.

3.3.4.2 Analysis of the visualization

The explicit formula of the time-dependent FS of elasticity for 3D QCs has been derived by the matrix transformations, solutions of some ordinary differential equations depending on the Fourier parameters and the inverse Fourier transform. The formula for FS of elasticity for 3D QCs has been presented in the form convenient for computation of the transient phonon and phason displacement fields.

The simulation of the phonon and phason displacements in general anisotropic media by modern computer tools allow us to see and evaluate dependence between media structures and behavior of these displacement. The approach of the method allows users to observe the elastic wave propagation arising from pulse point sources of the form $\mathsf{E}^m \delta(x_1)\delta(x_2)\delta(x_3)\delta(t)$ in 3D QCs (icosahedral). Here $\mathsf{E}^m = (\delta_1^m, \delta_2^m, \delta_3^m, \delta_4^m, \delta_5^m, \delta_6^m)$.

3.4 Concluding Remarks

In this chapter of the thesis fundamental solution of the dynamic three dimensional motion equations of 1D, 2D and 3D QCs are obtained using Fourier transformation and some matrix computations. Computational images of phonon and phason displacements for anisotropic 1D, 2D and 3D QCs are given.

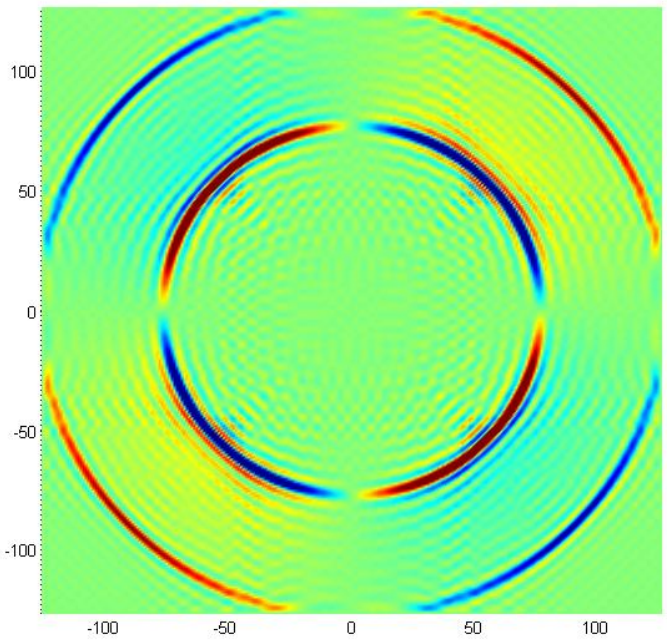

Figure 3.57: The map surface plot (plan) of 3D surface $z = u_1^3(x_1, 0, x_3, 0.3)$ in Al-Cu-Li.

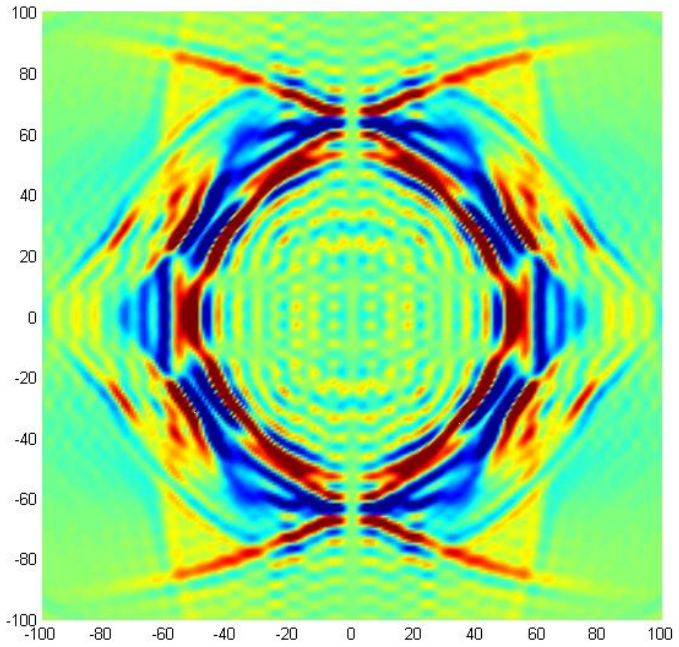

Figure 3.58: The map surface plot (plan) of 3D surface $z = w_1^3(0, x_2, x_3, 0.19)$ in Al-Cu-Li.

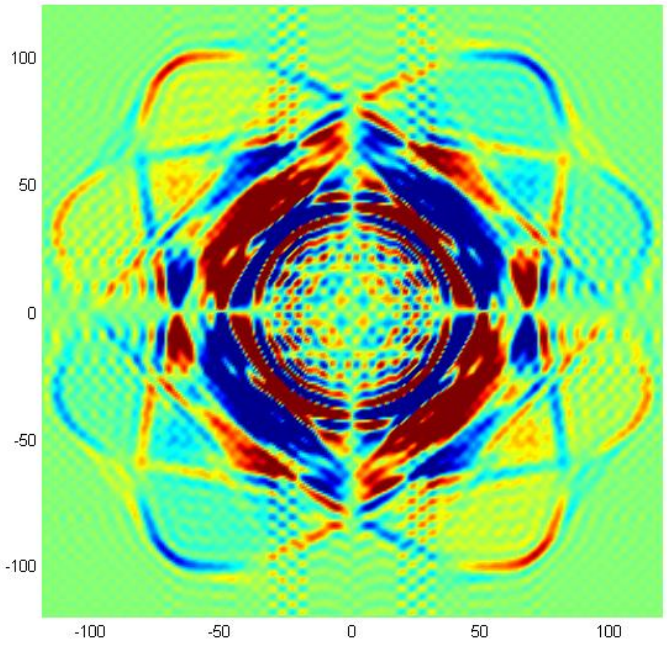

Figure 3.59: The map surface plot (plan) of 3D surface $z = w_2^3(x_1, x_2, 0, 0.15)$ in Al-Cu-Li.

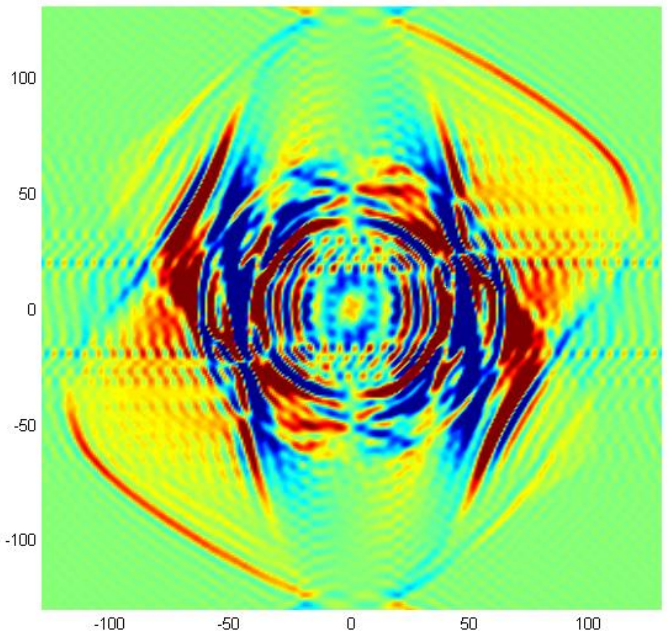

Figure 3.60: The map surface plot (plan) of 3D surface $z = u_1^6(x_1, 0, x_3, 0.15)$ in Al-Cu-Li .

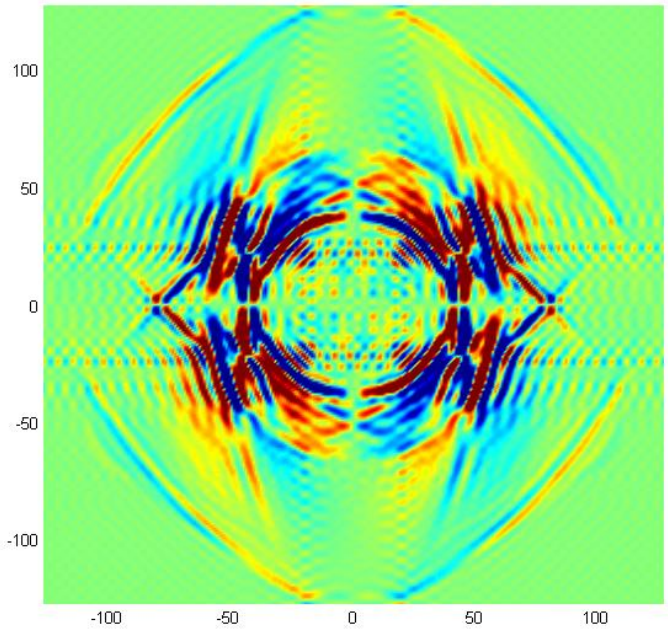

Figure 3.61: The map surface plot (plan) of 3D surface $z = u_2^6(0, x_2, x_3, 0.15)$ in Al-Cu-Li .

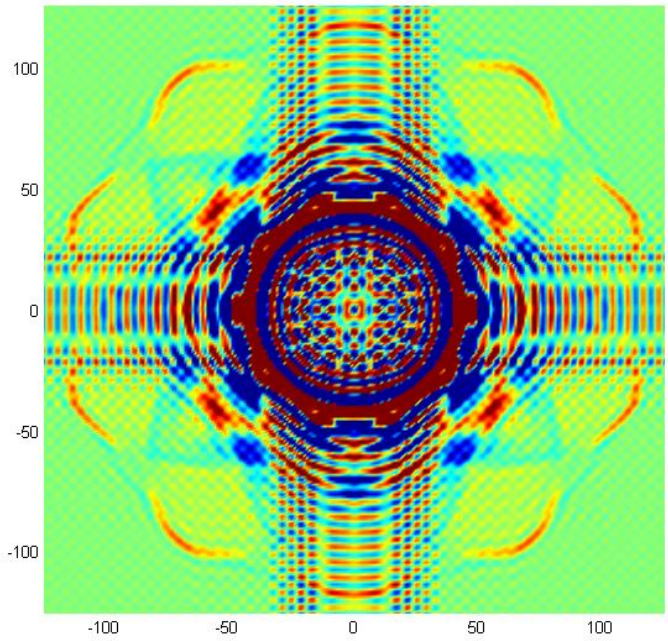

Figure 3.62: The map surface plot (plan) of 3D surface $z = u_3^6(x_1, x_2, 0, 0.15)$ in Al-Cu-Li .

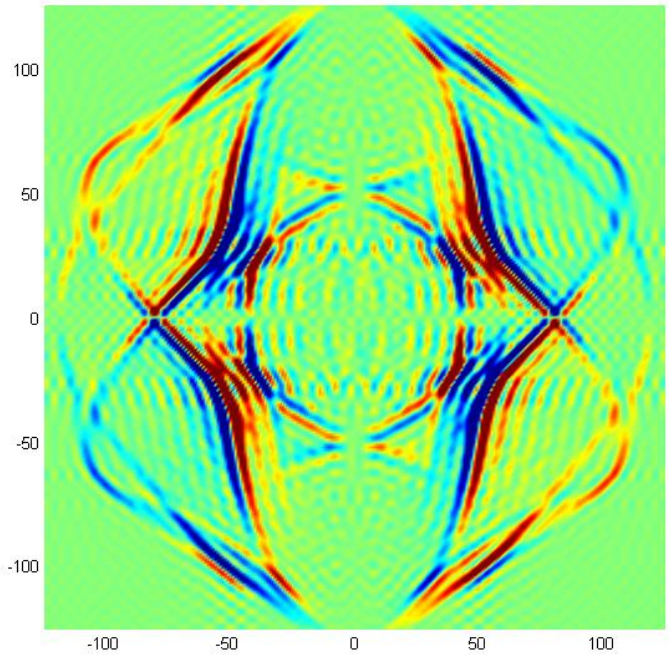

Figure 3.63: The map surface plot (plan) of 3D surface $z = w_2^6(0, x_2, x_3, 0.15)$ in Al-Cu-Li .

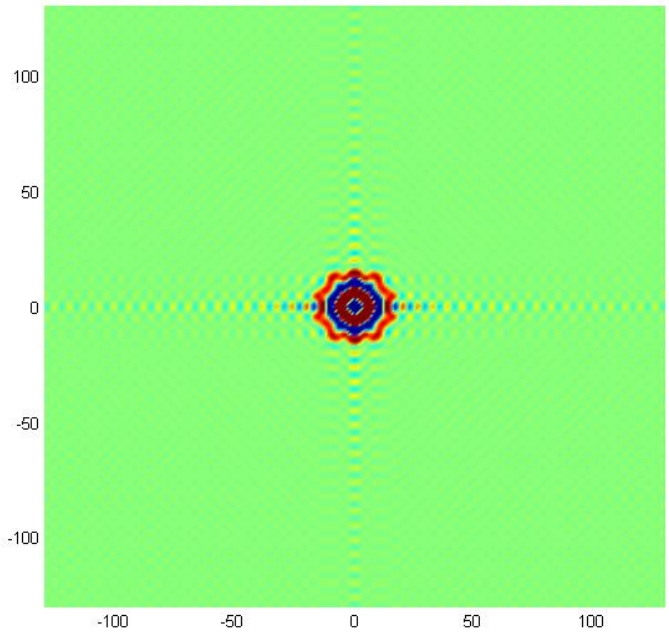

Figure 3.64: The map surface plot (plan) of 3D surface $z = w_3^6(x_1, x_2, 0, 0.02)$ in Al-Cu-Li .

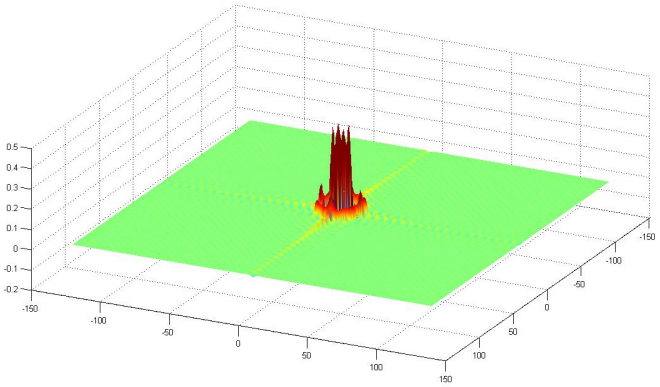

Figure 3.65: 3D surface $zw_3^6(x_1,x_2,0,0.02)$ in Al-Cu-Li
.

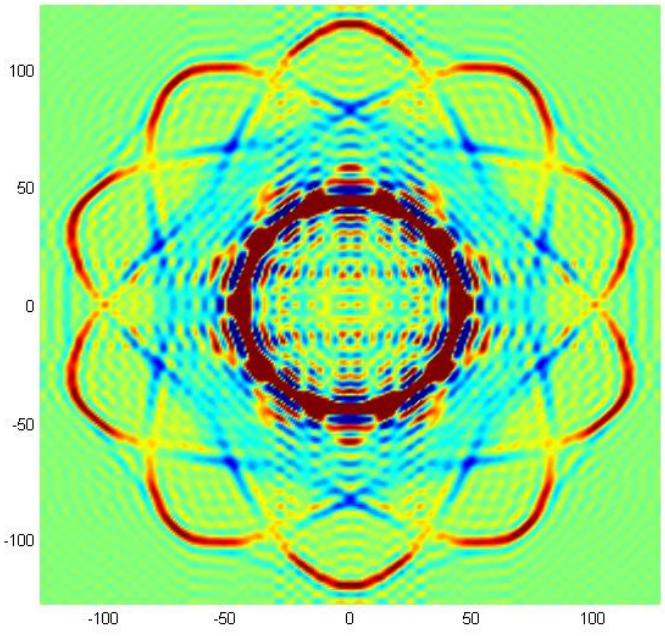

Figure 3.66: The map surface plot (plan) of 3D surface $z = w_3^6(x_1,x_2,0,0.15)$ in Al-Cu-Li .

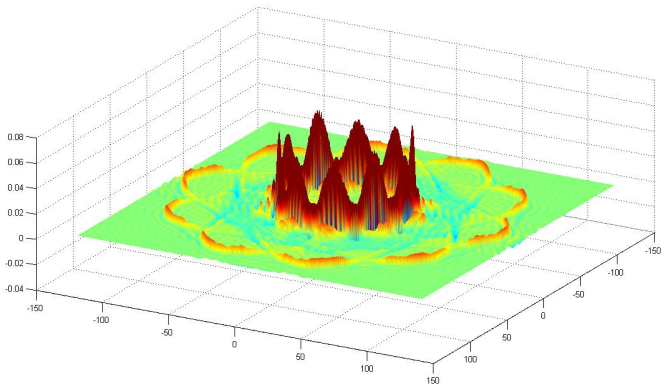

Figure 3.67: 3D surface $z = w_3^6(x_1, x_2, 0, 0.15)$ in Al-Cu-Li .

CHAPTER FOUR

COMPUTATION OF FUNDAMENTAL SOLUTION FOR ELECTRICALLY AND MAGNETICALLY ANISOTROPIC MEDIA

In this chapter an analytic method for deriving the time-dependent fundamental solution (Green's function of the free space) in a homogeneous non-dispersive electrically and magnetically anisotropic media is studied.

4.1 Basic equations of Electromagnetism

The time-dependent electric and magnetic fields in homogeneous non-dispersive materials are governed by the following Maxwell's system in Gaussian units (Pope (2010), Tikhonov & Samarskii (1963))

$$curl_x\mathbf{H} = \frac{1}{c}\bar{\bar{\varepsilon}}\frac{\partial \mathbf{E}}{\partial t} + \frac{4\pi}{c}\mathbf{J},\ curl_x\mathbf{E} = -\frac{1}{c}\bar{\bar{\mu}}\frac{\partial \mathbf{H}}{\partial t}, \tag{4.181}$$

$$div_x(\bar{\bar{\varepsilon}}\mathbf{E}) = 4\pi\rho_e,\ div_x(\bar{\bar{\mu}}\mathbf{H}) = 0, \tag{4.182}$$

where $x = (x_1, x_2, x_3) \in R^3$ is a space variable, $t \in R$ is a time variable, $\mathbf{E} = (E_1, E_2, E_3)$ and $\mathbf{H} = (H_1, H_2, H_3)$ are the electric and magnetic fields with components: $E_i = E_i(x,t),\ H_i = H_i(x,t),\ i = 1,2,3;\ \mathbf{J} = (J_1, J_2, J_3)$ is the density of the electric current with components $J_i = J_i(x,t);\ c = 1/\sqrt{\varepsilon_0\mu_0}$ is the light velocity, ε_0 and μ_0 are the permittivity and permeability of the free space, respectively. And $\mu_0 = 1.257 \times 10^{-6}$(farad/meter), $\varepsilon_0 = 8.854 \times 10^{-12}$(henry/meter). $\bar{\bar{\varepsilon}} = (\varepsilon_{ij})_{3\times 3}$ is the 3×3 permittivity matrix ; $\bar{\bar{\mu}} = (\mu_{ij})_{3\times 3}$ is the 3×3 permeability matrix; ρ_e is the density of electric charges. The electric charges and current are sources of electromagnetic

waves. We assume these sources are given. It follows from (4.181)-(4.182) that electric charges and current have to satisfy the conservation law of charges

$$\frac{\partial \rho_e}{\partial t} + div_x \mathbf{J} = 0. \tag{4.183}$$

A medium is said to be electrically and magnetically anisotropic if $\overline{\overline{\varepsilon}}$ and $\overline{\overline{\mu}}$ are arbitrary matrices (see, for example, Kong (1986)). Some of materials have the magnetic permeability as a matrix $\overline{\overline{\mu}}$ and the permittivity as a identity matrix (i.e. $\overline{\overline{\varepsilon}} = \mathbf{I}$, where $\mathbf{I}$ is the identity matrix). These materials are said to be magnetically anisotropic. Materials which have the permittivity as a matrix $\overline{\overline{\varepsilon}}$ and the magnetic permeability as a a identity matrix (i.e. $\overline{\overline{\mu}} = \mathbf{I}$) are said to be electrically anisotropic. Crystals (dielectrics) are electrically anisotropic materials.

In this chapter a homogeneous non-dispersive electrically and magnetically anisotropic media, characterized by a symmetric positive definite permittivity and permeability tensors are considered. An analytic method for deriving the time-dependent fundamental solution (FS) in these anisotropic media is suggested. This method consists of the following: equations for each column of the FS are reduced to a symmetric hyperbolic system; using the Fourier transform with respect to the space variables and matrix transformations we obtain explicit formulae for Fourier images of the FS columns; finally, the FS is computed by the inverse Fourier transform. Computational examples confirm the robustness of the suggested method.

In this chapter we suppose that

$$\mathbf{E} = 0,\ \mathbf{H} = 0,\ \mathbf{J} = 0,\ \rho_e = 0,\ \textit{for } t < 0. \tag{4.184}$$

Remark 1. The equations (4.181) under conditions (4.184) imply the equalities of (4.182) (we assume here that (4.183) is satisfied).

Proof. Applying divergence operator to the first equation of (4.181) and using the first equation of (4.182) we have the conservation law of charges (4.183). Using the divergence operator to the first equation of (4.181)

$$\frac{1}{c}\frac{\partial}{\partial t} div_x(\bar{\bar{\varepsilon}}\mathbf{E}) + \frac{4\pi}{c} div_x \mathbf{J} = 0. \tag{4.185}$$

Substituting (4.183) into (4.185)

$$\frac{1}{c}\frac{\partial}{\partial t}(div_x(\bar{\bar{\varepsilon}}\mathbf{E}) - 4\pi\rho_e) = 0, \tag{4.186}$$

and using the initial conditions (4.184) we have the first equalities of (4.182).

Similarly applying divergence operator to the second equation of (4.181) we have

$$\frac{1}{c}\frac{\partial}{\partial t} div_x(\bar{\bar{\mu}}\mathbf{H}) = 0,$$

and using the initial conditions (4.184) we have the second equalities of (4.182). □

4.2 Maxwell's equations as a first order symmetric hyperbolic system

In this section we reduce the first and second equations of (4.181) to a first order symmetric hyperbolic system.

Using definition of $curl_x$ the first equation of (4.181) can be rewritten in the following form:

$$\frac{1}{c}\bar{\bar{\varepsilon}}\frac{\partial \mathbf{E}}{\partial t} + \sum_{j=1}^{3} \mathbf{A}_j^1 \frac{\partial \mathbf{H}}{\partial x_j} = -\frac{4\pi}{c}\mathbf{J}, \tag{4.187}$$

where

$$\mathbf{A}_1^1 = \begin{bmatrix} 0 & 0 & 0 \\ 0 & 0 & 1 \\ 0 & -1 & 0 \end{bmatrix}, \mathbf{A}_2^1 = \begin{bmatrix} 0 & 0 & -1 \\ 0 & 0 & 0 \\ 1 & 0 & 0 \end{bmatrix}, \mathbf{A}_3^1 = \begin{bmatrix} 0 & 1 & 0 \\ -1 & 0 & 0 \\ 0 & 0 & 0 \end{bmatrix}. \tag{4.188}$$

Similarly, the second equation of (4.181) can be rewritten in the following form:

$$\frac{1}{c}\bar{\bar{\mu}}\frac{\partial \mathbf{H}}{\partial t} + \sum_{j=1}^{3} (\mathbf{A}_j^1)^* \frac{\partial \mathbf{E}}{\partial x_j} = 0. \tag{4.189}$$

Then the first and second equations of (4.181) can be written as the following first order symmetric hyperbolic system

$$\frac{1}{c}\mathbf{A}_0 \frac{\partial \mathbf{V}}{\partial t} + \sum_{j=1}^{3} \mathbf{A}_j \frac{\partial \mathbf{V}}{\partial x_j} = \mathbf{F} \tag{4.190}$$

where

$$\mathbf{V} = (E_1, E_2, E_3, H_1, H_2, H_3), \ \mathbf{F} = \frac{4\pi}{c}(-J_1, -J_2, -J_3, 0, 0, 0),$$

$$\mathbf{A}_0 = \begin{bmatrix} \bar{\bar{\varepsilon}} & 0_{3,3} \\ 0_{3,3} & \bar{\bar{\mu}} \end{bmatrix}_{6\times 6}, \ \mathbf{A}_j = \begin{bmatrix} 0_{3,3} & \mathbf{A}_j^1 \\ (\mathbf{A}_j^1)^* & 0_{3,3} \end{bmatrix}_{3\times 3},$$

$*$ denotes transposition, $0_{3,3}$ is the zero matrix which has the order 3×3.

4.3 Equations for the time-dependent fundamental solution(FS) of electrically and magnetically anisotropic media

The FS for the time-dependent Maxwell's equations (4.181) is defined as a matrix $\mathbf{G}(x,t)$ of the order 6×3 whose columns $(\mathbf{E}^m, \mathbf{H}^m) = (E_1^m, E_2^m, E_3^m, H_1^m, H_2^m, H_3^m)$, $m =$

$1,2,3$, satisfy

$$\begin{aligned} curl_x\mathbf{H}^m &= \frac{1}{c}\bar{\bar{\varepsilon}}\frac{\partial \mathbf{E}^m}{\partial t} + \frac{4\pi \mathbf{e}^m}{c}\delta(x)\delta(t),\ curl_x\mathbf{E}^m = -\frac{1}{c}\bar{\bar{\mu}}\frac{\partial \mathbf{H}^m}{\partial t}, \\ \mathbf{E}^m\mid_{t<0} &= 0,\ \mathbf{H}^m\mid_{t<0}= 0, \end{aligned} \tag{4.191}$$

Here $\mathbf{e}^1 = (1,0,0),\ \mathbf{e}^2 = (0,1,0),\ \mathbf{e}^3 = (0,0,1)$ are basis vectors of the Cartesian coordinates; $\delta(x) = \delta(x_1)\delta(x_2)\delta(x_3)$ is the Dirac delta function of the space variable concentrated at $x_1 = 0,\ x_2 = 0,\ x_3 = 0$; $\delta(t)$ is the Dirac delta function of the time variable concentrated at $t = 0$.

Elements of the m-th column $(\mathbf{E}^m, \mathbf{H}^m)$ of the FS are the electric and magnetic fields in the considered anisotropic medium arising from the pulse dipole $\mathbf{e}^m\delta(x)\delta(t)$.

Equalities (4.191) can be written as

$$\frac{1}{c}\mathbf{A}_0\frac{\partial \mathbf{V}^m}{\partial t} + \sum_{j=1}^{3}\mathbf{A}_j\frac{\partial \mathbf{V}^m}{\partial x_j} = \frac{4\pi}{c}\mathsf{E}^m\delta(x)\delta(t),\ \mathbf{V}^m\mid_{t<0}= 0,\ m = 1,2,3, \tag{4.192}$$

where $\mathsf{E}^m = (-\mathbf{e}^m, 0,0,0)$ is such vector with six components that the first three components are components of $-\mathbf{e}^m$ and other components are equal to zero.

4.4 Deriving formulae for electric and magnetic fields

Let $\tilde{\mathbf{V}}^m(\nu,t) = (\tilde{V_1}^m(\nu,t), \tilde{V_2}^m(\nu,t), \tilde{V_3}^m(\nu,t), \tilde{V_4}^m(\nu,t), \tilde{V_5}^m(\nu,t), \tilde{V_6}^m(\nu,t))$ be the Fourier image of $\mathbf{V}^m(x,t)$ with respect to $x = (x_1,x_2,x_3) \in R^3$, i.e. for $j = 1,2,3$

$$\begin{aligned} &\tilde{V_j}^m(\nu,t) = \int_{-\infty}^{\infty}\int_{-\infty}^{\infty}\int_{-\infty}^{\infty} V_j^m(x,t)e^{ix\cdot\nu}dx_1dx_2dx_3, \\ &\nu = (\nu_1,\nu_2,\nu_3) \in R^3,\ x\cdot\nu = x_1\nu_1 + x_2\nu_2 + x_3\nu_3,\ i^2 = -1. \end{aligned}$$

Equalities (4.192) can be written in terms of $\tilde{\mathbf{V}}^m(\nu,t)$ as follows

$$\mathbf{A}_0\frac{\partial\tilde{\mathbf{V}}^m}{\partial t}-ic\mathbf{B}(\nu)\tilde{\mathbf{V}}^m=4\pi\mathsf{E}^m\delta(t),\ \ \tilde{\mathbf{V}}^m(\nu,t)|_{t<0}=0, \tag{4.193}$$

where $\mathbf{B}(\nu)=(\nu_1\mathbf{A}_1+\nu_2\mathbf{A}_2+\nu_3\mathbf{A}_3)$.

Diagonalization $\mathbf{A}_0$ and $\mathbf{B}(\nu)$ simultaneously. The matrix $\mathbf{A}_0$ is symmetric positive definite and $\mathbf{B}(\nu)$ is symmetric. In this step we construct a non-singular matrix $\mathbf{T}(\nu)$ and a diagonal matrix $\mathbf{D}(\nu)=diag(d_k(\nu),\ k=1,2,...,6)$ with real valued elements such that

$$\mathbf{T}^*(\nu)\mathbf{A}_0\mathbf{T}(\nu)=\mathbf{I},\ \ \mathbf{T}^*(\nu)\mathbf{B}(\nu)\mathbf{T}(\nu)\ \ =\ \ \mathbf{D}(\nu), \tag{4.194}$$

where $\mathbf{I}$ is the identity matrix, $\mathbf{T}^*(\nu)$ is the transposed matrix to $\mathbf{T}(\nu)$.

Computing $\mathbf{T}(\nu)$ and $\mathbf{D}(\nu)$ can be made by the following way: we find $\mathbf{A}_0^{-1/2}$ and then using the matrix $\mathbf{A}_0^{-1/2}\mathbf{B}(\nu)\mathbf{A}_0^{-1/2}$ we construct $\mathbf{T}(\nu)$ and $\mathbf{D}(\nu)$.

Finding $\mathbf{A}_0^{-1/2}$. For the given positive definite matrix $\mathbf{A}_0$ we compute an orthogonal matrix $\mathcal{R}$ by the eigenfunctions of $\mathbf{A}_0$ such that $\mathcal{R}^*\mathbf{A}_0\mathcal{R}=\mathcal{L}$, where $\mathcal{R}^*$ is the transpose matrix to $\mathcal{R}$ and $\mathcal{L}=diag(\lambda_k,\ k=1,2,...,6)$ is the diagonal matrix with positive elements λ_k which are eigenvalues of $\mathbf{A}_0$. The matrix $\mathcal{L}^{1/2}$ is defined by the formula $\mathcal{L}^{1/2}=diag(\sqrt{\lambda_k},\ k=1,2,...,6)$ and $\mathbf{A}_0^{1/2}$ is defined by $\mathbf{A}_0^{1/2}=\mathcal{R}\mathcal{L}^{1/2}\mathcal{R}^*$. The matrix $\mathbf{A}_0^{-1/2}$ is the inverse to $\mathbf{A}_0^{1/2}$.

Finding $\mathbf{T}(\nu)$ and $\mathbf{D}(\nu)$. Let matrix $\mathbf{B}(\nu)$ be given and matrix $\mathbf{A}_0^{-1/2}$ be found. Let us consider the matrix $\mathbf{A}_0^{-1/2}\mathbf{B}(\nu)\mathbf{A}_0^{-1/2}$ which is symmetric with real valued elements. The diagonal matrix $\mathbf{D}(\nu)$ is constructed by eigenvalues of $\mathbf{A}_0^{-1/2}\mathbf{B}(\nu)\mathbf{A}_0^{-1/2}$. The columns of the orthogonal matrix $\mathbf{Q}(\nu)$ are formed by normalized orthogonal eigenfunctions of $\mathbf{A}_0^{-1/2}\mathbf{B}(\nu)\mathbf{A}_0^{-1/2}$ corresponding to eigenvalues $d_k(\nu),\ k=1,2,...,6$.

The matrix $\mathbf{T}(\nu)$ is defined by the formula $\mathbf{T}(\nu) = \mathbf{A}_0^{-1/2}\mathbf{Q}(\nu)$.

Deriving a solution of IVP (4.192). Let $\mathbf{D}(\nu)$ and $\mathbf{T}(\nu)$, satisfying (4.194), be constructed. We find a solution of (4.193) in the form $\tilde{\mathbf{V}}^m(\nu,t) = \mathbf{T}(\nu)\mathbf{Y}^m(\nu,t)$, where $\mathbf{Y}^m(\nu,t)$ is unknown vector function. Substituting $\tilde{\mathbf{V}}^m(\nu,t) = \mathbf{T}(\nu)\mathbf{Y}^m(\nu,t)$ into (4.193) and then multiplying the obtained vector differential equation by $\mathbf{T}^*(\nu)$ and using (4.194) we find

$$\frac{\partial \mathbf{Y}^m}{\partial t} - ic\mathbf{D}(\nu)\mathbf{Y}^m = 4\pi\mathbf{T}^*(\nu)\mathsf{E}^m\delta(t),\ t \in R,\ \mathbf{Y}^m(\nu,t)|_{t\le 0} = 0. \tag{4.195}$$

Using the ordinary differential equations technique a solution of the initial value problem (4.195) is given by

$$\mathbf{Y}^m(\nu,t) = 4\pi\theta(t)\left[\cos(c\mathbf{D}(\nu)t) + i\sin(c\mathbf{D}(\nu)t)\right]\mathbf{T}^*(\nu)\mathsf{E}^m,$$

where $\theta(t)$ is the Heaviside function, i.e. $\theta(t) = 1$ for $t \ge 0$ and $\theta(t) = 0$ for $t < 0$; $\cos(c\mathbf{D}(\nu)t)$ and $\sin(c\mathbf{D}(\nu)t)$ are diagonal matrices whose diagonal elements are $\cos(cd_k(\nu)t)$ and $\sin(cd_k(\nu)t)$, $k = 1,2,...,6$, respectively.

A solution of (4.193) is determined by

$$\tilde{\mathbf{V}}^m(\nu,t) = 4\pi\theta(t)\mathbf{T}(\nu)\left[\cos(c\mathbf{D}(\nu)t) + i\sin(c\mathbf{D}(\nu)t)\right]\mathbf{T}^*(\nu)\mathsf{E}^m. \tag{4.196}$$

Finally the vector function $\mathbf{V}^m(\nu,t)$ satisfying (4.192) can be found by the inverse Fourier transform

$$\mathbf{V}^m(x,t) = \frac{1}{(2\pi)^3}\int_{-\infty}^{\infty}\int_{-\infty}^{\infty}\int_{-\infty}^{\infty}\tilde{\mathbf{V}}^m(\nu,t)e^{-i\nu\cdot x}d\nu_1 d\nu_2 d\nu_3. \tag{4.197}$$

Noting that every solution of (4.192) is a real valued vector function and using formulae

(4.196), (4.197) we find that a solution of IVP (4.192) is given by

$$\mathbf{V}^m(x,t) = \frac{\theta(t)}{2\pi^2} \int_{-\infty}^{\infty} \int_{-\infty}^{\infty} \int_{-\infty}^{\infty} \mathbf{T}(\nu) \cos\Big(c\mathbf{D}(\nu)t - \mathbf{I}(\nu \cdot x)\Big) \mathbf{T}^*(\nu) \mathsf{E}^m d\nu_1 d\nu_2 d\nu_3, \quad (4.198)$$

where $\cos\Big(c\mathbf{D}(\nu)t - \mathbf{I}(\nu \cdot x)\Big)$ is the diagonal matrix with diagonal elements $\cos\Big(cd_k(\nu)t - \nu \cdot x\Big)$, $k = 1,2,...,6$.

4.5 Computation of scalar-vector potentials and FS of Maxwell's equations in isotropic media

4.5.1 Scalar and vector potentials for Maxwell's equations

Let $\overline{\overline{\varepsilon}} = \varepsilon \mathbf{I}_{3,3}$ and $\overline{\overline{\mu}} = \mu \mathbf{I}_{3,3}$ in (4.181)-(4.182), where ε and μ are positive constants. Let us consider the following Cauchy problem,

$$\frac{\partial}{\partial t}(div_x(\mu \mathbf{H})) = 0, \quad (4.199)$$

$$div_x(\mu \mathbf{H})|_{t<0} = 0 \quad (4.200)$$

Therefore, $div_x(\mu \mathbf{H}) = 0$ for $t \in R$. The vector $\mu \mathbf{H}$ can be written in the following form,

$$\mu\, \mathbf{H}(x,t) = curl_x \overrightarrow{A}(x,t) + \nabla_x \psi(x,t) \quad (4.201)$$

where $\overrightarrow{A}$ is a vector function and $\psi(x,t)$ is a scalar function. We choose $\overrightarrow{A}$ and ψ satisfying (4.201) such that $\overrightarrow{A} \neq \overrightarrow{0}$ and $\psi = 0$. Then $\mathbf{H}$ can be represented as

$$\mathbf{H}(x,t) = \frac{1}{\mu} curl_x \overrightarrow{A}(x,t), \quad (4.202)$$

where $\overrightarrow{A}$ is called the electrodynamic potential vector. Substituting (4.202) into the second equation of (4.181) we have

$$curl_x\mathbf{E} = -\frac{\mu}{c}\frac{\partial}{\partial t}(\frac{1}{\mu}curl_x\overrightarrow{A}(x,t)) \tag{4.203}$$

$$curl_x(\mathbf{E}+\frac{1}{c}\frac{\partial}{\partial t}\overrightarrow{A}(x,t)) = 0. \tag{4.204}$$

From the theory of vector analysis the vector $\mathbf{E}+\frac{1}{c}\frac{\partial}{\partial t}\overrightarrow{A}$ can be written as,

$$\mathbf{E}+\frac{1}{c}\frac{\partial}{\partial t}\overrightarrow{A} = curl_x\overrightarrow{B}(x,t)+\nabla_x\varphi(x,t) \tag{4.205}$$

we choose $\overrightarrow{B}$ and φ such that $\overrightarrow{B} = 0$ and $\varphi \neq 0$. $\varphi(x,t)$ is a scalar function and called the scalar electrodynamic potential and also $curl_x\nabla_x\varphi = 0$. Then $\mathbf{E}$ can be represented as,

$$\mathbf{E}(x,t) = -\frac{1}{c}\frac{\partial}{\partial t}\overrightarrow{A}(x,t)+\nabla_x\varphi(x,t) \tag{4.206}$$

Substituting (4.202), (4.206) into the first equation (4.181) we have

$$curl_x(\frac{1}{\mu}curl_x\overrightarrow{A}) = \frac{1}{c}\varepsilon\frac{\partial}{\partial t}\left(-\frac{1}{c}\frac{\partial\overrightarrow{A}}{\partial t}+\nabla_x\varphi\right)+\frac{4\pi}{c}\mathbf{J}. \tag{4.207}$$

Using $curl_xcurl_x\overrightarrow{A} = -\triangle_x\overrightarrow{A}+\nabla_x div_x\overrightarrow{A}$, the last equation becomes

$$\frac{1}{\mu}(-\triangle_x\overrightarrow{A}+\nabla_x div_x\overrightarrow{A}) = -\frac{1}{c^2}\varepsilon\frac{\partial^2\overrightarrow{A}}{\partial t^2}+\frac{1}{c}\varepsilon\nabla_x\frac{\partial\varphi}{\partial t}+\frac{4\pi}{c}\mathbf{J} \tag{4.208}$$

equivalently,

$$\nabla_x\left(-\frac{\varepsilon}{c}\frac{\partial\varphi}{\partial t}+\frac{1}{\mu}div_x\overrightarrow{A}\right)+\left(\frac{\varepsilon}{c^2}\frac{\partial^2\overrightarrow{A}}{\partial t^2}-\frac{1}{\mu}\triangle_x\overrightarrow{A}-\frac{4\pi}{c}\mathbf{J}\right) = 0 \tag{4.209}$$

equality (4.209) holds if $\overrightarrow{A}$ and φ are chosen from relations

$$\frac{\partial\varphi(x,t)}{\partial t} = \frac{c}{\varepsilon\mu} div_x \overrightarrow{A}(x,t), \tag{4.210}$$

$$\frac{\partial^2 \overrightarrow{A}(x,t)}{\partial t^2} - \frac{c^2}{\varepsilon\mu}\triangle_x \overrightarrow{A}(x,t) = \frac{4\pi c}{\varepsilon}\mathbf{J}(x,t). \tag{4.211}$$

For holding the equations

$$\varphi(x,t)|_{t<0} = 0, \tag{4.212}$$

$$\overrightarrow{A}(x,t)|_{t<0} = 0 \tag{4.213}$$

are sufficient.

4.5.2 FS for equations of scalar and vector potentials

FS for the equation of vector potential is a matrix G^A of the order 3×3 whose columns $A^m = (A_1^m, A_2^m, A_3^m)$, $m = 1,2,3$, satisfy

$$\frac{\partial^2 \overrightarrow{A^m}(x,t)}{\partial t^2} - \frac{c^2}{\varepsilon\mu}\triangle_x \overrightarrow{A^m}(x,t) = \frac{4\pi c}{\varepsilon}\delta(x)\delta(t)\mathbf{e}^m,$$

$$\overrightarrow{A^m}(x,t)|_{t<0} = 0, \tag{4.214}$$

where $\mathbf{e}^1 = (1,0,0),\ \mathbf{e}^2 = (0,1,0),\ \mathbf{e}^3 = (0,0,1)$ are basis vectors of the Cartesian coordinates; $\delta(x) = \delta(x_1)\delta(x_2)\delta(x_3)$ is the Dirac delta function of the space variable concentrated at $x_1 = 0,\ x_2 = 0,\ x_3 = 0$; $\delta(t)$ is the Dirac delta function of the time variable concentrated at $t = 0$.

Applying the Fourier transformation with respect to x to (4.214) we have the

following IVP

$$\begin{aligned} \frac{\partial^2 \overrightarrow{\tilde{A}^m}(\nu,t)}{\partial t^2} + \frac{c^2 \mid \nu \mid^2}{\varepsilon\mu} \overrightarrow{\tilde{A}^m}(\nu,t) &= \frac{4\pi c}{\varepsilon}\delta(t)\mathbf{e}^m, \\ \overrightarrow{\tilde{A}^m}(\nu,t) \mid_{t<0} &= 0. \end{aligned} \tag{4.215}$$

Solving IVP (4.215) we have

$$\overrightarrow{\tilde{A}^m_j}(\nu,t) = \theta(t)\frac{4\pi}{\mid \nu \mid}\sqrt{\frac{\mu}{\varepsilon}}\sin(\frac{c}{\sqrt{\mu\varepsilon}} \mid \nu \mid t)\delta^m_j. \tag{4.216}$$

Here δ^m_j is the Kronecker symbol, i.e. $\delta^m_j = 1$ if $j = m$ and $\delta^m_j = 0$ if $j \neq m$; $j = 1,2,3$; $m = 1,2,3$.

FS for the equation of scalar potential is a vector G^φ whose components φ^m, $m = 1,2,3$ satisfy the following IVP

$$\begin{aligned} \frac{\partial \varphi^m(x,t)}{\partial t} &= \frac{c}{\varepsilon\mu} div_x \overrightarrow{A^m}(x,t), \\ \varphi^m(x,t) \mid_{t<0} &= 0 \end{aligned} \tag{4.217}$$

Applying Fourier transformation with respect to x to (4.217) we have the following IVP

$$\begin{aligned} \frac{\partial \tilde{\varphi}^m(\nu,t)}{\partial t} &= \frac{c}{\varepsilon\mu}(-i\nu_1\tilde{A}^m_1 - i\nu_2\tilde{A}^m_2 - i\nu_3\tilde{A}^m_3)(\nu,t), \\ \tilde{\varphi}^m(\nu,t) \mid_{t<0} &= 0 \end{aligned} \tag{4.218}$$

Using (4.216) and solving IVP (4.218) we have

$$\tilde{\varphi}^m_j(\nu,t) = i\nu_j\frac{4\pi}{\varepsilon \mid \nu \mid^2}(\cos(\frac{c}{\sqrt{\varepsilon\mu}} \mid \nu \mid t) - 1), \ j = 1,2,3. \tag{4.219}$$

4.5.3 FS of Maxwell equations in isotropic media

The FS for the time-dependent Maxwell's equations (4.181) in isotropic medium is defined as a matrix $\mathbf{G}^{\mathbf{I}}(x,t)$ of the order 6×3 whose columns $(\mathbf{E}^{\mathbf{I}^m},\mathbf{H}^{\mathbf{I}^m}) = (\mathcal{E}_1^m,\mathcal{E}_2^m,\mathcal{E}_3^m,\mathcal{H}_1^m,\mathcal{H}_2^m,\mathcal{H}_3^m)$, $m=1,2,3$, satisfy

$$\begin{aligned} curl_x\mathbf{H}^{\mathbf{I}^m} &= \frac{1}{c}\varepsilon\frac{\partial\mathbf{E}^{\mathbf{I}^m}}{\partial t}+\frac{4\pi\mathbf{e}^m}{c}\delta(x)\delta(t),\ curl_x\mathbf{E}^{\mathbf{I}^m}=-\frac{1}{c}\mu\frac{\partial\mathbf{H}^{\mathbf{I}^m}}{\partial t},\\ \mathbf{E}^{\mathbf{I}^m}\mid_{t<0} &= 0,\ \mathbf{H}^{\mathbf{I}^m}\mid_{t<0}=0. \end{aligned} \tag{4.220}$$

From (4.202) and (4.206) we can write

$$\mathbf{H}^{\mathbf{I}^m}(x,t)=\frac{1}{\mu}curl_x\overrightarrow{A}^m(x,t), \tag{4.221}$$

$$\mathbf{E}^{\mathbf{I}^m}(x,t)=-\frac{1}{c}\frac{\partial}{\partial t}\overrightarrow{A}^m(x,t)+\nabla_x\varphi^m(x,t). \tag{4.222}$$

Applying Fourier transformation with respect to x to (4.221) and (4.222) and using the (4.216) and (4.219) the Fourier image of FS $\mathbf{G}^{\mathbf{I}}(x,t)=(\mathbf{E}^{\mathbf{I}}(x,t),\mathbf{H}^{\mathbf{I}}(x,t))$ for the time-dependent Maxwell's equations in isotropic medium can be written as follows

$$\begin{aligned} \tilde{\mathbf{E}}^{\mathbf{I}}(\nu,t) &= -\mathbf{I}_{3,3}\frac{4\pi}{\varepsilon}\cos(\frac{c}{\sqrt{\varepsilon\mu}}\mid\nu\mid t)\\ &+ \begin{bmatrix} \nu_1^2 & \nu_1\nu_2 & \nu_1\nu_3\\ \nu_1\nu_2 & \nu_2^2 & \nu_3\nu_2\\ \nu_1\nu_3 & \nu_3\nu_2 & \nu_3^2 \end{bmatrix}\frac{4\pi}{\varepsilon\mid\nu\mid^2}(\cos(\frac{c}{\sqrt{\varepsilon\mu}}\mid\nu\mid t)-1). \end{aligned} \tag{4.223}$$

$$\tilde{\mathbf{H}}^{\mathbf{I}}(\nu,t)=\begin{bmatrix} 0 & i\nu_3 & -i\nu_2\\ -i\nu_3 & 0 & i\nu_1\\ i\nu_3 & -i\nu_1 & 0 \end{bmatrix}\theta(t)\frac{4\pi}{\sqrt{\mu\varepsilon}\mid\nu\mid}(\sin(\frac{c}{\sqrt{\varepsilon\mu}}\mid\nu\mid t), \tag{4.224}$$

where $\mathbf{I}_{3,3}$ is the identity matrix of order 3×3.

4.6 Computation of the fundamental solution of (4.190) with arbitrary source

The computation of the fundamental solution for the system of the form (4.190) arising from an arbitrary given force $\mathbf{F}(x,t) = (f_1(x,t), f_2(x,t), f_3(x,t), 0, 0, 0)$, whose components $f_i(x,t), i = 1,2,3$ are arbitrary functions for $t \geq 0$ and equal to zero for $t < 0$, can be defined as a matrix $\mathcal{G}(x,t)$ of the order 6×6 for which the formula

$$V(x,t) = \int_{-\infty}^{\infty}\int_{-\infty}^{\infty}\int_{-\infty}^{\infty}\int_{-\infty}^{\infty} \mathcal{G}(x-\xi, t-\eta)\mathbf{F}(\xi,\eta)d\xi_1 d\xi_2 d\xi_3 d\eta \tag{4.225}$$

gives a solution of (4.190). Here the columns of $\mathbf{G}$ are defined by (4.192), $\xi = (\xi_1, \xi_2, \xi_3) \in R^3$, $x = (x_1, x_2, x_3) \in R^3$, $t \in R$, $\eta \in R$.

Using the fact that the first three components of

$$\mathbf{F} = (f_1(\xi,\eta), f_2(\xi,\eta), f_3(\xi,\eta), 0, 0, 0)$$

are nonzero and other components are identically equal to zero we find that columns of $\mathcal{G}(x,t)$ started from fourth do not have any influence on the solution $V(x,t)$ defined by (4.225). Therefore the fundamental solution of (4.190) is naturally defined as a matrix $\mathbf{G}(x,t)$ of the order 6×3 for which the formula

$$V(x,t) = \int_{-\infty}^{\infty}\int_{-\infty}^{\infty}\int_{-\infty}^{\infty}\int_{-\infty}^{\infty} \mathbf{G}(x-\xi, t-\eta)\mathbf{f}(\xi,\eta)d\xi_1 d\xi_2 d\xi_3 d\eta$$

gives a solution of (4.190), where $\mathbf{f}(\xi,\eta) = (f_1(\xi,\eta), f_2(\xi,\eta), f_3(\xi,\eta))$ is 3D vector column. We note also that each column of the fundamental solution $\mathbf{G}(x,t)$ of (4.190) satisfies (4.192).

4.7 Computational examples

We have implemented two types of computational experiments. The first one shows a high accuracy in computing values of FS for Maxwell equations in isotropic media. The values of Fourier image of FS have been derived for isotropic material in two ways: by explicit formulae as well as by the method of Section 4.4. The results of the comparison are presented in Tables 4.1.-4.2. And Fourier images of FS in isotropic medium have been given by Figs. 4.68-4.71.

In the second type of computational experiments we consider five homogeneous non-dispersive anisotropic materials: a biaxial crystal, positive uniaxial crystal (sapphire), monoclinic dielectric, triclinic dielectric, an electrically and magnetically anisotropic medium. The point pulse current situating in each material radiates diverging electromagnetic waves. The interference figures of the electric and magnetic fields into these five media computed by obtained explicit formula (4.198) are presented and analyzed in this section. The interference patterns of electric and magnetic fields and diverging spherical fronts emitted by this special type of the current (a pulse dipole with a fixed polarization) will accumulate astigmatism on wave propagations arising from the anisotropy of the materials. For all applications the current density $\mathbf{J}$ is taken in the form

$$\mathbf{J}(x,t) = \mathbf{e}^3\delta(x_1)\delta(x_2)\delta(x_3)\delta(t)$$

where $\delta(x_1)\delta(x_2)\delta(x_3)\delta(t)$ is the Dirac delta function concentrated at the origin of the coordinates at the time $t = 0$ in the direction $\mathbf{e}^3 = (0,0,1)$. This is a pulse dipole with the polarization $\mathbf{e}^3$.

Using the procedure of Section 4.4 the matrices $\mathbf{T}$, $\mathbf{T}^*$, $\mathbf{D}$ were computed for every given symmetric positive definite matrices $\overline{\overline{\varepsilon}}$ and $\overline{\overline{\mu}}$. Further, using formula (4.198)

we have found explicit formulae for the electric field components and magnetic field components.

4.7.1 Accuracy of the method

Taking $\mu = 1$ and $\varepsilon = 9.4$ and using formulae (4.223)-(4.224) we have calculated exact solution of the Fourier images of FS $\mathbf{G^I}$ corresponding to source $\mathbf{J} = \mathbf{e}^3\delta(x)\delta(t)$, i.e. $\tilde{\mathcal{E}_1}^3(\nu,t)$, $\tilde{\mathcal{E}_2}^3(\nu,t)$, $\tilde{\mathcal{E}_3}^3(\nu,t)$, $\tilde{\mathcal{H}_1}^3(\nu,t)$, $\tilde{\mathcal{H}_2}^3(\nu,t)$, $\tilde{\mathcal{H}_3}^3(\nu,t)$ in $t = 1/c$. Using the method of Section 4.4 we have computed $\mathbf{T}(\nu)$, $\mathbf{T}^*(\nu)$, $\mathbf{D}(\nu)$ and then using the formula (4.196) we have found Fourier image of the third column of FS $\tilde{\mathbf{G}}(\nu,t)$ in terms of values $\nu = (\nu_1,\nu_2,\nu_3)$ for time $t = 1/c$, i.e we have calculated values of $\tilde{E}_1^3(\nu,t)$, $\tilde{E}_2^3(\nu,t)$, $\tilde{E}_3^3(\nu,t)$, $\tilde{H}_1^3(\nu,t)$, $\tilde{H}_2^3(\nu,t)$, $\tilde{H}_3^3(\nu,t)$ in $t = 1/c$. Some values of $\tilde{E}_j^3(\nu,t)$ and $\tilde{H}_j^3(\nu,t)$, $j = 1,2,3$ and their comparison are given in Table 4.1. and Table 4.2., respectively.

In these table the following notations are used: $\tilde{\mathcal{E}_j}^3(\nu_1,\nu_2,\nu_3,t)$, $\tilde{\mathcal{H}_j}^3(\nu_1,\nu_2,\nu_3,t)$ are values computed by the formula (4.223), (4.224); $\tilde{E}_j^3(\nu_1,\nu_2,\nu_3,t)$ and $\tilde{H}_j^3(\nu_1,\nu_2,\nu_3,t)$ are values of the third column of FS $\tilde{\mathbf{G}}(\nu_1,\nu_2,\nu_3,t)$ computed by our method; $\tilde{E}_j^3 - \tilde{\mathcal{E}_j}^3$ are values of $\tilde{E}_j^3(\nu_1,\nu_2,\nu_3,t) - \tilde{\mathcal{E}_j}^3(\nu_1,\nu_2,\nu_3,t)$ which mean the error between values $\tilde{E}_j^3(\nu_1,\nu_2,\nu_3,t)$ found by our method and exact values $\tilde{\mathcal{E}_j}^3(\nu_1,\nu_2,\nu_3,t)$; $\tilde{H}_j^3 - \tilde{\mathcal{H}_j}^3$ are values of $\tilde{H}_j^3(\nu_1,\nu_2,\nu_3,t) - \tilde{\mathcal{H}_j}^3(\nu_1,\nu_2,\nu_3,t)$ which mean the error between values $\tilde{H}_j^3(\nu_1,\nu_2,\nu_3,t)$ found by our method and exact values $\tilde{\mathcal{H}_j}^3(\nu_1,\nu_2,\nu_3,t)$.

The graphs of functions $\tilde{E}_j^3(z,t)$, $\tilde{\mathcal{E}}_j^3(z,t)$, $j = 1,2,3$ obtained by our method and by formula (4.223) are presented in Figs. 4.68-4.69; the graphs of functions $\tilde{H}_j^3(z,t)$, $\tilde{\mathcal{H}}_j^3(z,t)$, $j = 1,2$ obtained by our method and by formula (4.224) are presented in Figs. 4.70-4.71. Here $\nu_1 = \nu_2 = \nu_3 = z$ and $t = 1/c$.

Table 4.1. The accuracy of computing of electric field (isotropic case) for $t = 1/c$.

ν_1	ν_2	ν_3	$\tilde{E}_1^3$	$\tilde{E}_1^3 - \tilde{\mathcal{E}}_1^3$	$\tilde{E}_2^3$	$\tilde{E}_2^3 - \tilde{\mathcal{E}}_2^3$	$\tilde{E}_3^3$	$\tilde{E}_3^3 - \tilde{\mathcal{E}}_3^3$
10^{-4}	10^{-5}	10^{-6}	-5.7×10^{-13}	-3×10^{-17}	-5.7×10^{-14}	2×10^{-17}	-0.1064	1×10^{-15}
10^{-2}	10^{-3}	10^{-4}	-5.7×10^{-9}	1×10^{-17}	-6×10^{-10}	5×10^{-18}	-0.1064	2×10^{-16}
10^{-1}	10^{-2}	10^{-3}	-5.7×10^{-7}	-1×10^{-18}	-6×10^{-8}	1×10^{-17}	-0.1063	2×10^{-16}
1	1	1	-0.0055	-7×10^{-17}	-0.0055	4×10^{-17}	-0.0954	4×10^{-16}
10^1	10^2	10^3	-5.6×10^{-4}	2×10^{-15}	-0.0056	8×10^{-15}	-0.1058	-7×10^{-16}
10^2	10^3	10^4	-0.0012	1×10^{-14}	-0.0124	-3×10^{-15}	-0.1051	4×10^{-16}
10^4	10^5	10^6	-2.4×10^{-4}	-1×10^{-12}	-0.0024	-1×10^{-11}	-0.1061	1×10^{-11}

Table 4.2. The accuracy of computing of magnetic field (isotropic case) for $t = 1/c$.

ν_1	ν_2	ν_3	$\tilde{H}_1^3$	$\tilde{H}_1^3 - \tilde{\mathcal{H}}_1^3$	$\tilde{H}_2^3$	$\tilde{H}_2^3 - \tilde{\mathcal{H}}_2^3$	$\tilde{H}_3^3 - \tilde{\mathcal{H}}_3^3$
10^{-4}	10^{-5}	10^{-6}	-1.1×10^{-6}	2×10^{-20}	1.1×10^{-5}	-1×10^{-19}	1×10^{-22}
10^{-2}	10^{-3}	10^{-4}	-1.1×10^{-4}	-6×10^{-19}	0.0011	-5×10^{-18}	1×10^{-22}
10^{-1}	10^{-2}	10^{-3}	-0.0011	5×10^{-18}	0.0106	-6×10^{-17}	2×10^{-19}
1	1	1	-0.1008	7×10^{-16}	0.1008	-1×10^{-15}	6×10^{-18}
10^1	10^2	10^3	-0.0286	1×10^{-14}	0.0029	-4×10^{-15}	3×10^{-18}
10^2	10^3	10^4	0.0319	-2×10^{-15}	-0.0032	-1×10^{-14}	1×10^{-15}
10^4	10^5	10^6	-0.0205	-5×10^{-11}	0.002	5×10^{-11}	6×10^{-30}

4.7.2 Simulation of electric and magnetic field in different materials

Example 1. A biaxial crystal. The matrix of the dielectric permittivity $\overline{\overline{\varepsilon}}$ and magnetic permeability $\overline{\overline{\mu}}$ have been taken from Burridge & Qian (2006). They are $\overline{\overline{\varepsilon}} = diag(2.25, 1, 0.25)$, $\overline{\overline{\mu}} = diag(1,1,1)$. We have taken these data similar to Burridge & Qian (2006) for clarity in the graphical illustrations of the behavior of electric and magnetic fields in a biaxial crystal (an electrically anisotropic media). Examples of images of electric and magnetic fields in the bi-axial anisotropic material are presented in Fig.4.72 and Fig.4.73. These figures include several geometrical objects. The object in the center of each picture looks like ellipse. The 3D surfaces plots of $z = E_2^3(x_1, x_2, -\sqrt{1/3}x_1, 1/c)$ and $z = H_2^3(x_1, x_2, -\sqrt{1/3}x_1, 1/c)$ are given in Fig.4.72b and Fig.4.73b. Here the horizontal axes are x_1 and x_2. The vertical axis is the magnitude of $z = E_2^3(x_1, x_2, -\sqrt{1/3}x_1, 1/c)$ and $z = H_2^3(x_1, x_2, -\sqrt{1/3}x_1, 1/c)$, respectively. The different colors correspond to different values of $z = E_2^3(x_1, x_2, -\sqrt{1/3}x_1, 1/c)$ and

$z = H_2^3(x_1, x_2, -\sqrt{1/3}x_1, 1/c)$. Fig.4.72a and Fig.4.73a contain screen shots of 2D level plots of the same surfaces, i.e. view of these surfaces from the top of z axis.

Example 2. A positive uniaxial crystal (sapphire) in the principal symmetry axes. We take the matrix $\overline{\overline{\varepsilon}} = diag(9.4, 9.4, 11.6)$, $\overline{\overline{\mu}} = diag(1,1,1)$. Fig.4.74 shows dynamic of the distribution of the electric field component $z = E_3^3(x_1, x_2, -\sqrt{1/2}x_1 - \sqrt{1/2}x_2, t)$. In Fig.4.74 there is a circle for different times. So we can see how the circle are progressing. Fig.4.74a,b are 2D plots $z = E_3^3(x_1, x_2, -\sqrt{1/2}x_1 - \sqrt{1/2}x_2, t)$ for $t = 1/c, 8/c$, respectively.

Example 3. Monoclinic Dielectric. The matrix $\overline{\overline{\varepsilon}}$ is given by (Yakhno & Yakhno & Kasap (2006))

$$\overline{\overline{\varepsilon}} = \begin{bmatrix} 17.1598 & 13.0178 & 0 \\ 13.0178 & 23.6686 & 0 \\ 0 & 0 & 44.4444 \end{bmatrix}.$$

And we take $\overline{\overline{\mu}} = diag(1,1,1)$. The results of the simulation of the electric and magnetic wave propagation in this monoclinic dielectric are presented in Fig.4.75. In Fig.4.75 there is a ellipse. Inside of this ellipse there is a circle and ellipse with the same center. Fig.4.75a show dynamic of the distribution of the electric field component $E_2^3(x_1, 0, x_3, 6/c)$. Fig.4.75b show dynamic of the distribution of the magnetic field component $H_3^3(x_1, 0, x_3, 6/c)$. The results of the simulations are 2D plots. Here x_1 and x_3 are axis.

Example 4. Triclinic Dielectric. $\overline{\overline{\varepsilon}}$ is given by (Yakhno & Yakhno & Kasap (2006))

$$\overline{\overline{\varepsilon}} = \begin{bmatrix} 30.7929 & -12.7337 & -14.3432 \\ -12.7337 & 5.51479 & 5.86982 \\ -14.3432 & 5.86982 & 6.74556 \end{bmatrix}.$$

And we take $\overline{\overline{\mu}} = diag(1,1,1)$. Fig.4.76a contain screen shot of 2D level plot of $E_2^3(x_1,0,x_3,(0.5)/c)$. Fig.4.76b contain screen shot of 2D level plot of $H_1^3(x_1,x_2,0,(0.5)/c)$.

Example 5. An electrically and magnetically anisotropic medium. The matrix of dielectric permittivity is given by $\overline{\overline{\varepsilon}} = diag(16,25,36)$ and the matrix of magnetic permeability is defined by $\overline{\overline{\mu}} = diag(36,25,16)$ (Yakhno (2008)). The medium is electrically and magnetically anisotropic. The 3D surfaces plots of $z = E_1^3(x_1,0,x_3,50/c)$ and $z = H_2^3(x_1,0,x_3,50/c)$ are given in Fig.4.77b and Fig.4.78b. Here the horizontal axes are x_1 and x_3. The vertical axis is the magnitude of $z = E_1^3(x_1,0,x_3,50/c)$ and $z = H_2^3(x_1,0,x_3,50/c)$, respectively. The different colors correspond to different values of $z = E_1^3(x_1,0,x_3,50/c)$ and $z = H_2^3(x_1,0,x_3,50/c)$. Fig.4.77a and Fig.4.78a contain screen shots of 2D level plots of the same surfaces, i.e. view of these surfaces from the top of z axis. In these figures include ellipse. And the object in the center of Fig.4.77 has the complex configuration.

4.7.3 Analysis of the visualization

The simulation of electric and magnetic fields in anisotropic media by modern computer tools allow us to see dependence between media structures and behavior of electric and magnetic fields. Using the presented method we have generated images of electric and magnetic fields components which are a result of the electromagnetic radiations arising from a pulse dipole with a fixed polarization in different electrically and magnetically anisotropic homogeneous media. The different structures of electrically and magnetically anisotropic media produce different responses of electromagnetic radiation inside these anisotropic media. The various shapes of electric and magnetic waves (different forms of fronts and magnitude

fluctuations) are shown in Examples 1-5.

4.8 Concluding Remarks

In this chapter of the thesis an analytic method for deriving the time-dependent fundamental solution (FS) in a homogeneous, non-dispersive, electrically and magnetically anisotropic media is studied. This method is based on Fourier transformation and some matrix computations. Accuracy of the method is shown by some numerical computations. Computational images of FS in a homogeneous, non-dispersive, different anisotropic materials are given.

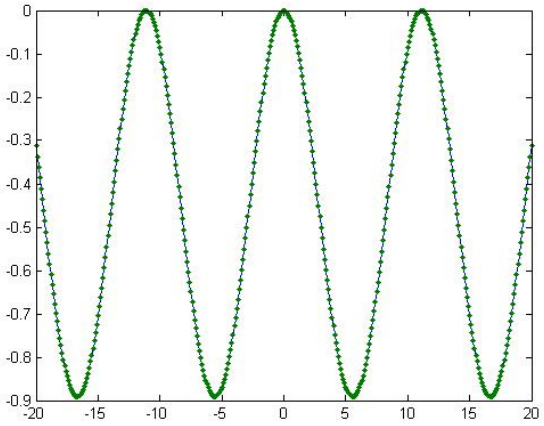

Figure 4.68: Graphs of $\tilde{\mathcal{E}}_j^{\,3}(z,t)$ and $\tilde{E}_j^{\,3}(z,t)$. The dotted line represents $\tilde{E}_j^{\,3}(\nu,t)(z,t)$ at $t = 1/c$ (our method). The continuous line represents $\tilde{\mathcal{E}}_j^{\,3}(z,t)$ at $t = 1/c$ (the explicit formula (4.223)), $j = 1,2$.

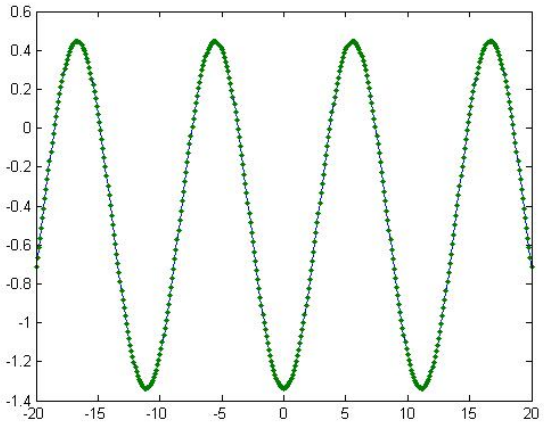

Figure 4.69: Graphs of $\tilde{\mathcal{E}_3}^3(z,t)$ and $\tilde{E_3}^3(z,t)$. The dotted line represents $\tilde{E_3}^3(\nu,t)(z,t)$ at $t = 1/c$ (our method). The continuous line represents $\tilde{\mathcal{E}_3}^3(z,t)$ at $t = 1/c$ (the explicit formula (4.223)).

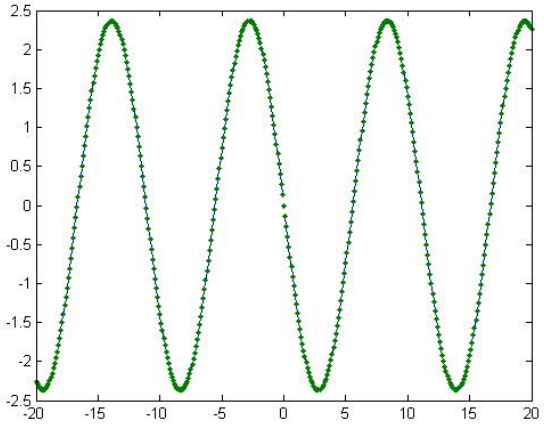

Figure 4.70: Graphs of $\tilde{\mathcal{H}_1}^3(z,t)$ and $\tilde{H_1}^3(z,t)$. The dotted line represents $\tilde{H_1}^3(\nu,t)(z,t)$ at $t = 1/c$ (our method). The continuous line represents $\tilde{\mathcal{H}_1}^3(z,t)$ at $t = 1/c$ (the explicit formula (4.224)).

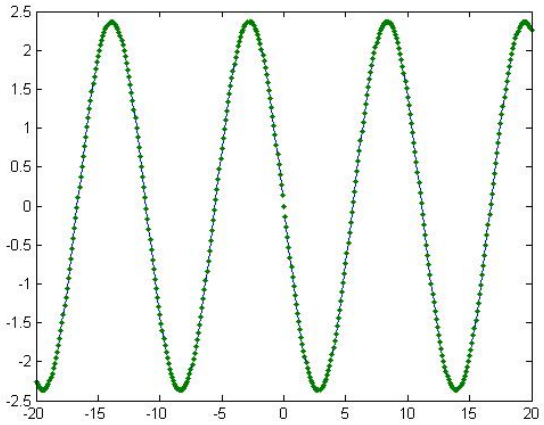

Figure 4.71: Graphs of $\tilde{\mathcal{H}_2}^3(z,t)$ and $\tilde{H_2}^3(z,t)$. The dotted line represents $\tilde{H_2}^3(\nu,t)(z,t)$ at $t = 1/c$ (our method). The continuous line represents $\tilde{\mathcal{H}_2}^3(z,t)$ at $t = 1/c$ (the explicit formula (4.224)).

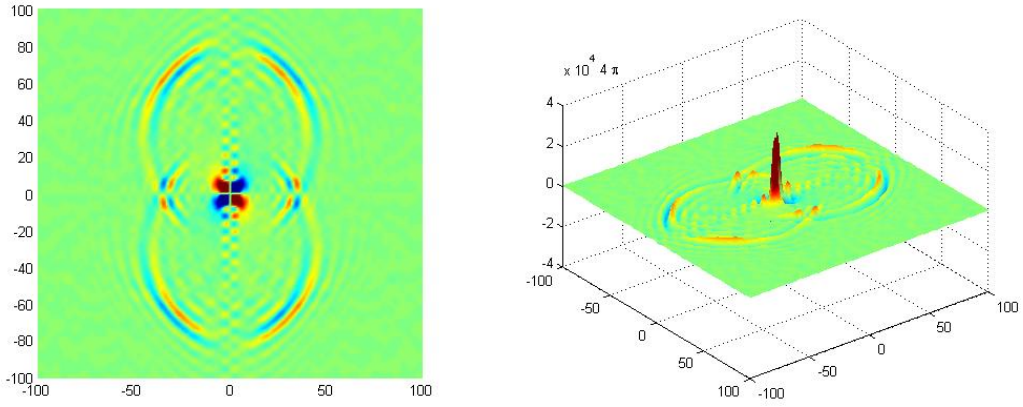

(a) $E_2^3(x_1,x_2,-\sqrt{1/3}x_1,1/c)$ (b) $E_2^3(x_1,x_2,-\sqrt{1/3}x_1,1/c)$

Figure 4.72: 2D and 3D plots of electric field in a biaxial crystal.

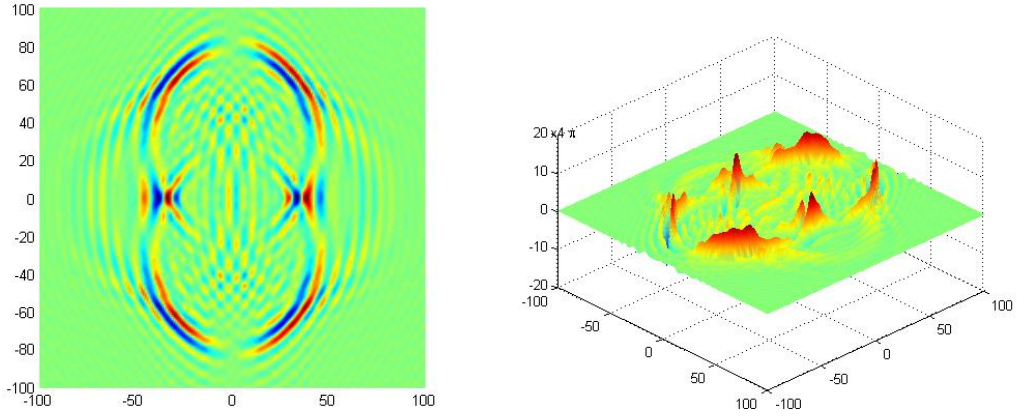

(a) $H_2^3(x_1, x_2, -\sqrt{1/3}x_1, 1/c)$ (b) $H_2^3(x_1, x_2, -\sqrt{1/3}x_1, 1/c)$

Figure 4.73: 2D and 3D plots of magnetic field in a biaxial crystal.

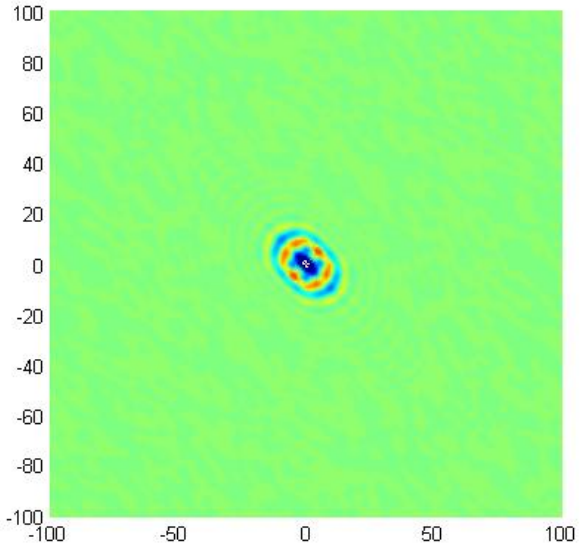

(a) $t = 1/c$

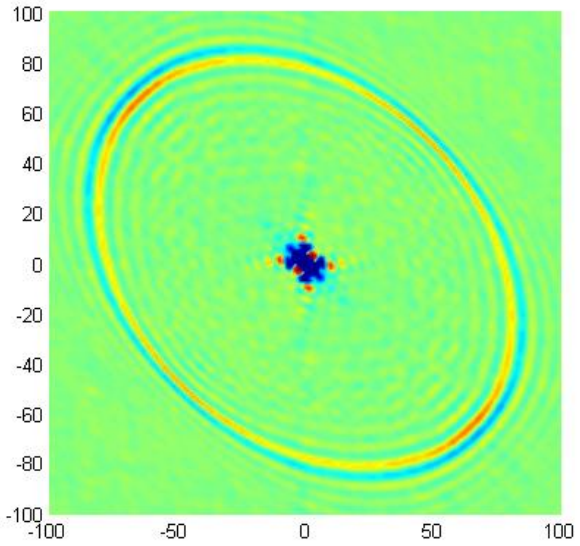

(b) $t = 8/c$

Figure 4.74: 2D plots of electric field in sapphire (uniaxial crystal in principal axes) of $E_3^3(x_1, x_2, -\sqrt{1/2}x_1 - \sqrt{1/2}x_2, t)$, $t = 1/c, 6/c, 8/c$.

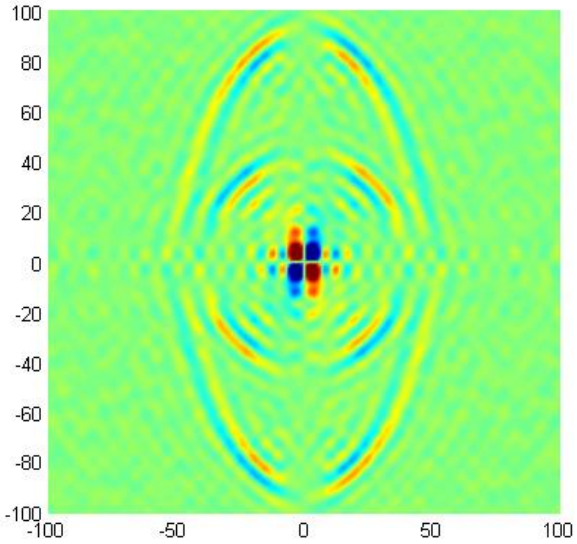

(a) $E_2^3(x_1,0,x_3,6/c)$

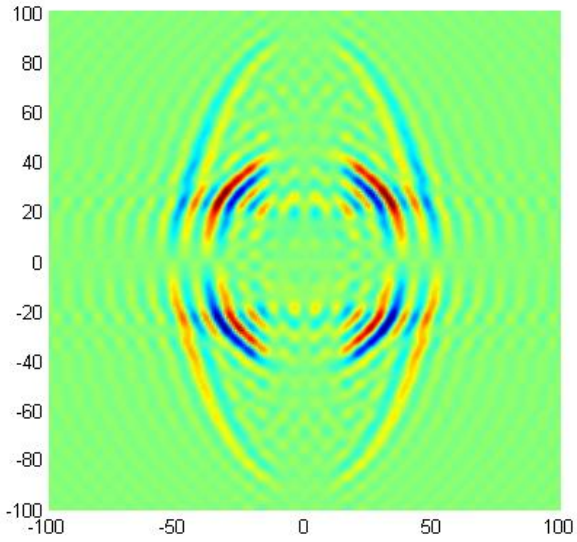

(b) $H_3^3(x_1,0,x_3,6/c)$

Figure 4.75: 2-D level plots of $E_2^3(x_1,0,x_3,6/c)$ and $H_3^3(x_1,0,x_3,6/c)$ for monoclinic dielectric.

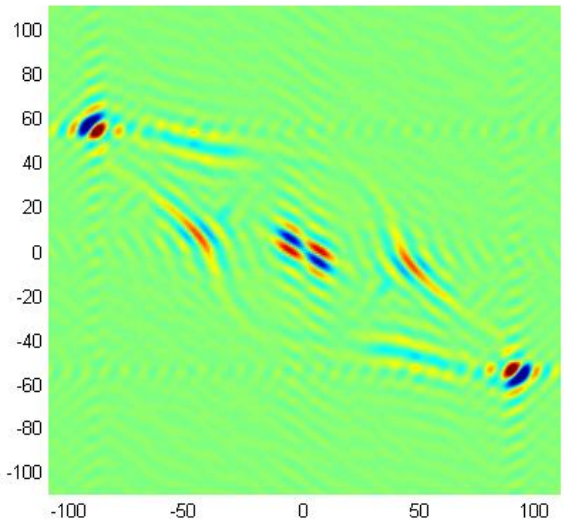

(a) $E_2^3(x_1, 0, x_3, (0.5)/c)$

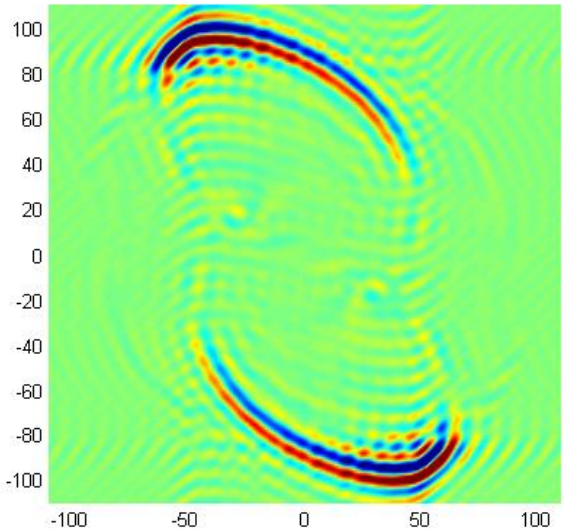

(b) $H_1^3(x_1, x_2, 0, (0.5)/c)$

Figure 4.76: 2D of the electric and magnetic field in electrically triclinic medium.

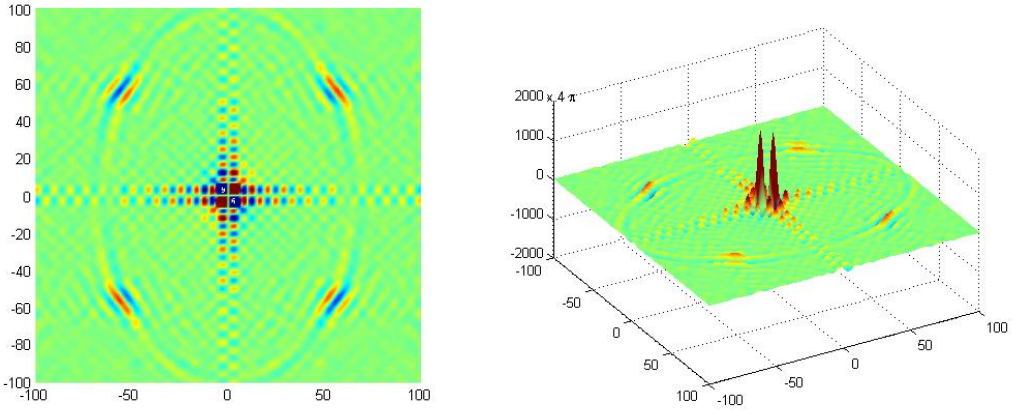

(a) $E_1^3(x_1,0,x_3,50/c)$ (b) $E_1^3(x_1,0,x_3,50/c)$

Figure 4.77: 2D and 3D plots of electric field in an electrically and magnetically anisotropic medium.

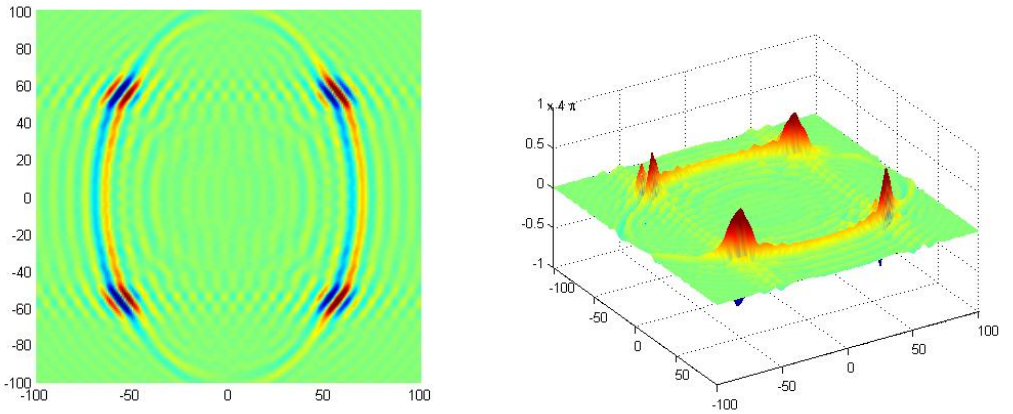

(a) $H_2^3(x_1,0,x_3,50/c)$ (b) $H_2^3(x_1,0,x_3,50/c)$

Figure 4.78: 2D and 3D plots of magnetic field in an electrically and magnetically anisotropic medium.

CHAPTER FIVE
AN ANALYTIC METHOD OF SOLVING IVP FOR ELECTROMAGNETOELASTIC SYSTEM

In this chapter an analytic method for deriving for the initial value problem of linear, inhomogenous, anisotropic dynamics of electromagnetoelasticity (EME) is studied.

5.1 Basic equations for system of electromagnetoelasticity

The basic equations for the linear, inhomogenous, anisotropic dynamics of electromagnetoelasticity (EME) can be expressed by (Yakhno & Merazhov (2000), Dunkin & Eringen (1963))

$$\rho \frac{\partial^2 u_i}{\partial t^2} = \sum_{j=1}^{3} \frac{\partial \sigma_{ij}}{\partial x_j} + f_i, \ i = 1,2,3, \tag{5.226}$$

$$curl_x \mathbf{H} = \frac{\partial D}{\partial t} + \mathbf{J}, \tag{5.227}$$

$$curl_x \mathbf{E} = -\frac{\partial B}{\partial t}, \tag{5.228}$$

$$div_x B = 0, \ div_x D = \rho_e \tag{5.229}$$

Due to the coupling of elastic, electric and magnetic behaviors, the constitutive equations for a inhomogeneous, linear and fully anisotropic magnetoelectroelastic solid are given by (Chen & Shen (2007), Tsai & Wu (2008))

$$\sigma_{ij} = \sum_{k,l=1}^{3} c_{ijkl} \frac{\partial u_k}{\partial x_l} - \sum_{k=1}^{3} e_{kij} E_k - \sum_{k=1}^{3} h_{kij} H_k, \ i,j = 1,2,3, \tag{5.230}$$

$$D_i = \sum_{k=1}^{3} \varepsilon_{ik} E_k + \sum_{k,j=1}^{3} e_{ijk} \frac{\partial u_k}{\partial x_j} + \sum_{k=1}^{3} d_{ik} H_k, \ i = 1,2,3, \tag{5.231}$$

$$B_i = \sum_{k=1}^{3} d_{ik} E_k + \sum_{k,j=1}^{3} h_{ijk} \frac{\partial u_k}{\partial x_j} + \sum_{k=1}^{3} \mu_{ik} H_k, \ i = 1,2,3. \tag{5.232}$$

Let us consider the following initial conditions

$$\begin{aligned} \mathbf{u}(x,t) \mid_{t=0} &= \gamma(x), \ \frac{\partial \mathbf{u}(x,t)}{\partial t} \mid_{t=0} = \psi(x), \\ \mathbf{E}(x,t) \mid_{t=0} &= 0, \ \mathbf{H}(x,t) \mid_{t=0} = 0, \ x \in R^3, \ t \in R, \end{aligned} \tag{5.233}$$

where $x = (x_1, x_2, x_3) \in R^3$ is the space variable, $t \in R$ is the time variable, $\gamma(x), \ \psi(x)$ are given vector functions with components: $\gamma_i = \gamma_i(x), \ \psi_i = \psi_i(x), \ i = 1,2,3$; $\rho = \rho(x_3) > 0$ is the density of the inhomogeneous medium; $\mathbf{u} = (u_1, u_2, u_3)$ is the displacement vector with component $u_i = u_i(x,t), \ i = 1,2,3$; $\rho_e(x,t)$ is the density of electric charges; $\mathbf{E} = (E_1, E_2, E_3)$ and $\mathbf{H} = (H_1, H_2, H_3)$ are the electric and magnetic fields with components: $E_i = E_i(x,t), \ H_i = H_i(x,t), \ i = 1,2,3; \ B = (B_1, B_2, B_3)$ is the magnetic induction with components: $B_i = B_i(x,t); \ D = (D_1, D_2, D_3)$ is the electric displacement with components: $D_i = D_i(x,t), \ i = 1,2,3$; $\sigma_{ij}(x,t)$ are the components of the stress tensor; $\mathbf{J} = (J_1, J_2, J_3)$ is electric current with components $J_i = J_i(x,t)$; $\mathbf{f} = (f_1, f_2, f_3)$ is external force with components $f_i = f_i(x,t)$. $c_{ijkl} = c_{ijkl}(x_3)$ are the elastic moduli of the medium; $e_{kij} = e_{kij}(x_3)$ are the piezoelectric moduli of the medium; $h_{kij} = h_{kij}(x_3)$ are the piezomagnetic moduli of the medium; $\varepsilon_{ij}(x_3)$ are the dielectric moduli of the medium; $d_{ki}(x_3)$ are the electromagnetic moduli of the medium; $\mu_{ik}(x_3)$ are moduli of magnetic permeability of the medium. These coefficients satisfy following symmetric properties (Diaz & Saez & Sanchez & Zhang (2008), Wang & Mai (2004))

$$\begin{aligned} c_{ijkl} &= c_{jikl} = c_{ijlk} = c_{klij}, \ e_{kij} = e_{kji}, \ h_{kij} = h_{kji}, \\ d_{ki} &= d_{ik}, \mu_{ki} = \mu_{ik}, \varepsilon_{ij} = \varepsilon_{ji}. \end{aligned} \tag{5.234}$$

Using the symmetry properties (5.234) it is convenient to describe the elastic moduli in terms of a 6×6 matrix according to the following conventions relating pairs of indices (ij) and (kl) to single indices α and β:

$$\begin{gathered}(11) \leftrightarrow 1,\ (22) \leftrightarrow 2,\ (33) \leftrightarrow 3, \\ (23),(32) \leftrightarrow 4,\ (13),(31) \leftrightarrow 5\ (12),(21) \leftrightarrow 6.\end{gathered} \tag{5.235}$$

The obtained matrix $\mathbf{C} = (c_{\alpha\beta})_{6\times 6}$ of all moduli, where $\alpha = (ij)$, $\beta = (kl)$, is symmetric. Similarly the matrices

$$\mathcal{E} = (\varepsilon_{ij}(x_3)),\ \mathcal{D} = (d_{ij}(x_3)),\ \mathcal{M} = (\mu_{ij}(x_3)),\ i,j = 1,2,3,$$

are symmetric. And $\mathbf{C}$, $\mathcal{E}$, $\mathcal{M}$ are positive definite matrices (Yakhno & Merazhov (2000), Wang & Mai (2004), Diaz & Saez & Sanchez & Zhang (2008)). And also $\mathbf{C}^{-1}$ which is the inverse matrix of $\mathbf{C}$ is positive definite.

The electric charges and current have to satisfy the conservation law of charges

$$\frac{\partial \rho_e}{\partial t} + div_x \mathbf{J} = 0. \tag{5.236}$$

In this chapter we also suppose that

$$\mathbf{J} = 0,\ \rho_e = 0,\ \texttt{for}\ \ t = 0. \tag{5.237}$$

Remark 1. The equations of (5.227)-(5.228) under conditions (5.233)-(5.237) imply the equalities of (5.229) (we assume here that (5.236) is satisfied).

5.2 Reduction of IVP for Electromagnetoelastic System to IVP for a First-Order Symmetric Hyperbolic System

Let

$$U_i = \frac{\partial u_i}{\partial t},\ i = 1,2,3,\ \tau_\alpha = \sum_{k,l=1}^{3} c_{\alpha kl}\frac{\partial u_l}{\partial x_k},\ \ \alpha = 1,2,...,6. \tag{5.238}$$

Using the symmetry properties of the elastic moduli, Eq.(5.238) and the rule (5.235) we can write for $\alpha = 1,2,3,4,5,6$

$$\frac{\partial \tau_\alpha}{\partial t} = c_{\alpha 1}\frac{\partial U_1}{\partial x_1} + c_{\alpha 6}\frac{\partial U_1}{\partial x_2} + c_{\alpha 5}\frac{\partial U_1}{\partial x_3} + c_{\alpha 6}\frac{\partial U_2}{\partial x_1}$$

$$+c_{\alpha 2}\frac{\partial U_2}{\partial x_2} + c_{\alpha 4}\frac{\partial U_2}{\partial x_3} + c_{\alpha 5}\frac{\partial U_3}{\partial x_1} + c_{\alpha 4}\frac{\partial U_3}{\partial x_2} + c_{\alpha 3}\frac{\partial U_3}{\partial x_3}. \tag{5.239}$$

Let us define

$$\mathbf{Y} = (\frac{\partial U_1}{\partial x_1}, \frac{\partial U_2}{\partial x_2}, \frac{\partial U_3}{\partial x_3}, (\frac{\partial U_3}{\partial x_2} + \frac{\partial U_2}{\partial x_3}), (\frac{\partial U_3}{\partial x_1} + \frac{\partial U_1}{\partial x_3}), (\frac{\partial U_2}{\partial x_1} + \frac{\partial U_1}{\partial x_2}))$$

and

$$\tau = (\tau_1, \tau_2, \tau_3, \tau_4, \tau_5, \tau_6).$$

Eq.(5.239) can be written in the form

$$\frac{\partial \tau}{\partial t} = \mathbf{C}\mathbf{Y}, \tag{5.240}$$

where $\mathbf{C} = (c_{\alpha\beta})_{6\times 6}$. Multiplying both sides by the inverse of $\mathbf{C}$, denoted $\mathbf{C}^{-1}$, we find

$$\mathbf{C}^{-1}\frac{\partial \tau}{\partial t} - \mathbf{Y} = 0. \tag{5.241}$$

Letting

$$\mathbf{V} = (U_1, U_2, U_3, T_1, T_2, T_3, T_4, T_5, T_6, E_1, E_2, E_3, H_1, H_2, H_3),$$

(5.241) can be written in the form

$$\mathbf{M}_0 \frac{\partial \mathbf{V}}{\partial t} + \sum_{j=1}^{3} \mathbf{M}_j \frac{\partial \mathbf{V}}{\partial x_j} = 0, \tag{5.242}$$

where $0_{m,n}$ is the zero matrix which has the order $m \times n$, here m is the number of lines, n is the number of columns.

$$\mathbf{M}_0 = \begin{bmatrix} 0_{6,3} & \mathbf{C}^{-1} & 0_{6,6} \end{bmatrix}; \ \mathbf{M}_j = \begin{bmatrix} (\mathbf{A}_j^1)^* & 0_{6,6} & 0_{6,6} \end{bmatrix}, \ j = 1,2,3,$$

$$\mathbf{A}_1^1 = \begin{bmatrix} -1 & 0 & 0 & 0 & 0 & 0 \\ 0 & 0 & 0 & 0 & 0 & -1 \\ 0 & 0 & 0 & 0 & -1 & 0 \end{bmatrix}, \ \mathbf{A}_2^1 = \begin{bmatrix} 0 & 0 & 0 & 0 & 0 & -1 \\ 0 & -1 & 0 & 0 & 0 & 0 \\ 0 & 0 & 0 & -1 & 0 & 0 \end{bmatrix},$$

$$\mathbf{A}_3^1 = \begin{bmatrix} 0 & 0 & 0 & 0 & -1 & 0 \\ 0 & 0 & 0 & -1 & 0 & 0 \\ 0 & 0 & -1 & 0 & 0 & 0 \end{bmatrix}. \tag{5.243}$$

Here $*$ denotes the transposition of sign. Let us consider Eq.(5.230). Using the symmetry properties of elastic moduli, piezoelectric moduli, piezomagnetic moduli and the rule (5.235), Eq.(5.230) can be written in the following form for $\alpha =$

$1,2,3,4,5,6$

$$\begin{aligned}\sigma_\alpha &= c_{\alpha1}\frac{\partial u_1}{\partial x_1}+c_{\alpha6}\frac{\partial u_1}{\partial x_2}+c_{\alpha5}\frac{\partial u_1}{\partial x_3}+c_{\alpha6}\frac{\partial u_2}{\partial x_1}+c_{\alpha2}\frac{\partial u_2}{\partial x_2}+c_{\alpha4}\frac{\partial u_2}{\partial x_3}\\ &+ c_{\alpha5}\frac{\partial u_3}{\partial x_1}+c_{\alpha4}\frac{\partial u_3}{\partial x_2}+c_{\alpha3}\frac{\partial u_3}{\partial x_3}-e_{1\alpha}E_1\\ &- e_{2\alpha}E_2-e_{3\alpha}E_3-h_{1\alpha}H_1-h_{2\alpha}H_2-h_{3\alpha}H_3\end{aligned}$$

or

$$\sigma_\alpha=\tau_\alpha-e_{1\alpha}E_1-e_{2\alpha}E_2-e_{3\alpha}E_3-h_{1\alpha}H_1-h_{2\alpha}H_2-h_{3\alpha}H_3. \tag{5.244}$$

The left-hand side of (5.226) can be written in the vector form

$$\rho\frac{\partial^2\mathbf{u}}{\partial t^2}=\rho\frac{\partial\mathbf{U}}{\partial t}. \tag{5.245}$$

Now consider the term $\sum\limits_{j=1}^{3}\frac{\partial\sigma_{ij}}{\partial x_j}$ on the right-hand side of (5.226). Applying rule (5.235) for $i=1,2,3$ gives

$$\sum_{j=1}^{3}\frac{\partial\sigma_{1j}}{\partial x_j}=\frac{\partial\sigma_{11}}{\partial x_1}+\frac{\partial\sigma_{12}}{\partial x_2}+\frac{\partial\sigma_{13}}{\partial x_3}=\frac{\partial\sigma_1}{\partial x_1}+\frac{\partial\sigma_6}{\partial x_2}+\frac{\partial\sigma_5}{\partial x_3}, \tag{5.246}$$

$$\sum_{j=1}^{3}\frac{\partial\sigma_{2j}}{\partial x_j}=\frac{\partial\sigma_{21}}{\partial x_1}+\frac{\partial\sigma_{22}}{\partial x_2}+\frac{\partial\sigma_{23}}{\partial x_3}=\frac{\partial\sigma_6}{\partial x_1}+\frac{\partial\sigma_2}{\partial x_2}+\frac{\partial\sigma_4}{\partial x_3}, \tag{5.247}$$

$$\sum_{j=1}^{3}\frac{\partial\sigma_{3j}}{\partial x_j}=\frac{\partial\sigma_{31}}{\partial x_1}+\frac{\partial\sigma_{32}}{\partial x_2}+\frac{\partial\sigma_{33}}{\partial x_3}=\frac{\partial\sigma_5}{\partial x_1}+\frac{\partial\sigma_4}{\partial x_2}+\frac{\partial\sigma_3}{\partial x_3}. \tag{5.248}$$

Substituting (5.244) into (5.246)-(5.248) and using (5.245), (5.226) can be written as

$$\mathbf{R}_0\frac{\partial\mathbf{V}}{\partial t}+\sum_{j=1}^{3}\mathbf{R}_j\frac{\partial\mathbf{V}}{\partial x_j}+\bar{\mathbf{Q}}\mathbf{V}=\mathbf{f}, \tag{5.249}$$

where $\mathbf{I}_{m,m}$ is the identity matrix of the order $m \times m$.

$$\mathbf{R}_0 = \left[\begin{array}{ccc} \rho\mathbf{I}_{3,3} & 0_{3,6} & 0_{3,6} \end{array} \right];\ \mathbf{R}_j = \left[\begin{array}{cccc} 0_{3,3} & (\mathbf{A}_j^1) & (\mathbf{A}_j^2) & (\mathbf{A}_j^3) \end{array} \right],\ j = 1,2,3,$$

$$\mathbf{A}_1^2 = \left[\begin{array}{ccc} e_{11} & e_{21} & e_{31} \\ e_{16} & e_{26} & e_{36} \\ e_{15} & e_{25} & e_{35} \end{array} \right], \mathbf{A}_2^2 = \left[\begin{array}{ccc} e_{16} & e_{26} & e_{36} \\ e_{12} & e_{22} & e_{32} \\ e_{14} & e_{24} & e_{34} \end{array} \right], \mathbf{A}_3^2 = \left[\begin{array}{ccc} e_{15} & e_{25} & e_{35} \\ e_{14} & e_{24} & e_{34} \\ e_{13} & e_{23} & e_{33} \end{array} \right],$$

$$\mathbf{A}_1^3 = \left[\begin{array}{ccc} h_{11} & h_{21} & h_{31} \\ h_{16} & h_{26} & h_{36} \\ h_{15} & h_{25} & h_{35} \end{array} \right], \mathbf{A}_2^3 = \left[\begin{array}{ccc} h_{16} & h_{26} & h_{36} \\ h_{12} & h_{22} & h_{32} \\ h_{14} & h_{24} & h_{34} \end{array} \right], \mathbf{A}_3^3 = \left[\begin{array}{ccc} h_{15} & h_{25} & h_{35} \\ h_{14} & h_{24} & h_{34} \\ h_{13} & h_{23} & h_{33} \end{array} \right];$$

$$\bar{\mathbf{Q}} = \left[\begin{array}{ccc} 0_{3,9} & \mathbf{Q}_1 & \mathbf{Q}_2 \end{array} \right],\ \mathbf{Q}_1 = \frac{d}{dx_3}\mathbf{A}_3^2,\ \mathbf{Q}_2 = \frac{d}{dx_3}\mathbf{A}_3^3. \tag{5.250}$$

Let us consider (5.227). Taking derivative with respect to t of (5.231) we obtain

$$\begin{aligned} \frac{\partial D_i}{\partial t} &= (\varepsilon_{i1}, \varepsilon_{i2}, \varepsilon_{i3})\frac{\partial \mathbf{E}}{\partial t} + (e_{i1}, e_{i6}, e_{i5})\frac{\partial \mathbf{U}}{\partial x_1} + (e_{i6}, e_{i2}, e_{i4})\frac{\partial \mathbf{U}}{\partial x_2} \\ &+ (e_{i5}, e_{i4}, e_{i3})\frac{\partial \mathbf{U}}{\partial x_3} + (d_{i1}, d_{i2}, d_{i3})\frac{\partial \mathbf{H}}{\partial t}. \end{aligned} \tag{5.251}$$

Substituting this equality into (5.227), we obtain

$$\mathbf{S}_0\frac{\partial \mathbf{V}}{\partial t} + \sum_{j=1}^{3} \mathbf{S}_j\frac{\partial \mathbf{V}}{\partial x_j} = -\mathbf{J}, \tag{5.252}$$

where

$$\mathbf{S}_0 = \left[\begin{array}{cccc} 0_{3,3} & 0_{3,6} & \mathcal{E} & \mathcal{D} \end{array} \right];\ \mathbf{S}_j = \left[\begin{array}{cccc} (\mathbf{A}_j^2)^* & 0_{3,6} & 0_{3,3} & (\mathbf{A}_j^4) \end{array} \right],\ j = 1,2,3;$$

$$\mathbf{A}_1^4 = \begin{bmatrix} 0 & 0 & 0 \\ 0 & 0 & 1 \\ 0 & -1 & 0 \end{bmatrix}, \mathbf{A}_2^4 = \begin{bmatrix} 0 & 0 & -1 \\ 0 & 0 & 0 \\ 1 & 0 & 0 \end{bmatrix}, \mathbf{A}_3^4 = \begin{bmatrix} 0 & 1 & 0 \\ -1 & 0 & 0 \\ 0 & 0 & 0 \end{bmatrix}. \quad (5.253)$$

Similarly let us consider (5.228). Taking derivative with respect to t of (5.232) we obtain in the following form

$$\begin{aligned} \frac{\partial B_i}{\partial t} &= (d_{i1}, d_{i2}, d_{i3})\frac{\partial \mathbf{E}}{\partial t} + (h_{i1}, h_{i6}, h_{i5})\frac{\partial \mathbf{U}}{\partial x_1} + (h_{i6}, h_{i2}, h_{i4})\frac{\partial \mathbf{U}}{\partial x_2} \\ &+ (h_{i5}, h_{i4}, h_{i3})\frac{\partial \mathbf{U}}{\partial x_3} + (\mu_{i1}, \mu_{i2}, \mu_{i3})\frac{\partial \mathbf{H}}{\partial t}. \end{aligned} \quad (5.254)$$

Substituting this equality into (5.228), we obtain

$$\mathbf{N}_0 \frac{\partial \mathbf{V}}{\partial t} + \sum_{j=1}^{3} \mathbf{N}_j \frac{\partial \mathbf{V}}{\partial x_j} = 0, \quad (5.255)$$

where $\mathcal{M} = (\mu_{ij}),\ i, j = 1,2,3,$

$$\mathbf{N}_0 = \begin{bmatrix} 0_{3,3} & 0_{3,6} & \mathcal{D} & \mathcal{M} \end{bmatrix};\ \mathbf{N}_j = \begin{bmatrix} (\mathbf{A}_j^3)^* & 0_{3,6} & (\mathbf{A}_j^4)^* & 0_{3,3} \end{bmatrix},\ j = 1,2,3;$$

Combining (5.242), (5.249), (5.252) and (5.255), we obtain the matrix representation of EME in the form

$$\mathbf{A}_0 \frac{\partial \mathbf{V}}{\partial t} + \sum_{j=1}^{3} \mathbf{A}_j \frac{\partial \mathbf{V}}{\partial x_j} + \mathbf{Q}\mathbf{V} = \mathbf{F}. \quad (5.256)$$

Here

$$\mathbf{V} = (U_1, U_2, U_3, \tau_1, \tau_2, \tau_3, \tau_4, \tau_5, \tau_6, E_1, E_2, E_3, H_1, H_2, H_3),$$

$$\mathbf{A}_j = \begin{bmatrix} 0_{3,3} & \mathbf{A}_j^1 & \mathbf{A}_j^2 & \mathbf{A}_j^3 \\ (\mathbf{A}_j^1)^* & 0_{6,6} & 0_{6,3} & 0_{6,3} \\ (\mathbf{A}_j^2)^* & 0_{3,6} & 0_{3,3} & \mathbf{A}_j^4 \\ (\mathbf{A}_j^3)^* & 0_{3,6} & (\mathbf{A}_j^4)^* & 0_{3,3} \end{bmatrix}, \ j = 1,2,3; \ \mathbf{A}_0 = \begin{bmatrix} \rho(x_3)\mathbf{I}_{3,3} & 0_{3,6} & 0_{3,6} \\ 0_{6,3} & \mathbf{C}^{-1} & 0_{6,6} \\ 0_{6,3} & 0_{6,6} & \mathbf{L} \end{bmatrix},$$

$$\mathbf{L} = \begin{bmatrix} \mathcal{E} & \mathcal{D} \\ \mathcal{D} & \mathcal{M} \end{bmatrix}; \ \mathbf{Q} = \begin{bmatrix} \bar{\mathbf{Q}} \\ 0_{12,15} \end{bmatrix}; \ \mathbf{F} = (\mathbf{f}, 0_{6,1}, -\mathbf{J}, 0_{3,1})^*.$$

The matrices $\mathbf{A}_j^k$, $j = 1,2,3$, $k = 1,2,3,4$, and $\bar{\mathbf{Q}}$ are defined by (5.243), (5.250), (5.253).

Since the matrix $\mathbf{L}$ is positive definite (Karamany (2009)), $\rho > 0$, the inverse matrix $\mathbf{C}^{-1}$ is positive definite $\mathbf{A}_0(x_3)$ is also positive definite and symmetric matrix. And $\mathbf{A}_i(x_3)$, $i = 1,2,3$, are symmetric matrices.

The initial conditions (5.233) can be written as

$$\mathbf{V}(x,t)\,|_{t=0} \ = \ \mathbf{V}^0(x), \ x \in R^3, \ t \in R, \tag{5.257}$$

where

$$\begin{aligned} \mathbf{V}^0(x) &= (\psi_1, \psi_2, \psi_3, \tau_1^0, \tau_2^0, \tau_3^0, \tau_4^0, \tau_5^0, \tau_6^0, 0, 0, 0, 0, 0, 0)^*, \\ \tau_\alpha^0 &= \sum_{k,l=1}^{3} c_{\alpha kl} \frac{\partial \gamma_l}{\partial x_k}, \ \alpha = 1,2,...,6. \end{aligned}$$

Assumptions

In this chapter we suppose that

1. There exits a constant $\rho_0 > 0$ such that for $x_3 \in (-\infty, \infty)$, $\rho(x_3) \geq \rho_0 > 0$.

2 . There exits a constant $c_0 > 0$ such that for the inverse matrix $\mathbf{C}^{-1}(x_3)$ and $x_3 \in (-\infty, \infty)$ and for every nonzero vector $\eta \in R^6$, $< \mathbf{C}^{-1}(x_3)\eta, \eta > \geq c_0|\eta|^2$.

3 . There exits a constant $L_0 > 0$ such that for all $x_3 \in (-\infty, \infty)$ and for every nonzero vector $\eta \in R^6$ the matrix

$$\mathbf{L}(x_3) = \begin{bmatrix} \mathcal{E}(x_3) & \mathcal{D}(x_3) \\ \mathcal{D}(x_3) & \mathcal{M}(x_3) \end{bmatrix}$$

satisfies $< \mathbf{L}(x_3)\eta, \eta > \geq L_0|\eta|^2$.

4 . There exit constants $a_{23} > 0$ and $a_{33} > 0$ such that for $x_3 \in (-\infty, \infty)$

$$| (\mathbf{A}_{23}(x_3))_{ij} | \leq a_{23}, \ | (\mathbf{A}_3^3(x_3))_{ij} | \leq a_{33}, \ \ i, j = 1, ..., 15.$$

5. Let T be a given positive number; $a_0 = max\{\rho_0, c_0, L_0\}$, $a_3 = max\{a_{23}, a_{33}\}$, $M = \frac{a_3}{a_0}$

$$\Delta(M,T) = \{(x_3,t); \ 0 \leq t \leq T, \ -M(T-t) \leq x_3 \leq M(T-t)\}. \qquad (5.258)$$

6.The function $\rho(x_3) \in C^2([-MT, MT]) \cap C(R)$; elements of matrices $\mathcal{E}(x_3), \mathcal{M}(x_3), \mathcal{D}(x_3), \mathbf{C}^{-1}(x_3)$, $\mathbf{A}_3^2$ and $\mathbf{A}_3^3$ from the class $C^2([-MT, MT]) \cap C(R)$; elements of matrices $\mathbf{A}_1^2$, $\mathbf{A}_2^2$, $\mathbf{A}_1^3$ and $\mathbf{A}_2^3$ from the class $C^1([-MT, MT])$.

7. $\tilde{\mathbf{f}}(\nu, x_3, t)$, $\tilde{\mathbf{J}}(\nu, x_3, t)$, $\tilde{\gamma}(\nu, x_3)$, $\tilde{\psi}(\nu, x_3)$ be Fourier images with respect to x_1, x_2 of

$\mathbf{f}(x,t)$, $\mathbf{J}(x,t)$, $\gamma(x)$, $\psi(x)$, respectively.

$$\tilde{\mathbf{f}}(\nu,x_3,t),\ \tilde{J}(\nu,x_3,t) \in C_0(R^2,C^1(\Delta(M,T))),$$
$$\tilde{\gamma}(\nu,x_3) \in C_0(R^2,C^2([-MT,MT])),\ \tilde{\psi}(\nu,x_3) \in C_0(R^2,C^1([-MT,MT])),$$

where $C_0(R^2)$ denotes the class of all functions from $C(R^2)$ with compact support. $C_0(R^2;C^1(\Delta(M,T)))$ is a class of all continuous mapping of $\nu \in R^2$ into the class $C^1(\Delta(M,T))$ of functions $(x_3,t) \in \Delta(M,T)$ and these functions have finite support with respect to ν. $C_0(R^2;C^2(\Delta(M,T)))$ is a class of all continuous mapping of $\nu \in R^2$ into the class $C^2(\Delta(M,T))$ of functions $(x_3,t) \in \Delta(M,T)$ and have finite support with respect to ν.

For any fixed $x_3 \in [-MT,MT]$ functions $\tilde{\gamma}(\nu,x_3)$, $\tilde{\psi}(\nu,x_3)$ have finite supports lying in S_A; for any fixed $(x_3,t) \in \Delta(M,T)$ functions $\tilde{\mathbf{f}}(\nu,x_3,t),\tilde{\mathbf{J}}(\nu,x_3,t)$ have finite supports lying in S_A. Here

$$S_A = \{\nu \in R^2;\ \nu_1^2+\nu_2^2 \le A^2\},$$

and A is a positive number.

5.3 Diagonalization of matrices $\mathbf{A}_0(x_3)$ and $\mathbf{A}_3(x_3)$ simulteneously

In this section we will find nonsingular matrix $\mathbf{T}(x_3)$ and diagonal $\mathbf{D}(x_3)$ satisfying the following relations (Goldberg (1992))

$$\mathbf{T}^*(x_3)\mathbf{A}_0(x_3)\mathbf{T}(x_3) = \mathbf{I}, \mathbf{T}^*(x_3)\mathbf{A}_3(x_3)\mathbf{T}(x_3) = \mathbf{D}(x_3), \tag{5.259}$$

where $\mathbf{I}$ is the identity matrix, $\mathbf{T}^*(x_3)$ is the transposed matrix to $\mathbf{T}(x_3)$.

Since $\mathbf{A}_0(x_3)$ is the symmetric and positive definite matrix and we can find a matrix

$\mathbf{S}(x_3)$ such that $\mathbf{S}^2 = \mathbf{A}_0$. $\mathbf{S}(x_3)$ is denoted as $\mathbf{A}_0^{1/2}(x_3)$. The inverse matrix to $\mathbf{A}_0^{1/2}(x_3)$ is denoted as $\mathbf{A}_0^{-1/2}(x_3)$, i.e. $\mathbf{A}_0^{-1/2}(x_3) = (\mathbf{A}_0^{1/2})^{-1}(x_3)$. There are the following properties of $\mathbf{A}_0^{-1/2}(x_3)$

$$\mathbf{A}_0^{-1/2}(x_3) = \mathbf{P}(x_3)\mathbf{S}^{-1/2}(x_3)\mathbf{P}^*(x_3), \tag{5.260}$$

where $\mathbf{P}(x_3)$ is an orthogonal matrix and $\mathbf{S}(x_3)$ is a diagonal matrix. The diagonal element of $\mathbf{S}(x_3)$ are the eigenvalues of $\mathbf{A}_0(x_3)$ and the columns of $\mathbf{P}(x_3)$ are the corresponding eigenvectors. Using the facts we have

$$\mathbf{A}_0^{1/2}(x_3) = \mathbf{P}(x_3)\mathbf{S}^{1/2}(x_3)\mathbf{P}^{-1}(x_3).$$

Let us consider the matrix $\mathbf{A}_0^{-1/2}(x_3)\mathbf{A}_3(x_3)\mathbf{A}_0^{-1/2}(x_3)$. Using the symmetric property we can write

$$\mathbf{A}_0^{-1/2}(x_3)\mathbf{A}_3(x_3)\mathbf{A}_0^{-1/2}(x_3) = \mathbf{Z}(x_3)\mathbf{D}(x_3)\mathbf{Z}^{-1}(x_3),$$

where the orthogonal matrix $\mathbf{Z}(x_3)$ consists of eigenvectors and the diagonal matrix $\mathbf{D}(x_3)$ consists of eigenvalues of given matrix. From the last equality we have

$$\mathbf{Z}^{-1}(x_3)\mathbf{A}_0^{-1/2}(x_3)\mathbf{A}_3(x_3)\mathbf{A}_0^{-1/2}(x_3)\mathbf{Z}(x_3) = \mathbf{D}(x_3).$$

For $\mathbf{T}(x_3) = \mathbf{A}_0^{-1/2}(x_3)\mathbf{Z}(x_3)$, we can say that there exists the matrix $\mathbf{T}$ such that (5.259) are satisfied.

Properties of matrices $\mathbf{A}_0$, $\mathbf{D}$, $\mathbf{T}$:

Property 1. Let $a_0 = max\{\rho_0, c_0, L_0\}$. Then for $x_3 \in (-\infty, \infty)$ and every nonzero vector $\eta \in R^{15} < \mathbf{A}_0(x_3)\eta, \eta > \geq a_0|\eta|^2$.

Proof of property 1. Proof of property 1 follows from assumptions 1-3.

Property 2. Let $x_3 \in R$ and $\mathbf{A}_0^{-1/2}$ be defined in (5.260). Then

$$\| \mathbf{A}_0^{-1/2} \| \leq \| \mathbf{S}^{-1/2} \| \leq \frac{1}{\sqrt{a_0}}, \tag{5.261}$$

where

$$\| \mathbf{A}_0 \| = \max_{i,k=1,...,15,\ x_3 \in (-\infty,\infty)} | (\mathbf{A}_0)_{i,k}(x_3) | . \tag{5.262}$$

Proof of property 2. If $v_j(x_3),\ j = 1,2,...,15$, are eigenfunctions of $\mathbf{A}_0(x_3)$ and $\lambda_j,\ j = 1,2,...,15$, are corresponding eigenvalues then

$$(\mathbf{A}_0)_j(x_3)v_j(x_3) = \lambda_j(x_3)v_j(x_3).$$

And using property 1 we have

$$< (\mathbf{A}_0)_j(x_3)v_j(x_3), v_j(x_3) > \geq a_0|v_j(x_3)|^2,\ \ j = 1,2,...,15,$$

and

$$\lambda_j(x_3)|v_j(x_3)|^2 \geq a_0|v_j(x_3)|^2,\ \ j = 1,2,...,15,$$

$$\frac{1}{\sqrt{\lambda_j(x_3)}} \leq \frac{1}{\sqrt{a_0}},\ \ j = 1,2,...,15.$$

and so

$$\| \mathbf{A}_0^{-1/2} \| \leq \| \mathbf{S}^{-1/2} \| \leq \frac{1}{\sqrt{a_0}}. \tag{5.263}$$

Property 3. If $x_3 \in R$ and $\mathbf{D}(x_3)$ is defined by (5.259). Then

$$\| \mathbf{D} \| \leq \frac{a_3}{a_0},$$

where $\| . \|$ is defined by (5.262).

Proof of property 3. Since $\mathbf{A}_0$ is the symmetric and positive definite matrix and $\mathbf{A}_3$ is the symmetric matrix we have

$$\mathbf{Z}^{-1}(x_3)\mathbf{A}_0^{-1/2}(x_3)\mathbf{A}_3(x_3)\mathbf{A}_0^{-1/2}(x_3)\mathbf{Z}(x_3) = \mathbf{D}(x_3).$$

From assumption 4 we have

$$\| \mathbf{A}_3 \| \leq a_3.$$

And

$$\begin{aligned} \| \mathbf{D} \| &\leq \| \mathbf{Z}^{-1} \| \| \mathbf{A}_0^{-1/2} \| \| \mathbf{A}_3 \| \| \mathbf{A}_0^{-1/2} \| \| \mathbf{Z} \|, \\ &\leq 1.\frac{1}{\sqrt{a_0}}.a_3.\frac{1}{\sqrt{a_0}}.1 \leq \frac{a_3}{a_0}. \end{aligned}$$

Property 4. If $x_3 \in R$ and $\mathbf{T}(x_3)$ is defined by (5.259). Then

$$\| \mathbf{T} \| \leq \frac{1}{\sqrt{a_0}},$$

where $\| . \|$ is defined by (5.262).

Proof of property 4. Using $\mathbf{T}(x_3) = \mathbf{A}_0^{-1/2}(x_3)\mathbf{Z}(x_3)$ we have

$$\begin{aligned} \| \mathbf{T} \| &\leq \| \mathbf{A}_0^{-1/2} \| \| \mathbf{Z} \| \\ &\leq \frac{1}{\sqrt{a_0}}.1 \leq \frac{1}{\sqrt{a_0}}. \end{aligned}$$

5.4 IVP (5.256)-(5.257) in terms of the Fourier transform and its reduction to a vector integral equation

In this section IVP (5.256)-(5.257) is written in terms of the Fourier images with respect to the space variables x_1, x_2, we denote FIVP. We show that FIVP is equivalent to a second kind vector integral equation of Volterra type. Properties of this vector integral equation are described. This FIVP consists of a system of fifteen partial differential equations with two independent variables x_3, t. The two-dimensional Fourier transform parameter $\nu = (\nu_1, \nu_2) \in R^2$ is appeared in the obtained system. The principal part of this system contains function-coefficients depending on x_3.

5.4.1 IVP (5.256)-(5.257) in terms of the Fourier transform

Let components of vector functions $\tilde{\mathbf{V}}(\nu, x_3, t)$ and $\tilde{\mathbf{F}}(\nu, x_3, t)$ be defined by

$$\tilde{\mathbf{V}}_j(\nu, x_3, t) = F_{x_1,x_2}[\mathbf{V}_j](\nu, x_3, t),\ \tilde{\mathbf{F}}_j(\nu, x_3, t) = F_{x_1,x_2}[\mathbf{F}_j](\nu, x_3, t),$$
$$j = 1, 2, ..., 15,\ \nu = (\nu_1, \nu_2) \in R^2,$$

where F_{x_1,x_2} is the Fourier transform with respect to x_1, x_2, i.e.

$$F_{x_1,x_2}[\mathbf{V}](\nu, x_3, t) = \int_{-\infty}^{\infty}\int_{-\infty}^{\infty} \mathbf{V}(x, t) e^{i(x_1\nu_1 + x_2\nu_2)} dx_1 dx_2,\ i^2 = -1.$$

Lemma 5.5. *The IVP (5.256)-(5.257) can be written as*

$$\mathbf{A}_0(x_3)\frac{\partial \tilde{\mathbf{V}}}{\partial t} + \mathbf{A}_3(x_3)\frac{\partial \tilde{\mathbf{V}}}{\partial x_3} = \overline{\mathbf{B}}(\nu, x_3)\tilde{\mathbf{V}} - \mathbf{Q}(x_3)\tilde{\mathbf{V}} + \tilde{\mathbf{F}}(\nu, x_3, t), \quad (5.264)$$

$$\tilde{\mathbf{V}}(\nu, x_3, t)\mid_{t=0} = \tilde{\mathbf{V}}^0(\nu, x_3),\ \nu \in R^2,\ x_3 \in R,\ t \in R, \quad (5.265)$$

where $\overline{\mathbf{B}}(\nu,x_3) = i(\nu_1\mathbf{A}_1(x_3) + \nu_2\mathbf{A}_2(x_3))$, $\tilde{\mathbf{V}}(\nu,x_3,t)$ *and* $\tilde{\mathbf{F}}(\nu,x_3,t)$ *are the Fourier images of* $\mathbf{V}(x,t)$ *and* $\mathbf{F}(x,t)$ *with respect to* x_1,x_2*, respectively.*

Proof. Applying the operator F_{x_1,x_2} to (5.256)-(5.257) we can write the problem (5.256)-(5.257) in terms of the Fourier image $\tilde{\mathbf{V}}(\nu,x_3,t)$ as follows

$$\mathbf{A}_0\frac{\partial\tilde{\mathbf{V}}}{\partial t} + \mathbf{A}_3\frac{\partial\tilde{\mathbf{V}}}{\partial x_3} - i(\nu_1\mathbf{A}_1 + \nu_2\mathbf{A}_2)\tilde{\mathbf{V}} + \mathbf{Q}\tilde{\mathbf{V}} = \tilde{\mathbf{F}}(\nu,x_3,t),$$
$$\tilde{\mathbf{V}}(\nu_1,\nu_2,x_3,t)\mid_{t=0} = \tilde{\mathbf{V}}^0(\nu,x_3),\ x_3 \in R,\ (\nu_1,\nu_2) \in R^2,\ t \in R.$$

□

Lemma 5.6. *The IVP (5.264)-(5.265) can be written as*

$$\frac{\partial\tilde{\mathbf{W}}}{\partial t} + \mathbf{D}(x_3)\frac{\partial\tilde{\mathbf{W}}}{\partial x_3} = \mathbf{B}(\nu,x_3)\tilde{\mathbf{W}} + \bar{\mathbf{F}}(\nu,x_3,t), \tag{5.266}$$
$$\tilde{\mathbf{W}}(\nu,x_3,t)\mid_{t=0} = \tilde{\mathbf{W}}^0(\nu,x_3),\ \nu \in R^2,\ x_3 \in R,\ t \in R, \tag{5.267}$$

where

$$\begin{aligned}\mathbf{B}(\nu,x_3) &= \mathbf{T}^*(x_3)\overline{\mathbf{B}}(\nu,x_3)\mathbf{T}(x_3) - \mathbf{T}^*(x_3)\mathbf{A}_3(x_3)\frac{d\mathbf{T}}{dx_3}(x_3)\\ &- \mathbf{T}^*(x_3)\mathbf{Q}(x_3)\mathbf{T}(x_3),\\ \bar{\mathbf{F}}(\nu,x_3,t) &= \mathbf{T}^*(x_3)\tilde{\mathbf{F}}(\nu,x_3,t),\ \tilde{\mathbf{W}}^0(\nu,x_3) = \mathbf{T}^{-1}(x_3)\tilde{\mathbf{V}}^0(\nu,x_3).\end{aligned} \tag{5.268}$$

And $\mathbf{T}(x_3)$, $\mathbf{D}(x_3)$ *are defined by (5.259).*

Proof. Using the following transformation in (5.264)

$$\tilde{\mathbf{V}}(\nu,x_3,t) = \mathbf{T}(x_3)\tilde{\mathbf{W}}(\nu,x_3,t)$$

we have

$$\mathbf{A}_0\mathbf{T}\frac{\partial\tilde{\mathbf{W}}}{\partial t}+\mathbf{A}_3\mathbf{T}\frac{\partial\tilde{\mathbf{W}}}{\partial x_3}+\mathbf{A}_3\frac{d\mathbf{T}}{dx_3}\tilde{\mathbf{W}}=\overline{\mathbf{B}}\mathbf{T}\tilde{\mathbf{W}}-\mathbf{Q}\mathbf{T}\tilde{\mathbf{W}}+\tilde{\mathbf{F}}.$$

Multiplying the above system by $\mathbf{T}^*$ and using relations (5.259)

$$\frac{\partial\tilde{\mathbf{W}}}{\partial t}+\mathbf{D}\frac{\partial\tilde{\mathbf{W}}}{\partial x_3}=-\mathbf{T}^*\mathbf{A}_3\frac{d\mathbf{T}}{dx_3}\tilde{\mathbf{W}}+\mathbf{T}^*\overline{\mathbf{B}}\mathbf{T}\tilde{\mathbf{W}}-\mathbf{T}^*\mathbf{Q}\mathbf{T}\tilde{\mathbf{W}}+\mathbf{T}^*\tilde{\mathbf{F}}.$$

Now let us consider the initial condition (5.265)

$$\begin{aligned}\mathbf{T}(x_3)\tilde{\mathbf{W}}(\nu,x_3,t)\mid_{t=0} &= \tilde{\mathbf{V}}^0(\nu,x_3),\\ \tilde{\mathbf{W}}(\nu,x_3,t)\mid_{t=0} &= \mathbf{T}^{-1}(x_3)\tilde{\mathbf{V}}^0(\nu,x_3).\end{aligned}$$

□

5.4.2 Construction of characteristics for $\frac{\partial u(x,t)}{\partial t}+d(x)\frac{\partial u(x,t)}{\partial x}=f(x,t)$

Let T,M be arbitrary positive numbers; $\Delta(M,T)$ be defined by (5.258). Let us consider the following partial differential equation

$$\frac{\partial u(x,t)}{\partial t}+d(x)\frac{\partial u(x,t)}{\partial x}=f(x,t),\ \ (x,t)\in\Delta(M,T). \tag{5.269}$$

Here $d(x)\in C(-\infty,\infty)$, $\mid d(x)\mid\leq M$ for all $x\in R$, $d(x)\in C^2([-MT,MT])$.

The partial differential equation (5.269) can be written as

$$\frac{\partial u(\xi,\tau)}{\partial\tau}+d(\xi)\frac{\partial u(\xi,\tau)}{\partial\xi}=f(\xi,\tau).$$

And characteristics equations are

$$\frac{d}{d\tau}\xi(\tau) = d(\xi(\tau)),\ \tau \in [0,t], \tag{5.270}$$

$$\xi(\tau)\mid_{\tau=t} = x. \tag{5.271}$$

IVP (5.270)-(5.271) can be written as

$$\xi(\tau;x,t) = x + \int_t^\tau d(\xi(\eta;x,t))d\eta. \tag{5.272}$$

Applying method of successive approximations to the above integral equation we have

$$\begin{aligned} \xi_0(\tau;x,t) &= x, \\ \xi_n(\tau;x,t) &= x + \int_t^\tau d(\xi_{n-1}(\eta;x,t))d\eta. \end{aligned} \tag{5.273}$$

Lemma 5.7. *Let T,M be arbitrary positive numbers; $\Delta(M,T)$ be defined by (5.258); (x,t) be fixed point from $\Delta(M,T)$; $\xi_n(\tau;x,t)$ be functions defined by (5.273). Then the values of $\xi_n(\tau;x,t)$ satisfies*

1.

$$\xi_n(\tau;x,t) \in [x-M(t-\tau), x+M(t-\tau)] \subset [-MT,MT]\ for\ 0 \le \tau \le t \le T. \tag{5.274}$$

2. There exits a positive constant $K = K(M,T)$ such that

$$\mid \xi_{n+1}(\tau;x,t) - \xi_n(\tau;x,t) \mid \le K \int_\tau^t \mid \xi_n(\eta;x,t) - \xi_{n-1}(\eta;x,t) \mid d\eta. \tag{5.275}$$

Proof. **1.** From (5.273) we have

$$\mid \xi_n(\tau;x,t) - x \mid \le \int_\tau^t \mid d(\xi_{n-1}(\eta;x,t)) \mid d\eta \le M(t-\tau).$$

From the last inequality

$$x - M(t-\tau) \leq \xi_n(\tau) \leq x + M(t-\tau).$$

Now, we will show $[x-M(t-\tau), x+M(t-\tau)] \subset [-MT, MT]$. From

$$\Delta(M,T) = \{(x,t);\ 0 \leq t \leq T,\ -M(T-t) \leq x \leq M(T-t)\}$$

we can write

$$x + M(t-\tau) \leq M(T-t) + M(t-\tau) \leq MT - M\tau \leq MT.$$

Similarly

$$x - M(t-\tau) \geq -M(T-t) - M(t-\tau) \geq -MT + M\tau \geq -MT.$$

So

$$[x-M(t-\tau), x+M(t-\tau)] \subset [-MT, MT].$$

2.

From (5.273) we have

$$\xi_{n+1}(\tau;x,t) - \xi_n(\tau;x,t) = \int_t^\tau \{d(\xi_n(\eta;x,t)) - d(\xi_{n-1}(\eta;x,t))\} d\eta. \tag{5.276}$$

Using the following relation

$$d(z) - d(y) = \int_y^z d'(s) ds,\ \ [y,z] \subset [-MT, MT], \tag{5.277}$$

(5.276) can be written as

$$\xi_{n+1}(\tau;x,t)-\xi_n(\tau;x,t)=\int_t^\tau\int_{\xi_{n-1}(\eta;x,t)}^{\xi_n(\eta;x,t)}d'(s)dsd\eta.$$

$$\begin{aligned}|\,\xi_{n+1}(\tau;x,t)-\xi_n(\tau;x,t)\,| &\leq \int_\tau^t|\int_{\xi_{n-1}(\eta;x,t)}^{\xi_n(\eta;x,t)}d'(s)ds\,|\,d\eta\\ &\leq \int_\tau^t K|\int_{\xi_{n-1}(\eta;x,t)}^{\xi_n(\eta;x,t)}ds\,|\,d\eta\\ &\leq K\int_\tau^t|\,\xi_{n-1}(\eta;x,t)-\xi_n(\eta;x,t)\,|\,d\eta.\end{aligned}$$

□

Lemma 5.8. *Let us consider the following Neumann series*

$$\xi_0(\tau;x,t)+\sum_{n=0}^{\infty}\{\xi_{n+1}(\tau;x,t)-\xi_n(\tau;x,t)\}. \tag{5.278}$$

The series (5.278) uniformly converges to a continuous function $\xi(\tau;x,t)\in C([0,t])$ *for any* $(x,t)\in\Delta(M,T)$.

Proof. The partial sum of the series (5.278) is

$$S_N(\tau;x,t)=\xi_0(\tau;x,t)+\sum_{n=0}^{N-1}\{\xi_{n+1}(\tau;x,t)-\xi_n(\tau;x,t)\}=\xi_N(\tau;x,t). \tag{5.279}$$

Let us denote

$$\begin{aligned}z_0(\tau;x,t) &= x\\ z_{n+1}(\tau;x,t) &= \xi_{n+1}(\tau;x,t)-\xi_n(\tau;x,t).\end{aligned} \tag{5.280}$$

From (5.273)

$$\begin{aligned}\xi_1(\tau;x,t) &= x+\int_t^\tau d(\xi_0(\tau;x,t))d\tau \\ \xi_1(\tau;x,t)-x &= \int_t^\tau d(\xi_0(\tau))d\tau.\end{aligned}$$

From (5.280)

$$\begin{aligned}|\, z_1(\tau;x,t)\,| &= |\, \xi_1(\tau;x,t)-\xi_0(\tau;x,t)\,|\leq|\, \xi_1(\tau)-x\,|\leq \int_\tau^t |\, d(\xi_0(\tau))\,|\, d\tau \\ &\leq \int_\tau^t M d\tau \leq M(t-\tau)\leq MT,\ \ 0\leq\tau\leq t\leq T.\end{aligned}$$

Using (5.275) we can write

$$|\, z_{n+1}(\tau;x,t)\,|\leq K\int_\tau^t |\, z_n(\eta;x,t)\,|\, d\eta. \tag{5.281}$$

For $n=1$

$$\begin{aligned}|\, z_2(\tau;x,t)\,| &\leq K\int_\tau^t |\, z_1(\eta;x,t)\,|\, d\eta \\ &\leq K\int_\tau^t M(t-\eta)d\eta = KM\frac{(t-\tau)^2}{2!}.\end{aligned}$$

And we have

$$|\, z_{n+1}(\tau;x,t)\,|\leq \frac{M}{K}\frac{(KT)^{n+1}}{(n+1)!}.$$

The series

$$\sum_{k=0}^{\infty}\frac{(KT)^{k+1}}{(k+1)!}$$

is convergent to $\exp(KT)$. And from (5.273) $\xi_n(\tau;x,t)$ are continuous functions with

respect to τ for any $(x,t) \in \Delta(M,T)$. By Weierstrass theorem (Apostol (1967))

$$\sum_{k=0}^{\infty} z_k(\tau;x,t)$$

uniformly converges to continuous function $\xi(\tau;x,t) \in C([0,t])$ for any $(x,t) \in \Delta(M,T)$. Consequently, from (5.279) the series (5.278) uniformly converges to a continuous function $\xi(\tau;x,t) \in C([0,t])$ for any $(x,t) \in \Delta(M,T)$. □

Lemma 5.9. *Let T,M be arbitrary positive numbers; $\Delta(M,T)$ be defined by (5.258); (x,t) be fixed point from $\Delta(M,T)$; $\xi_n(\tau;x,t) \in C([0,t])$ be a sequence of functions defined by (5.273); $\xi_n(\tau;x,t)$ be uniformly converges to a continuous function $\xi(\tau;x,t) \in C([0,t])$ for any $(x,t) \in \Delta(M,T)$; $d(x)$ be a continuous function in R. Then $d(\xi_n(\tau;x,t))$ uniformly converges to a continuous function $d(\xi(\tau;x,t))$.*

Proof. If $\xi_n(\tau)$ uniformly converges to a continuous function $\xi(\tau)$ then for $\forall\ \varepsilon > 0$, $\exists\ N = N(\varepsilon)$: $\forall\ k \geq N \sup\limits_{\eta\in[0,t]} \mid \xi_k(\eta) - \xi(\eta) \mid < \frac{\varepsilon}{K}$. From (5.277) we can write

$$\mid d(\xi_k(\eta)) - d(\xi(\eta)) \mid = \mid \int_{\xi_k(\eta)}^{\xi(\eta)} d'(s)ds \mid \leq K \int_{\xi_k(\eta)}^{\xi(\eta)} ds \leq K \mid \xi_k(\eta) - \xi(\eta) \mid .$$

And

$$\sup_{\eta\in[0,t]} \mid d(\xi_k(\eta)) - d(\xi(\eta)) \mid \leq K \sup_{\eta\in[0,t]} \mid \xi_k(\eta) - \xi(\eta) \mid < \varepsilon.$$

□

Theorem 5.10. *Let T,M be arbitrary positive numbers; $\Delta(M,T)$ be defined by (5.258); (x,t) be fixed point from $\Delta(M,T)$. Then $\xi(\tau;x,t) \in C([0,t])$ is a unique solution of IVP (5.270)-(5.271).*

Proof. From lemma 5.8 the sequence of functions $\xi_n(\tau;x,t)$ defined by (5.273) uniformly converges to a function $\xi(\tau;x,t) \in C([0,t])$ for any $(x,t) \in \Delta(M,T)$. Now,

we will show that function $\xi(\tau;x,t)$ is a solution of IVP (5.270)-(5.271). Taking limit as $n \to \infty$ in (5.273) we have

$$\lim_{n\to\infty} \xi_n(\tau;x,t) = x + \lim_{n\to\infty} \int_t^\tau d(\xi_{n-1}(\eta;x,t))d\eta.$$

From lemma (5.8)

$$\xi(\tau;x,t) = x + \lim_{n\to\infty} \int_t^\tau d(\xi_{n-1}(\eta;x,t))d\eta.$$

From the second Weierstrass theorem (Apostol (1967)) and lemma (5.9)

$$\xi(\tau;x,t) = x + \int_t^\tau \lim_{n\to\infty} d(\xi_{n-1}(\eta;x,t))d\eta = x + \int_t^\tau d(\xi(\eta;x,t))d\eta.$$

To show uniqueness let $\xi_1(\tau;x,t)$ and $\xi_2(\tau;x,t)$ be two solutions of (5.270)-(5.271) and $\bar{\xi}(\tau;x,t) = \xi_1(\tau;x,t) - \xi_2(\tau;x,t)$ then $\bar{\xi}(\tau;x,t)$ satisfies the following integral equality

$$\bar{\xi}(\tau;x,t) = \int_t^\tau (d(\xi_1(\eta;x,t)) - d(\xi_2(\eta;x,t)))d\eta,\ (x,t) \in \Delta(M,T),\ 0 \le \tau \le t \le T.$$

And we have

$$\begin{aligned} \mid \bar{\xi}(\tau;x,t) \mid &\le \int_\tau^t \mid d(\xi_1(\eta;x,t)) - d(\xi_2(\eta;x,t)) \mid d\eta \le \int_\tau^t \mid \int_{\xi_2}^{\xi_1} d'(y)dy \mid d\eta \\ &\le K \int_\tau^t \mid \xi_1(\eta;x,t) - \xi_2(\eta;x,t) \mid d\eta \\ &\le K \int_0^t \mid \bar{\xi}(\eta;x,t) \mid d\eta. \end{aligned} \tag{5.282}$$

Applying Grownwall's lemma (Nagle & Saff & Snider (2005)) to (5.282) we find

$$\xi_1(\tau;x,t) \equiv \xi_2(\tau;x,t),\ (x,t) \in \Delta(M,T),\ 0 \le \tau \le t \le T.$$

□

Lemma 5.11. *Let T, M be arbitrary positive numbers; $\Delta(M,T)$ be defined by (5.258);*

(x,t) be fixed point from $\Delta(M,T)$; $\xi(\tau;x,t)$ be the solution of IVP (5.270)-(5.271). Then $\xi(\tau;x,t) \in C^1(\Delta(M,T);C([0,t]))$.

Proof. Let us consider integral equation (5.272). Taking derivative with respect to x we obtain

$$\frac{d}{dx}\xi(\tau;x,t) = 1 + \int_t^\tau d'(\xi(\eta;x,t))\frac{d}{dx}\xi(\eta;x,t)d\eta. \tag{5.283}$$

Let us denote $\phi(\tau;x,t) \equiv \frac{d}{dx}\xi(\tau;x,t)$. Let us consider the following equality

$$\begin{aligned}\phi(\tau;x+\Delta x,t+\Delta t) - \phi(\tau;x,t) &= \int_{t+\Delta t}^{\tau} \{d'(\xi(\eta;x+\Delta x,t+\Delta t))\phi(\eta,x+\Delta x,t+\Delta t) \\ - \quad d'(\xi(\eta;x,t))\phi(\eta,x,t)\}d\eta &+ \int_{t+\Delta t}^{t} d'(\xi(\eta;x,t))\phi(\eta,x,t)d\eta.\end{aligned}$$

From the integral equation (5.283) and $d(x) \in C^2[-MT,MT]$ we can say that there exits positive constant K_1 such that

$$|\ \phi(\tau;x,t)\ | \leq K_1,\ \forall (x,t) \in \Delta(M,T),\ 0 \leq \tau \leq t.$$

Then we can write

$$\begin{aligned}|\ \phi(\tau;x+\Delta x,t+\Delta t) - \phi(\tau;x,t)\ | &\leq K \int_{\tau}^{t+\Delta t} |\ \phi(\eta,x+\Delta x,t+\Delta t) - \phi(\eta,x,t)\ |\, d\eta \\ + \quad \int_{\tau}^{t+\Delta t} |\ d'(\eta,x+\Delta x,t+\Delta t) - d'(\eta,x,t)\ ||\ \phi(\tau;x+\Delta x,t+\Delta t)\ |\, d\eta &+ K_1 K\Delta t\end{aligned}$$

From the Grownwall's Lemma

$$\begin{aligned}|\ \phi(\tau;x+\Delta x,t+\Delta t) - \phi(\tau;x,t)\ | &\leq (K_1 K\Delta t + \int_{\tau}^{t+\Delta t} |\ d'(\eta,x+\Delta x,t+\Delta t) - d'(\eta,x,t)\ | \\ . \quad |\ \phi(\tau;x+\Delta x,t+\Delta t)\ |\, d\eta).\exp K(t+\Delta t-\tau).\end{aligned}$$

If Δx and Δt approaches to zero then $\mid \phi(\tau;x+\Delta x,t+\Delta t)-\phi(\tau;x,t) \mid$ approaches to zero. This means that $\phi(\tau;x,t)$ is a continuous function with respect to x and t for $(x,t)\in\Delta(M,T)$. And we have $\xi(\tau;x,t)\in C_x^1(\Delta(M,T);C([0,t]))$.

Now, we will show that the solution of IVP (5.270)-(5.271) from the space $C_t^1(\Delta(M,T);C([0,t]))$. Taking derivative with respect to t in (5.272) we obtain

$$\varsigma(\tau;x,t)=\int_t^\tau d'(\xi(\eta;x,t))\varsigma(\eta;x,t)d\eta-d(\xi(t;x,t)), \tag{5.284}$$

where $\varsigma(\tau;x,t)\equiv\frac{d}{dt}\xi(\tau;x,t)$.

$$\begin{aligned}
&\varsigma(\tau;x+\Delta x,t+\Delta t)-\varsigma(\tau;x,t)=\int_{t+\Delta t}^{\tau}\{d'(\xi(\eta;x+\Delta x,t+\Delta t))\varsigma(\eta,x+\Delta x,t+\Delta t)\\
-\;& d'(\xi(\eta;x,t))\varsigma(\eta,x,t)\}d\eta+\int_{t+\Delta t}^{t} d'(\xi(\eta;x,t))\varsigma(\eta,x,t)d\eta\\
+\;& d(\xi(t;x,t))-d(\xi(t+\Delta t;x+\Delta x,t+\Delta t)).
\end{aligned}$$

And we can write

$$\begin{aligned}
&\mid \varsigma(\tau;x+\Delta x,t+\Delta t)-\varsigma(\tau;x,t)\mid\leq K_1\int_{\tau}^{t+\Delta t}\mid d'(\xi(\eta;x+\Delta x,t+\Delta t))-d'(\xi(\eta;,t))\mid d\eta\\
+\;& K\int_{\tau}^{t+\Delta t}\mid \varsigma(\eta;x+\Delta x,t+\Delta t)-\varsigma(\eta;x,t)\mid d\eta+K_1K\Delta t\\
+\;& \mid d(\xi(t;x+,t))-d(\xi(t+\Delta t;x+\Delta x,t+\Delta t))\mid .
\end{aligned}$$

Applying the Grownwall's Lemma and taking limit as Δx and Δt approaches to zero then we find $\mid \varsigma(\tau;x+\Delta x,t+\Delta t)-\varsigma(\tau;x,t)\mid$ approaches to zero. This means that $\varsigma(\tau;x,t)$ is a continuous function with respect to x and t for $(x,t)\in\Delta(M,T)$. And we have $\xi(\tau;x,t)\in C_t^1(\Delta(M,T);C([0,t]))$. This complete proof of the lemma. □

5.4.3 Reduction of IVP (5.266)-(5.267) to an equivalent vector integral equation

Lemma 5.12. *Let T be a given positive number; $\Delta(M,T)$ be defined by (5.258). IVP (5.266)-(5.267) can be written the following Volterra type integral equation*

$$\widetilde{\mathbf{W}}_j(\nu,x_3,t) = \mathbf{G}_j(\nu,x_3,t) + \int_0^t (\mathbf{K}_j\widetilde{\mathbf{W}})(\nu,\varphi_j(\tau;x_3,t),\tau)d\tau,\ \ j=1,2,...,15, \quad (5.285)$$

where $\varphi_j(\tau;x_3,t),\ \ j=1,2,...,15$, are characteristics of IVP (5.266)-(5.267),

$$\mathbf{G}_j(\nu,x_3,t) = \widetilde{\mathbf{W}}(\nu,\varphi_j(0;x_3,t),0) + \int_0^t \bar{\mathbf{F}}_j(\nu,\varphi_j(\tau;x_3,t),\tau)d\tau,\ \ j=1,2,...,15, \quad (5.286)$$

and operator $\mathbf{K}_j,\ \ j=1,2,...,15$, is

$$(\mathbf{K}_j\widetilde{\mathbf{W}})(\nu,x_3,t,\tau) = [\mathbf{B}(\nu,\varphi_j(\tau;x_3,t))\widetilde{\mathbf{W}}(\nu,\varphi_j(\tau;x_3,t),\tau)]_j. \quad (5.287)$$

(5.285) can be written as

$$\begin{aligned} \widetilde{\mathbf{W}}(\nu,x_3,t) &= \mathbf{G}(\nu,x_3,t) + \int_0^t (\mathbf{K}\widetilde{\mathbf{W}})(\nu,x_3,t,\tau)d\tau, \quad (5.288)\\ \mathbf{K} &= (\mathbf{K}_1,\mathbf{K}_2,...,\mathbf{K}_{15}),\ \mathbf{G} = (\mathbf{G}_1,\mathbf{G}_2,...,\mathbf{G}_{15}). \end{aligned}$$

Proof. Applying the method of characteristics to IVP (5.266)-(5.267) characteristic equation of (5.266) is

$$\begin{aligned} \frac{d\varphi_j(\tau;x_3,t)}{d\tau} &= \mathbf{D}_j(\varphi_j(\tau;x_3,t)),\ \ j=1,2,...,15,\\ \varphi_j(\tau;x_3,t)\mid_{\tau=t} &= x_3. \quad (5.289) \end{aligned}$$

From lemma 5.11 (5.289) has a solution from $C^1(\Delta(M,T);C([0,t]))$. (5.266) along of

the characteristics may be written in the form

$$\frac{\partial \widetilde{\mathbf{W}}_j(\nu,\varphi_j,\tau)}{\partial \tau} = (\mathbf{B}(\nu,\varphi_j)\widetilde{\mathbf{W}}(\nu,\varphi_j,\tau))_j + \bar{\mathbf{F}}_j(\nu,\varphi_j,\tau)$$

integrating from $\tau = 0$ to $\tau = t$

$$\begin{aligned}\widetilde{\mathbf{W}}_j(\nu,x_3,t) &= \widetilde{\mathbf{W}}_j(\nu,\varphi_j(0;x_3,t),0) + \int_0^t \{[\mathbf{B}(\nu,\varphi_j(\tau;x_3,t))\widetilde{\mathbf{W}}(\nu,\varphi_j(\tau;x_3,t),\tau)]_j \\ &+ \bar{\mathbf{F}}_j(\nu,\varphi_j(\tau;x_3,t),\tau)\}d\tau,\ \ j = 1,2,...,15,\end{aligned}$$

where

$$\widetilde{\mathbf{W}}_j(\nu,\varphi_j(0;x_3,t),0) = (\mathbf{T}^{-1}(\varphi_j(0;x_3,t))\widetilde{\mathbf{V}^0}(\nu,\varphi_j(0;x_3,t)))_j\ \ j = 1,2,...,15.$$

□

5.4.4 Properties of the vector integral equation (5.288)

In this section the properties of the inhomogeneous term and the kernel of (5.288) are described. These properties will be used for solving (5.288). We state these properties in the form of the following lemmas.

Lemma 5.13. *Let T be a fixed positive number, components of* $\mathbf{G} = (\mathbf{G}_1,\mathbf{G}_2,...,\mathbf{G}_{15})$ *be defined by (5.286). Then under assumptions 1-6 the functions* $\mathbf{G}_j(\nu,x_3,t)$, $j = 1,2,...,15$ *belong the space* $C(R^2;C^1(\Delta(M,T)))$.

Proof. From the assumptions 5-6 $\mathbf{T}^{-1}(x_3)$, $\mathbf{T}^*(x_3) \in C^2([-MT,MT])$ and $\tilde{\mathbf{V}}^0(\nu,x_3) \in C_0(R^2;C^1([-MT,MT]))$, $\bar{\mathbf{F}}(\nu,x_3,t) \in C_0(R^2;C^1([-MT,MT]))$. From lemma 5.11 $\varphi_j(\tau;x_3,t) \in C^1(\Delta(M,T);C([0,t]))$, $j = 1,2,...,15$. Using formula (5.286) we find that the functions $\mathbf{G}_j(\nu,x_3,t) \in C(R^2;C^1(\Delta(M,T)))$, $j = 1,2,...,15$. □

Lemma 5.14. *Let T be a fixed positive number and $\Delta(M,T)$ be defined by (5.258). Suppose that the Assumptions 1-6 are true and the components of the vector operator $\mathbf{K} = (\mathbf{K}_1, \mathbf{K}_2, ..., \mathbf{K}_{15})$ are defined by (5.287). Then for any vector function $\widetilde{\mathbf{W}}(\nu, x_3, t)$ with continuous components in $R^2 \times C^1(\Delta(M,T))$*

1. $\mathbf{K}_j$, $j = 1,2,...,15$, *is a linear operator and*

$$\int_0^t (\mathbf{K}_j \widetilde{\mathbf{W}})(\nu, x_3, t, \tau) d\tau, \;\; j = 1,2,...,15 \tag{5.290}$$

belongs to the space $C(R^2; C^1(\Delta(M,T)))$;

2.for any positive number Ω the following inequalities are satisfied

$$| \int_0^t (\mathbf{K}_j \widetilde{\mathbf{W}})(\nu, x_3, t, \tau) d\tau | \leq B_0 \int_0^t \| \widetilde{\mathbf{W}} \| (\nu, \tau, M, T) d\tau, \;\; j = 1,2,...,15; \tag{5.291}$$

where

$$\| \widetilde{\mathbf{W}} \| (\nu, \tau, M, T) = \max_{k,j=1,2,...,15, \;\; 0 \leq \eta \leq \tau, \;\; (\varphi_j, \tau) \in \Delta(M,T)} | \widetilde{\mathbf{W}}_k(\nu, \varphi_j, \eta) |,$$

$(x_3, t) \in \Delta(M,T)$, $| \nu | \leq \Omega$, *and B_0 is a positive number depending on values of T, M, Ω.*

Proof. From assumptions 5-6 the matrix $\mathbf{B}(\nu, x_3)$ has continuous components for $(\nu, x_3) \in R^2 \times C^1([-MT, MT])$. From lemma 5.11 $\varphi_j(\tau; x_3, t) \in C^1(\Delta(M,T); C([0,t]))$, $j = 1,2,...,15$. $\varphi_j(\tau; x_3, t) \subset [-MT, MT]$ for any $(x_3, t) \in \Delta(M,T)$ and $0 \leq \tau \leq t \leq T$. Using the equalities

$$\begin{aligned} & (\mathbf{K}_j \widetilde{\mathbf{W}})(\nu, x_3, t, \tau) = [\mathbf{B}(\nu, \varphi_j(\tau; x_3, t)) \widetilde{\mathbf{W}}(\nu, \varphi_j(\tau; x_3, t), \tau)]_j, \\ & \mathbf{B}(\nu, x_3) = i\mathbf{T}^*(x_3)(\nu_1 \mathbf{A}_1(x_3) + \nu_2 \mathbf{A}_2(x_3))\mathbf{T}(x_3) - \mathbf{T}^*(x_3)\mathbf{A}_3(x_3)\frac{d\mathbf{T}}{dx_3}(x_3) \\ - \;\; & \mathbf{T}^*(x_3)\mathbf{Q}(x_3)\mathbf{T}(x_3), \end{aligned} \tag{5.292}$$

linearity of the operator $\mathbf{K}_j$ is satisfied.

Let (x_3,t) be an arbitrary point from $\Delta(M,T)$; the components of the matrices $\mathbf{T}(x_3)$, $\mathbf{A}_3(x_3)$ are twice continuously differentiable functions for $x_3 \in [-MT,MT]$; the components of the matrices $\frac{d\mathbf{T}(x_3)}{dx_3}$, $\mathbf{A}_1(x_3)$, $\mathbf{A}_2(x_3)$ and $\mathbf{Q}(x_3)$ are continuously differentiable functions for $x_3 \in [-MT,MT]$. From lemma 5.11 $\varphi_j(\tau;x_3,t) \in C^1(\Delta(M,T);C([0,t]))$, $j = 1,2,...,15$. And $\varphi_j(\tau;x_3,t) \subset [-MT,MT]$ for any $(x_3,t) \in \Delta(M,T)$ and $0 \le \tau \le t \le T$. Using formulae (5.292) for any vector functions $\widetilde{\mathbf{W}} = (\widetilde{\mathbf{W}}_1,...,\widetilde{\mathbf{W}}_{15})$ with components $\widetilde{\mathbf{W}}_j(\nu,x_3,t)$ in $C(R^2 \times C^1(\Delta(M,T)))$ we find that (5.290) is from $C(R^2;C^1(\Delta(M,T)))$.

From assumptions 5-6 we know $\mathbf{A}_l(x_3) \in C^1([-MT,MT])$, $l = 1,2$; $\mathbf{T}(x_3) \in C^2([-MT,MT])$; $\mathbf{Q}(x_3) \in C^1([-MT,MT])$. From lemma 5.11 we have $\varphi_j(\tau;x_3,t) \in C^1(\Delta(M,T);C([0,t]))$; $\varphi_j(\tau;x_3,t) \subset [-MT,MT]$ for any $(x_3,t) \in \Delta(M,T)$ and $0 \le \tau \le t \le T$. Using the facts we find positive constants $a_1(M,T)$, $a_2(M,T)$, $q(M,T)$, $c(M,T)$ such that

$$\begin{aligned}
&\max_{k=1,2,...,15,\ \varphi_j \in [-MT,MT]} |\ (\mathbf{A}_l)_{jk}(\varphi_j)\ | \le a_l(M,T); l = 1,2; j = 1,...,15,\\
&\max_{k=1,2,...,15,\ \varphi_j \in [-MT,MT]} |\ \frac{dT_{jk}(\xi)}{d\xi}\ |_{\xi=\varphi_j(\tau;x_3,t)} \le c; j = 1,...,15,\\
&\max_{k=1,2,...,15,\ \varphi_j \in [-MT,MT]} |\ \mathbf{Q}_{jk}(\varphi_j)\ | \le q(M,T); j = 1,...,15. \qquad (5.293)
\end{aligned}$$

Using (5.292) and the inequalities (5.293) we can obtain the following inequality

$$
\begin{aligned}
&| \int_0^t (\mathbf{K}_j \widetilde{\mathbf{W}})(\nu, x_3, t, \tau) d\tau | \leq \int_0^t | [\mathbf{B}(\nu, \varphi_j(\tau; x_3, t)) \widetilde{\mathbf{W}}(\nu, \varphi_j(\tau; x_3, t), \tau)]_j | \, d\tau, \\
&= \int_0^t | [\mathbf{B}_{j,1}(\nu, \varphi_j(\tau; x_3, t)) \widetilde{\mathbf{W}}_1(\nu, \varphi_j(\tau; x_3, t), \tau) \\
+ \quad &\mathbf{B}_{j,2}(\nu, \varphi_j(\tau; x_3, t)) \widetilde{\mathbf{W}}_2(\nu, \varphi_j(\tau; x_3, t), \tau) + ... \\
+ \quad &\mathbf{B}_{j,15}(\nu, \varphi_j(\tau; x_3, t)) \widetilde{\mathbf{W}_{15}}(\nu, \varphi_j(\tau; x_3, t), \tau)] | \, d\tau, \\
&\leq 15 \int_0^t \max_{k=1,2,...,15, \ \varphi_j \in [-MT, MT]} | \mathbf{B}_{jk}(\varphi_j) | \| \widetilde{\mathbf{W}} \| (\nu, \tau, M, T) d\tau, \\
&\leq B_0(M, T, \Omega) \int_0^t \| \widetilde{\mathbf{W}} \| (\nu, \tau, M, T) d\tau, \\
&j = 1, 2, ..., 15, \ (x_3, t) \in \Delta(M, T), \ 0 \leq \tau \leq T, \ | \nu | \leq \Omega.
\end{aligned}
$$

Here $\xi(\tau; x_3, t) = \varphi_j(\tau; x_3, t), j = 1, 2, ...15$, for all $(x_3, t) \in \Delta(M, T), \ | \nu | \leq \Omega$ and

$$
B_0(M, T, \Omega) = 15\{ | \nu_1 | \frac{a_1}{a_0} + | \nu_2 | \frac{a_2}{a_0} + \frac{a_3 c}{\sqrt{a_0}} + \frac{q}{a_0} \}.
$$

□

5.5 Solving the integral equation (5.288) by successive approximations

Let T be a fixed positive number, $\Delta(M, T)$ be defined by (5.258). In this section we solve the integral equation (5.288) by the method of successive approximations and then show that this solution is unique in the class of vector functions with components (5.285) from $C(R^2, C^1(\Delta(M, T)))$.

5.5.1 Solving integral equation (5.285) by successive approximations

Let us consider integral equation (5.285) for $\nu \in R^2$, $(x_3,t) \in \Delta(M,T)$. For finding a solution of this equation we apply the following successive approximations for $j = 1,2,...,15$

$$\widetilde{\mathbf{W}_j}^{0}(\nu,x_3,t) = \mathbf{G}_j(\nu,x_3,t), \tag{5.294}$$

$$\widetilde{\mathbf{W}_j}^{(p)}(\nu,x_3,t) = \int_0^t (\mathbf{K}_j \widetilde{\mathbf{W}}^{(p-1)})(\nu,\varphi_j(\tau;x_3,t),\tau)d\tau \ \ p = 1,2,.... \tag{5.295}$$

Let Ω be an arbitrary positive number. We will show that for $|\nu| \leq \Omega$, $(x_3,t) \in \Delta(M,T)$ the series $\sum\limits_{k=0}^{\infty} \widetilde{\mathbf{W}}^{(k)}(\nu,x_3,t) = (\sum\limits_{k=0}^{\infty} \widetilde{\mathbf{W}_1}^{(k)}(\nu,x_3,t),...,\sum\limits_{k=0}^{\infty} \widetilde{\mathbf{W}_{15}}^{(k)}(\nu,x_3,t))$ is uniformly convergent to a vector function $\widetilde{\mathbf{W}}(\nu,x_3,t) = (\widetilde{\mathbf{W}_1}(\nu,x_3,t),...,\widetilde{\mathbf{W}_{15}}(\nu,x_3,t))$ and this vector function $\widetilde{\mathbf{W}}(\nu,x_3,t)$ is a solution of (5.288). Indeed, we find from (5.294) and Lemmas (5.13)-(5.14) that $\widetilde{\mathbf{W}}^k(\nu,x_3,t)$, $k = 0,1,...$ are vector functions with components $\widetilde{\mathbf{W}_j}^{(k)}(\nu,x_3,t) \in C(R^2;C^1(\Delta(M,T)))$, $j = 1,...,15$, $k = 0,1,...$ for $|\nu| \leq \Omega$, $(x_3,t) \in \Delta(M,T)$ and

$$|\widetilde{\mathbf{W}_j}^{(k)}(\nu,x_3,t)| \leq B_0 \int_0^t \|\widetilde{\mathbf{W}}^{(k-1)}\|(\nu,\tau,M,T)d\tau, \ \ t \in [0,T], \tag{5.296}$$

where $\|.\|(\nu,\tau,M,T)$ and B_0 are defined in Lemma (5.14).

It follows from (5.296) that

$$|\widetilde{\mathbf{W}_j}^{(k)}(\nu,x_3,t)| \leq \frac{(B_0T)^k}{k!}\|\mathbf{G}\|(\nu,t,M,T), \ \ k = 0,1,..., \ \ |\nu| \leq \Omega, \tag{5.297}$$

where

$$\|\mathbf{G}\|(\nu,t,M,T) = \max_{j=1,...,15} \max_{0\leq\tau\leq t, \ (x_3,t)\in\Delta(M,T)} |\mathbf{G}_j(\nu,x_3,\tau)|.$$

The uniform convergence of $\sum_{k=0}^{\infty} \widetilde{\mathbf{W}}_j^{\,k}(\nu,x_3,t)$ to a continuous function $\widetilde{\mathbf{W}}_j(\nu,x_3,t)$ for $|\,\nu\,| \leq \Omega$, $(x_3,t) \in \Delta(M,T)$ follows from inequality (5.297) and the first Weierstrass theorem (Apostol (1967)). Let us consider the vector function $\widetilde{\mathbf{W}}(\nu,x_3,t) = (\widetilde{\mathbf{W}}_1(\nu,x_3,t),...,\widetilde{\mathbf{W}_{15}}(\nu,x_3,t))$ for $|\,\nu\,| \leq \Omega$, $(x_3,t) \in \Delta(M,T)$. We show below that the vector function $\widetilde{\mathbf{W}}(\nu,x_3,t) \in C(R^2;C^1(\Delta(M,T)))$ is a solution of (5.288). Summing the Eq.(5.294) from 1 to N we have

$$\sum_{k=1}^{N} \widetilde{\mathbf{W}}^{(k)}(\nu,x_3,t) = \sum_{k=0}^{N-1} \int_0^t (\mathbf{K}\widetilde{\mathbf{W}}^{(k)})(\nu,x_3,t,\tau)d\tau, \tag{5.298}$$

where

$$\sum_{k=0}^{\infty} \widetilde{\mathbf{W}}^{(k)}(\nu,x_3,t) = (\sum_{k=0}^{\infty} \widetilde{\mathbf{W}_1}^{(k)}(\nu,x_3,t),...,\sum_{k=0}^{\infty} \widetilde{\mathbf{W}_{15}}^{(k)}(\nu,x_3,t)).$$

Adding both sides $\mathbf{G}(\nu,x_3,t)$ of Eq.(5.298) we have

$$\sum_{k=0}^{N} \widetilde{\mathbf{W}}^{(k)}(\nu,x_3,t) = \mathbf{G}(\nu,x_3,t) + \int_0^t \sum_{k=0}^{N-1} (\mathbf{K}\widetilde{\mathbf{W}}^{(k)})(\nu,x_3,t,\tau)d\tau. \tag{5.299}$$

Approaching N the infinity and using the second Weierstrass theorem (Apostol (1967)) we find that $\widetilde{\mathbf{W}}(\nu,x_3,t)$ satisfies (5.288) for $|\,\nu\,| \leq \Omega$, $(x_3,t) \in \Delta(M,T)$. Since Ω is an arbitrary positive number we find that $\widetilde{\mathbf{W}}(\nu,x_3,t) \in C(R^2;C^1(\Delta(M,T)))$ is a solution of (5.288) for $\nu \in R^2$, $(x_3,t) \in \Delta(M,T)$.

5.5.2 Uniqueness of solution

We prove here that a solution $\widetilde{\mathbf{W}}(\nu,x_3,t)$ of (5.288) is unique in the class of vector functions with components $\widetilde{\mathbf{W}}_j(\nu,x_3,t) \in C(R^2,C^1(\Delta(M,T)))$, $j = 1,...,15$. Indeed, let $\widetilde{\mathbf{W}}(\nu,x_3,t)$ and $\widetilde{\mathbf{W}}^*(\nu,x_3,t)$ be two solutions of (5.288) corresponding to the same vector function $\mathbf{G}(\nu,x_3,t)$ and $\widetilde{\hat{\mathbf{W}}}(\nu,x_3,t) = \widetilde{\mathbf{W}}(\nu,x_3,t) - \widetilde{\mathbf{W}}^*(\nu,x_3,t)$ for $\nu \in R^2$, $(x_3,t) \in \Delta(M,T)$.

The vector function $\widetilde{\hat{\mathbf{W}}}(\nu,x_3,t)$ satisfies the following operator integral equality

$$\widetilde{\hat{\mathbf{W}}}(\nu,x_3,t)=\int_0^t(\mathbf{K}\widetilde{\hat{\mathbf{W}}})(\nu,x_3,t,\tau)d\tau,\ \nu\in R^2,\ (x_3,t)\in\Delta(M,T). \tag{5.300}$$

Let Ω be an arbitrary positive number. Using the Lemma 5.14 and (5.300) we have

$$\|\widetilde{\hat{\mathbf{W}}}\|(\nu,t,M,T)\le B_0\int_0^t\|\widetilde{\hat{\mathbf{W}}}\|(\nu,\tau,M,T)d\tau,\ |\nu|\le\Omega,\ t\in[0,T], \tag{5.301}$$

where $\|.\|(\nu,\tau,M,T)$ and B_0 are defined in Lemma (5.14).

Applying Grownwall's lemma (Nagle & Saff & Snider (2005)) to (5.301) we have

$$\|\widetilde{\hat{\mathbf{W}}}\|(\nu,t,M,T)\le 0,\ |\nu|\le\Omega,\ t\in[0,T]. \tag{5.302}$$

Since Ω is an arbitrary and $\widetilde{\hat{\mathbf{W}}}(\nu,x_3,t)$ is continuous we find from (5.302)

$$\widetilde{\hat{\mathbf{W}}}(\nu,x_3,t)\equiv 0,\ \nu\in R^2,\ (x_3,t)\in\Delta(M,T).$$

This means that $\widetilde{\mathbf{W}}(\nu,x_3,t)\equiv\widetilde{\mathbf{W}}^*(\nu,x_3,t)$ for $\nu\in R^2$, $(x_3,t)\in\Delta(M,T)$.

5.6 Solving IVP for EMES (5.226)-(5.233)

In this section we describe a class of functions where this inverse Fourier transform works correctly (similar reasoning in Yakhno & Sevimlican (2010)). We will use the following notions and notations. For the exponent $\alpha=(\alpha_1,\alpha_2)$ with $\alpha_j\in 0,1,2,...$ and $|\alpha|=\alpha_1+\alpha_2$, the partial derivatives of higher order

$$\frac{\partial^{|\alpha|}}{\partial\nu_l}\widetilde{\mathbf{W}}_j(\nu,x_3,t),\ j=1,...,15,\ l=1,2,$$

will be denoted by

$$D_\nu^\alpha \widetilde{\mathbf{W}}_j(\nu, x_3, t).$$

For vector functions $\widetilde{\mathbf{W}}(\nu, x_3, t) = (\widetilde{\mathbf{W}}_1(\nu, x_3, t), ..., \widetilde{\mathbf{W}_{15}}(\nu, x_3, t))$ and each α we define $D_\nu^\alpha \widetilde{\mathbf{W}}(\nu, x_3, t)$ by

$$D_\nu^\alpha \widetilde{\mathbf{W}} = (\mathbf{D}_\nu^\alpha \widetilde{\mathbf{W}}_1, ..., \mathbf{D}_\nu^\alpha \widetilde{\mathbf{W}_{15}}).$$

The Paley-Wiener space is denoted by PW. $C(PW(R^2); C^1(\Delta(M,T)))$ is a class of all continuous mapping of $PW(R^2)$ into the class $C^1(\Delta(M,T))$.

Theorem 5.15. *Let T be a positive number; $\tilde{\mathbf{f}} = (\tilde{f}_1, \tilde{f}_2, \tilde{f}_3)$, $\tilde{\mathbf{J}} = (\tilde{J}_1, \tilde{J}_2, \tilde{J}_3)$, $\tilde{\gamma} = (\tilde{\gamma}_1, \tilde{\gamma}_2, \tilde{\gamma}_3)$ and $\tilde{\psi} = (\tilde{\psi}_1, \tilde{\psi}_2, \tilde{\psi}_3)$ be the Fourier transform with respect to x_1, x_2 of the inhomogenous term $\mathbf{f}$, $\mathbf{J}$, γ and ψ in (5.226)-(5.233) such that for each α*

$$D_\nu^\alpha \tilde{\mathbf{f}}_j,\ D_\nu^\alpha \tilde{\mathbf{J}}_j \in C_0(R^2; C^1(\Delta(M,T))),\ \ j = 1,2,3.$$

$$D_\nu^\alpha \tilde{\psi}_j \in C_0(R^2; C^1(\Delta(M,T))),\ D_\nu^\alpha \tilde{\gamma}_j \in C_0(R^2; C^2(\Delta(M,T))),\ \ j = 1,2,3.$$

Then under Assumptions1-6, there exits a unique generalized solution of IVP (5.226)-(5.233) such that

$$\begin{aligned} \mathbf{u}(x,t) &\in C^2(\Delta(M,T); PW(R^2)),\ \mathbf{E}(x,t) \in C^1(\Delta(M,T); PW(R^2)), \\ \mathbf{H}(x,t) &\in C^1(\Delta(M,T); PW(R^2)). \end{aligned}$$

Proof. We note that under hypothesis of the theorem the functions $\mathbf{G}_j(\nu, x_3, t), j = 1, ..., 15$, defined by (5.286) for any α satisfy the following conditions

$$D_\nu^\alpha \mathbf{G}_j(\nu, x_3, t) \in C_0(R^2; C^1(\Delta(M,T))),\ \ j = 1, ..., 15. \tag{5.303}$$

$\alpha = (\alpha_1, \alpha_2)$, $\alpha_j \in 0, 1, ...$, $\nu = (\nu_1, \nu_2) \in R^2$, $(x_3, t) \in \Delta(M,T)$. Applying D_ν^α to the

vector integral equation (5.288) we obtain for $\nu \in R^2$, $(x_3,t) \in \Delta(M,T)$

$$D_\nu^\alpha \widetilde{\mathbf{W}}(\nu,x_3,t) = D_\nu^\alpha \mathbf{G}(\nu,x_3,t) + \int_0^t (\mathbf{K} D_\nu^\alpha \widetilde{\mathbf{W}})(\nu,x_3,t,\tau)d\tau. \tag{5.304}$$

Eq.(5.304) has the same form as (5.288). Using the reasoning of Section 5.5 for any α we have

$$D_\nu^\alpha \widetilde{\mathbf{W}}(\nu,x_3,t) \in C(R^2;C^1(\Delta(M,T))).$$

Let Ω be an arbitrary positive number. Then using (5.304) and (5.291) for any α and $|\nu| \leq \Omega$ we obtain the following inequality

$$\| D_\nu^\alpha \widetilde{\mathbf{W}} \|(\nu,t,M,T) \leq \| D_\nu^\alpha \mathbf{G} \|(\nu,t,M,T) + B_0 \int_0^t \| D_\nu^\alpha \widetilde{\mathbf{W}} \|(\nu,\tau,M,T)d\tau, \tag{5.305}$$

where $\| . \|(\nu,\tau,M,T)$ and B_0 are defined in Lemma (5.14). Applying the Grownwall's lemma (Nagle & Saff & Snider (2005)) for the inequality (5.305) we find

$$\| D_\nu^\alpha \widetilde{\mathbf{W}} \|(\nu,t,M,T) \leq \exp(B_0 T) \max_{|\nu|\leq\Omega} \| D_\nu^\alpha \mathbf{G} \|(\nu,t,M,T), \nu \in R^2, t \in [0,T]. \tag{5.306}$$

Since Ω is an arbitrary positive number then we find from (5.303), (5.306) that the solution $\widetilde{W}(\nu,x_3,t)$ of (5.288) satisfies for any α the following property

$$D_\nu^\alpha \widetilde{\mathbf{W}}(\nu,x_3,t) \in C_0(R^2;C^1(\Delta(M,T))).$$

So

$$\widetilde{\mathbf{W}}(\nu,x_3,t) \in C_0^\infty(R^2;C^1(\Delta(M,T))).$$

From the equality

$$\tilde{\mathbf{V}}(\nu,x_3,t) = \mathbf{T}(x_3)\tilde{\mathbf{W}}(\nu,x_3,t)$$

there exits a unique solution of IVP (5.264)-(5.265) such that $\tilde{V}(\nu,x_3,t) \in$

$C_0^\infty(R^2;C^1(\Delta(M,T)))$. Applying the inverse Fourier transform with respect to ν_1,ν_2 to the $\tilde{V}(\nu,x_3,t)$ and using the real version of the Paley-Wiener theorem (Reed & Simon (2005)) we find that $V(x,t) = F^{-1}[\tilde{V}]$ is a unique generalized solution of (5.256)-(5.257) such that $V(x,t) \in C^1(\Delta(M,T);PW(R^2))$.

Consequently, IVP for EMES (5.226)-(5.233) has a unique generalized solution such that

$$\begin{aligned} \mathbf{u}(x,t) &\in C^2(\Delta(M,T);PW(R^2)),\ \mathbf{E}(x,t) \in C^1(\Delta(M,T);PW(R^2)), \\ \mathbf{H}(x,t) &\in C^1(\Delta(M,T);PW(R^2)). \end{aligned}$$

□

5.7 Concluding Remarks

In this chapter of the thesis an analytic method of solving IVP for linear, inhomogenous, anisotropic dynamics of electromagnetoelasticity is given. This method is based on the Fourier transform, successive approximations and Paley-Wiener theorem. Theorems about existence and uniqueness of the solution are proved.

CHAPTER SIX

CONCLUSION

New methods for the computation of fundamental solutions of differential equations of elastodynamics and electrodynamics for general anisotropic solids, crystals, electrically and magnetically anisotropic materials have been developed.

In particular three new analytical methods are developed for computation of fundamental solution of anisotropic elastodynamics. In the first method dynamical equations of the motion of homogeneous elastic anisotropic media have been written in the form of the symmetric hyperbolic system of the first order partial differential equations. If initial data and inhomogenous terms have finite supports then solutions of hyperbolic systems have finite supports with respect to space variables for any fixed time variable. This property is proved in the thesis for the system of anisotropic elasticity. Using Paley-Wiener theorem we find that the Fourier image of the solutions with finite supports with respect to space variables are analytic functions with respect to Fourier parameters. Using the presentation of unknown solution in the form of a power series with respect to Fourier parameters we can find the recurrence relations for unknown coefficients of the power series from the considered system of anisotropic elasticity and initial data. Using these relations we recover all unknown coefficients. Finally, the inverse Fourier transform is applied for the considered power series for Fourier image of the solution. We have justified the suggested method using the explicit formula of the fundamental solution for the isotropic elastic media. The computational experiments confirm the robustness of our method to produce images of elements of fundamental solution of symmetric hyperbolic system of elasticity.

In the second method the fundamental solution (FS) of anisotropic elastodynamics is a matrix whose columns are solutions of motion equations with pulse point forces. The direction of these forces are basic vectors. The columns of FS are vector functions with finite supports and their Fourier transforms with respect to space variables are

analytic vector functions. The FSs in terms of wave-vector variables are differentiable matrix functions without singularities. The time-dependent FSs of electrodynamics in general anisotropic media in terms of wave-vector variables is derived by matrix transformations and solutions of some ordinary differential equations depending on 3D wave-vector variables and the time variable. The computational demonstrate that the accuracy of values of FSs in terms of wave-vector variables computed by the suggested method is less then 10^{-10}. The values of FSs in terms of space and time variables are derived numerically from the values of FS in terms of wave-vector variables and 3D integration of the inverse Fourier transform. The computational illustrate that integrals of FSs are found with high accuracy in the case of isotropic (or transversely isotropic) solids. The computational examples show that the suggested method is applicable for the computation of all elements of the time-dependent FSs of elastodynamics in general homogeneous anisotropic solids (trigonal, monoclinic, triclinic) as well as the computation of the displacement speed, stress components arising from arbitrary force. The computational examples have confirmed the robustness of the suggested approach. In the third method a new method of computation of the fundamental solution for anisotropic elastodynamics is proposed. Applying the Fourier transform with respect to space variables to system of anisotropic elastodynamic we obtain a system of second order ordinary differential equations whose coefficients depend on Fourier parameters. Using the matrix transformations and properties of coefficients the Fourier image of the fundamental solution is computed. Finally, the fundamental solution is computed by the inverse Fourier transform to obtained Fourier image. The implementation and justification of the suggested method have been made by computational experiments in MATLAB. Computational experiments confirm the robustness of the suggested method.

The explicit formula of the time-dependent fundamental solution of elastodynamics in 1D, 2D and 3D QCs has been derived by the matrix transformations, solutions

of some ordinary differential equations depending on the Fourier parameters and the inverse Fourier transform. The formula for the FS of elastodynamics in 1D, 2D and 3D QCs has been presented in the form convenient for computation of the transient phonon and phason displacement fields. Computational experiment confirms the robustness of our method for the computation of the time-dependent fundamental solution in quasicrystals.

A novel efficient method of constructing the time-dependent fundamental solution (Green's function of the free space) for electrically and magnetically anisotropic homogeneous media is developed. This method is based on matrix computations and the inverse Fourier transform which is done numerically. This method combines in a rational way analytical techniques and numerical computations.

The visualization of the elastic waves, phonon and phason elastic fields, electric and magnetic waves in different anisotropic crystals, quasicrystals and electrically and magnetically anisotropic materials has been obtained. These images are the simulation of wave propagations arising from directional pulse point forces in homogeneous elastic crystals and quasicrystals. We have generated images of electric and magnetic fields components which are a result of the electromagnetic radiations arising from a pulse dipole with a fixed polarization in different electrically and magnetically anisotropic homogeneous media. The visualization of wave propagations in general homogeneous anisotropic materials and solids by modern computer tools allows us to see and evaluate the dependence between the structure of solids, crystals, quasicrystals, electrically and magnetically anisotropic materials and the behavior of the waves. Our method allows users to observe the wave propagations arising from pulse point sources of the form $\mathbf{e}^m \delta(x)\delta(t)$ in general anisotropic solids, crsyals, quasicrystals and electrically and magnetically anisotropic materials.

A new analytical method of finding a solution of the initial value problem (IVP)

for equations of electromagnetoelasticity (EMES) in a general anisotropic vertically inhomogenous electromagnetoelastic material has been suggested. This method consists of the following. The Fourier transform of IVP for EMEs with respect to lateral variables is obtained. Transformed IVP reduces to a second kind vector integral equation of the Volterra type. Solving this integral equation by the method of successive approximations. The inverse Fourier transform with the real Paley-Wiener theorem to the obtained Fourier images is applied. At the same time a theorem about the existence of a unique solution of IVP for EME is proved.

The main results of the thesis were published in the following papers:

- Yakhno, V.G., Çerdik Yaslan, H. (2011). Three dimensional elastodynamics of 2D quasicrystals: The derivation of the time-dependent fundamental solution. Applied Mathematical Modelling 35, 3092-3110.
- Yakhno, V.G., Çerdik Yaslan, H. (2011). Equations of anisotropic elastodynamics as a symmetric hyperbolic system: Deriving the time-dependent fundamental solution. Journal of Computational and Applied Mathematics. doi: 10.1016/j.cam.2010.10.048.
- Yakhno, V.G., Çerdik Yaslan, H. (2011). Computation of the time-dependent fundamental solution for equations of elastodynamics in general anisotropic media. Computers and Structures. 89, 646-655.

One of the results of this thesis was presented in *14th International Congress on Computational and Applied Mathematics*, September 2009, Antalya.

REFERENCES

Achenbach, J. D. (1973). *Wave propagation in elastic solids.* North-holland, Amsterdam.

Akmaz, H., & Akinci, U. (2009). On dynamic plane elasticity problems of 2D quasicrystals. *Phys. Lett. A,* 373, 1901-1905.

Akmaz, H.K. (2009). Three-dimensional elastic problems of three-dimensional quasicrystals. *Appl. Math. Comp.,* 207, 327-332.

Aki, K., & Richards, P.G. (1980). *Quantitative Seismology. Theory and Methods.* Freeman and company, San Francisco.

Alexandrov, K. S. *Sov. Phys. Cryst.,* 8, 589-591.

Albuquerque, E. L., Sollero, P., & Aliabadi, M. H. (2002). The boundary element method applied to time dependent problems in anisotropic materials. *International Journal of Solids and Structures,* 39, 1405-1422.

Apostol, T. M. (1967) *M* Calculus I. John Wiley and Sons, New York.

Bachteler, J., & Trebin, H.R. (1998). Elastic Green's function of icosahedral quasicrystals. *Eur. Phys. J. B,* 4, 299-306.

Banerjee, P. K., & Watson, J. O. (1986). *Developments in boundary element methods.* Elsevier, London.

Batra, R. C., Qian, L. F., & Chen, L. M. (2004). Natural frequencies of thick square plates made of orthotropic, trigonal, monoclinic, hexagonal and triclinic materials. *Journal of Sound and Vibration,* 270, 1074-1086.

Belytschko, .T, & Hughes, T. J. R. (1983) *Computational methods for transient analysis.* North-Holland, Amsterdam.

Berger, J. R., & Tewary, V. K. (1996). *Green's Functions and Boundary Element Analysis for Modelling of Mechanical Behavior of Advanced Materails.* National Institute of Standarts and Techonology, Special Publication 910, Boulder, Colorado.

Berrini, P., & Wu, K. (1996). Modelling lossy anisotropic dielectric waveguides with the method of lines. *IEEE Tran. Microwave Techn.,* 44(5), 749-59.

Blaaderen, A. (2009). Quasicrystals from nanocrystals. *Mater. Sci.,* 461, 892-893.

Boyce, W.E., & DiPrima, R.C. (1992). *Elementary Differential Equations and Boundary Value Problems.* John Wiley and Sons, New York.

Brown, J. M., Abramson, E. H., & Angel, R. J. (2006). Triclinic elastic constants for low albite. *Phys. Chem. Minerals.,* 33, 256-265.

Buchanan, G. R. (2003). Free vibration of an infinite magneto-electro-elastic cylinder. *J*ournal of Sound and Vibration, 268, 413-426.

Buchwald, V. T. (1959). Elastic waves in anisotropic media. *Proc. R. Soc. Lond. A,* 253, 563-580.

Budreck, D. E. (1992). An eigenfunction expansion of elastic wave Green's function for anisotropic media. *Q. J. Mech. Appl. Math.,* 46, 1-26.

Burridge, R. (1967a). The singularity on the plane lids of the wave surface of elastic media with cubic symmetry. *Q. J. Mech. Appl. Math.,* 20, 41-56.

Burridge, R. (1967b). Lacunas in two-dimensional wave propagation. *Proc. Camb. Phil. Soc.,* 63, 819-845.

Burridge, R. (1971). Lamb's problem for an anisotropic half-space. *Q. J. Mech. Appl. Math.,* 24, 81-98.

Burridge, R., & Qian, J. (2006). The fundamental solution of the time-dependent system of crystal optics. *European Journal of Applied Mathematics,* 17, 63-94.

Carcione, J. M. (2000). *Wave Fields in Real media: Wave Propagation in Anisotropic, Anelastic and Porous media.* Pergamon.

Carrer, J. A. M., & Mansur, W. J. (1999). Stress and velocity in 2D transient elastodynamic analysis by the boundary element method. *Eng. Anal. Boundary Elem.,* 23, 233-245.

Chang, J. H., & Wu, D. J. (2003). Finite element calculation of elastodynamic stress field around a notch tip via contour integrals. *Int. J. Solids Struct.,* 40, 1189-1202.

Chen, W. F., & Lewis, A. D. M. (1983). *Recent advances in engineering mechanics and their impact on civil engineering practice.* ASCE, New Yok.

Chen, W. Q., & Lee, K. Y. (2003). Alternative state space formulations for magnetoelectric thermoelasticity with transverse isotropy and the application to bending analysis of nonhomogeneous plates. *Int. J. Solid. Struct.,* 40, 5689-705.

Chen, W. Q., Ma, Y. L., & Ding, H. J. (2004). On three-dimensional elastic problems of one-dimensional hexagonal quasicrystal bodies. *Mechanics Research Communications,* 31, 633-641.

Chen, W. Q., Lee, K. Y., & Ding, H. J. (2005). On free vibration of non-homogeneous transversely isotropic magneto-electro-elastic plates. *J. Sound Vib.,* 279, 237-51.

Chen, P., Shen, Y., & Tian, X. (2006). Dynamic potentials and Greens functions of a quasi-plane magneto-electro-elastic medium with inclusion. *International Journal of Engineering Science,* 44, 540-553.

Chen, P., & Shen, Y. (2007). Propagation of axial shear magnetoûelectro-elastic waves in piezoelectricûpiezomagnetic composites with randomly distributed cylindrical inhomogeneities. *International Journal of Solids and Structures,* 44, 1511-1532.

Chen, J., Pan, E., & Chen, H. (2007). Wave propagation in magneto-electro-elastic multilayered plates. *International Journal of Solids and Structures,* 44, 1073-1085.

Chen, J., Chen, H., Pan, E., & Heyliger, P. R. (2007). Modal analysis of magneto-electro-elastic plates using the state-vector approach. *Journal of Sound and Vibration,* 304, 722-734.

Chernikov, M. A., Ott, H. R., Bianchi, A., & Darling, T. W. (1998). Elastic Moduli of a Single Quasicrystal of Decagonal Al-Ni-Co: Evidence for Transverse Elastic Isotropy. *Physics Review Letters,* 80, 321-324.

Cohen, G. C. (2002). *Higher-order numerical methods for transient wave equations*. Springer-Verlag, Berlin.

Cohen, G. C., Heikkola, E., Joly, P., Neittaanmaki, P. (2003). *Mathematical and Numerical Aspects of Wave Propagation*. Springer, Berlin.

Courant, R., & Hilbert, D. (1963). *Methods of Mathematical Physics.* Interscience, New York.

Cruse, T. A., & Rizzo, F. J. (1975). *Boundary integral equation method: Computational applications in applied mechanics.* ASME, New York.

Cruse, T. A, Pifko, A. B, & Armen, H. (1985). *Advanced topics in boundary element analysis.* ASME, New York.

Cruse, T. A. (1987). Recent advances in boundary element analysis methods. *Comput. Methods Appl. Mech. Eng.,* 62, 227-244.

Dauksher, W., & Emery, A. F. (2000). The solution of elastostatic and elastodynamic problems with Chebyshev spectral finite elements. *Comput. Methods Appl. Mech. Engrg.* 88, 217-233.

De, P., & Pelcovits, R. A. (1987). Linear elasticity theory of pentagonal quasicrystals. *Phys. Lett. B,* 35, 8609-8620.

Dıaz, R. R., Saez, A., Sanchez, F. G., & Zhang, C. (2008). Time-harmonic Greens functions for anisotropic magnetoelectroelasticity. *International Journal of Solids and Structures,* 45, 144-158.

Dieulesaint, E., & Royer, D. (1980). *Elastic waves in solids.* John Wiley and Sons, Chichester.

Dieulesaint, E. & Royer, D. (2000). *Elastic waves in solids I.* Springer-Verlag, Berlin, Heidelberg.

Ding, D.H., Yang, W.G., Hu, C.Z., & Wang, R.H. (1993). Generalized elasticity theory of quasicrystals. *Phys. Rev. B,* 48, 7003-7010.

Ding, D., Wang, R., Yang, W., Hu, C. (1995). General expressions for the elastic displacement fields induced by dislocations in quasicrystals. *J. Phys. Condens. Matter.,* 7, 5423-5436.

Dmitriev, V. I., Silkin, A. N., & Farzan, R. (2002). Tensor Green function for the system of Maxwell's equations in a layered medium. *Computational Mathematics and Modeling,* 13(2), 107-118.

Donida, G., & Bernetti, R. (1991). Finite element approximation of dynamic problems for semi-infinite solids in elasticity.*Computers and Structures,* 41, 835-842.

Dubois, J. M. (2000). New prospects from potential applications of quasicrystalline materials.*Mater. Sci. Eng.,* 294 - 296, 4 - 9.

Dubois, J. M. (2005). *Useful quasicrystals.* World Scientific, London.

Dunkin, J. W., & Eringen, A. C. (1963). On the propagation of waves in an electromagnetic elastic solid. *Int. J. Engng. Sci.,* 1, 461-495.

Ehrenpreis, L. (1960). Solution of some problems of division. IV. Invertible and elliptic operators. *Amer. J. Math.,* 82, 522-588.

Evans, L. C. (1998). *Partial differential Equationss*. American Mathematical Society, Providence, Rhode Island.

Fan, T. Y. (1999). *The mathematical theory of elasticity of quasicrystals and applications.* Beijing Institute of Technology Press, Beijing (in Chinese).

Fan, T.Y., & Mai, Y.W. (2004). Elasticity theory, fracture mechanics and some relevant thermal properties of quasicrystalline materials. *Appl. Mech. Rev.,* 57 (5), 325-343.

Fan, T.Y., & Guo, L. H. (2005). The final governing equation and fundamental solution of plane elasticity of icosahedral quasicrystals. *Phys. Lett. A,* 341, 235-239.

Federov, I. F. (1968). *Theory of Elastic Waves in Crystals.* Plenum Press, New York.

Fredholm, I. (1908). Sur l'intgrale fondamentale d'une quation differentielle elliptique coefficients constants. *Rend. Circ. Mat. Palermo*, 25, 346-351.

Freund, L. B. (1998). *Dynamic Fracture Mechanics.* Cambridge University Press.

Gao, Y., & Zhao, B.S. (2006). A general treatment of three-dimensional elasticity of quasicrystals by an operator method. *Phys. Stat. Sol. b,* 243, 4007-4019.

Gao, Y., Zhao, B. S., & Xu, S. P. (2008). A Theory of General Solutions of Plane Problems in Two-Dimensional Octagonal Quasicrystals. *J. Elast.,* 93, 263-277.

Gao, Y., Xu, S. P., & Zhao, B. S. (2008). A theory of general solutions of 3D problems in 1D hexagonal quasicrystals. *Phys. Scr.,* 77, 015601 (6pp).

Gao, Y. (2009). Governing equations and general solutions of plane elasticity of cubic quasicrystals. *Phys. Lett. A,* 373, 885-889.

Gao, Y., Xu, S. P., & Zhao, B. S. (2009). General solutions of equilibrium equations for 1D hexagonal quasicrystals . *Mechanics Research Communications,* 36, 302-308.

Garg, N. R., Goel, A., Miglani, A., & Kumar, R. (2004). Elastodynamic response of an anisotropic medium due to a line-load. *Earth Planets Space,* 56, 407-417.

Goldberg, J. L. (1992). *M*atrix theory with applications. McGrawHill International Editions.

Gottis, P. G., & Kondylis, G. D. (1995). Properties of the dyadic Green's function for unbounded anisotropic medium. *IEEE Trans. Anten. Propag.,* 45, 154-61.

Grimmer, H. (2008). Elasticity properties of two-dimensional quasicrystals. *Acta Cryst.,* A64, 459-464.

Hu, C., Yang, W., Wang, R., & Ding, D. H. (1996). Point groups and elastic properties of two-dimensional quasicrystals. *Acta Crystallogr.,* 52, 251-256.

Haba, Z. (2004). Green functions and propagation of waves strongly inhomogeneous media. *J. Phys A: Math Gen.*, 37, 9295-302

Harada, K., & Sasahara, H. (2009). Effect of dynamic response and displacement/stress amplitude on ultrasonic vibration cutting. *Journal of Materials Processing Technology,* 209, 4490-4495.

Hachemi, M. E. (2008). Callé, S., Remenieras, J. P. (2008). Transient displacement induced in shear wave elastography: Comparison between analytical results and ultrasound measurements. *Ultrasonics,* 44, e221-e225.

Hearmon, R. F. S. (1956). *Adv. Phys.,* 5, 323-382.

Hormander, L. (1963). *Linear Partial Differential Operators.* Springer, Berlin.

Hu, C., Wang, R., & Ding, D. H. (2000). Symmetry groups, physical property tensors, elasticity and dislocations in quasicrystals. *Rep. Prog. Phys.,* 63, 1-39.

Huang, K., & Wang, M. (1991). Fundamental solution of bi-material elastic space. *Sci. China.,* 34, 309-315.

Karamany, A. S. (2009). Uniqueness theorem and Hamiltons principle in linear micropolar thermopiezoelectric/piezomagnetic continuum with two relaxation times. *M*eccanica, 44, 47-59.

Kausel, E. (2006). *Fundamental Solutions in Elastodynamics,* Cambridge University Press.

Khojasteh, A., Rahimian, M., & Pak, R. Y. S. (2008). Three-dimensional dynamic Greens functions in transversely isotropic bi-materials. *International Journal of Solids and Structures,* 45, 4952-4972.

Kocak, H., & Yildirim, A. (2009). Numerical solution of 3D Fundamental solution for the dynamic system of anisotropic elasticity. *Physics Letters A,* 373, 3145-3150.

Kong, J. A. (1986). *E*lectromagnetic Wave Theory. Wiley, New York.

Kraut, E. A. (1963). Advances in the theory of anisotropic elastic wave propagation. *Rev. Geophys.,* 1, 401-448.

Lax, P. T. (2006). *Hyperbolic Partial Differential Equations*. American Mathematical Society, Providence, Rhode Island.

Lei, J., Wang, R., Hu, C., & Ding, D. (1998). Diffuse scattering from pentagonal quasicrystals. *Phys. Lett. A,* 247, 343-352.

Lei, J., Hu, C., Wang, R., & Ding, D. (1999). Diffuse scattering from octagonal quasicrystals. *J. Phys.: Condens. Matter,* 11, 1211-1223.

Lei, J., Wang, R., Hu, C., & Ding, D. (2000). Diffuse scattering from dodecagonal quasicrystals. *Eur. Phys. J. B,* 13, 21-30.

Levine, D., Lubensky, T. C., Ostlund, S., Ramaswamy, S., Steinhardt, P. J., & Toner, J. (1985). Elasticity and dislocations in pentagonal and icosahedral quasicrystals. *Phys. Rev. Lett.,* 54, 1520-1523.

Li, L. W., Liu, S., Leong, M. S., & Yeo, T. S. (2001). *Circular cylindrical waveguide filled with uniaxial anisotropic media-electromagnetic fields and dyadic Green's functions*. IEEE Tran. Microwave Techn., 49 (7), 1361–4.

Li, L. H., & Fan, T. Y. (2006). Final governing equation of plane elasticity of icosahedral quasicrystals and general solution based on stress potential function. *Chin. Phys. Lett.* 23, 2519-2521.

Li, L. H., & Fan, T. Y. (2006). Final Governing Equation of Plane Elasticity of Icosahedral Quasicrystals and General Solution Based on Stress Potential Function. *Chin. Phys. Lett.,* 23, 2519-2521.

Li, W., Fan, T.Y., & Wu, Y. L. (2009). Plastic analysis of crack problems in three-dimensional icosahedral quasicrystalline material. *Phil. Mag.,* 89, 2823-2831.

Lighthill, M. J. (1960). Anisotropic wave motions. *Phil. Trans. R. Soc. Lond. A* 252, 397-470.

Lindell 1990. IV. Time-domain TE/TM decomposition of electromagnetic sources. *IEEE Transi Anteni Propag.*, 38(3), 353-8.

Liu, Y. Y., Fu, X. J., & Dong, X. Q. (1997). Physical properties of one dimensional quasicrystals. *Prog. Phys.,* 17, 1-63 (in Chinese).

Liu, G. T., Fan, T. Y., & Guo, R. P. (2003). Displacement function and simplifying of plane elasticity problems of two-dimensional quasicrystals with noncrystal rotational symmetry. *Mechanics Research Communications,* 30, 335-344.

Liu, G. T., Fan, T. Y., & Guo, R. P. (2004). Governing equations and general solutions of plane elasticity of one-dimensional quasicrystals. *International Journal of Solids and Structures,* 41, 3949-3959.

Love, A. E. H. (1944). *A treatise on the mathematical theory of elasticity.* 4th ed., Dover, New York.

Malgrange, B. (1955-1956). Existence et approximation des solutions des équations aux dérivées partielles et des équations de convolution.(French) *Ann. Inst. Fourier, Grenoble,* 6, 271-355.

Manolis, G. D., Shaw, R. P., & Pavlou, S. (1998). A first order system solution for the vector wave equation in a restricted class of heterogeneous media. *Journal of Sound and Vibration,* 209, (5), 723-752.

Mansur, W. J., Loureiro, F. S., Soares, Jr., & Dors, C. (2007). Explicit time-domain approach based on numerical Green's functions computed by finite differences-the ExGA family. *J. Comput. Phys.,* 227, 851-870.

Mansur, W. J., & Loureiro, F. S. (2009). An efficient hybrid time-Laplace domain method for elastodynamic analysis based on the explicit Greens approach. *Int. J. Solids Struct.,* 46, 3093-3102.

Merlin, R., Bajema, K., Clarke, R., Juang, F. Y., & Bhattacharya, P. K. (1985). Quasiperiodic GaAs-AlAs Heterostructures. *Physical Review Letters,* 55, 1768-1770.

Mindlin, R. D. (1936). Force at point in the interior of a semi-infinite solid. *Physics,* 7, 195-202.

Mizohata, J. (1973). *The theory of partial differential equations*. Translated from the Japanese by Katsumi Miyahara. New York: Cambridge University Press.

Monk, P. (2003). *Finite Element Methods for Maxwell's Equations*. Oxford, Clarendon Press.

Moosavi, M. R., & Khelil, A. (2009). Finite volume meshless local Petrov-Galerkin method in elastodynamic problems. *Eng. Anal. Boundary Elem.,* 33, 1016-1021.

Musgrave, M. J. P. (1970). *Crystal Acoustics.* Holden-Day, Inc., San Francisco, CA.

Nagle, R. K., Saff, E. B., & Snider, A. D. (2004)) *Fundamentals of Differential Equations and Boundary Value Problems,* Addison Wesley, Boston.

Niwa, Y., Fukui, T., Kato, S., & Fujiki, K. (1980). An application of the integral equation method to two-dimensional elastodynamics. *Theoretical and applied mechanics,* 28, 281-290.

Nye, J.F., (1957). *Physicsal Properties of Crystals*. Oxford Univesity Press, Oxford.

Nye, J.F., (1967). *Physical Properties of Crystals: Their Presentation by Tensors and Matrices*. Clarendon Press, Oxford.

Ortner N., & Wagner P. (2004). Fundamental matrices of homogeneous hyperbolic systems. Application to crystal optics, electrodynamics, and piezoelectromagnetism. *Z Angew Math. Mech.,* 84 (5), 314-46.

Ovidko, I. A. (1998). Plastic deformation and decay of dislocations in quasi-crystals. *Mater. Sci. Eng. A,* 154, 29-33.

Pan, E., Heyliger, P. R. (2002). Free vibration of simply supported and multilayered magneto-electro-elastic plates. *Journal of Sound and Vibration,* 252, 429-442.

Payton, R. G. (1983). *Elastic wave propagation in transversely isotropic media.* Martinus Nijhoff, Dordrecht.

Payton, R. G. (1992). Wave propagation in a restricted transversely isotropic solid whose slowness surface contains conical points. *Q.J. Mech. Appl. Math.,* 45, 183-197.

Peng, Y., & Fan, T. (2000). Elastic theory of 1D-quasiperiodic stacking of 2D crystals. *J. Phys.: Condens. Matter,* 12, 9381-9387.

Peng, Y. & Fan, T. (2001). Crack and indentation problems for one-dimensional hexagonal quasicrystals. *Eur. Phys. J. B,* 21, 39-44.

Peng, Y., Fan, T., Zhang, W., & Sun, Y. (2001). Perturbative method for solving elastic problems of one-dimensional hexagonal quasicrystals. *J. Phys. Condens. Matter,* 13, 4123-4128.

Peng, Y., & Fan, T. Y. (2002). Perturbation theory of 2D decagonal quasicrystals. *Physica B,* 311, 326-330.

Pope, C. (2010). *Electromagnetic Theory II.* Retrieved April 5, 2011, from http://faculty.physics.tamu.edu/pope/EM611/em611-2010.pdf.

Poruchikov, V. B. (1993). *Methods of the Classical Theory of Elastodynamics.* Springer Verlag, Berlin.

Priimenko, V., & Vishnevskii, M. (2005). An inverse problem of electromagnetoelasticity in the case of complete nonlinear interaction. *J. Inverse Ill-Posed Probl.,* 13, 277-301.

Priimenko, V., & Vishnevskii, M. (2008). The first initial-boundary-value problem for a nonlinear model of the electrodynamics of vibrating elastic media. *Nonlinear Anal.,* 68, 2913-2932.

Priimenko, V., & Vishnevskii, M. (2010). Direct problem for a nonlinear evolutionary system. *Nonlinear Analysis,* 73, 1767-1782.

Ramo, S., Whinnery, J. R., & Duzer, T. (1994). *Fields and Waves in Communication Electronics*. Wiley, New York.

Rangelov, T. V. (2003). Scattering from cracks in an elasto-anisotropic plane. *J. Theoret. Appl. Mech.,* 33, 55-72.

Rangelov, T. V., Manolis, G. D., & Dineva, P. S. (2008). Elastodynamic fundamental solutions for certain families of 2d inhomogeneous anisotropic domains: basic derivations, *European Journal of Mechanics A/Solids,* 24, 820-836.

Reed, M., & Simon, B. (1975). *Methods of Modern Mathematical Physics II: Fourier analysis, Self-adjointness.* Academic Press, New York.

Reed M., & Simon B. (2005). *Methods of modern mathematical physics. II. Fourier analysis, self-adjointness*. Academic Press, New York.

Rochal, S.B., & Lorman, V.L. (2002). Minimal model of the phonon-phason dynamics in icosahedral quasicrystals and its application to the problem of internal friction in the i-AlPbMn alloy. *Phys. Rev. B,* 66, 144-204.

Ronchetti, M. (1987). Quasicrystals, an introduction overview. *Phil. Mag.,* 56, 237-249.

Shechtman, D., Blech, I., Gratias, D., & Cahn, J.W. (1984). Metallic phase with long-range orientational order and no translational symmetry. *Phys. Rev. Lett.,* 53, 1951û1953.

Sladek, J., Sladek, V., & Zhang, C. (2005). An advanced numerical method for computing elastodynamic fracture parameters in functionally graded materials. *Comp. Mater. Sci.,* 32, 532-543.

Soares, Jr., & Mansur, W. J. (2005). A time domain FEM approach based on implicit Green's functions for nonlinear dynamic analysis. *Int. J. Numer. Methods Eng.,* 62, 664-681.

Socolar, J. E. S., Lubensky, T. C., & Steinhardt, P. J. (1986). Phonons, phason and dislocations in quasicrystals. *Phys. Rev. B,* 34 (5), 3345-3360.

Socolar, J. E. S. (1989). Simple octagonal and dodecagonal quasicrystals. *Phys. Rev. B,* 39, 10519-10551.

Stokes, G. G. (1849). On the dynamical theory of diffraction. *Trans. Camb. Phil. Soc.,* 9, 1-62.

Stokes, G. G. (1883). *Mathematical and physical papers*. Cambridge University Press.

Tewary, V. K., & Fortunko, C. M. (1992). Computationally efficient representation for propagation of elastic waves in anisotropic solids. *J. Acoust. Soc. A.,* 91, 1888-1896.

Tewary, V. K. (1995). A computationally efficient representation for elastostatic and elastodynamic Fundamental solutions for anisotropic solids. *Physical Review B,* 51-22.

Tikhonov, A. N., & Samarskii, A. A. (1963). *Equations of mathematical physics.* Pergamon Press, New York.

Ting, T. C. T., Barnett, D. M., & Wu, J. J. *Modern Theory of Anisotropic Elasticity and Applications,* SIAM, Philadelphia (1990).

Ting, T. C. T. (1996). *Anisotropic Elasticity: Theory and Applications.* Oxford University Press, Oxford.

Tsai, Y. H., & Wu, C. P. (2008). Dynamic responses of functionally graded magnetoelectro- elastic shells with open-circuit surface conditions. *Int. J. Eng. Sci.,* 46, 843-857.

Tsvankin, I. D., & Chesnokov, Y. M. (1989). Wave fields of point sources in arbitrarily anisotropic media. *Izv. Earth Phys.,* 25, 528-540.

Vavrycuk, V. (2001). Exact elastodynamic Green functions for simple types of anisotropy derived from higher-order ray theory. *Stud. Geophys. Geod.,* 45, 67-84.

Vavrycuk, V. (2002). Asymptotic elastodynamic Green function in the kiss singularity in homogeneous anisotropic solids. *Stud. Geophys. Geod.,* 46, 249-266.

Vera-Tudela, C. A. R., & Telles, J. C. F. (2005). A numerical Greens function and dual reciprocity BEM method to solve elastodynamic crack problems. *Eng. Anal. Boundary Elem.,* 29, 204-209.

Vladimirov, J.V.S. (1971). *Equations of Mathematical Physics.* Marcel Dekker, New York.

Vladimirov, V.S. (1979). *Generalized Functions in Mathematical Physics.* Mir Publishers, Moscow.

Volterra, V. (1894). Sur les vibrations des corps èlastiques isotropes. *Acta Mathematica*, 18(1), 161-232.

Wang, N., Chen, H., & Kuo, K. H. (1987). Two-dimensional quasicrystal with eight-fold rotational symmetry.*Phys. Rev. Lett.,* 59, 1010-1013.

Wang, N., Chen, H., & Kuo, K. H. (1987). Two-dimensional quasicrystal with eight-fold rotational symmetry. *Phys. Rev. Lett.* 59, 1010-1013.

Wang, C. Y., & Achenbach, J. D. (1992). A new look at 2D time domain elastodynamic Green's functions for general anisotropic solids. *Wave motion,* 16, 389-405.

Wang, C. Y., & Achenbach, J. D. (1994). Elastodynamic fundamental solutions for anisotropic solids. *Geophys. J. Int.,* 118, 384-392.

Wang, C. Y., & Achenbach, J. D. (1995). Three-Dimensional Time-Harmonic Elastodynamic Fundamental solutions for anisotropic solids. *Proc. R. coc. Lond.,* A449, 441-458.

Wang, C. Y., Achenbach, J. D., & Hirose, S. (1996). Two-dimensional time domain BEM for scattering of elastic waves in solids of general anisotropy. *Int. J. Solids Structures,* 33, 3843-3864.

Wang, R. H., Yang, W. G., & Hu, C. Z. (1997). Point and space groups and elastic behaviors of one dimensional quasicrystals. *J. Phys: Condens. Matter,* 9, 2411-2422.

Wang, B. L., & Mai, Y. W. (2004). Fracture of piezoelectromagnetic materials. *Mechanics Research Communications.,* 31, 65-73.

Wang, X. (2006). The general solution of one-dimensional hexagonal quasicrystal.*Mech. Res. Commun.,* 33, 576-580.

Wang, X., Pan, E., & Feng, W. J. (2007). Time-dependent Green's functions for an anisotropic bimaterial with viscous interface. *European Journal of Mechanics A/Solid,* 26, 901-908.

Wijnands F., Pendry, J. B., Garcia-Vidal, F. J., Bell, P. M., Roberts, P. J., & Moreno, L. M. (1997). Green's functions for Maxwell's equations; application to spontaneous emission. *Opt. Quantum Electron,* 29, 199-216.

Willis, J. R. (1973). Self-similar problems in elastodynamics. *Phil. Trans. R. Soc. London A,* 274, 435-491.

Wollgarten, M., Beyss, M., Urban, K., Liebertz, H., & Koster, U. (1993). Direct evidence for plastic deformation of quasicrystals by means of a dislocation mechanism. *Phys. Rev. Lett.,* 71, 549-552.

Wu, J. J., Ting, T. C. T., & Barnett, D. M. (1990). *Modern Theory of Anisotropic Elasticity and Applications.* SIAM, Philadelphia, PA.

Wu, B., Yu, J., & He, C. (2008). Wave propagation in non-homogeneous magneto-electro-elastic plates . *J. Sound Vib.,* 317, 250-264.

Wu, C. P., & Lu, Y. C. (2009). A modified Pagano method for the 3D dynamic responses of functionally graded magneto-electro-elastic plates. *Compos. Struct.,* 90, 363 - 372.

Wu, C. P., & Tsai, Y. H. (2010). Dynamic responses of functionally graded magneto-electro-elastic shells with closed-circuit surface conditions using the method of multiple scales. *European Journal of Mechanics A/Solids.,* 29, 166-181.

Yagawa, G., & Atluri, S. N. *Computational mechanics.* Springer-Verlag, Tokyo (1986).

Yakhno, V. G., & Merazhov, I. Z. (2000).Direct Problems and a One-Dimensional Inverse Problem of Electromagnetoelasticity for ôSlow Waves. *Siberian Advances in Mathematics,* 10, 87-150.

Yakhno, V. G., & Akmaz, H. K. (2005). Initial value problem for dynamic problem of anisotropic elasticity. *International Journal of Solids and Structures,* 42, 855-876.

Yakhno, V. G. (2005). Constructing Green's functions for time-depending Maxwell system in anisotropic dielectrics. *J. Phys. A: Math. Gen.,* 38, 2277-2287.

Yakhno, V. G., Yakhno, T. M., & Kasap, M. (2006). A novel approach for modelling and simulation of electromagnetic waves in anisotropic dielectrics. *International Journal of Solids and Structures,* 43, 6261-6276.

Yakhno, V. G., & Akmaz, H. K. (2007). Anisotropic elastodynamics in a half space: An analytic method for polynomial data. *Journal of Computational and Applied Math.,* 204, 268-281.

Yakhno, V. G., & Yakhno, T. M. (2007). Modelling and simulation of electric and magnetic fields in homogeneous non-dispersive anisotropic nmmaterials. *Computers and Structures,* 85, 1623-1634.

Yakhno, V. G. (2008). Computing and Simulation of time-dependent electromagnetic fields in homogeneous anisotropic materials. *International Journal of Engineering Science,* 46, 411-426.

Yakhno, V., & Altunkaynak, M. (2008). A new method for computing a solution of the Cauchy problem with polynomial data for the system of crystal optics. *Internatioan Journal of Computer Mathematics,* 1-16.

Yakhno, V. G., & Sevimlican, A. (2010). Solving an initial value problem in inhomogeneous electrically and magnetically anisotropic uniaxial media. *App. Math. Comp.,* 215, 3839-3850.

Yahkhno, V.G., & Yaslan H.C. (2011). Three dimensional elastodynamics of 2D quasicrystals: The derivation of the time-dependent fundamental solution. *Appl. Math. Modell.* 35, 3092-3110.

Yang, W. G., Wang, R. H., Ding, D. H., & Hu, C. Z. (1993). Linear elasticity theory of cubic quasicrystals. *Phys. Rev. B,* 48, 6999-7002.

Yang, W. G., Hu, C. Z., Ding, D. H., & Wang, R. (1995a). *Phys. Rev. B,* 51, 3906.

Yang W. G., Hu C. Z., Ding D. H. and Wang R. (1995b). *J. Phys. Condens. Matter,* 7, 7099.

Yang, B., Pan, E., & Tewary, V. K. (2004). Three-dimensional Greens functions of steady-state motion in anisotropic half-spaces and bimaterial. *Engineering Analysis with Boundary Elements,* 28, 1069-1082.

Yao, D., Wang, R., Ding, D., & Hu, C. (1997). Evaluation of some useful integrals in the theory of dislocations in quasicrystals. *Phys. Lett. A,* 225, 127-133.

Yu, J., Ma, Q., & Su, S. (2008). Wave propagation in non-homogeneous magneto-electro-elastic hollow cylinders. *Ultrasonics.,* 48, 664-667.

Yu, J., & Wu, B. (2009).Circumferential wave in magneto-electro-elastic functionally graded cylindrical curved plates . *European Journal of Mechanics A/Solids.,* 28, 560-568.

Zhong, Z., & Yu, T. (2006). Vibration of a simply supported functionally graded piezoelectric rectangular plate. *Smart Mater. Struct.,* 15, 1404-1412.

Zhou, W. M., & Fan, T.Y. (2000). Axisymmetric elasticity problem of cubic quasicrystal. *Chinese Phys.,* 9, 295-303.

Zhu, H. (1992). A method to evaluate three-dimensional time-harmonic elastodynamic Green's functions in transversely isotropic media. *J. Appl. Mech., ASME,* 59, 587-590.

CHAPTER

APPENDIX

A.1 Some Facts From Matrix Theory

This section contains some basic facts from matrix theory related with symmetric and positive-definite matrices, which are used inside the thesis (Goldberg (1992)).

Theorem A.16. *Let* $\mathbf{C}$ *be a real, symmetric, positive-definite matrix of dimension* $m \times m$*. Then* $\mathbf{C}^{-1}$ *is a real, symmetric, positive-definite matrix.*

Proof. Since $\mathbf{C}^{-1}\mathbf{C} = \mathbf{C}\mathbf{C}^{-1} = \mathbf{I}$, using the symmetry property of $\mathbf{C}$ and the rule $(\mathbf{AB})^* = \mathbf{B}^*\mathbf{A}^*$ we get $\mathbf{I} = \mathbf{C}(\mathbf{C}^{-1})^*$. Multiplying both sides of the last equality by $\mathbf{C}^{-1}$ from left-hand side we get $\mathbf{C}^{-1} = (\mathbf{C}^{-1})^*$, which implies symmetry property of $\mathbf{C}^{-1}$.

If λ is an eigenvalue of $\mathbf{C}$, then $\frac{1}{\lambda}$ is an eigenvalue of $\mathbf{C}^{-1}$. Since the eigenvalues of a positive-definite matrix are positive, all eigenvalues of $\mathbf{C}$ are positive, which implies that $\mathbf{C}^{-1}$ has all positive eigenvalues. Hence $\mathbf{C}^{-1}$ is positive-definite. □

Theorem A.17. *Let* $\mathbf{C}$ *be a real, symmetric, positive-definite matrix of dimension* $m \times m$*. Then there exists a real, symmetric, positive-definite matrix* $\mathbf{M}$ *such that* $\mathbf{C}^{-1} = \mathbf{M}^2$.

Proof. According to Theorem A.16, $\mathbf{C}^{-1}$ is real, symmetric, positive-definite and is congruent to a diagonal matrix of its eigenvalues. That is, there exists an orthogonal matrix $\mathbf{Q}$ such that

$$\mathbf{Q}^*\mathbf{C}^{-1}\mathbf{Q} = \Lambda, \qquad \mathbf{Q}^* = \mathbf{Q}^{-1}.$$

Since $\mathbf{C}^{-1}$ is symmetric and positive-definite, its eigenvalues λ_i, $i = 1,2,\ldots,m$ are real and positive. Let $\Lambda^{\frac{1}{2}}$ and $\mathbf{M}$ be defined as follows

$$\Lambda^{\frac{1}{2}} = \mathrm{diag}(\lambda_i^{\frac{1}{2}}, i = 1,2,\ldots,m), \qquad \mathbf{M} = \mathbf{Q}\Lambda^{\frac{1}{2}}\mathbf{Q}^*.$$

Noting that $\mathbf{Q}$ is orthogonal we have $\mathbf{Q}^*\mathbf{Q} = \mathbf{I}$, and therefore

$$\mathbf{M}^2 = (\mathbf{Q}\Lambda^{\frac{1}{2}}\mathbf{Q}^*)(\mathbf{Q}\Lambda^{\frac{1}{2}}\mathbf{Q}^*) = \mathbf{Q}\Lambda\mathbf{Q}^* = \mathbf{C}^{-1}.$$

Clearly, $\mathbf{M} = \mathbf{Q}\Lambda^{\frac{1}{2}}\mathbf{Q}^*$ is positive-definite. □

Theorem A.18. *Let $\mathbf{A}_j, \mathbf{S}$ be real and symmetric matrices of dimension $m \times m$. Then the matrix $\tilde{\mathbf{A}}_j = \mathbf{S}\mathbf{A}_j\mathbf{S}$ is real and symmetric.*

Proof. The proof follows from equalities

$$\tilde{\mathbf{A}}_j^* = (\mathbf{S}\mathbf{A}_j\mathbf{S})^* = \mathbf{S}^*(\mathbf{S}\mathbf{A}_j)^* = \mathbf{S}^*\mathbf{A}_j^*\mathbf{S}^* = \mathbf{S}\mathbf{A}_j\mathbf{S} = \tilde{\mathbf{A}}_j.$$

□

A.2 Some Existence and Uniqueness Theorems for Symmetric Hyperbolic Systems

In this section we present the existence and uniqueness theorems for symmetric hyperbolic systems of the first order. For the statements of these theorems we will use the following notation. $L^2(R^n, R^m)$, $C^k(R^n, R^m)$, $H^k(R^n, R^m)$, $k = 0,1,...$, consist of all vector functions $\mathbf{w} = (w_1, w_2, ..., w_n)$ such that w_j belongs to $L^2(R^n)$, $C^k(R^n)$, $H^k(R^n)$, $L^2(R^n)$, $j = 1,2,...,m$, respectively. Here C^k is the space of k times continuously differentiable functions; H^k is Sobolev space (Evans (1998)) and $L^2 = H^0$, $C = C^0$.

The spaces $C^1([0,T];H^k(R^n;R^m))$, $C^1([0,T];C^k(R^n;R^m))$ are the spaces of all k times continuously differentiable functions with respect to t which is defined by from $[0,T]$ to $H^k(R^n;R^m)$ and $[0,T]$ to $C^k(R^n;R^m)$, respectively. The space $M^{m\times m}$ is the space of all matrices of dimension $m\times m$.

Let $x=(x_1,x_2,...,x_n)\in R^n$, $t\in[0,\infty)$. Consider the system (Evans, 1998)

$$u_t+\sum_{i=1}^{n}A_i(x,t)u_{x_i}+B(x,t)u(x,t)=F(x,t). \tag{A.307}$$

Here the unknown $u:R^n\times[0,\infty)\to R^m$, and the functions $A_i(x,t),B(x,t):R^n\times[0,\infty)\to M^{m\times m}(i=1,2,...n),F:R^n\times[0,\infty)\to R^m$ are given. Fix $\xi\in R^n$. Let

$$A(x,t,\xi)=\sum_{i=1}^{n}A_i(x,t)\xi_i,$$

The system (A.307) is called hyperbolic if the matrix $A(x,t,\xi)$ is diagonalizable for all $x,\xi\in R^n,t>0$.

In particular, a system is hyperbolic if the matrix $A(x,t,\xi)$ has m real eigenvalue

$$\lambda_1(x,t,\xi)\le\lambda_2(x,t,\xi)\le...\le\lambda_m(x,t,\xi),$$

and corresponding eigenvectors $r_i(x,t,\xi)(i=1,2,...n)$ which form a basis of R^m for all $\xi,x\in R^n,t>0$. There are two special cases of hyperbolocity which we now define.

1) If $A_i(x,t)$ is symmetric for $i=1,2,...n$, then $A(x,t,\xi)$ is symmetric for all $\xi\in R^n$. Recall that if the $m\times m$ matrix $A(x,t,\xi)$ is symmetric, then it is diagonalizable. For the case when the matrices $A_i(x,t)$ are all symmetric we say that the system (A.307) is symmetric hyperbolic.

2) If $A(x,t,\xi)$ has m real, distinct eigenvalues

$$\lambda_1(x,t,\xi) < \lambda_1(x,t,\xi) < ... < \lambda_m(x,t,\xi),$$

for all $x,\xi \in R^n, t > 0$, then $A(x,t,\xi)$ is diagonalizable. In this case, we say system (A.307) is strictly hyperbolic.

Consider the initial value problem a symmetric hyperbolic system of the first order. Let the symmetric hyperbolic system be written in the form

$$\frac{\partial \mathbf{V}}{\partial t} + \sum_{j=1}^{3} \mathbf{A}_j \frac{\partial \mathbf{V}}{\partial x_j} = \mathbf{F}, \ x \in R^n, \ t \in (0,T) \tag{A.308}$$

$$\mathbf{V}(x,0) = \phi(x) \ x \in R^n, \tag{A.309}$$

where T is a fixed positive number, $\mathbf{V} = (V_1,...,V_n)$ is the vector function with components $V_j = V_j(x,t)$, $j = 1,2,...,n$, $\mathbf{A}_j$, $j = 1,2,...,n$ are real, symmetric, $m \times m$ matrices with constant elements.

In this part of the section, we adjust the general approach (Courant & Hilbert (1962)) for finding stability estimates of solutions for the symmetric hyperbolic system. Let the symmetric hyperbolic system be written in the form given with the equations (A.308)-(A.309).

Let $\xi = (\xi_1,...,\xi_n) \in R^n$ and $\mathbf{A}(\xi) = \sum_{j=1}^{n} \mathbf{A}_j \xi_j$ and $\lambda_j(\xi)$, $j = 1,\ldots,9$ be the eigenvalues of $\mathbf{A}(\xi)$. We define the constant M as

$$M = \max_{i=1,...,9} \max_{|\xi|=1} |\lambda_i(\xi)|. \tag{A.310}$$

Let T be a given positive number. Using M and T we define the following domains

$$\Gamma(P) = \{(x,t) : 0 \le t \le T, |x| \le M(T-t)\}, \tag{A.311}$$

$$S(h) = \{x \in R^n : |x| \le M|T-h|, \quad 0 \le h \le T\}, \tag{A.312}$$

$$R(h) = \{(x,t) : 0 \le t \le h, |x| = M|T-t|\}. \tag{A.313}$$

Here Γ is the conoid with vertex $(0,T)$; $S(h)$ is the surface constructed by the intersection of the plane $t = h$ and the conoid Γ; $R(h)$ is the lateral surface of the conoid Γ bounded by $S(0)$ and $S(h)$. Let Ω be the region in $R^n \times (0,\infty)$ bounded by $S(0)$, $S(h)$ and $R(h)$ with boundary $\partial\Omega = S(0) \cup S(h) \cup R(h)$. Further we assume that $\phi(x)$, $\mathbf{F}(x,t)$, $\mathbf{V}(x,t)$ are vector functions with continuously differentiable components in $S(0)$ and Γ, respectively. Multiplying (A.308) with $\mathbf{V}$ and integrating over Ω we have

$$\int_\Omega \mathbf{V}.\frac{\partial \mathbf{V}}{\partial t} + \mathbf{V}.\left(\sum_{j=1}^{n} \mathbf{A}_j \frac{\partial \mathbf{V}}{\partial x_j}\right) dxdt = \int_\Omega \mathbf{F}.\mathbf{V} dxdt. \tag{A.314}$$

Noting the relations

$$\mathbf{V}.\frac{\partial \mathbf{V}}{\partial t} = \frac{1}{2}\frac{\partial |\mathbf{V}|^2}{\partial t},$$
$$\mathbf{V}.\left(\sum_{j=1}^{n} \mathbf{A}_j \frac{\partial \mathbf{V}}{\partial x_j}\right) = \frac{1}{2}\sum_{j=1}^{n} \frac{\partial}{\partial x_j}\left(\mathbf{V}.\mathbf{A}_j\mathbf{V}\right)$$

we rewrite (A.314) as

$$\frac{1}{2}\int_\Omega \frac{\partial |\mathbf{V}|^2}{\partial t} + \sum_{j=1}^{n} \frac{\partial}{\partial x_j}\left(\mathbf{V}.\mathbf{A}_j\mathbf{V}\right) dxdt = \int_\Omega \mathbf{F}.\mathbf{V} dxdt.$$

Applying divergence theorem to left hand side of the last equality we find

$$\frac{1}{2}\int_{\partial\Omega} |\mathbf{V}|^2 \nu_t + \sum_{j=1}^{n} \left(\mathbf{V}.\mathbf{A}_j\mathbf{V}\right)\nu_j dS = \int_\Omega \mathbf{F}.B\mathbf{V} dxdt, \tag{A.315}$$

where $\nu = (\nu_1, \ldots, \nu_n, \nu_t)$ is the outward unit normal on $\partial\Omega$. Since $\partial\Omega = S(0) \cup S(h) \cup$

$R(h)$ and

$$\begin{aligned}
\nu &= (0,\ldots,1) \quad \text{on} \quad S(h),\\
\nu &= (0,\ldots,-1) \quad \text{on} \quad S(0),\\
\nu &= \frac{(x_1,\ldots,x_n,M^2(T-t))}{(T-t)M\sqrt{1+M^2}} \quad \text{on} \quad R(h),
\end{aligned}$$

formula (A.315) takes the form

$$\begin{aligned}
\frac{1}{2}\int_{S(h)}|\mathbf{V}(x,h)|^2dx &- \frac{1}{2}\int_{S(0)}|\mathbf{V}(x,0)|^2dx+\frac{1}{2}\int_{R(h)}|\mathbf{V}(x,t)|^2\frac{M}{\sqrt{1+M^2}}dS\\
&+ \frac{1}{2}\int_{R(h)}\sum_{j=1}^{n}\left(\mathbf{V}.\mathbf{A}_j\mathbf{V}\right)\frac{x_j}{(T-t)M\sqrt{1+M^2}}dS\\
&= \frac{1}{2}\int_0^h\int_{S(t)}\mathbf{F}(x,t).\mathbf{V}(x,t)dxdt \qquad (A.316)
\end{aligned}$$

Let us denote

$$\xi_j=\frac{(x_j)}{(T-t)M}\,,\quad j=1,\ldots,n,$$

which satisfies $|\xi|=\sqrt{\xi_1^2+\ldots+\xi_n^2}=1$. Using

$$\mathbf{A}(\xi)=\sum_{j=1}^{n}\mathbf{A}_j\xi_j$$

we write the following equality

$$\begin{aligned}
&\frac{1}{2}\int_{R(h)}\sum_{j=1}^{n}\left(\mathbf{V}.\mathbf{A}_j\mathbf{V}\right)\frac{x_j}{(T-t)M\sqrt{1+M^2}}dS\\
&\quad=\frac{1}{2\sqrt{1+M^2}}\int_{R(h)}\sum_{j=1}^{n}\left(\mathbf{V}.\mathbf{A}_j\xi_j\mathbf{V}\right)dS\\
&\quad=\frac{1}{2\sqrt{1+M^2}}\int_{R(h)}\left(\mathbf{V}.\mathbf{A}(\xi)\mathbf{V}\right)dS \qquad (A.317)
\end{aligned}$$

Substituting (A.317) into (A.316) we get

$$\begin{aligned} & \frac{1}{2}\int_{S(h)} |\mathbf{V}(x,h)|^2 dx - \frac{1}{2}\int_{S(0)} |\mathbf{V}(x,0)|^2 dx \\ + & \frac{1}{2\sqrt{1+M^2}}\int_{R(h)} \left[|\mathbf{V}|^2 M + \mathbf{V}.\mathbf{A}(\xi)\mathbf{V}\right] dS \\ = & \int_0^h \int_{S(t)} \mathbf{V}(x,t).\mathbf{F}(x,t) dx dt \end{aligned} \tag{A.318}$$

Let us consider the matrix $M\mathbf{I}+\mathbf{A}(\xi)$, where $\mathbf{I}$ is the identity matrix of order $m \times m$. Since $\mathbf{A}(\xi)$ is diagonalizable we can find a matrix $\mathbf{Z}$ which reduces $\mathbf{A}(\xi)$ to a diagonal matrix of its eigenvalues, denoted $\Lambda = \mathrm{diag}(\lambda_1, \lambda_2, \ldots, \lambda_m)$. Multiplying $M\mathbf{I}+\mathbf{A}(\xi)$ with matrix $\mathbf{Z}$ from right, and with its inverse $\mathbf{Z}^{-1}$, from left we have

$$\begin{aligned} \mathbf{Z}^{-1}\left(M\mathbf{I}+\mathbf{A}(\xi)\right)\mathbf{Z} &= \mathbf{Z}^{-1}M\mathbf{I}\mathbf{Z} + \mathbf{Z}^{-1}\mathbf{A}(\xi)\mathbf{Z} = M\mathbf{I} + \mathbf{Z}^{-1}\mathbf{A}(\xi)\mathbf{Z} \\ &= M\mathbf{I}+\Lambda. \end{aligned} \tag{A.319}$$

Noting (A.310), we conclude that the matrix $M\mathbf{I}+\Lambda$ has non-negative elements on the diagonal. It means that the matrix $M\mathbf{I}+\mathbf{A}(\xi)$ has non-negative eigenvalues. This fact Goldberg (1992) implies the positive semi-definiteness of the matrix $M\mathbf{I}+\mathbf{A}(\xi)$, i.e. $\mathbf{V}.(M\mathbf{I}+\mathbf{A}(\xi))\mathbf{V} \geq 0$ for any $\xi \in R^n$, $|\,\xi\,| = 1$ and any vector-function $\mathbf{V}(x,t)$. Using this remark and denoting $\frac{1}{2}\int\limits_{S(\tau)} |\mathbf{V}(x,t)|^2 dx = w(\tau)$, we find from (A.318)

$$w(h) \leq w(0) + \int_0^h w(\tau)d\tau + \frac{1}{2}\int_0^h \int_{S(t)} |\mathbf{F}|^2 dx dt$$

or

$$w(h) \leq g(h) + \int_0^h w(\tau)d\tau, \tag{A.320}$$

where $g(h) = \frac{1}{2}\int_0^h \int_{S(t)} |\mathbf{F}|^2 dxdt + \frac{1}{2}\int_{S(0)} |\phi(x)|^2 dx$. Using Gronwall's Lemma (Nagle & Saff & Snider (2005)) we find from (A.320)

$$w(h) \leq g(h)e^h,$$

or

$$\int_{S(h)} |\mathbf{V}(x,h)|^2 dx \leq e^h \Big[\int_{S(0)} |\phi(x)|^2 dx + \int_0^h \Big(\int_{S(t)} |\widetilde{\mathbf{F}}(x,t)|^2 dx \Big) dt \Big].$$

Theorem A.19. *(see, for example, work Mizohata (1973)). Let $\mathbf{A}_j(x,t)$, $j = 1,...,n$, be $N \times N$ symmetric matrices, $\phi(x) \in H^m(R^n;R^m)$, $\mathbf{F}(x,t) \in C([0,T];H^m(R^n;R^m))$, where $m = 1,2,....$ Then there exits a unique solution $\mathbf{V}(x,t)$ of the problem (A.308)-(A.309) such that*

$$\mathbf{V}(x,t) \in C([0,T];H^m(R^n;R^m)) \cap C^1([0,T];H^{m-1}(R^n;R^m)).$$

Theorem A.20. *Let $m \geq [|\frac{n}{2}|] + 2$ in Theorem A.19. Then $\mathbf{V}(x,t)$ is a classical solution of (A.308)-(A.309) such that*

$$\mathbf{V}(x,t) \in C([0,T];C^{m-[|\frac{n}{2}|]-1}(R^n;R^m)) \cap C^1([0,T];H^{m-[|\frac{n}{2}|]-2}(R^n;R^m)).$$

Theorem A.21. *A special case of Sobolev Lemma (see, for example, work Mizohata (1973)). Let $H^m(R^n;R^m)$ be Sobolev space and*

$$\mathbb{B}^p(R^n;R^m) = \{f : R^n \to R^m;\ D^\alpha f \text{ is bounded and continuous},\ |\alpha| \leq p\}.$$

Then $H^{1+p+[|\frac{n}{2}|]} \subset \mathbb{B}^p$, $p = 0,1,2,...$

Theorem A.22. *Hormander-Lojasiezwicz Theorem (see, for example, work Vladimirov*

(1979)). The equation

$$P(D)u = f,$$

where $P(D) \neq 0$*, is solvable in* $\mathbb{S}'$ *for all* $f \in \mathbb{S}'$.

Corollary: Every nonzero linear differential operator with constant coefficients has a fundamental solution of slow growth.

Theorem A.23. *Paley-Wiener Theorem (see, for example, work Reed & Simon (1975)). A distribution* $T \in \mathbb{S}'(R^3)$ *has compact support if and only if Fourier transform of* T*,* $\widehat{T}$*, has an analytic continuation to an entire analytic function of n variables* $\widehat{T}(\eta)$ *that satisfies*

$$| \widehat{T}(\eta) | \leq C(1+ | \eta |)^N \exp(R \mid Im\eta \mid)$$

for all $\eta \in \mathbb{C}^n$ *and some constants* $C,\ N,\ R$*. Moreover, if A.23 holds, the support of* T *is contained in the ball of radius* R.

A.3 Positive definiteness of $\mathbf{A}(\nu)$, defined by (2.88)

The matrix $\mathbf{A}(\nu)$, defined by (2.88), is symmetric with real valued elements. Let us show that $\mathbf{A}(\nu)$ is positive-definite for any nonzero (ν_1, ν_2, ν_3) from R^3, i.e. the matrix $\mathbf{A}(\nu)$ has to satisfy

$$\mathbf{V}^* \mathbf{A}(\nu) \mathbf{V} > 0 \tag{A.321}$$

for arbitrary nonzero vectors $(u_1, u_2, u_3) \in R^3$ and $(\nu_1, \nu_2, \nu_3) \in R^3$.

We assume that c_{ijkl} satisfy condition (2.13) for any non-zero real symmetric tensor

ε_{ij}. The relations (2.13) can be written in the form

$$\sum_{j,l,i,k=1}^{3} c_{ijkl} u_i u_k \nu_j \nu_l > 0 \tag{A.322}$$

when

$$\varepsilon_{ij} = \frac{1}{2}(u_i \nu_j + u_j \nu_i),$$

here $\nu_1,\ \nu_2,\ \nu_3, u_1,\ u_2,\ u_3$ are arbitrary nonzero real numbers.

From (4.201) we can write

$$\mathbf{u}^* \mathbf{A}(\nu)\mathbf{u} = \sum_{j,l,i,k=1}^{3} c_{ijkl} u_i u_k \nu_j \nu_l \tag{A.323}$$

where $\mathbf{u} = (u_1, u_2, u_3) \in R^3$ and $(\nu_1, \nu_2, \nu_3) \in R^3$ are arbitrary nonzero vectors.

The inequality (A.321) follows from (A.322) and (A.323) for all nonzero $\mathbf{u} = (u_1, u_2, u_3) \in R^3$ and $(\nu_1, \nu_2, \nu_3) \in R^3$.

Remark: For all $(\nu_1, \nu_2, \nu_3) \in R^3$ the matrix $\mathbf{A}(\nu)$ defined by (4.201) is positive semi definite matrix.

A.4 Properties of 1D QCs

There exits the following classification of 1-D QCs (Wang & Yang & Hu (1997)):

`Triclinic`: In the triclinic 1-D QC system, the point group may be 1 or $\overline{1}$. There are 21 independent phonon elastic constants, 6 independent phason elastic constants and 18 independent phonon-phason coupling constants in the triclinic crystal system. Therefore, the total number of independent elastic constants is 45.

`Monoclinic`: In the monoclinic 1-D QC system, there are two Laue classes, i.e. $2/m_h$ and $2_h/m$. For invariants of the point groups $2/m_h$ we obtain the non-zero elastic constants as follows

$$\begin{aligned}
&c_{1111} \quad , \quad c_{2222},\ c_{3333},\ c_{1122},\ c_{1133},\ c_{1112},\ c_{2233},\ c_{2212},\ c_{3312},\\
&c_{3232} \quad , \quad c_{3231},\ c_{3131},\ c_{1212},\ K_{3333},\ K_{3131},\ K_{3232},\ K_{3132}\\
&R_{1133} \quad , \quad R_{2233},\ R_{3333},\ R_{1233},\ R_{2331},\ R_{2332},\ R_{3131},\ R_{3132}.
\end{aligned}$$

Therefore, the total number of independent elastic constants is 25.

For invariants of the point groups $2_h/m$ we obtain the non-zero elastic constants as follows

$$\begin{aligned}
&c_{1111} \quad , \quad c_{2222},\ c_{3333},\ c_{1122},\ c_{1133},\ c_{1131},\ c_{2233},\ c_{2231},\ c_{3331},\\
&c_{2323} \quad , \quad c_{1212},\ c_{3131},\ c_{2312},\ K_{3333},\ K_{3131},\ K_{3232},\ K_{3331}\\
&R_{1133} \quad , \quad R_{2233},\ R_{3333},\ R_{3133},\ R_{1131},\ R_{2231},\ R_{3331},\ R_{3131},R_{2332},\ R_{1232}.
\end{aligned}$$

Therefore, the total number of independent elastic constants is 27.

`Orthorhombic`: The point groups 2_h2_h2, $mm2$, 2_hmm_h and mmm_h in this system belong to the same Laue class. And the non-zero elastic constants

$$\begin{aligned}
&c_{1111} \quad , \quad c_{2222},\ c_{3333},\ c_{1122},\ c_{1133},\ c_{2233},\ c_{2323},\ c_{1212},\ c_{3131},\\
&K_{3333} \quad , \quad K_{3131},\ K_{3232},\ R_{1133},\ R_{2233},\ R_{3333},\ R_{3131},R_{2332}.
\end{aligned}$$

Therefore, the total number of independent elastic constants is 17.

`Tetragonal`: Two Laue classes, i.e. $4/m_h$ and $4/m_hmm$ belong to this system. For

the Laue class $4/m_h$ the non-zero elastic constants are

$$\begin{aligned} c_{1111} &= c_{2222},\ c_{3333},\ c_{2323} = c_{3131},\ c_{1122},\ c_{1212},\ c_{1133} = c_{2233}, \\ c_{1112} &= -c_{2212},\ K_{3333},\ K_{3131} = K_{3232}, \\ R_{1133} &= R_{2233},\ R_{3333},\ R_{3131} = R_{2332},\ R_{2331} = -R_{3132}. \end{aligned}$$

Therefore, the total number of independent elastic constants is 13.

For the Laue class $4/m_h mm$ the non-zero elastic constants are

$$\begin{aligned} c_{1111} &= c_{2222},\ c_{3333},\ c_{1133} = c_{2233},\ c_{1122},\ c_{1212},\ c_{2323} = c_{3131}, \\ K_{3131} &= K_{3232},\ K_{3333},\ R_{1133} = R_{2233},\ R_{3333},\ R_{3131} = R_{2332}. \end{aligned}$$

Therefore, the total number of independent elastic constants is 11.

`Trigonal`: Two Laue classes, i.e. $\overline{3}$ and $\overline{3}$m belong to the trigonal 1D QC system. For the first Laue class the non-zero elastic constants are

$$\begin{aligned} c_{1111} &= c_{2222},\ c_{3333},\ c_{2323} = c_{3131}\ c_{1133} = c_{2233},\ c_{1122}, \\ 2c_{1212} &= (c_{1111} - c_{1122}),\ c_{1123} = -c_{2223} = c_{3112}, \\ c_{2231} &= c_{2312} = -c_{1131},\ K_{3131} = K_{3232}, K_{3333},\ R_{1133} = R_{2233},\ R_{3333}, \\ R_{3131} &= R_{2332},\ R_{2331} = -R_{3132},\ R_{1131} = -R_{2231} = -R_{1232}, \\ R_{1132} &= -R_{2232} = R_{1231}. \end{aligned} \tag{A.324}$$

Therefore, the total number of independent elastic constants is 15. For the Laue class in (A.324) $c_{1131} = 0$, $R_{1131} = 0$ and $R_{2331} = 0$ and hence the total number of independent elastic constants is 12.

`Hexagonal`: Two Laue classes, i.e. $6/m_h$ and $6/m_h mm$, belong to the hexagonal

1D QC system. For the first Laue class the non-zero elastic constants are

$$\begin{aligned} c_{1111} &= c_{2222},\ c_{3333},\ c_{2323}=c_{3131}\ c_{1133}=c_{2233},\ c_{1122}, \\ 2c_{1212} &= (c_{1111}-c_{1122}),\ K_{3333},\ K_{3131}=K_{3232}, \\ R_{1133} &= R_{2233},\ R_{3333},\ R_{3131}=R_{2332},\ R_{2331}=-R_{3132}. \end{aligned} \tag{A.325}$$

Therefore, the total number of independent elastic constants is 11. For the latter Laue class their elastic constants are the same as (A.325) except that $R_{2331}=0$.

Positive definiteness of $\mathbf{A}(\nu)$, defined by (3.129): The matrix $\mathbf{A}(\nu)$, defined by (3.129), is symmetric with real valued elements. Let us show that $\mathbf{A}(\nu)$ is positive-definite for any nonzero (ν_1,ν_2,ν_3) from R^3, i.e. the matrix $\mathbf{A}(\nu)$ has to satisfy

$$\mathbf{V}^*\mathbf{A}(\nu)\mathbf{V}>0 \tag{A.326}$$

for arbitrary nonzero vectors $\mathbf{V}=(u_1,u_2,u_3,w_3)\in R^4$ and $(\nu_1,\nu_2,\nu_3)\in R^3$.

We assume that $c_{ijkl},\ R_{ij3l},\ K_{3j3l}$ satisfy conditions (3.118) for any symmetric matrix $(\varepsilon_{ij})_{3\times 3}$ and any vector $(w_{3l})_{1\times 3}$.

The relations (3.118) can be written in the form

$$\sum_{j,l,i,k=1}^{3} c_{ijkl}u_iu_k\nu_j\nu_l>0,\ \sum_{j,l,i=1}^{3} R_{ij3l}u_iw_3\nu_j\nu_l>0,\ \sum_{j,l=1}^{3} K_{3j3l}w_3^2\nu_j\nu_l>0 \tag{A.327}$$

when

$$\varepsilon_{ij}=\frac{1}{2}(u_i\nu_j+u_j\nu_i),\ w_{3l}=\nu_l w_3,$$

here $\nu_1,\ \nu_2,\ \nu_3, u_1,\ u_2,\ u_3, w_3$ are arbitrary nonzero real numbers.

Using (3.129) we can write

$$\mathbf{V}^*\mathbf{A}(\nu)\mathbf{V} = \frac{1}{2}\sum_{j,l,i,k=1}^{3}(c_{ijkl}+c_{ilkj})u_iu_k\nu_j\nu_l + \sum_{j,l,i=1}^{3}(R_{ij3l}+R_{il3j})u_iw_3\nu_j\nu_l$$
$$+ \quad \frac{1}{2}\sum_{j,l=1}^{3}(K_{3j3l}+K_{3l3j})w_3^2\nu_j\nu_l, \tag{A.328}$$

where $\mathbf{V} = (u_1, u_2, u_3, w_3) \in R^4$ and $(\nu_1, \nu_2, \nu_3) \in R^3$ are arbitrary nonzero vectors.

The inequality (A.326) follows from (A.327) and (A.328) for all nonzero $(\nu_1, \nu_2, \nu_3) \in R^3$ and $\mathbf{V} = (u_1, u_2, u_3, w_3) \in R^4$.

Remark: For all $(\nu_1, \nu_2, \nu_3) \in R^3$ the matrix $\mathbf{A}(\nu)$ defined by (3.129) is positive semi definite matrix.

A.5 Properties of 2D QCs

Follow works Lei & Wang & Hu & Ding (1998), Lei & Hu & Wang & Ding (1999), Lei & Wang & Hu & Ding (2000), Gao (2009), Peng & Fan (2002), Hu & Wang & Ding (2000) we consider the following types of anisotropic 2D QCs: dodecagonal, octagonal, decagonal, pentagonal, hexagonal, triclinic. Similar to Ding & Yang & Hu & Wang (1993) we assume that elastic constants c_{ijkl}, $K_{\beta j\alpha l}$, $R_{ij\alpha l}$ satisfy conditions (3.139) for all types of anisotropic QCs. Moreover these elastic constants satisfy specific properties for each type of anisotropy for 2D QCs. Let us point out these specific properties.

Dodecagonal: Nonzero elastic constants are (see, for example, Lei & Wang & Hu

& Ding (2000))

$$
\begin{aligned}
c_{1111} &= c_{2222},\ c_{1122},\ c_{1133}=c_{2233},\ c_{3333},\ c_{4444}=c_{5555},\ c_{1212}=\frac{c_{1111}-c_{1122}}{2},\\
K_{1111} &= K_{2222},\ K_{1122},\ K_{1221},\ K_{2323}=K_{1313},\ K_{1212}=K_{2121}=K_{1111}+K_{1122}+K_{1221},\\
K_{1112} &= K_{1121}=-K_{2212}=-K_{2221}.
\end{aligned}
$$

Octagonal: Nonzero elastic constants are (see, for example, Lei & Hu & Wang & Ding (1999))

$$
\begin{aligned}
c_{1111} &= c_{2222},\ c_{1122},\ c_{1133}=c_{2233},\ c_{3333},\ c_{4444}=c_{5555},\ c_{1212}=\frac{c_{1111}-c_{1122}}{2},\\
R_{1111} &= R_{1122}=-R_{2211}=-R_{2222}=R_{1221}=-R_{1212},\\
R_{1112} &= -R_{1121}=-R_{2212}=R_{2221}=R_{1211}=R_{1222},\ K_{1111}=K_{2222},\ K_{1122},\ K_{1221},\\
K_{1313} &= K_{2323}, K_{1212}=K_{2121}=K_{1111}+K_{1122}+K_{1221},\\
K_{1112} &= K_{1121}=-K_{2212}=-K_{2221}.
\end{aligned}
$$

Decagonal: Nonzero elastic constants are (see, for example, Peng & Fan (2002))

$$
\begin{aligned}
c_{1111} &= c_{2222},\ c_{1122},\ c_{1133}=c_{2233},\ c_{3333},\ c_{4444}=c_{5555},\ c_{1212}=\frac{c_{1111}-c_{1122}}{2},\\
R_{1111} &= R_{1122}=R_{1221}=-R_{2211}=-R_{2222}=-R_{1212},\\
K_{1111} &= K_{2222}=K_{1212}=K_{2121},\ K_{1122}=-K_{1221},\ K_{2323}=K_{1313}.
\end{aligned}
$$

Pentagonal: Nonzero elastic constants are (see, for example, Lei & Wang & Hu &

Ding (1998))

$$
\begin{aligned}
c_{1111} &= c_{2222},\ c_{1122},\ c_{1133}=c_{2233},\ c_{3333},\ c_{4444}=c_{5555},\ c_{1212}=\frac{c_{1111}-c_{1122}}{2},\\
R_{1111} &= R_{1122}=-R_{2211}=-R_{2222}=R_{1221}=-R_{1212},\\
R_{1112} &= -R_{1121}=-R_{2212}=R_{2221}=R_{1211}=R_{1222},\\
R_{2312} &= R_{2321}=-R_{3111}=R_{3122},\ R_{2311}=-R_{2322}=R_{3112}=R_{3121},\\
R_{1113} &= -R_{2213}=-R_{1223}, R_{1123}=-R_{2223}=R_{1213},\ K_{1111}=K_{2222}=K_{1212}=K_{2121},\\
K_{1122} &= -K_{1221},\ K_{1313}=K_{2323},\ K_{1113}=K_{2213}=K_{2312}=-K_{2321},\\
K_{1123} &= K_{2223}=-K_{1213}=K_{1321}.
\end{aligned}
$$

Hexagonal: Nonzero elastic constants are (see, for example, Gao (2009))

$$
\begin{aligned}
c_{1111} &= c_{2222},\ c_{1122},\ c_{1133}=c_{2233},\ c_{3333},\ c_{4444}=c_{5555}, c_{1212}=\frac{c_{1111}-c_{1122}}{2},\\
R_{1111} &= R_{2222},\ R_{1122}=R_{2211},\ R_{3322}=R_{3311},\ R_{1313},\\
R_{1212} &= R_{1221}=\frac{R_{1111}-R_{2222}}{2},\ K_{1111}=K_{2222},\ K_{1122},\\
K_{1212} &= K_{2121},\ K_{2323}=K_{1313},\ K_{1221}=K_{1111}-K_{1122}-K_{1212}.
\end{aligned}
$$

Triclinic: The total number of independent elastic constants is 78 (see, for example, Hu & Wang & Ding (2000)) in the triclinic 2-D QC system. There are 21 independent phonon elastic constants, 21 independent phason elastic constants and 36 independent phonon-phason coupling constants.

The classification of 2D QCs is given by Table A.1(Hu & Wang & Ding (2000)).

Positive definiteness of $\mathbf{A}(\nu)$, defined by (3.149)

The matrix $\mathbf{A}(\nu)$, defined by (3.149), is symmetric with real valued elements.

Table A.1. Systems, Laue classes, point groups and the number of independent elastic constants for 2D QCs. N_C, N_K and N_R are the numbers of independent elastic constants associated with the phonon field, the phason field and the phonon-phason coupling,respectively.

Systems	No of Laue classes	Point groups	N_C	N_K	N_R	Sum
Triclinic	1	$1,\ \bar{1}$	21	21	36	78
Monoclinic	2	$2,\ m,\ 2/m$	13	13	20	46
	3	$12,\ 1m,\ 12/m$	13	12	18	43
Orthorhombic	4	$2mm,\ 222,\ mmm,\ mm2$	9	8	10	27
Tetragonal	5	$4,\ \bar{4},\ 4/m$	7	7	10	24
	6	$4mm,\ 422,\ \bar{4}m2,\ 4/mmm$	6	5	5	16
Trigonal	7	$3,\ \bar{3}$	7	7	12	26
	8	$3m,\ 32,\ \bar{3}m$	6	5	6	17
Hexagonal	9	$6,\ \bar{6}m,\ 6/m$	5	5	8	18
	10	$6mm,\ 622,\ \bar{6}m2,\ 6/mmm$	5	4	4	13
Pentagonal	11	$5,\ \bar{5}$	5	5	6	16
	12	$5m,\ 52,\ \bar{5}m$	5	4	3	12
Decagonal	13	$10,\ \overline{10},\ 10/m$	5	3	2	10
	14	$10mm,\ 1022,\ \overline{10}m2,\ 10/mmm$	5	3	1	9
Octagonal	15	$8,\ \bar{8},\ 8/m$	5	5	2	12
	16	$8mm,\ 822,\ \bar{8}m2,\ 8/mmm$	5	4	1	10
Dodecagonal	17	$12,\ \overline{12},\ 12/m$	5	5	0	10
	18	$12mm,\ 1222,\ \overline{12}m2,\ 12/mmm$	5	4	0	9

Let us show that $\mathbf{A}(\nu)$ is positive-definite for any nonzero (ν_1,ν_2,ν_3) from R^3, i.e. the matrix $\mathbf{A}(\nu)$ has to satisfy

$$\mathbf{V}^*\mathbf{A}(\nu)\mathbf{V} > 0 \tag{A.329}$$

for arbitrary nonzero vectors $\mathbf{V} = (u_1,u_2,u_3,w_1,w_2) \in R^5$ and $(\nu_1,\nu_2,\nu_3) \in R^3$.

We assume that $c_{ijkl},\ R_{ij\alpha l},\ K_{\beta j\alpha l}$ satisfy conditions (3.140) for any symmetric matrix $(\varepsilon_{ij})_{3\times 3}$ and any matrix $(w_{\alpha l})_{2\times 3}$.

The relations (3.140) can be written in the form

$$\sum_{j,l,i,k=1}^{3} C_{ijkl}u_iu_k\nu_j\nu_l > 0,\ \sum_{j,l,i=1}^{3}\sum_{\alpha=1}^{2} R_{ij\alpha l}u_iw_\alpha\nu_j\nu_l > 0,$$
$$\sum_{j,l=1}^{3}\sum_{\alpha,\beta=1}^{2} K_{\beta j\alpha l}w_\beta w_\alpha\nu_j\nu_l > 0 \tag{A.330}$$

when

$$\varepsilon_{ij} = \frac{1}{2}(u_i\nu_j + u_j\nu_i),\ w_{\alpha l} = \nu_l w_\alpha,$$

here $\nu_1,\ \nu_2,\ \nu_3, u_1,\ u_2,\ u_3, w_1,\ w_2$ are arbitrary nonzero real numbers.

Using (3.149) we can write

$$\mathbf{V}^*\mathbf{A}(\nu)\mathbf{V} = \frac{1}{2}\sum_{j,l,i,k=1}^{3}(c_{ijkl}+c_{ilkj})u_iu_k\nu_j\nu_l + \sum_{j,l,i=1}^{3}\sum_{\alpha=1}^{2}(R_{ij\alpha l}$$
$$+R_{il\alpha j})u_iw_\alpha\nu_j\nu_l + \frac{1}{2}\sum_{j,l=1}^{3}\sum_{\alpha,\beta=1}^{2}(K_{\beta j\alpha l}+K_{\beta l\alpha j})w_\beta w_\alpha\nu_j\nu_l, \tag{A.331}$$

where $\mathbf{V} = (u_1,u_2,u_3,w_1,w_2) \in R^5$ and $(\nu_1,\nu_2,\nu_3) \in R^3$ are arbitrary nonzero vectors.

The inequality (A.329) follows from (A.330) and (A.331) for all nonzero $(\nu_1,\nu_2,\nu_3) \in R^3$ and $\mathbf{V} = (u_1,u_2,u_3,w_1,w_2) \in R^5$.

Remark: For all $(\nu_1,\nu_2,\nu_3) \in R^3$ the matrix $\mathbf{A}(\nu)$ defined by (3.149) is positive semi definite matrix.

A.6 Positive definiteness of $\mathbf{A}(\nu)$, defined by (3.172)

The matrix $\mathbf{A}(\nu)$, defined by (3.172), is symmetric with real valued elements. Let us show that $\mathbf{A}(\nu)$ is positive-definite for any nonzero (ν_1,ν_2,ν_3) from R^3, i.e. the

matrix $\mathbf{A}(\nu)$ has to satisfy

$$\mathbf{V}^*\mathbf{A}(\nu)\mathbf{V} > 0 \tag{A.332}$$

for arbitrary nonzero vectors $\mathbf{V} = (u_1, u_2, u_3, w_1, w_2, w_3) \in R^6$ and $(\nu_1, \nu_2, \nu_3) \in R^3$.

We assume that $c_{ijkl},\ R_{ijkl},\ K_{ijkl}$ satisfy conditions (3.162) for any symmetric matrix $(\varepsilon_{ij})_{3\times 3}$ and any matrix $(w_{ij})_{3\times 3}$.

The relations (3.162) can be written in the form

$$\sum_{j,l,i,k=1}^{3} C_{ijkl}u_iu_k\nu_j\nu_l > 0, \sum_{i,j,k,l=1}^{3} R_{ijkl}u_iw_k\nu_j\nu_l > 0,$$
$$\sum_{i,j,k,l=1}^{3} K_{ijkl}w_iw_k\nu_j\nu_l > 0 \tag{A.333}$$

when

$$\varepsilon_{ij} = \frac{1}{2}(u_i\nu_j + u_j\nu_i),\ w_{kl} = \nu_l w_k,$$

here $\nu_1,\ \nu_2,\ \nu_3, u_1,\ u_2,\ u_3, w_1,\ w_2,\ w_3$ are arbitrary nonzero real numbers.

Using (3.172) we find

$$\mathbf{V}^*\mathbf{A}(\nu)\mathbf{V} = \frac{1}{2}\sum_{j,l,i,k=1}^{3}(c_{ijkl} + c_{ilkj})u_iu_k\nu_j\nu_l \ + \sum_{j,l,i,k=1}^{3}(R_{ijkl} + R_{ilkj})u_iw_k\nu_j\nu_l$$
$$+ \ \frac{1}{2}\sum_{j,l,i,k=1}^{3}(K_{ijkl} + K_{ilkj})w_iw_k\nu_j\nu_l, \tag{A.334}$$

where $\mathbf{V} = (u_1, u_2, u_3, w_1, w_2, w_3) \in R^6$ and $(\nu_1, \nu_2, \nu_3) \in R^3$ are arbitrary nonzero vectors.

The inequality (A.332) follows from (A.333) and (A.334) for all nonzero $\mathbf{V} = (u_1, u_2, u_3, w_1, w_2, w_3) \in R^6$ and $(\nu_1, \nu_2, \nu_3) \in R^3$.

Remark: For all $(\nu_1, \nu_2, \nu_3) \in R^3$ the matrix $\mathbf{A}(\nu)$ defined by (3.172) is positive semi definite matrix.